PH.D. THESIS

Control of Large Actuator Arrays Using Pattern-Forming Systems

by E.W. Justh
Advisor: P.S. Krishnaprasad

CDCSS Ph.D. 98-3
(ISR Ph.D. 98-6)

The Center for Dynamics and Control of Smart Structures (CDCSS) is a joint Harvard University, Boston University, University of Maryland center, supported by the Army Research Office under the ODDR&E MURI97 Program Grant No. DAAG55-97-1-0114 (through Harvard University). This document is a technical report in the CDCSS series originating at the University of Maryland.

Web site http://www.isr.umd.edu/CDCSS/cdcss.html

ABSTRACT

Title of dissertation: CONTROL OF LARGE ACTUATOR ARRAYS
USING PATTERN-FORMING SYSTEMS

Eric W. Justh, Doctor of Philosophy, 1998

Dissertation directed by: Professor P.S. Krishnaprasad
Department of Electrical Engineering

Pattern-forming systems are used to model many diverse phenomena from biology, chemistry, and physics. These systems of differential equations have the property that as a bifurcation (or control) parameter passes through a critical value, a stable spatially uniform equilibrium state gives way to a stable pattern state, which may have spatial variation, time variation, or both. There is a large body of experimental and mathematical work on pattern-forming systems. However, these ideas have not yet been adequately exploited in engineering, particularly in the control of smart systems; i.e., feedback systems having large numbers of actuators and sensors. With dramatic recent improvements in micro-actuator and micro-sensor technology, there is a need for control schemes better than the conventional approach of reading out all of the sensor information to a computer, performing all the necessary computations in a centralized fashion, and then sending out commands to each individual actuator. Potential applications for large arrays of micro-actuators

include adaptive optics (in particular, micromirror arrays), suppressing turbulence and vortices in fluid boundary-layers, micro-positioning small parts, and manipulating small quantities of chemical reactants.

The main theoretical result presented is a Lyapunov functional for the cubic nonlinearity activator-inhibitor model pattern-forming system. Analogous Lyapunov functionals then follow for certain generalizations of the basic cubic nonlinearity model. One such generalization is a complex activator-inhibitor equation which, under suitable hypotheses, models the amplitude and phase evolution in the continuum limit of a network of coupled van der Pol oscillators, coupled to a network of resonant circuits, with an external oscillating input. Potential applications for such coupled van der Pol oscillator networks include quasi-optical power combining and phased-array antennas.

In addition to the Lyapunov functional, a Lyapunov function for the truncated modal dynamics is derived, and the Lyapunov functional is also used to analyze the stability of certain equilibria. Basic existence, uniqueness, regularity, and dissipativity properties of solutions are also verified, engineering realizations of the dynamics are discussed, and finally, some of the potential applications are explored.

CONTROL OF LARGE ACTUATOR ARRAYS USING PATTERN-FORMING SYSTEMS

by

Eric W. Justh

Dissertation submitted to the Faculty of the Graduate School of the
University of Maryland, College Park in partial fulfillment
of the requirements for the degree of
Doctor of Philosophy
1998

Advisory Committee:

Professor P.S. Krishnaprasad, Chair/Advisor
Professor Shihab Shamma
Professor André Tits
Professor Steven Marcus
Professor Stuart Antman

ACKNOWLEDGEMENTS

I would like to thank my advisor, Dr. P.S. Krishnaprasad, for his help and guidance on the theoretical aspects of this dissertation.

This research was supported in part by grants from the National Science Foundation's Engineering Research Centers Program: NSFD CDR 8803012; by the Army Research Office under the ODDR&E MURI97 Program Grant No. DAAG55-97-1-0114 to the Center for Dynamics and Control of Smart Structures (through Harvard University); and by the AFOSR University Research Initiative Program, under grant AFOSR-90-0105 and AFOSR-F49620-92-J-0500. Also, this work was partially supported by a National Science Foundation fellowship and an Achievement Rewards for College Scientists (ARCS) scholarship.

TABLE OF CONTENTS

1 Introduction **1**

1.1 Background 1

1.2 Overview 12

2 Standard Approaches for Analyzing Pattern-Forming Systems **13**

2.1 Introduction 13

2.2 Amplitude equations 14

2.2.1 Amplitude equation for K-systems 18

2.2.2 Amplitude equation for Ω-systems 20

2.2.3 Amplitude equation for $K\Omega$-systems 22

2.3 Phase equations 26

2.3.1 Linearized phase equation derivation from the amplitude equation 26

2.3.2 Derivation of the phase equation using the reaction-diffusion equation 29

2.4 Results for general activator-inhibitor equations 32

2.4.1 Linearized analyses of spatially uniform equilibria and bifurcations 32

2.4.2 Classification of general activator-inhibitor systems 37

2.5 Analysis of spike solutions 39

2.5.1 Active transmission line without inhibitor diffusion or dissipation 39

2.5.2 General activator-inhibitor system 42

3 Engineering Realizations of Activator-Inhibitor Equations **46**

3.1 Basic cubic nonlinearity model 46

3.2 Active transmission line 50

3.3 Complex activator-inhibitor equation 54

4 Basic Properties of Solutions **64**

4.1 Introduction 64

4.2 Existence and uniqueness of weak solutions for the general polynomial-nonlinearity model 67

4.2.1 Definition of weak solutions 67

4.2.2 Galerkin approximations 71

4.2.3 Inequality for uniformly parabolic bilinear forms 72

4.2.4 $L^2(0,T;L^2(\Omega))$ and $L^\infty(0,T;L^2(\Omega))$ bounds for θ_m and η_m 73

4.2.5 $L^2(0,T;L^2(\Omega))$ bounds for $\nabla\theta_m$ and $\nabla\eta_m$ 77

4.2.6 $L^{2p_\theta}(0,T;L^{2p_\theta}(\Omega))$ and $L^{2p_\eta}(0,T;L^{2p_\eta}(\Omega))$ bounds for θ_m and η_m 78

4.2.7 $L^2(0,T;H^{-1}(\Omega))$ bounds for $\partial_t\theta_m$ and $\partial_t\eta_m$ 79

4.2.8 Convergence lemma 85

4.2.9 Existence proof 86

4.2.10 Uniqueness proof 89

4.2.11 Continuous dependence on initial data 92

4.3 Generalizations of the basic existence and uniqueness results 93

4.3.1 Bounded nonlinearity model 93

4.3.2 Complex activator-inhibitor equation 93

4.3.3 Additional symmetric long-range coupling 94

4.4 Existence and uniqueness of weak solutions for the active transmission-line model without inhibitor diffusion 95

4.5 Regularity of weak solutions for the general polynomial-nonlinearity model 98

4.5.1 Further energy bounds for θ and $\partial_t\theta$ 98

4.5.2 Outline of regularity proof 102

4.6 Dissipativity results 104

4.6.1 The notion of dissipativity 104

4.6.2 Cubic nonlinearity model 107

4.6.3 Active transmission-line models 113

4.6.4 Cubic nonlinearity model with an additional advective term 114

4.6.5 Cubic nonlinearity model with additional symmetric long-range coupling 116

4.6.6 Complex activator-inhibitor equation 117

5 Lyapunov Functionals **119**

5.1 Introduction 119
5.2 Gradient dynamics property of the cubic nonlinearity model ..120
5.3 Lyapunov function derivation for the spatially discretized cubic nonlinearity model 121
5.4 Convergence result for the spatially discretized cubic nonlinearity model 127
5.5 Lyapunov functional derivation for the cubic nonlinearity model 128
5.6 Generalizations of the basic Lyapunov functional 134
5.6.1 Cubic nonlinearity model with additional symmetric long-range coupling 134
5.6.2 Complex activator-inhibitor equation 135
5.6.3 Bounded nonlinearity model 137
5.6.4 Active transmission line (with inhibitor diffusion and dissipation) 139
5.6.5 Spatially-varying coefficients 141

6 Analyzing Equilibria Using Lyapunov Functionals **142**

6.1 Introduction 142
6.2 Form of the Lyapunov functional at equilibria 143
6.2.1 Basic cubic nonlinearity model 143
6.2.2 Complex activator-inhibitor equation 146
6.3 Stability analysis for spatially uniform equilibria 147
6.3.1 Basic cubic nonlinearity model 147
6.3.2 Active transmission line (with inhibitor diffusion and dissipation) 151
6.4 Analysis of equilibria for the complex activator-inhibitor equation 153
6.4.1 Polar coordinate transformation 154
6.4.2 Analysis of the ideal helical equilibria in the $C = 0$ case 156
6.4.3 Analysis of the spatially uniform equilibrium in the large-$|C|$ case 168
6.4.4 Bifurcation from the spatially uniform equilibrium solution 170

6.5 Analysis of equilibria using modal equations 171
6.5.1 Derivation of the modal dynamics 172
6.5.2 Lyapunov function for the modal dynamics 174
6.5.3 Bounding the higher-order modes 176
6.5.4 Modal results for the real cubic nonlinearity model 179
6.6 Numerical results for the spatially discretized cubic nonlinearity model 180

7 Smart Systems Applications **183**

7.1 Introduction 183
7.2 MEMS actuator-array applications 189
7.2.1 Derivation of torsional flap dynamical equations 191
7.2.2 Manipulation of micro-scale items 200
7.2.3 Micropositioning small (but not micro-scale) items 202
7.3 Phased-array antenna applications 204
7.3.1 Linear array 204
7.3.2 Endfire array 207
7.4 Real-time image processing application 212

8 Conclusions and Directions for Future Research **217**

A Derivations **219**

A.1 Derivation of the phase equation for K-systems 219
A.2 Derivation of the complex activator-inhibitor dynamics in polar coordinates 225

B Simulations **229**

References **232**

LIST OF FIGURES

1.1 Intersection of the curves $\eta(\theta) = \theta^3 - \theta$ and $\eta(\theta) = -\theta + C$ 4

1.2 Narrow spike equilibrium solution for the cubic nonlinearity model ... 5

1.3 Wide pulse equilibrium solution for the cubic nonlinearity model 5

1.4 Equilibrium pattern solution for the cubic nonlinearity model 6

1.5 An equilibrium pattern solution for the two-dimensional cubic nonlinearity model 7

1.6 Narrow spike solution for the two-dimensional cubic nonlinearity model 7

1.7 An actual pattern for the two-dimensional cubic nonlinearity model .. 8

2.1 Growth rate of a linear disturbance as a function of wave number and ϵ 17

2.2 Phase plane for the potential function $V(x) = -(1/4)x^4 + (1/2)x^2 - Cx$ 41

2.3 Traveling spike solution corresponding to the separatrix trajectory .. 42

2.4 Traveling spike for the cubic nonlinearity model with additional advective term 45

3.1 An implementation of the spatially discretized cubic nonlinearity model dynamics 48

3.2 Active transmission-line circuit with inhibitor diffusion and dissipation 52

3.3 Active transmission-line circuit without inhibitor diffusion or dissipation 54

3.4 Oscillator array with linear coupling network 56

3.5 Van der Pol oscillator circuit model 57

6.1 Plot of R_θ versus ϕ 159

6.2 Complex activator-inhibitor equation near the bifurcation threshold 171

6.3 V^* energy for the cubic nonlinearity model equilibria as a function of β 181

6.4 Wide pulse equilibrium shape as a function of β 181

6.5 Narrow spike equilibrium shape as a function of β 182

7.1 One cycle of the pattern solution excited by locally raising the control parameter for the one-dimensional discretization of the cubic nonlinearity model 184

7.2 The resulting spike when the control parameter is restored to its original value after a cycle of the pattern solution has been excited as in figure 7.1 185

7.3 One cycle of the pattern solution excited by locally raising the control parameter for the two-dimensional discretization of the cubic nonlinearity model 185

7.4 The resulting spike when the control parameter is restored to its original value after a cycle of the pattern solution has been excited as in figure 7.3 186

7.5 The pattern solution excited by locally raising the control parameter over a circular region larger than that of figure 7.3 187

7.6 The resulting circularly symmetric solution when the control parameter is restored to its original value after the pattern solution of figure 7.5 has been excited 187

7.7 The pattern solution excited by locally raising the control parameter over a non-circular region larger than that of figure 7.3 ... 188

7.8 The resulting spikes when the control parameter is restored to its original value after the pattern solution of figure 7.7 188

7.9 Torsional flap above a conducting sheet 192

7.10 Electrostatics problem for the torsional flap above a conducting sheet 193

7.11 Torsional flap above two electrodes 197

7.12 Ideal roll pattern for the endfire phased-array antenna with long-range coupling 208

7.13 Antenna pattern for the ideal roll pattern of figure 7.12 209

7.14 Roll pattern in a circular network with the oscillators turned on using a bistable activator-inhibitor network 211

7.15 The roll pattern of figure 7.14 in the process of being formed as the wave in the bistable system sweeps across 211

Chapter 1

Introduction

1.1 Background

Pattern-forming systems are used to model many diverse phenomena from biology, chemistry, and physics. Biological examples include models for describing population dynamics, animal coloration patterns, various aspects of nervous systems, human visual hallucination patterns, and cardiac fibrillation [1, 2]. Examples from chemistry include certain catalyzed reactions, including the catalytic converters used to convert carbon monoxide to carbon dioxide in motor vehicles [1, 3, 4, 5]. Physics examples include patterns observed in shaken collections of small spherical particles, gas discharge tubes, semiconductor electron-hole plasmas, and Josephson-junction arrays [6, 7, 8, 9, 10, 11]. Despite the diversity of underlying phenomena, all such pattern-forming systems share certain basic mathematical features, which is reflected in the similarities among the observed patterns.

The philosophy underlying the study of pattern formation is that while each of the various physical systems has its own unique characteristics, certain basic features of the pattern-forming behavior are universal; i.e., independent of the details of the model. However, given some physical model that is known to exhibit patterns, it is not generally clear how to extract the part responsible for the pattern-forming behavior. Therefore, the standard approach to studying patterns is to write down simplified model equations, which do not necessarily have a specific physical origin, but which can be shown analytically to give rise to the patterns under study. The cubic nonlinearity activator-

inhibitor model equation, which is the main equation analyzed in this work, is an example of a pattern-forming system model equation. Because of its relatively simple form, a number of strong results can be derived for it [12].

There is a large body of experimental and mathematical work on pattern-forming systems that arise in biology, chemistry, and physics. However, these ideas have not yet been adequately exploited in engineering, particularly in the control of smart systems; i.e., feedback systems having large numbers of actuators and sensors. With dramatic recent improvements in micro-actuator and micro-sensor technology, there is a need for control schemes better than the conventional approach of reading out all of the sensor information to a computer, performing all the necessary computations in a centralized fashion, and then sending out commands to each individual actuator.

Potential applications for large arrays of micro-actuators include adaptive optics (in particular, micromirror arrays), suppressing turbulence and vortices in fluid boundary-layers, micro-positioning small parts, and manipulating small quantities of chemical reactants [13, 14, 15, 16, 17, 18, 19, 20]. As the number of actuators increases, so does the bandwidth required to command each actuator individually. The goals of using pattern-forming systems for control of large actuator arrays are to

- enable the external control inputs to be lower-bandwidth, either by having the same control input influence many actuators, or by having the control input set quasistatic parameters which determine how the (much faster) pattern-forming system dynamics evolve;
- allow the actuator control signals to be computed in parallel at each actuator site using mostly local information; and

- permit large arrays to be treated mathematically using nonlinear dynamical systems theory so that control schemes can be developed.

Biology provides the best examples of how information from large numbers of sensors can be incorporated effectively into the control of large numbers of actuators. Experimental and theoretical biologists have made and continue to make considerable progress in explaining how various aspects of animal nervous systems function. However, there is still not enough known to suggest rules for the design of a smart system. The pattern-forming system level seems to be the correct level of analysis for certain aspects of biological nervous systems (most dramatically, human visual hallucination patterns) [1, 2]. So trying to base the control of a smart system on pattern-forming system ideas is at least biologically reasonable.

The model equation we focus on is the cubic nonlinearity activator-inhibitor system

$$\begin{aligned} \tau_\theta \partial_t \theta &= l^2 \Delta\theta - \theta^3 + \theta + \eta, \\ \tau_\eta \partial_t \eta &= L^2 \Delta\eta - \eta - \theta + C \end{aligned} \tag{1.1}$$

in either one or two space dimensions, where Δ denotes the Laplacian, and

$$\begin{aligned} \theta &= \text{activator}, \\ \eta &= \text{inhibitor}, \\ \tau_\theta &= \text{time constant for the activator}, \\ \tau_\eta &= \text{time constant for the inhibitor}, \\ l &= \text{diffusion length for the activator}, \\ L &= \text{diffusion length for the inhibitor}, \\ C &= \text{control (or bifurcation) parameter}. \end{aligned}$$

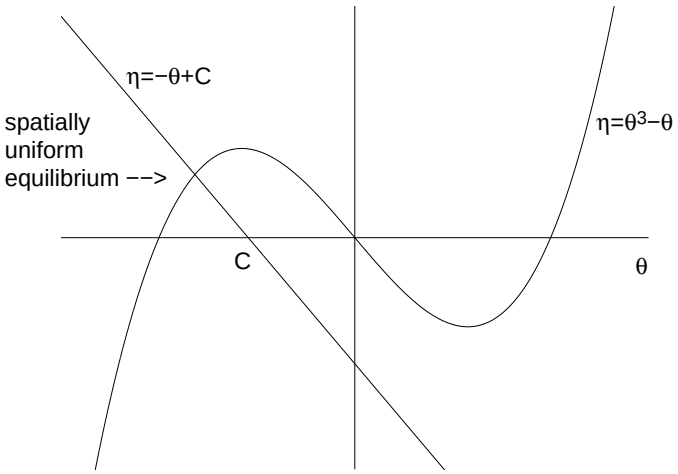

Figure 1.1: Intersection of the curves $\eta(\theta) = \theta^3 - \theta$ and $\eta(\theta) = -\theta + C$

We also define

$$\begin{aligned} \alpha &= \tau_\theta/\tau_\eta = \text{ ratio of time constants,} \\ \beta &= l/L = \text{ ratio of length scales.} \end{aligned} \tag{1.2}$$

The system has a spatially uniform equilibrium solution given by the intersection of the curve $\eta(\theta) = \theta^3 - \theta$ with the line $\eta(\theta) = -\theta + C$, as shown in figure 1.1.

We are primarily interested in $\beta << 1$, in which case the spatially uniform equilibrium solution is stable for $|C| > \frac{1}{3\sqrt{3}}$. When the spatially uniform equilibrium solution is unstable, a pattern solution is stable. When $\alpha << 1$, there is an ideal pattern solution which is periodic in both space and time. However, for the case we are primarily interested in, $\alpha > 1$, the pattern solution is in fact a spatially periodic equilibrium. Furthermore, when $\beta << 1$ and $\alpha > 1$, when the spatially uniform equilibrium is stable, other interesting equilibria may also be stable. These interesting equilibria, and a spatially periodic pattern equilibrium, are illustrated in figures 1.2, 1.3, and 1.4. (In figures 1.1, 1.2, and 1.3, $C = -\frac{2\sqrt{2}}{3\sqrt{3}}$; in figure 1.4, $C = 0$.)

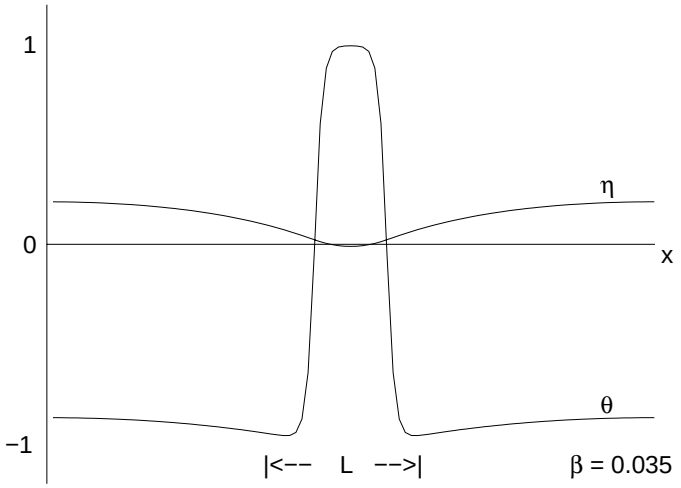

Figure 1.2: Narrow spike equilibrium solution for the cubic nonlinearity model

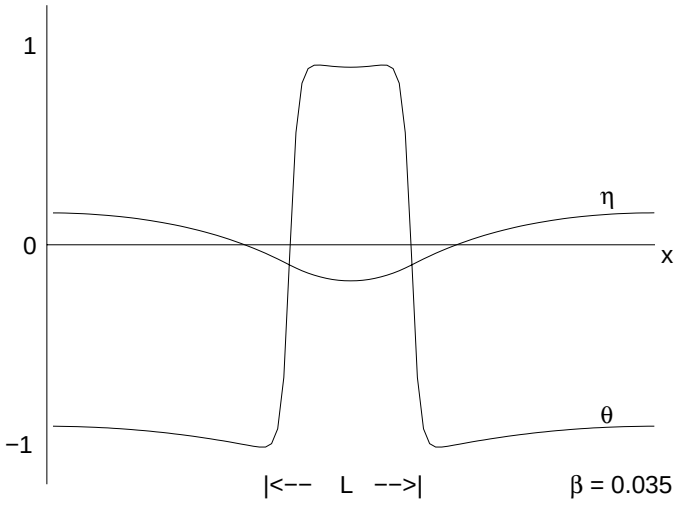

Figure 1.3: Wide pulse equilibrium solution for the cubic nonlinearity model

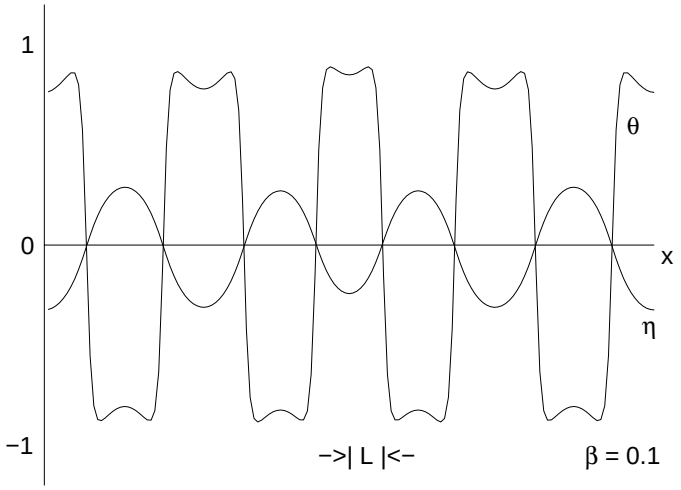

Figure 1.4: Equilibrium pattern solution for the cubic nonlinearity model

A pattern of spikes in one dimension corresponds to more interesting equilibria for a two-dimensional system. Two (approximately) radially symmetric equilibria in two dimensions are pictured in figures 1.5 and 1.6. Since the boundary conditions are periodic, the radial symmetry of the pattern solution breaks down toward the edges of the domain. The two-dimensional system also has an ideal pattern consisting of parallel rolls.

Actual patterns observed in pattern-forming systems generally differ from the ideal patterns, unless at least one of several special conditions is met:

- the system is highly homogeneous and is uniformly maintained very close to the bifurcation point where stability of the spatially uniform equilibrium has just given way to stability of the pattern solution;
- the system is excited into the pattern state in a carefully controlled way so that the ideal pattern is obtained; or
- there is long-range coupling present so that an ideal pattern is energetically favorable as compared with a more disordered pattern.

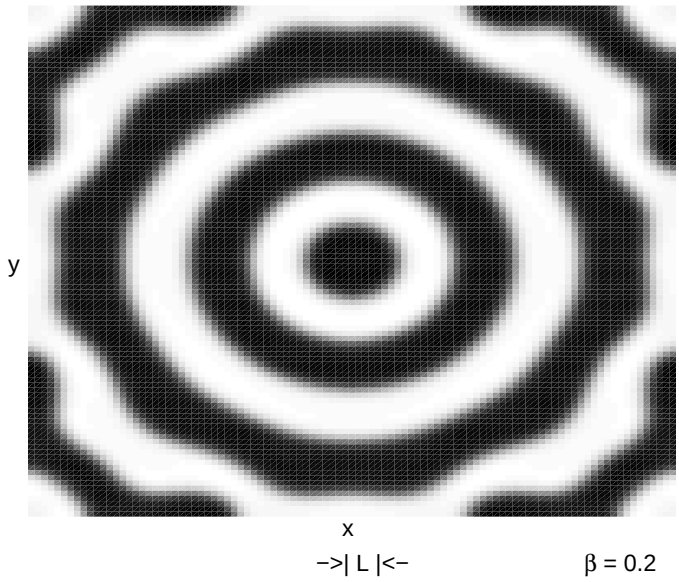

Figure 1.5: An equilibrium pattern solution for the two-dimensional cubic nonlinearity model

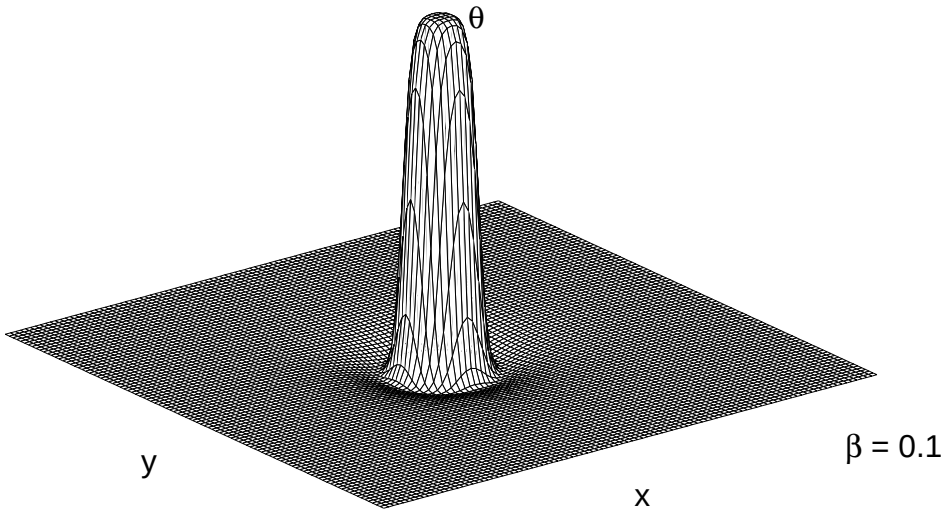

Figure 1.6: Narrow spike solution for the two-dimensional cubic nonlinearity model

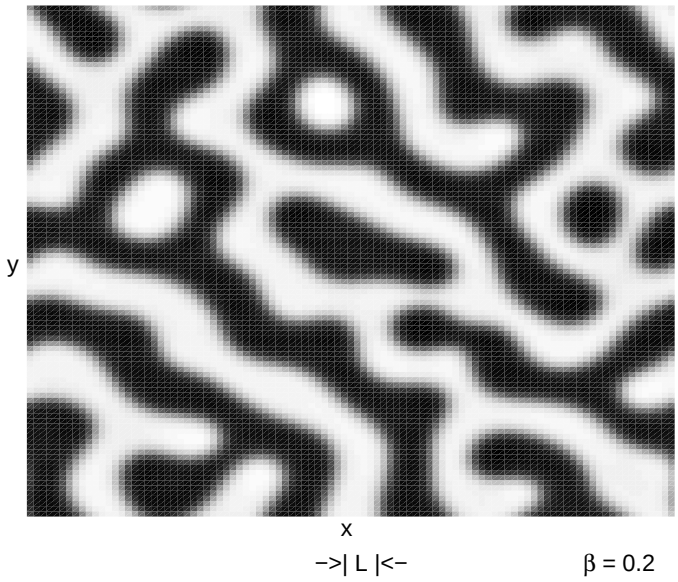

Figure 1.7: An actual pattern for the two-dimensional cubic nonlinearity model

Unless one of these special conditions is met, the actual pattern observed looks locally like the ideal pattern, but exhibits disorder over long ranges, as illustrated in figure 1.7. Similarly, when $\beta << 1$, $\alpha > 1$, and the spatially uniform equilibrium state of the cubic nonlinearity model is stable, the spike solutions essentially do not interact with each other as long as they are separated by several inhibitor diffusion lengths, unless the system is highly homogeneous. If the system is highly homogeneous, the effect spikes have on each other decreases exponentially with the distance between them [21]. (In figures 1.5 and 1.7, $C = 0$; in figure 1.6, $C = -\frac{2\sqrt{2}}{3\sqrt{3}}$.)

The factors that influence actual patterns are initial conditions, boundary conditions, inhomogeneities, and symmetry-breaking. Initial conditions, boundary conditions, and inhomogeneities might be used for pattern control. (During symmetry breaking, tiny perturbations beyond our control select the position and orientation of the pattern.) Although ideal patterns have been the focus of much of the theoretical and experimental work with pattern-forming

systems, the fact that actual patterns have the flexibility to deviate from ideal patterns means that a rich variety of patterns can be realized, at the expense, of course, of having to devise control schemes.

For the cubic nonlinearity model with $\beta << 1$ and $\alpha > 1$, both the pattern regime and the spike regime might be useful, depending on the particular application. Two surfaces with micro-actuator arrays in contact with each other could change the coefficient of friction between them by alternating between the spatially uniform equilibrium state (low friction), and a state of disordered interlocking rolls (high friction), under the control of parameter common to all of the actuators. Alternatively, interlocking patterns of parallel rolls would produce a high coefficient of friction normal to the rolls, and low friction in the direction parallel to the rolls. In the friction example, the pattern regime would be the regime of interest. Alternatively, if one wanted an analog memory, so that a sensor input would excite a spike at a particular point that could persist until a single control input to all the actuators were changed to eliminate all the spikes, that would be an application where the spike regime would be of interest.

For $\beta << 1$ and $\alpha > 1$, the stable solutions for the cubic nonlinearity model are equilibria. When $\alpha << 1$, time-periodic patterns and traveling spikes are also possible. However, the pattern-selection problem (or the problem of selecting stationary versus traveling spikes and prescribing the direction the traveling spikes travel) is quite difficult. There are, however, alternative approaches to taking $\alpha << 1$ in the cubic nonlinearity model in order to obtain interesting time-varying patterns of activity in an array of actuators, namely

- the active transmission-line model,

- the complex activator-inhibitor equation (which, under appropriate hypotheses, models a type of coupled oscillator network), or
- the cubic nonlinearity model with an additional advective term.

One type of active transmission line acts like a linear transmission line for the particular pulse shapes that it supports, and pulses applied to the active transmission line decay to one of those pulse shapes (or else decay to a stable spatially uniform equilibrium). If two pulses traveling in opposite directions encounter each other, they both are attenuated as they pass through each other, but then each one grows back toward a pulse shape supported by the active transmission line. Furthermore, certain pulse shapes supported by the active transmission line are readily characterized.

The complex activator-inhibitor equation represents the phase envelope of the coupled oscillator network it models, so equilibria of the complex activator-inhibitor equation can actually represent rotating waves in the underlying coupled oscillator network. Therefore, traveling waves can be achieved in the physical system, while the control and modeling still involves equilibria.

An additional advective term in the basic cubic nonlinearity model dynamics can be used to move around individual spikes or whole patterns. One possibility would be to have a digital memory at each actuator site that could store a velocity vector. The velocity vectors could be updated slowly, so that they would act as quasistatic parameters governing the (much faster) motion of spikes. In this way, a rapidly changing (but somewhat stereotypical) pattern of activity could be achieved in an array of actuators with only low-bandwidth access to the individual actuator memories. This is in contrast to the approach used in the Texas Instruments digital micromirror chip for

high-definition television applications, a state-of-the-art example of a micro-actuator array [22, 23].

In the Texas Instruments micromirror chip, each mirror in a 1000 by 1000 array is not only individually updated for each high-definition television frame, but is also pulse-width-modulated at an even faster rate to provide the gray-scale (and an additional three times faster to provide all three colors using the same mirrors). It is not difficult to calculate that

$$10^6 \text{ mirrors} \times 24 \text{ frames/second} \times 3 \text{ colors} \times 8 \text{ bits of grayscale resolution}$$
$$= \quad 576 \text{ megabits/second},$$

which can be accomodated with a dozen 50MHz input pins. This calculation shows how the number of actuators and mechanical bandwidth required for each actuator translate into a system bandwidth requirement. The entire 1000 by 1000 array of micromirrors fits into a square inch, so requiring a computer to provide 576 megabits per second for each square inch of active area would be the primary limitation to the Texas Instruments micromirror chip control approach if the active area were to be many square inches. (Of course, the HDTV application requires that each actuator be independently controlled, so in that case, there is no choice but to provide enough high-bandwidth input signals to do the job.)

It should be emphasized that although there has been a huge amount of work (theoretical and experimental) on pattern-forming systems, there has been little done by way of applying those ideas in an engineering context. As the Texas Instruments micromirror chip example shows, the number of actuators needs to be rather large before alternatives to the direct computer-controlled approach are worth considering. But now, with the coming-of-age of MEMS technology, it is possible to start envisioning engineering systems

with so many actuators and sensors that alternatives to the direct computer-controlled approach are worth considering.

1.2 Overview

First, some of the standard analysis techniques for pattern-forming systems are reviewed, including envelope equations and analysis of equilibria. Second, engineering realizations of the cubic nonlinearity model, and the related active transmission line and complex activator-inhibitor systems are discussed. Third, basic existence and uniqueness results are proved for solutions of these systems of PDEs, and some dissipativity results are also proved. Fourth, a Lyapunov functional for the cubic nonlinearity model is derived, and then generalized to several related systems, including the complex activator-inhibitor equation and a version of the active transmission line. Fifth, some smart-system applications are discussed, and finally, conclusions and future research directions are indicated.

Chapter 2

Standard Approaches for Analyzing Pattern-Forming Systems

2.1 Introduction

Pattern-forming systems that arise in nature are, of course, governed by the fundamental equations underlying the media in which the patterns appear. These fundamental governing equations, which are also sometimes called "microscopic equations," tend to be complicated to analyze. (The same equations referred to as microscopic equations in the pattern-forming-system context may also be considered macroscopic equations in a continuum-mechanics context, but we adopt the pattern-forming system terminology.) For example, the Navier-Stokes equations for fluid systems, reaction-diffusion equations for chemical systems, and equations of mechanics for shaken-particle systems, are all examples of microscopic equations. Even when the microscopic equations for a process giving rise to patterns can be confidently written down, directly analyzing the pattern-forming properties of the microscopic equations is generally difficult or impossible. Particularly in fluid systems, much analysis of patterns has been carried out even though it is quite difficult [1, 24, 25, 26]. But often in physical systems, the microscopic equations are not even known with certainty, and the goal of the pattern analysis may be to discern properties of systems from the patterns, rather than the other way around.

There are two main standard approaches for dealing with the difficulties encountered in analyzing pattern-forming systems. The first approach is to distill from microscopic equations the essential part which gives rise to the

pattern-forming properties. The second approach is to derive envelope equations, which are intimately connected to the patterns, but also have some parameters depending on the microscopic equations (or on the underlying system) [1, 27]. The two approaches are interrelated, because microscopic equations can be informally classified by the envelope equations they give rise to.

While envelope equations are useful for understanding pattern-forming systems, from an engineering standpoint, we generally want stronger results than envelope equations alone can provide. But demanding stronger results necessitates narrowing the microscopic equations we consider. We therefore focus on "model equations," the simplest microscopic equations that give rise to the pattern-forming properties of interest. While the model equations are not the fundamental governing equations of any systems arising in nature, we hope that they capture the pattern properties of many physical systems.

After discussing envelope equations, we review the standard linear analysis of general activator-inhibitor equations and describe the type of activator-inhibitor equation for which the cubic nonlinearity model is a suitable model equation. The standard approach to analyzing spike solutions is also briefly discussed.

2.2 Amplitude equations

In narrowband wireless communications, a sinusoidal carrier signal is modulated by the voice or data signal to be transmitted. The resulting transmitted signal has high-frequency sinusoidal variation due to the carrier, but it is the slowly-varying envelope that contains the information of interest. For amplitude modulation, the amplitude envelope contains the transmitted information, and for frequency modulation or phase modulation, the phase envelope

contains the transmitted information. The same concepts can be applied to pattern-forming systems. The ideal pattern (analogous to the sinusoidal communications carrier signal) may have time periodicity, spatial periodicity, or both. Envelope equations (either amplitude equations or phase equations) capture the slow variations in the pattern, which may be slow time variations, long-length-scale spatial variations, or both. The envelope equations for a particular pattern-forming system can be derived from the microscopic equations and from knowledge of whether the ideal patterns are time-periodic, spatially periodic, or both. However, different microscopic equations with similar ideal patterns can give rise to similar envelope equations, so envelope equations can be associated with patterns rather than with specific microscopic equations (provided the microscopic equations satisfy certain assumptions). The properties of the specific microscopic equations are then captured in parameters that appear in the envelope equations.

Envelope equations are used to study how patterns evolve analytically when the microscopic equations are too difficult to analyze directly (e.g., where secondary instability boundaries lie). Envelope equations are also used for numerical investigations of pattern-forming system behavior, to study pattern behavior that is difficult to extract analytically even from the envelope equations. However, envelope equations have a limited domain of validity (generally the pattern-forming system has to be close to the bifurcation threshold), and therefore, there is a limit to how much information envelope equations can provide. Nevertheless, envelope equations do help us categorize pattern-forming systems, illustrate the important feature of "phase diffusion" (discussed in section 2.3), and provide insight into how patterns are established in pattern-forming systems as the bifurcation parameter passes through threshold (during which time it is briefly in the near-threshold regime of validity of the envelope

equations).

Amplitude equations are the simplest type of envelope equations. Their form is determined by the type of pattern under consideration, and the only other features of the original microscopic equations retained in the amplitude equations are the values of several constants. Amplitude equations only apply near the bifurcation threshold, and they also only apply to spatially localized regions (although there is also an equivariant form of the amplitude equations which can be used over the entire domain [30]).

The first step in deriving amplitude equations is to define the normalized control parameter ϵ so that the bifurcation to the pattern solution occurs at $\epsilon = 0$. If C is the control parameter in the microscopic equations, and C_0 is the critical value at which the bifurcation occurs, then we can take $\epsilon = (C - C_0)/C_0$.

The second step is to assume a form for the growth rate of linear disturbances for ϵ near zero. We will make the standard assumption that the linear disturbance growth rate is quadratic in wave number. The two most commonly assumed forms of linear growth rate versus wave number and ϵ are illustrated in figure 2.1. We define K-systems as systems having a steady, supercritical pitchfork bifurcation at threshold, and we define Ω-systems as having a Hopf bifurcation at threshold [24, 28]. For K-systems, then, the instability occurs first for a nonzero wave number k_0, and for Ω-systems, the instability occurs first for a spatially uniform perturbation with temporal frequency ω_0. In figure 2.1, $\mathrm{Re}\{\sigma\}$ represents the exponential growth rate of a spatially sinusoidal perturbation.

For K-systems, a real eigenvalue of the linearization passes from the left half-plane to the right half-plane at threshold. For Ω-systems, a pair of

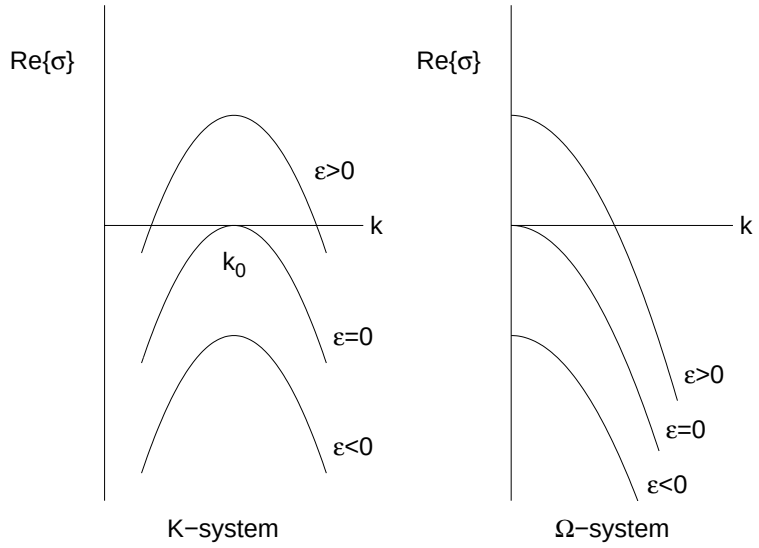

Figure 2.1: Growth rate of a linear disturbance as a function of wave number and ϵ

complex-conjugate eigenvalues of the linearization pass from the left half-plane to the right half-plane at threshold. If a system has the property that both a real eigenvalue and a pair of complex-conjugate eigenvalues of the linearization pass from the left half-plane to the right half-plane at threshold, we call such a system a $K\Omega$-system, since such a system would have both a nonzero wave number k_0 and a nonzero temporal frequency ω_0 at threshold. However, we do not define $K\Omega$-systems this way, because if a real eigenvalue and pair of complex-conjugate eigenvalues of the linearization cross the imaginary axis at approximately (but not exactly) the same value of the control parameter, we still consider the system to be a $K\Omega$-system [8, 9, 29]. Therefore, we defer the definition of $K\Omega$-systems until section 2.4. Since envelope equation analysis requires the system to be close to threshold, in the envelope equation context, the real eigenvalue and pair of complex-conjugate eigenvalues of a $K\Omega$-system would be thought of as crossing into the right half-plane for essentially the same value of control parameter. Therefore, $K\Omega$-systems have a linear instability growth rate plot identical to that for K-systems: figure 2.1 only depicts the

spatial instability.

2.2.1 Amplitude equation for *K*-systems

Since K-systems have spatially periodic equilibrium patterns, for deriving the amplitude equation we assume that at threshold (i.e., for $\epsilon = 0$), the unstable perturbation has the form

$$u(\mathbf{x}, t) = U_0 \mathrm{e}^{i\mathbf{k}_0 \cdot \mathbf{x} + \sigma t}, \tag{2.1}$$

where $\mathbf{k}_0$ is the wave vector of the pattern at threshold, and σ is purely real. Next, we suppose that our unstable perturbation saturates in amplitude (instead of growing exponentially forever), but the amplitude is a (slowly varying) function of time and position:

$$u(\mathbf{x}, t) = [U_0 A(x, y, t) \mathrm{e}^{ik_0 x} + \text{c.c.}] + O(\epsilon), \tag{2.2}$$

where "c.c." denotes the complex conjugate, and we also restrict our attention to the case of two space dimensions with $\mathbf{k}_0$ aligned along the x-direction. (The scalar $k = |\mathbf{k}|$ is the wave number associated with wave vector $\mathbf{k}$.)

It is possible to derive the amplitude equation directly from the PDE for $u(\mathbf{x}, t)$, but the form of the amplitude equation can actually be deduced more simply [1, 27]. From figure 2.1, the linear disturbance growth rate as a function of wave number has the form

$$\sigma(k) = \tau_0^{-1}[\epsilon - \xi_0^2 (k - k_0)^2], \tag{2.3}$$

where τ_0 and ξ_0 can be thought of as scaling factors for time and space, respectively. Writing $\mathbf{k} = k_0 \hat{\mathbf{x}} + \boldsymbol{\kappa}$, where $\hat{\mathbf{x}}$ is the unit vector in the x-direction, we can expand $|k_0 \hat{\mathbf{x}} + \boldsymbol{\kappa}| - k_0$ for small $|\boldsymbol{\kappa}|$ as follows:

$$|k_0 \hat{\mathbf{x}} + \boldsymbol{\kappa}| - k_0 \quad = \quad \sqrt{(k_0 + \kappa_x)^2 + \kappa_y^2} - k_0$$

$$
\begin{aligned}
&= \left(k_0 + \kappa_x + \frac{1}{2}\frac{1}{k_0+\kappa_x}\kappa_y^2 + \cdots\right) - k_0 \\
&\approx \kappa_x + \frac{\kappa_y^2}{2k_0}, \qquad (2.4)
\end{aligned}
$$

so that

$$\sigma(k) \approx \tau_0^{-1}\left[\epsilon - \xi_0^2\left(\kappa_x + \frac{\kappa_y^2}{2k_0}\right)^2\right]. \qquad (2.5)$$

Performing the standard substitutions $\sigma \to \partial_t$, $\kappa_x \to -i\partial_x$, and $\kappa_y \to -i\partial_y$, and adding the cubic saturation term $-g_0|A|^2A$, yields the amplitude equation

$$\tau_0\partial_t A = \epsilon A + \xi_0^2\left[\partial_x - \left(\frac{i}{2k_0}\right)\partial_{yy}\right]^2 A - g_0|A|^2A, \qquad (2.6)$$

where τ_0, ξ_0, and g_0 set the scales of variation in time, space, and amplitude. The cubic saturation term is the lowest-order nonlinearity that can saturate the linear amplitude growth while also preserving the invariance of the amplitude equation with respect to global phase shifts $A \to Ae^{i\phi}$.

The amplitude equation describes the variations in the pattern on the slow time scale ϵt and on the long spatial scales $\epsilon^{1/2}x$ and $\epsilon^{1/4}y$. The amplitude equation can be rescaled and put in the form

$$\partial_T\tilde{A} = \tilde{A} + (\partial_X - (1/2)i\partial_{YY})^2\tilde{A} - |\tilde{A}|^2\tilde{A}, \qquad (2.7)$$

when $\epsilon > 0$.

The amplitude equation (2.6) possesses the Lyapunov functional

$$V = \int\int\left[-\epsilon|A|^2 + \left(\frac{g_0}{2}\right)|A|^4 + \left|\xi_0\left(\partial_x - \left(\frac{i}{2k_0}\right)\partial_{yy}\right)A\right|^2\right]dxdy, \qquad (2.8)$$

so that

$$\partial_t V = \frac{\delta V}{\delta\bar{A}}\cdot(\partial_t A) = -2\tau_0\int\int|\partial_t A|^2 dxdy. \qquad (2.9)$$

This Lyapunov functional is radially unbounded, and the dynamics are gradient dynamics, so the behavior of the amplitude equation is relaxation toward equilibria.

The attractive features of the amplitude equation (2.6) are that it takes the same relatively simple form for all microscopic equations that give rise (only) to spatially periodic equilibrium patterns beyond the bifurcation threshold in two spatial dimensions (and that satisfy the assumption about the linear disturbance growth rate as a function of wave number). Because of the Lyapunov functional and gradient dynamics for this amplitude equation, we know that the system relaxes toward equilibria. Furthermore, we are able to eliminate all of the constants from the equation simply by rescaling the variables appropriately.

The most serious limitation of the amplitude equation (2.6) is that it is not equivariant with respect to rotations. Suppose the microscopic equations are invariant under rotations. Then two patterns that are related to each other through a rotation evolve identically. However, the amplitude equation (2.6) produces completely different solutions for initial patterns that are the same except for a rotation. Equivariant amplitude equations were derived by Gunaratne et. al. [30]. The equivariant amplitude equation approach also leads to an equivariant measure of the disorder in a pattern [31].

Another limitation of amplitude equations is that they are only valid for ϵ close to zero; i.e., when the system is near threshold. Phase equations can give better information when the system is further from threshold, but at the cost of a much more complicated derivation.

2.2.2 Amplitude equation for Ω-systems

Since Ω-systems have spatially uniform but time-periodic patterns, we assume that near threshold the solution in two space dimensions has the form

$$U(\mathbf{x},t) = [U_0 A(x,y,t)\mathrm{e}^{-i\omega_\epsilon t} + \text{c.c.}] + O(\epsilon), \tag{2.10}$$

where $A(x, y, t)$ is the complex amplitude. For $\epsilon = 0$, the oscillation frequency is $\omega_0 \neq 0$, and for $\epsilon > 0$, the oscillation frequency ω_ϵ is given by

$$\omega_\epsilon = \omega_0 - c_0\epsilon, \tag{2.11}$$

an affine relationship between reduced control parameter and frequency.

The amplitude equation is

$$\partial_t A = \epsilon A + (1 + ic_1)\Delta A - (1 - ic_3)|A|^2 A, \tag{2.12}$$

and its form is justified as follows [1]. First, there is a linear growth term ϵA, just as in the K-system case. Second, there is a diffusive term ΔA, which leads to a spatially uniform steady-state solution. Third, there is a nonlinearity to saturate the amplitude, $|A|^2 A$. The main difference from the K-system amplitude equation is that the coefficients of the ΔA and $|A|^2 A$ terms are now complex instead of real, and these complex coefficients admit the possibility of traveling-wave solutions.

Before considering traveling-wave solutions, consider a spatially uniform solution:

$$A(\mathbf{x}, t) = a_0 \mathrm{e}^{-i\Omega_0 t}. \tag{2.13}$$

Plugging this solution into the amplitude equation (2.12), we find

$$\begin{aligned} -i\Omega_0 a_0 \mathrm{e}^{-i\Omega_0 t} &= \epsilon a_0 \mathrm{e}^{-i\Omega_0 t} - (1 - ic_3) a_0^3 \mathrm{e}^{-i\Omega_0 t} \\ -i\Omega_0 &= \epsilon - (1 - ic_3) a_0^2, \end{aligned} \tag{2.14}$$

so that $a_0^2 = \epsilon$ and $\Omega_0 = -c_3\epsilon$.

Now consider a traveling wave solution:

$$A_\kappa(\mathbf{x}, t) = a_\kappa \mathrm{e}^{i(\kappa \cdot \mathbf{x} - \Omega_\kappa t)}. \tag{2.15}$$

Plugging this solution into the amplitude equation (2.12), we find

$$-i\Omega_\kappa = \epsilon - (1 + ic_1)\kappa^2 - (1 - ic_3)a_\kappa^2, \tag{2.16}$$

so that $a_\kappa^2 = \epsilon - \kappa^2$ and

$$\begin{aligned} \Omega_\kappa &= c_1\kappa^2 - c_3 a_\kappa^2 = c_1\kappa^2 - c_3(\epsilon - \kappa^2) \\ &= -c_3\epsilon + (c_1 + c_3)\kappa^2. \end{aligned} \tag{2.17}$$

These solutions are also known as rotating waves.

We are not considering Ω-systems as top candidates for control of large actuator arrays. However, it is important to understand the distinction between K-systems and $K\Omega$-systems, and the amplitude equation for Ω-systems is the first step in understanding the amplitude equation for $K\Omega$-systems.

2.2.3 Amplitude equation for $K\Omega$-systems

Recall that for K-systems there was a wave number $k_0 \neq 0$ at threshold, and for Ω-systems there was an oscillation frequency $\omega_0 \neq 0$ at threshold. For $K\Omega$-systems there are both a nonzero wave number k_0 and a nonzero oscillation frequency ω_0, and the solution in two spatial dimensions is described by

$$U(\mathbf{x}, t) = U_0[A_R(x, y, t)\mathrm{e}^{i(k_0 x - \omega_\epsilon t)} + A_L(x, y, t)\mathrm{e}^{-i(k_0 x + \omega_\epsilon t)} + \text{c.c.}] + O(\epsilon), \tag{2.18}$$

where $A_R(x, y, t)$ and $A_L(x, y, t)$ are the complex right-traveling and left-traveling waves for which we are deriving the amplitude equation.

The amplitude equation for $K\Omega$-systems can be deduced in a fashion similar to the derivation for K-systems. We start with the equation for the exponential growth term of the instability, equation (2.3), and set $\mathbf{k} = k_0\hat{\mathbf{x}} + \boldsymbol{\kappa}$. However, for $K\Omega$-systems, the exponential instability term also has an

imaginary part, $\sigma(k) \pm i\omega(k)$, with the dispersion relation $\omega(k)$ given by

$$\omega(k) = \omega_\epsilon + (k - k_0)s_0, \tag{2.19}$$

where s_0 is the "linear group speed," $\partial\omega/\partial k|_{k=k_0}$. The expansion of $(k-k_0)$ in terms of κ_x and κ_y is slightly more involved than in the K-system case, because $(k - k_0)$ appears linearly in the expression for $\omega(k)$ as well as quadratically in the expression for $\sigma(k)$:

$$\begin{aligned}
k - k_0 &= \sqrt{(k_0 + \kappa_x)^2 + \kappa_y^2} - k_0 \\
&= \left([(k_0 + \kappa_x)^2]^{1/2} + \frac{1}{2}[(k_0 + \kappa_x)^2]^{-1/2}\kappa_y^2 - \frac{1}{2!}\frac{1}{2}\frac{1}{2}[(k_0 + \kappa_x)^2]^{-3/2}\kappa_y^4 \right. \\
&\quad \left. + \cdots \right) - k_0 \\
&= \kappa_x + \frac{1}{2(k_0 + \kappa_x)}\kappa_y^2 - \frac{1}{8(k_0 + \kappa_x)^3}\kappa_y^4 + \cdots \\
&\approx \kappa_x + \frac{1}{2k_0}\left(1 - \frac{\kappa_x}{k_0}\right)\kappa_y^2 - \frac{1}{8k_0^3}\kappa_y^4 \\
&= \kappa_x + \frac{1}{2k_0}\kappa_y^2 - \frac{1}{2k_0^2}\kappa_x\kappa_y^2 - \frac{1}{8k_0^3}\kappa_y^4,
\end{aligned} \tag{2.20}$$

where we have retained the lowest-order term in κ_x, the two lowest-order terms in κ_y, and the lowest-order cross term involving κ_x and κ_y. As in the K-system case, for $(k - k_0)^2$ in the $\sigma(k)$ term, we can use

$$(k - k_0)^2 \approx \left(\kappa_x + \frac{1}{2k_0}\kappa_y^2\right)^2. \tag{2.21}$$

Then using $\omega \to i\partial_t$, $\kappa_x \to -i\partial_x$, and $\kappa_y \to -i\partial_y$ to determine the linear PDE resulting in the exponential growth represented by $\sigma(k) \pm i\omega(k)$, we obtain

$$k - k_0 \;\to\; -i\left(\partial_x - \frac{i}{2k_0}\partial_{yy} + \frac{1}{2k_0^2}\partial_x\partial_{yy} - \frac{i}{8k_0^3}\partial_y^4\right), \tag{2.22}$$

$$(k - k_0)^2 \;\to\; -\left(\partial_x - \frac{i}{2k_0}\partial_{yy}\right)^2. \tag{2.23}$$

We could now use these expressions to write down the linear part of the amplitude equation, but to keep the amplitude equation from becoming too cluttered, for now consider the one-dimensional case so that

$$\begin{aligned} k - k_0 &\rightarrow -i\partial_x, \\ (k-k_0)^2 &\rightarrow -\partial_{xx}. \end{aligned} \tag{2.24}$$

Then $\sigma(k)$, the exponential growth term of the instability, contributes the terms

$$\begin{aligned} \partial_t A_R &= \epsilon A_R + \partial_{xx} A_R, \\ \partial_t A_L &= \epsilon A_L + \partial_{xx} A_L \end{aligned} \tag{2.25}$$

to the amplitude equation. Since $\sigma(k) - i\omega(k)$ is associated with A_R, and $\sigma(k) + i\omega(k)$ is associated with A_L, $\omega(k)$ contributes the terms

$$\begin{aligned} \partial_t A_R &= -s_0 \partial_x A_R, \\ \partial_t A_L &= s_0 \partial_x A_L \end{aligned} \tag{2.26}$$

to the amplitude equation (where we have eliminated the constants τ_0 and ξ_0 by rescaling). The linear terms of the one-dimensional amplitude equation are then

$$\begin{aligned} \partial_t A_R + s_0 \partial_x A_R &= \epsilon A_R + \partial_{xx} A_R, \\ \partial_t A_L - s_0 \partial_x A_L &= \epsilon A_L + \partial_{xx} A_L. \end{aligned} \tag{2.27}$$

As in the K-system case, cubic terms are added to saturate the nonlinearity, and as in the Ω-system case, complex coefficients are introduced, yielding

$$\begin{aligned} \partial_t A_R + s_0 \partial_x A_R &= \epsilon A_R + (1 + ic_1)\partial_{xx} A_R - (1 - ic_3)|A_R|^2 A_R, \\ \partial_t A_L - s_0 \partial_x A_L &= \epsilon A_L + (1 + ic_1)\partial_{xx} A_L - (1 - ic_3)|A_L|^2 A_L. \end{aligned} \tag{2.28}$$

So far we have not introduced any interaction between the left- and right-traveling waves. The form of the coupling between A_R and A_L should satisfy the following conditions:

(1). For small A_R and A_L, the coupling should be insignificant compared to the linear terms in the amplitude equation.

(2). The coupling should only affect the magnitude, and not the phase, of A_R and A_L.

(3). The coupling should determine whether traveling waves or standing waves are the stable solutions.

The simplest coupling between A_R and A_L that meets these criteria leads to the following final form for the one-dimensional amplitude equation for $K\Omega$-systems [1]:

$$\begin{aligned}
\partial_t A_R + s_0 \partial_x A_R &= \epsilon A_R + (1+ic_1)\partial_{xx} A_R - (1-ic_3)|A_R|^2 A_R \\
&\quad -g_1(1-ic_2)|A_L|^2 A_R, \\
\partial_t A_L - s_0 \partial_x A_L &= \epsilon A_L + (1+ic_1)\partial_{xx} A_L - (1-ic_3)|A_L|^2 A_L \\
&\quad -g_1(1-ic_2)|A_R|^2 A_L.
\end{aligned} \tag{2.29}$$

The amplitude equation in two space dimensions takes the form [1]:

$$\begin{aligned}
&\partial_t A_R + s_0[\partial_x - (i/2k_0)\partial_{yy} + (1/2k_0^2)\partial_x\partial_{yy} - (i/8k_0^3)\partial_y^4]A_R \\
&\quad = \epsilon A_R + (1+ic_1)[\partial_x - (i/2k_0)\partial_{yy}]^2 A_R - (1-ic_3)|A_R|^2 A_R \\
&\qquad -g_1(1-ic_2)|A_L|^2 A_R, \\
&\partial_t A_L - s_0[\partial_x - (i/2k_0)\partial_{yy} + (1/2k_0^2)\partial_x\partial_{yy} - (i/8k_0^3)\partial_y^4]A_L \\
&\quad = \epsilon A_L + (1+ic_1)[\partial_x - (i/2k_0)\partial_{yy}]^2 A_L - (1-ic_3)|A_L|^2 A_L \\
&\qquad -g_1(1-ic_2)|A_R|^2 A_L.
\end{aligned} \tag{2.30}$$

Unlike the K-system case, the amplitude equation for the $K\Omega$-system cannot be rescaled to remove the epsilon because it is not clear how to choose appropriate time, length, and amplitude scales to balance the various terms. This also means that solutions to the amplitude equation may not be slowly varying in space and time, as required for the amplitude equation approach to be valid [1].

Amplitude-equation-type ideas are also used in more complicated pattern analysis contexts, for example in the study of "blinking" states that arise from the combination of odd and even parity standing waves, and in the study of coupling between instability modes belonging to different instability "balloons" [32, 33].

2.3 Phase equations

Just as amplitude equations could only describe the pattern dynamics accurately over long time and long distance scales, the same limitation also applies to phase equations. In both cases, the long distance scales signify large numbers of basic (spatial) periods of the pattern over which the solution is permitted to change significantly, in keeping with the envelope equation concept. The phase equation has the advantages of capturing certain features which the amplitude equation does not and of being valid well beyond threshold, but at the price of a much more complicated derivation.

In contrast to the amplitude equation, which could be written down just from the properties of the instability without regard to the microscopic equations, the derivation of the phase equation requires microscopic equations (or model equations having similar pattern-forming properties) as a starting point.

Because phase equation derivations are lengthy, we will only examine the K-system case.

2.3.1 Linearized phase equation derivation from the amplitude equation

Although we cannot hope to derive the phase equation itself from the am-

plitude equation (because the phase equation contains more information than the amplitude equation), it is possible to derive from the amplitude equation the linearized phase equation for small perturbations. (The linearized phase equation can be considered the phase equation near threshold.) It is much easier to derive the linearized phase equation from the amplitude equation than it is to derive the full phase equation and then linearize it, and furthermore, the linearized phase equation possesses "phase diffusion," one of the main qualitative features of the phase equation.

Consider the K-system amplitude equation, rescaled slightly,

$$\partial_t A = \epsilon A + \left(\partial_x - \frac{i}{2k_0}\partial_{yy}\right)^2 A - |A|^2 A. \tag{2.31}$$

Suppose $a_\kappa e^{i\kappa x}$ is a solution (implying $a_\kappa^2 = \epsilon - \kappa^2$), and consider the perturbed solution

$$A = (a_\kappa + \delta a)e^{i(\kappa x + \delta\phi)}. \tag{2.32}$$

Computing the various terms in the amplitude equation, neglecting derivatives of δa that are higher than first-order, neglecting products of the derivatives of δa and $\delta\phi$, and neglecting higher-order powers of δa, we obtain

$$\begin{aligned}
\partial_t A &= (\partial_t \delta a)e^{i(\kappa x+\delta\phi)} + i(\partial_t\delta\phi)(a_\kappa+\delta a)e^{i(\kappa x+\delta\phi)} \\
\partial_x A &= (\partial_x \delta a)e^{i(\kappa x+\delta\phi)} + i\kappa(a_\kappa+\delta a)e^{i(\kappa x+\delta\phi)} \\
&\quad + i(\partial_x\delta\phi)(a_\kappa+\delta a)e^{i(\kappa x+\delta\phi)}, \\
\partial_{xx} A &\approx 2i\kappa(\partial_x\delta a)e^{i(\kappa x+\delta\phi)} - \kappa^2(a_\kappa+\delta a)e^{i(\kappa x+\delta\phi)} \\
&\quad - 2\kappa(\partial_x\delta\phi)(a_\kappa+\delta a)e^{i(\kappa x+\delta\phi)} + i(\partial_{xx}\delta\phi)(a_\kappa+\delta a)e^{i(\kappa x+\delta\phi)}, \\
\partial_{yy} A &\approx i(\partial_{yy}\delta\phi)(a_\kappa+\delta a)e^{i(\kappa x+\delta\phi)}, \\
\partial_x\partial_{yy} A &\approx i(\partial_x\partial_{yy}\delta\phi)(a_\kappa+\delta a)e^{i(\kappa x+\delta\phi)} - \kappa(\partial_{yy}\delta\phi)(a_\kappa+\delta a)e^{i(\kappa x+\delta\phi)}, \\
-\frac{i}{k_0}\partial_x\partial_{yy} A &\approx \frac{1}{k_0}(\partial_x\partial_{yy}\delta\phi)(a_\kappa+\delta a)e^{i(\kappa x+\delta\phi)} + i\frac{\kappa}{k_0}(\partial_{yy}\delta\phi)(a_\kappa+\delta a)e^{i(\kappa x+\delta\phi)},
\end{aligned}$$

$$
\begin{aligned}
-\frac{1}{4k_0^2}\partial_y^4 A &\approx -\frac{i}{4k_0^2}(\partial_y^4\delta\phi)(a_\kappa+\delta a)\mathrm{e}^{i(\kappa x+\delta\phi)}, \\
|A|^2 A &\approx (a_\kappa^3+3a_\kappa^2\delta a)\mathrm{e}^{i(\kappa x+\delta\phi)}.
\end{aligned} \tag{2.33}
$$

The amplitude equation then implies (for small δa, $\delta\phi$, and small derivatives of δa and $\delta\phi$),

$$
\begin{aligned}
&\partial_t\delta a + i(\partial_t\delta\phi)(a_\kappa+\delta a) \\
&\quad= \epsilon(a_\kappa+\delta a) + i2\kappa\partial_x\delta a - \kappa^2(a_\kappa+\delta a) - 2\kappa(\partial_x\delta\phi)(a_\kappa+\delta a) \\
&\qquad +i(\partial_{xx}\delta\phi)(a_\kappa+\delta a) + \frac{1}{k_0}(\partial_x\partial_{yy}\delta\phi)(a_\kappa+\delta a) \\
&\qquad +i\frac{\kappa}{k_0}(\partial_{yy}\delta\phi)(a_\kappa+\delta a) - \frac{i}{4k_0^2}(\partial_y^4\delta\phi)(a_\kappa+\delta a) - (a_\kappa^3+3a_\kappa^2\delta a) \\
&\quad= -2a_\kappa^2\delta a + i2\kappa\partial_x\delta a - 2\kappa(\partial_x\delta\phi)(a_\kappa+\delta a) + i(\partial_{xx}\delta\phi)(a_\kappa+\delta a) \\
&\qquad +\frac{1}{k_0}(\partial_x\partial_{yy}\delta\phi)(a_\kappa+\delta a) + i\frac{\kappa}{k_0}(\partial_{yy}\delta\phi)(a_\kappa+\delta a) - \frac{i}{4k_0^2}(\partial_y^4\delta\phi)(a_\kappa+\delta a),
\end{aligned} \tag{2.34}
$$

where we have used the fact that $a_\kappa^2 = \epsilon - \kappa^2$, since $a_\kappa \mathrm{e}^{i\kappa x}$ satisfies the amplitude equation. Breaking this equation into real and imaginary parts, we find that the real part yields

$$
\partial_t\delta a = -2a_\kappa^2\delta a - 2\kappa(\partial_x\delta\phi)(a_\kappa+\delta a) + \frac{1}{k_0}(\partial_x\partial_{yy}\delta\phi)(a_\kappa+\delta a). \tag{2.35}
$$

The essential simplification involved in this approach to the phase equation is to use the fact that magnitude perturbations relax much more quickly than phase perturbations. We consider the changes in magnitude to occur instantaneously in response to the much slower phase changes and thereby suppress the magnitude dynamics. This approach is physically meaningful after any initial (possibly large) magnitude transient has relaxed. So neglecting the derivatives (including the time derivative) of δa, neglecting the higher-order derivatives of $\delta\phi$, and neglecting other higher-order terms leads to

$$
a_\kappa\delta a = -\kappa\partial_x\delta\phi. \tag{2.36}
$$

Similarly, neglecting the higher-order derivatives of δa and $\delta\phi$ and other higher-order terms in the imaginary part of equation (2.34) yields

$$\begin{aligned}\partial_t\delta\phi(a_\kappa+\delta a) &= 2\kappa\partial_x\delta a+(\partial_{xx}\delta\phi)(a_\kappa+\delta a)+\frac{\kappa}{k_0}(\partial_{yy}\delta\phi)(a_\kappa+\delta a),\\ \partial_t\delta\phi &= \frac{2\kappa}{a_\kappa}\partial_x\delta a+\partial_{xx}\delta\phi+\frac{\kappa}{k_0^2}\partial_{yy}\delta\phi. \end{aligned}\tag{2.37}$$

Plugging into this expression the expression derived for δa then gives

$$\begin{aligned}\partial_t\delta\phi &= \frac{2\kappa}{a_\kappa}\partial_x\left(-\frac{\kappa\partial_x\delta\phi}{a_\kappa}\right)+\partial_{xx}\delta\phi+\frac{\kappa}{k_0}\partial_{yy}\delta\phi\\ &= -\frac{2\kappa^2}{\epsilon-\kappa^2}\partial_{xx}\delta\phi+\partial_{xx}\delta\phi+\frac{\kappa}{k_0}\partial_{yy}\delta\phi\\ &= \left(1-\frac{2\kappa^2}{\epsilon-\kappa^2}\right)\partial_{xx}\delta\phi+\frac{\kappa}{k_0}\partial_{yy}\delta\phi\\ &= \left(\frac{\epsilon-3\kappa^2}{\epsilon-\kappa^2}\right)\partial_{xx}\delta\phi+\frac{\kappa}{k_0}\partial_{yy}\delta\phi. \end{aligned}\tag{2.38}$$

Thus, the linearized phase equation can be put in the form

$$\partial_t\delta\phi=D_\parallel\partial_{xx}\delta\phi+D_\perp\partial_{yy}\delta\phi,\tag{2.39}$$

where $D_\parallel$ and $D_\perp$ are the diffusion coefficients (for phase perturbations parallel to and perpendicular to $\mathbf{k}_0$, respectively). This is the same form that results from finding the full phase equation and then linearizing it in an appropriate way.

2.3.2 Derivation of the phase equation using the reaction-diffusion equation

We derive the phase equation for the reaction-diffusion equation

$$\partial_t\mathbf{u}=\mathbf{D}\Delta\mathbf{u}+\mathbf{f}(\mathbf{u}),\tag{2.40}$$

where we assume that $\mathbf{D}$ is symmetric. In order to derive a phase equation, we need to assume a form for the ideal pattern, which we take to be parallel

rolls since we are considering K-systems in two space dimensions. An ideal solution has the general form

$$\mathbf{u}(\mathbf{x}, t; \mathbf{k}) = \mathbf{u}_{\text{ideal}}(\mathbf{k} \cdot \mathbf{x}, k), \tag{2.41}$$

where the wave vector $\mathbf{k}$ parametrizes the ideal solutions.

The procedure for deriving the phase equation is basically to define a phase variable, rescale the time and space variables, and then perform a perturbation analysis. Define the local phase $\phi(\mathbf{x}, t)$ in terms of the local wave vector $\mathbf{k}(\mathbf{x}, t)$ by

$$\nabla\phi(\mathbf{x}, t) = \mathbf{k}(\mathbf{x}, t). \tag{2.42}$$

The perturbation expansion involves introducing the slow variables $\mathbf{X}$ and T, and using the diffusive scaling

$$\mathbf{X} = \epsilon\mathbf{x}, \quad T = \epsilon^2 t. \tag{2.43}$$

Our solution is expanded as

$$\mathbf{u}(\phi, \mathbf{X}, T) = \mathbf{u}^{(0)}(\phi, \mathbf{X}, T) + \epsilon\mathbf{u}^{(1)}(\phi, \mathbf{X}, T) + \cdots, \tag{2.44}$$

where $\mathbf{u}^{(0)}$ is the ideal pattern, and each of the $\mathbf{u}^{(i)}$ are periodic in ϕ with period 2π:

$$\mathbf{u}^{(i)}(\phi, \mathbf{X}, T) = \mathbf{u}^{(i)}(\phi + 2\pi, \mathbf{X}, T). \tag{2.45}$$

For the ideal pattern $\mathbf{u}^{(0)}$, the dependence on $(\mathbf{X}, T)$ is actually a dependence on $|\nabla_{\mathbf{x}}\phi|$.

We next define the scaled phase variable

$$\Phi(\mathbf{X}, T, \epsilon) = \epsilon\phi(\mathbf{x}, t), \tag{2.46}$$

so that

$$\hat{\mathbf{k}}(\mathbf{X}, T) = \mathbf{k}(\mathbf{x}, t) = \nabla_{\mathbf{x}}\phi(\mathbf{x}, t) = \nabla_{\mathbf{X}}\Phi(\mathbf{X}, T). \tag{2.47}$$

A lengthy calculation (see Appendix A) yields the phase equation

$$\begin{aligned} \partial_t \phi &= f_1(k)(\nabla \cdot \mathbf{k}) + f_2(k)(\mathbf{k} \cdot \nabla)k, \\ \mathbf{k} &= \nabla \phi. \end{aligned} \tag{2.48}$$

The functions f_1 and f_2 are calculated from $\mathbf{u}^{(0)}$, the ideal pattern. Linearizing the phase equation (see Appendix A) yields an equation of the same form as equation (2.39), the linearized phase equation derived from the amplitude equation.

The phase equation, equation (2.48), contains more information than the linearized version, equation (2.39). However, the linearized version does capture the important phenomenon of phase diffusion. As long as the diffusion coefficients are positive (and where they change sign represent instability boundaries for the ideal pattern of parallel rolls), the linearized phase equation shows that very close to threshold (as required to be in the domain of validity for the linearized phase equation), the rolls tend to regularize toward the ideal pattern, at least locally. However, further from threshold, the higher-order terms of the full phase equation have some influence.

Although the full phase equation captures the pattern behavior of the system away from threshold better than the amplitude equation does, the approach of controlling the pattern behavior using the phase equation would be difficult. The phase equation is a complicated nonlinear PDE when $\nabla\phi$ is substituted in for $\mathbf{k}$, and also depending on how the control entered the original system equations, the control might enter the phase equation in a complicated way.

2.4 Results for general activator-inhibitor equations

2.4.1 Linearized analyses of spatially uniform equilibria and bifurcations

The general form for activator-inhibitor dynamics is

$$\begin{aligned} \tau_\theta \partial_t \theta &= l^2 \Delta\theta - q(\theta, \eta, C), \\ \tau_\eta \partial_t \eta &= L^2 \Delta\eta - Q(\theta, \eta, C), \end{aligned} \tag{2.49}$$

where θ is the activator, η is the inhibitor; τ_θ, τ_η, l, and L are positive constants setting the time and length scales for the variation of the activator and inhibitor; C is the control (or bifurcation) parameter; and q and Q are continuously differentiable functions satisfying

$$\partial_\eta Q > 0, \quad \partial_\theta q < 0, \tag{2.50}$$

for some range of values for C. Spatially uniform equilibria (or homogeneous states) of the system, denoted by θ_h and η_h, are determined from

$$q(\theta_h, \eta_h, C) = 0, \quad Q(\theta_h, \eta_h, C) = 0. \tag{2.51}$$

A monostable system is one for which, with constant control parameter C, there is only one solution (θ_h, η_h) of the equilibrium equations. (It is also possible to have bistable systems for which there are three solutions to equation (2.51), two of which are stable, and one of which is unstable.) For monostable systems, $\theta_h(C)$ and $\eta_h(C)$, the spatially uniform equilibrium activator and inhibitor values as a function of control parameter, are single-valued. Applying the local implicit function theorem about the spatially uniform equilibrium (θ_h, η_h), we can solve

$$\begin{bmatrix} q(\theta_h, \eta_h, C) \\ Q(\theta_h, \eta_h, C) \end{bmatrix} = \begin{bmatrix} 0 \\ 0 \end{bmatrix} \tag{2.52}$$

for (θ_h, η_h) as a function of C if

$$\det \begin{bmatrix} \partial_\theta q & \partial_\eta q \\ \partial_\theta Q & \partial_\eta Q \end{bmatrix} = (\partial_\theta q)(\partial_\eta Q) - (\partial_\eta q)(\partial_\theta Q) \neq 0. \tag{2.53}$$

There are two possibilities for the inequality, but the correct one to assume is

$$(\partial_\theta q)(\partial_\eta Q) - (\partial_\eta q)(\partial_\theta Q) > 0. \tag{2.54}$$

The reason is that we generally want to think of $\partial_\eta Q > 0$ as being satisfied all the time, but $\partial_\theta q < 0$ as only being satisfied for certain values of the control parameter. In the situation where both $\partial_\eta Q > 0$ and $\partial_\theta q > 0$, if we consider the linearization of the activator-inhibitor equations and ignore the Laplacian terms, we obtain

$$\begin{aligned} \partial_t \begin{bmatrix} \tau_\theta \theta \\ \tau_\eta \eta \end{bmatrix} &= -\begin{bmatrix} \partial_\theta q & \partial_\eta q \\ \partial_\theta Q & \partial_\eta Q \end{bmatrix} \begin{bmatrix} \theta \\ \eta \end{bmatrix} \\ &= -\begin{bmatrix} \tau_\theta^{-1}\partial_\theta q & \tau_\eta^{-1}\partial_\eta q \\ \tau_\theta^{-1}\partial_\theta Q & \tau_\eta^{-1}\partial_\eta Q \end{bmatrix} \begin{bmatrix} \tau_\theta \theta \\ \tau_\eta \eta \end{bmatrix}. \end{aligned} \tag{2.55}$$

The matrix has characteristic equation

$$\begin{aligned} &(\lambda - \tau_\theta^{-1}\partial_\theta q)(\lambda - \tau_\eta^{-1}\partial_\eta Q) - \tau_\theta^{-1}\tau_\eta^{-1}(\partial_\eta q)(\partial_\theta Q) \\ &\quad = \lambda^2 - (\tau_\theta^{-1}\partial_\theta q + \tau_\eta^{-1}\partial_\eta Q)\lambda + \tau_\theta^{-1}\tau_\eta^{-1}[(\partial_\theta q)(\partial_\eta Q) - (\partial_\eta q)(\partial_\theta Q)] \\ &\quad = 0, \end{aligned} \tag{2.56}$$

which leads to

$$\begin{aligned} \lambda &= \frac{1}{2}(\tau_\theta^{-1}\partial_\theta q + \tau_\eta^{-1}\partial_\eta Q) \\ &\quad \pm \sqrt{\left(\frac{\tau_\theta^{-1}\partial_\theta q + \tau_\eta^{-1}\partial_\eta Q}{2}\right)^2 - \tau_\theta^{-1}\tau_\eta^{-1}[(\partial_\theta q)(\partial_\eta Q) - (\partial_\eta q)(\partial_\theta Q)]}. \end{aligned} \tag{2.57}$$

The condition for the real parts of both roots to be positive is then inequality (2.54), and this corresponds to stability for the linearized system we were examining. Hence the choice of the "greater than" sign in inequality (2.54).

As the control parameter C is changed, the spatially uniform equilibrium can become unstable with respect to fluctuations of the form

$$\begin{aligned} \delta\theta &= \delta a_\theta \mathrm{e}^{\sigma t + i\mathbf{k}\cdot\mathbf{x}}, \\ \delta\eta &= \delta a_\eta \mathrm{e}^{\sigma t + i\mathbf{k}\cdot\mathbf{x}} \end{aligned} \tag{2.58}$$

about the homogenous solution (θ_h, η_h):

$$\begin{aligned} \theta &= \theta_h + \delta\theta, \\ \eta &= \eta_h + \delta\eta. \end{aligned} \tag{2.59}$$

Linearizing, we obtain

$$\begin{aligned} \tau_\theta \partial_t \delta\theta &= l^2 \Delta\delta\theta - (\partial_\theta q)\delta\theta - (\partial_\eta q)\delta\eta, \\ \tau_\eta \partial_t \delta\eta &= L^2 \Delta\delta\eta - (\partial_\theta Q)\delta\theta - (\partial_\eta Q)\delta\eta, \end{aligned} \tag{2.60}$$

and plugging in the form of the fluctuations gives

$$\begin{aligned} \tau_\theta \sigma \delta a_\theta &= -k^2 l^2 \delta a_\theta - (\partial_\theta q)\delta a_\theta - (\partial_\eta q)\delta a_\eta, \\ \tau_\eta \sigma \delta a_\eta &= -k^2 L^2 \delta a_\eta - (\partial_\theta Q)\delta a_\theta - (\partial_\eta Q)\delta a_\eta, \end{aligned} \tag{2.61}$$

i.e.,

$$\begin{bmatrix} (\partial_\theta q + k^2 l^2 + \tau_\theta \sigma) & \partial_\eta q \\ \partial_\theta Q & (\partial_\eta Q + k^2 L^2 + \tau_\eta \sigma) \end{bmatrix} \begin{bmatrix} \delta a_\theta \\ \delta a_\eta \end{bmatrix} = \begin{bmatrix} 0 \\ 0 \end{bmatrix}. \tag{2.62}$$

For nonzero amplitudes $(\delta a_\theta, \delta a_\eta)$ to be possible, the determinant of the matrix must be zero, leading to

$$\begin{aligned} (\partial_\theta q + k^2 l^2 + \tau_\theta \sigma)(\partial_\eta Q + k^2 L^2 + \tau_\eta \sigma) - (\partial_\theta Q)(\partial_\eta q) &= 0, \\ (\partial_\theta q)(\partial_\eta Q) + k^2 L^2 (\partial_\theta q) + k^2 l^2 (\partial_\eta Q) + k^4 l^2 L^2 + \tau_\eta \sigma (\partial_\theta q + k^2 l^2) & \\ + \tau_\theta \sigma (\partial_\eta Q + k^2 L^2) + \tau_\theta \tau_\eta \sigma^2 - (\partial_\theta Q)(\partial_\eta q) &= 0, \\ (\tau_\theta \tau_\eta)\sigma^2 + [\tau_\eta (\partial_\theta q + k^2 l^2) + \tau_\theta (\partial_\eta Q + k^2 L^2)]\sigma & \\ + [k^4 l^2 L^2 + k^2 L^2 (\partial_\theta q) + k^2 l^2 (\partial_\eta Q) + (\partial_\theta q)(\partial_\eta Q) - (\partial_\theta Q)(\partial_\eta q)] &= 0, \end{aligned}$$

$$\sigma = -\frac{\tau_\eta(\partial_\theta q + k^2 l^2) + \tau_\theta(\partial_\eta Q + k^2 L^2)}{2\tau_\theta \tau_\eta}$$

$$\pm \sqrt{\frac{[\tau_\eta(\partial_\theta q + k^2 l^2) + \tau_\theta(\partial_\eta Q + k^2 L^2)]^2}{4\tau_\theta^2 \tau_\eta^2} - \frac{k^4 l^2 L^2 + k^2 L^2(\partial_\theta q) + k^2 l^2(\partial_\eta Q) + (\partial_\theta q)(\partial_\eta Q) - (\partial_\theta Q)(\partial_\eta q)}{\tau_\theta \tau_\eta}}. \tag{2.63}$$

If $\mathrm{Re}(\sigma) > 0$, then the spatially uniform equilibrium is unstable, and this is the case if either of the following inequalities holds:

$$\begin{aligned} \tau_\eta(\partial_\theta q + k^2 l^2) + \tau_\theta(\partial_\eta Q + k^2 L^2) &< 0, \\ k^4 l^2 L^2 + k^2 L^2(\partial_\theta q) + k^2 l^2(\partial_\eta Q) + (\partial_\theta q)(\partial_\eta Q) - (\partial_\theta Q)(\partial_\eta q) &< 0. \end{aligned} \tag{2.64}$$

Examining the first inequality, we observe that since $\partial_\theta q < 0$, if $\alpha = \tau_\theta/\tau_\eta << 1$, then the first inequality can be satisfied for α sufficently small and for $k = 0$. At the particular value of α for which the first inequality is at the threshold of being satisfied, with $k = 0$, the frequency of oscillations is given by

$$\omega_0 = \mathrm{Im}(\sigma) = \sqrt{\frac{(\partial_\theta q)(\partial_\eta Q) - (\partial_\theta Q)(\partial_\eta q)}{\tau_\theta \tau_\eta}}, \tag{2.65}$$

where inequality (2.54) guarantees ω_0 is real.

As for the second inequality, at the threshold of it being satisfied, $\omega = \mathrm{Im}(\sigma) = 0$, so that the perturbation does not oscillate in time. In this case, the critical wave number can be found from

$$(l^2 L^2)(k^2)^2 + [L^2(\partial_\theta q) + l^2(\partial_\eta Q)](k^2) + (\partial_\theta q)(\partial_\eta Q) - (\partial_\theta Q)(\partial_\eta q) = 0. \tag{2.66}$$

In general, given an equation of the form

$$ak^4 + bk^2 + c = 0, \quad a, c > 0, \tag{2.67}$$

where we have the constraint that k must have a unique, real, positive value, it follows that $k = (c/a)^{1/4}$. Thus, the critical wave number is

$$k_0 = \left(\frac{(\partial_\theta q)(\partial_\eta Q) - (\partial_\theta Q)(\partial_\eta q)}{l^2 L^2} \right)^{1/4}. \tag{2.68}$$

The actual wave numbers of the bifurcating solutions are near k_0.

We will now show that the second inequality of equation (2.64) is more easily satisfied the smaller the quantity $\beta = l/L$ is. Plugging in the value of k_0 into the second inequality of equation (2.64) gives

$$\begin{aligned}
k_0^4 l^2 L^2 + k_0^2[L^2(\partial_\theta q) + l^2(\partial_\eta Q)] + (\partial_\theta q)(\partial_\eta Q) - (\partial_\theta Q)(\partial_\eta q) &< 0, \\
\frac{[(\partial_\theta q)(\partial_\eta Q) - (\partial_\theta Q)(\partial_\eta q)]^{1/2}}{lL}[L^2(\partial_\theta q) + l^2(\partial_\eta Q)] & \\
+2[(\partial_\theta q)(\partial_\eta Q) - (\partial_\theta Q)(\partial_\eta q)] &< 0, \\
\frac{L^2(\partial_\theta q) + l^2(\partial_\eta Q)}{lL} + 2[(\partial_\theta q)(\partial_\eta Q) - (\partial_\theta Q)(\partial_\eta q)]^{1/2} &< 0,
\end{aligned}$$

$$\begin{aligned}
L^2(\partial_\theta q) &< -l^2(\partial_\eta Q) - 2lL[(\partial_\theta q)(\partial_\eta Q) - (\partial_\theta Q)(\partial_\eta q)]^{1/2}, \\
\partial_\theta q &< -\left(\frac{l}{L}\right)^2 \partial_\eta Q - 2\left(\frac{l}{L}\right)[(\partial_\theta q)(\partial_\eta Q) - (\partial_\theta Q)(\partial_\eta q)]^{1/2}, \\
\partial_\theta q &< -\beta^2 \partial_\eta Q - 2\beta[(\partial_\theta q)(\partial_\eta Q) - (\partial_\theta Q)(\partial_\eta q)]^{1/2}.
\end{aligned} \tag{2.69}$$

Since from the formulation of the activator-inhibitor equations we have $\partial_\theta q < 0$, it follows that for β sufficiently small, the condition for bifurcating to the solution with $\omega = 0$ and $k = k_0$ is satisfied.

So for $\alpha << 1$, we expect a bifurcation with nonzero ω_0, and for $\beta << 1$, we expect a bifurcation with nonzero k_0. Therefore, when $\alpha << 1$ but $\beta > 1$, the activator-inhibitor equation (2.49) is an Ω-system, and when $\alpha > 1$ but

$\beta << 1$, it is a K-system. If $\alpha << 1$ and $\beta << 1$, then we define the activator-inhibitor system to be a $K\Omega$-system, since it is then possible for both ω_0 and k_0 to be nonzero.

2.4.2 Classification of general activator-inhibitor systems

We have already seen how activator-inhibitor equations of the general form given by equation (2.49) can be classified as K-systems, Ω-systems, or $K\Omega$-systems depending on the values of $\alpha = \tau_\theta/\tau_\eta$ and $\beta = l/L$. There is a second type of classification based on the type of nonlinearity. For simplicity, we assume that the significant nonlinearity is contained in the equilibrium equation $q(\theta, \eta, C) = 0$, which gives rise to the curve $\eta = \hat{\eta}(\theta)$ for a fixed value of C. For example, for the cubic nonlinearity model, $\hat{\eta}(\theta) = \theta^3 - \theta$.

The cubic nonlinearity (or any odd-order nonlinearity with positive leading coefficient) has the nice property of ensuring that the spike solutions remain modest in size. If the nonlinearity is quadratic instead of cubic, then it is possible for large-amplitude spike solutions (several orders of magnitude larger than the modest spike solutions of the cubic nonlinearity model) to be stable [8, 9]. Therefore, we focus on nonlinearities like the cubic nonlinearity, which rule out large-amplitude spike solutions.

The cubic nonlinearity model is a model equation for general activator-inhibitor equations having the same general shape for their $\hat{\eta}(\theta)$ curves. We expect that results obtained for the cubic nonlinearity model will apply qualitatively to any activator-inhibitor equation sharing the same important features (i.e., the magnitude of α and β, and the general shape of the nonlinearity).

To summarize the types of spike solutions possible in monostable activator-

inhibitor systems,

(1) narrow spike equilibria can occur in K-systems and in $K\Omega$-systems with either a cubic-type or quadratic-type nonlinearity;

(2) wide pulse equilibria can occur in K-systems and in $K\Omega$-systems with a cubic-type nonlinearity;

(3) pulsating and traveling narrow spike solutions can occur in $K\Omega$-systems with a cubic-type or quadratic-type nonlinearity;

(4) pulsating and traveling wide pulse solutions can occur in $K\Omega$-systems with a cubic-type nonlinearity;

(5) large-amplitude spike equilibria can occur in K-systems and in $K\Omega$-systems with a quadratic-type nonlinearity; and

(6) pulsating and traveling large-amplitude spike solutions can occur in $K\Omega$-systems with a quadratic-type nonlinearity [8, 9].

When traveling spike solutions collide, a static or pulsating spike solution may result, so in general, the analysis of traveling spike collisions is complicated [8, 9].

In bistable systems (which must have a cubic-type rather than quadratic-type nonlinearity for there to be one unstable and two stable spatially uniform equilibria), depending on the control parameter value, spike solutions analogous to those in monostable systems can be stable (static spikes for K-systems and $K\Omega$-systems, and pulsating or traveling spikes in $K\Omega$-systems). However, for other values of the control parameter, fronts (or domain boundaries)

between regions of the two stable spatially uniform equilibria become the interesting features. At a certain critical value of the control parameter, the domain boundaries are static in K-systems, but otherwise, the domain walls will move so that one of the spatially uniform equilibria takes over the entire domain. In $K\Omega$-systems, the same behavior can occur, but it is also possible for the domain boundary to pulsate instead of remaining static at the critical value of control parameter. The interesting feature of bistable systems is that domain walls can be excited, and then change the state of the entire domain from one spatially uniform equilibrium to the other [9]. Although we focus primarily on monostable systems, much of the analysis (such as the Lyapunov functional) also applies to bistable systems.

2.5 Analysis of spike solutions

2.5.1 Active transmission line without inhibitor diffusion or dissipation

An easy system to analyze for spike solutions is the active transmission-line model without inhibitor diffusion or dissipation,

$$\begin{aligned} \tau_\theta \partial_t \theta &= l^2 \partial_{xx} \theta - \theta^3 + \theta - C - \partial_x \eta, \\ \tau_\eta \partial_t \eta &= -\partial_x \theta. \end{aligned} \tag{2.70}$$

The electrical circuit that gives rise to this system in the continuum limit is discussed in section 3.2. The analysis of spike solutions for the activator-inhibitor equation (2.49) is a generalization of the technique that can be used to analyze traveling spike solutions for this active transmission-line model.

If we assume there is a steady-state traveling solution

$$\begin{aligned} \theta(x,t) &= \tilde{\theta}(x-vt), \\ \eta(x,t) &= \tilde{\eta}(x-vt), \end{aligned} \tag{2.71}$$

and we let $\xi = x - vt$, then we find

$$\begin{aligned} -\tau_\theta v \partial_\xi \tilde{\theta} &= l^2 \partial_{\xi\xi}\tilde{\theta} - \tilde{\theta}^3 + \tilde{\theta} - C - \partial_\xi \tilde{\eta}, \\ -\tau_\eta v \partial_\xi \tilde{\eta} &= -\partial_\xi \tilde{\theta}. \end{aligned} \tag{2.72}$$

If we take $v = 1/\sqrt{\tau_\theta \tau_\eta}$, we obtain

$$l^2 \partial_{\xi\xi}\tilde{\theta} - \tilde{\theta}^3 + \tilde{\theta} - C = 0. \tag{2.73}$$

If we consider equation (2.73) as a boundary-value problem, we can solve for possible steady state pulse shapes $\tilde{\theta}(\xi)$. In fact, we can write equation (2.73) as

$$l^2 \partial_{\xi\xi}\tilde{\theta} = -\frac{dV}{d\tilde{\theta}}, \tag{2.74}$$

where

$$V(\tilde{\theta}) = -\frac{1}{4}\tilde{\theta}^4 + \frac{1}{2}\tilde{\theta}^2 - C\tilde{\theta}. \tag{2.75}$$

Thus, if equation (2.73) is viewed as a dynamical system instead of as a boundary-value problem (i.e., if ξ is interpreted as time instead of as a spatial variable), then the dynamics are those of a particle with mass l^2 moving in a potential $V(\tilde{\theta})$.

The possible trajectories for a particle moving in the potential $V(\tilde{\theta})$ are easily visualized by using the standard graphical technique in which the phase-plane trajectories are derived from the plot of the potential. Changing to more familiar variables, suppose we have

$$\begin{aligned} m\frac{d^2x}{dt^2} &= -\frac{dV}{dx}, \\ V(x) &= -\frac{1}{4}x^4 + \frac{1}{2}x^2 - Cx. \end{aligned} \tag{2.76}$$

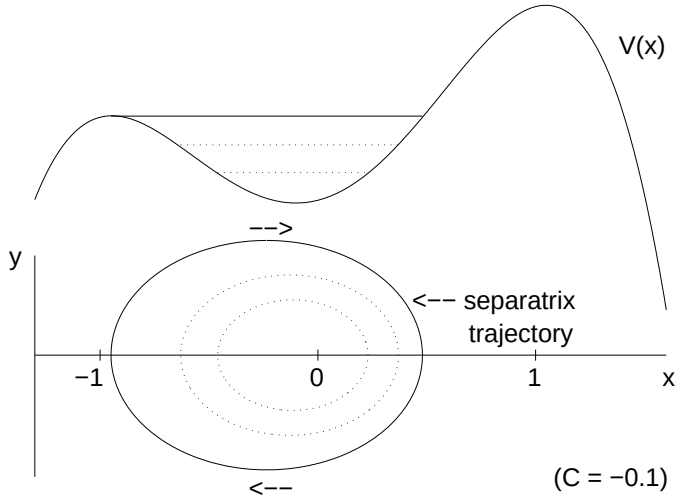

Figure 2.2: Phase plane for the potential function $V(x) = -(1/4)x^4 + (1/2)x^2 - Cx$

Taking $m = 1$ and letting $y = dx/dt$, we obtain the system of first-order ODEs,

$$\begin{aligned} \frac{dx}{dt} &= y, \\ \frac{dy}{dt} &= -\frac{dV}{dx}. \end{aligned} \tag{2.77}$$

The slope of the phase-plane trajectories are then found from

$$\frac{dy}{dx} = \frac{dy/dt}{dx/dt} = -\frac{dV/dx}{y}. \tag{2.78}$$

The phase plane is illustrated in figure 2.2. The trajectory of interest is the separatrix trajectory, because the separatrix trajectory corresponds to a single spike. The traveling spike corresponding to the separatrix trajectory is shown in figure 2.3.

An alternative approach to the phase-plane approach is to use elliptic functions to solve for $\tilde{\theta}$ in equation (2.73). Equation (2.73) is a special case of the general elliptic equation

$$\frac{d^2x}{dt^2} = a_0 + a_1 x + a_2 x^2 + a_3 x^3, \tag{2.79}$$

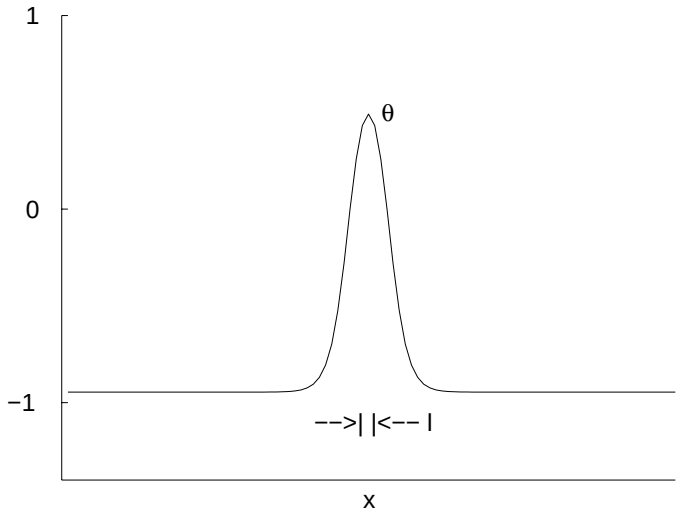

Figure 2.3: Traveling spike solution corresponding to the separatrix trajectory

where $a_1, ..., a_3$ are constants, which can be solved explicitly for $x(t)$ using elliptic functions [34].

There still remains the issue of determining other possible traveling solutions, and then assessing stability of the various traveling solutions.

2.5.2 General activator-inhibitor system

The analysis of spike solutions for the general activator-inhibitor system (2.49) involves simultaneously performing two particle-in-a-potential calculations like the one required for the active transmission line spike of the previous subsection. We assume that the system is monostable, and that the spatially uniform equilibrium solution is stable. We also assume one space dimension. We are looking for solutions of

$$\begin{aligned} l^2 \frac{d^2\theta}{dx^2} &= q(\theta, \eta, C), \\ L^2 \frac{d^2\eta}{dx^2} &= Q(\theta, \eta, C). \end{aligned} \tag{2.80}$$

Because both η and θ are functions of x, these equations are coupled, and there-

fore difficult to analyze. However, there are two limiting cases which we can analyze, and then try to argue that the actual solution is approximated by these limiting cases. The first case is $l \to 0$, which leads to the "smooth" distributions, and the second case is $L \to \infty$, which leads to the "sharp" distributions. (Mathematically, the smooth/sharp distribution analysis technique is related to singular perturbation analysis.)

For the smooth distribution case, setting $l \to 0$ in the above equations leads to

$$\begin{aligned} q(\theta, \eta, C) &= 0, \\ L^2 \frac{d^2\eta}{dx^2} &= Q(\theta, \eta, C). \end{aligned} \tag{2.81}$$

Both θ and η are functions of x, but for this case, θ can be viewed as a function of η, with the dependence given by $q(\theta(\eta), \eta, C) = 0$. With $\theta(\eta)$ known, the equation for η can be written as

$$L^2 \frac{d^2\eta}{dx^2} = -\frac{dU_\eta}{d\eta}, \quad U_\eta = -\int^\eta Q(\theta(\bar{\eta}), \bar{\eta}, C) d\bar{\eta}. \tag{2.82}$$

This equation is of the same form as the equation of the particle moving in a potential field. Since θ is actually a multivalued function of η, there are multiple branches of the potential function U_η that need to be properly pieced together.

For the sharp distribution case, setting $L \to \infty$ in the above equations leads to

$$\begin{aligned} l^2 \frac{d^2\theta}{dx^2} &= q(\theta, \eta, C), \\ \langle Q(\theta, \eta, C) \rangle &= \text{spatial average of } Q(\theta, \eta, C) = 0, \end{aligned} \tag{2.83}$$

with η =constant. To better see how the second equation is derived, we con-

sider the dynamical equation for the inhibitor,

$$\tau_\eta \partial_t \eta = L^2 \Delta \eta - Q(\theta, \eta, C). \tag{2.84}$$

For L very large, η varies significantly only over a very large distance. We therefore can consider η to be spatially uniform, and write

$$\tau_\eta \partial_t \eta = -\frac{1}{|\Omega|} \int_\Omega Q(\theta, \eta, C) d\mathbf{x} = -\langle Q(\theta, \eta, C) \rangle, \tag{2.85}$$

where $|\Omega| = \int_\Omega d\mathbf{x}$ is the system "volume," and the angle-bracket notation is being used to denote the spatial average over the system. Next, since we are concerned with equilibrium solutions, we set $\partial_t \eta = 0$, arriving at $\langle Q(\theta, \eta, C) \rangle = 0$ with η =constant. With η =constant, the equation for θ can be written as

$$l^2 \frac{d^2\theta}{dx^2} = -\frac{dU_\theta}{d\theta}, \;\; U_\theta = -\int^\theta q(\bar{\theta}, \eta, C) d\bar{\theta}. \tag{2.86}$$

Again, this equation is of the same form as the equation of the particle moving in a potential field.

Once the form of spike solutions (or other equilibria) have been found, the next task is to determine their stability. A linearized stability analysis technique gives conditions for stability of the wide pulse and narrow spike equilibria, and also leads to the conclusion that other equilibria (those having multiple peaks) are unstable [8, 9]. Actually checking the wide pulse and narrow spike stability criteria for a general activator-inhibitor system would be cumbersome. Formulas can also be found for the wide pulse solution pulse width [8, 9].

Traveling spike shapes in one space dimension appear qualitatively similar whether they arise in $K\Omega$-systems or in the cubic nonlinearity model with $\beta << 1$ and $\alpha > 1$ but with an additional advective term. A left-traveling spike in the latter type of system is shown in figure 2.4. The shape of the

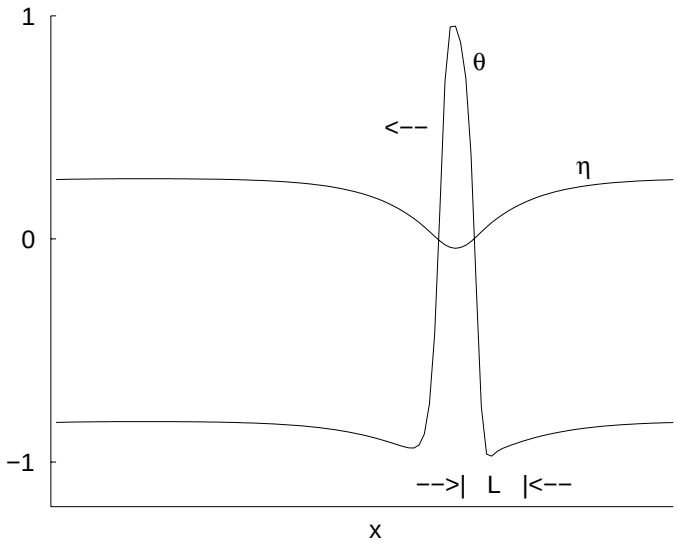

Figure 2.4: Traveling spike for the cubic nonlinearity model with an additional advective term

traveling spike can be derived using an approach similar to the approach used to find the equilibrium wide pulse and narrow spike shapes [8, 9].

Chapter 3

Engineering Realizations of Activator-Inhibitor Equations

3.1 Basic cubic nonlinearity model

There are several ways to think about implementing the basic cubic nonlinearity model dynamics,

$$\begin{aligned} \tau_\theta \partial_t \theta &= l^2 \Delta\theta - \theta^3 + \theta + \eta, \\ \tau_\eta \partial_t \eta &= L^2 \Delta\eta - \eta - \theta + C, \end{aligned} \tag{3.1}$$

for controlling a large array of actuators. We will focus on the MEMS applications, and consider implementations of spatial discretizations of the dynamics. In this context, there are two types of realizations we can consider: digital and analog. (A third possible realization, which is intermediate between digital and analog, is a pulse-train-based approach, where the frequency of pulse trains is used to encode analog values with high dynamic range [35].)

A digital implementation of the spatially discretized dynamics might be possible when relatively large MEMS actuators are to be controlled. The actuators would have to be large because of the area required for digital circuitry to perform the calculations at each site. At the expense of greater complexity, one could also design a digital implementation in which a number of actuators shared the same computational circuitry in order to keep the area of the digital circuitry small enough. Besides the usual advantages of a digital approach, such as simple biasing and highly accurate computations, the uniformity across the array would make it possible to work with the pattern-forming

system very close to the bifurcation threshold. With a digital approach, there might be hope of developing control schemes based on the equivariant amplitude equation, because keeping the system in the amplitude equation's domain of validity would be a possibiliy.

However, an analog implementation would inherently lack the uniformity required to operate very close to the bifurcation threshold, since analog circuits are sensitive to processing variations that lead to device nonuniformities across a chip. The main advantage of an analog implementation, however, is compact size, and if the actuators are small enough, an analog approach might be preferred for that reason. We are therefore led to consider how we might control the nonlinear dynamics themselves, rather than focusing on envelope equations. Implementation issues also lead to consideration of the bounded nonlinearity model, since an analog nonlinearity would necessarily saturate eventually.

There are different forms that an analog implementation could take, but the simplest approach is to consider both θ and η to be voltages. (By contrast, the active transmission line naturally leads to a realization with θ a voltage and η a current.) Resistive coupling can be used to implement the diffusion, capacitors can implement the time constants, an active element can be used for the nonlinearity and positive feedback, and all that remains is to implement the coupling. One possible scheme is illustrated in figure 3.1, where the diode symbol (representing a tunnel diode) denotes the nonlinear, negative-incremental-gain element. The biasing circuitry for the tunnel diode is not shown.

From figure 3.1, the equations for θ_k and η_k are

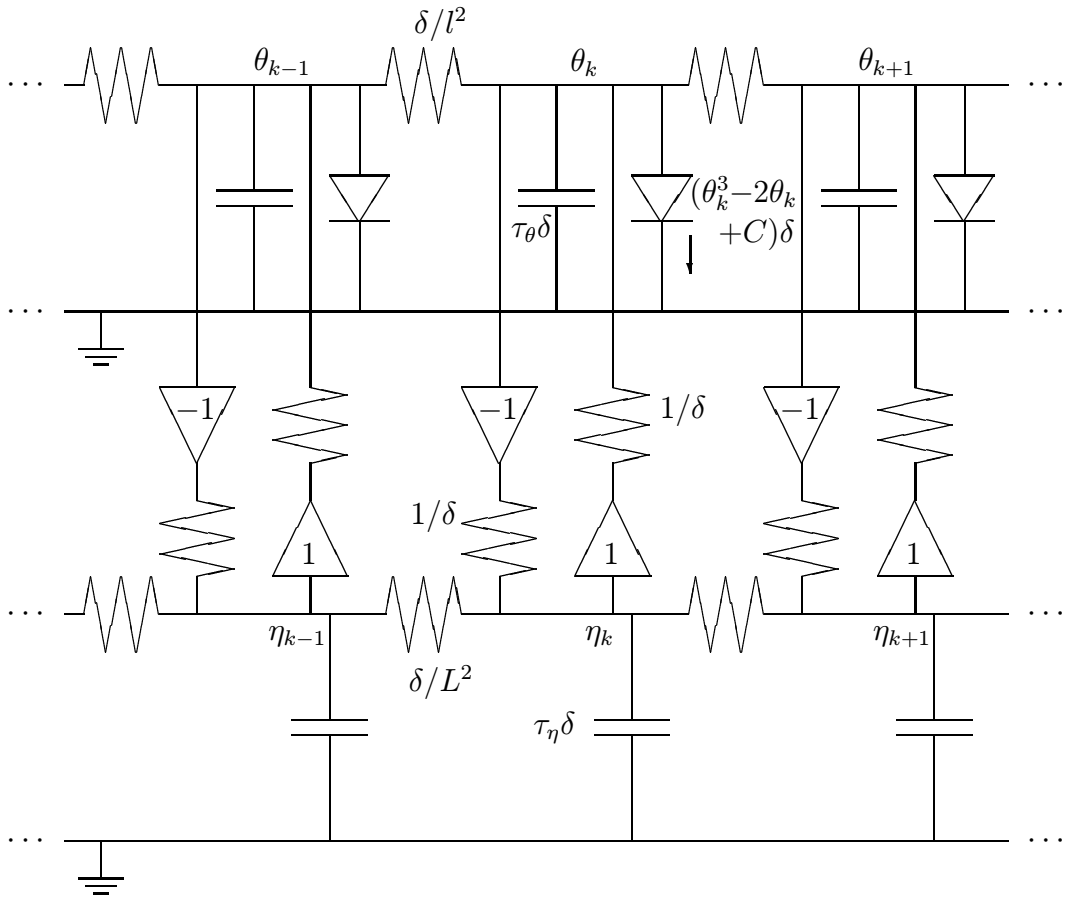

Figure 3.1: An implementation of the spatially discretized cubic nonlinearity model dynamics

$$
\begin{aligned}
(\tau_\theta \delta)\dot{\theta}_k &= \frac{l^2}{\delta}(\theta_{k+1} - \theta_k) + \frac{l^2}{\delta}(\theta_{k-1} - \theta_k) - (\theta_k^3 - 2\theta_k + C)\delta + (\eta_k - \theta_k)\delta, \\
(\tau_\eta \delta)\dot{\eta}_k &= \frac{L^2}{\delta}(\eta_{k+1} - \eta_k) + \frac{L^2}{\delta}(\eta_{k-1} - \eta_k) + (-\theta_k - \eta_k)\delta,
\end{aligned}
\tag{3.2}
$$

which simplifies to

$$
\begin{aligned}
\tau_\theta \dot{\theta}_k &= \frac{l^2}{\delta^2}(\theta_{k+1} - 2\theta_k + \theta_{k-1}) - \theta_k^3 + \theta_k + \eta_k - C, \\
\tau_\eta \dot{\eta}_k &= \frac{L^2}{\delta^2}(\eta_{k+1} - 2\eta_k + \eta_{k-1}) - \eta_k - \theta_k.
\end{aligned}
\tag{3.3}
$$

In the continuum limit (i.e., taking $\delta \to 0$), these equations become

$$
\begin{aligned}
\tau_\theta \partial_t \theta &= l^2 \partial_{xx}\theta - \theta^3 + \theta + \eta - C, \\
\tau_\eta \partial_t \eta &= L^2 \partial_{xx}\eta - \eta - \theta.
\end{aligned}
\tag{3.4}
$$

The control parameter can be moved to the inhibitor equation by taking $\tilde{\eta} = \eta - C$ (although there is no problem with having the control parameter in the activator equation as opposed to the inhibitor equation). The circuit of figure 3.1 generalizes to two dimensions by making the resistive grids two-dimensional.

An analog computer implementing essentially the cubic nonlinearity model was built by Purwins et. al. [36]. In their circuit, the inhibitor was the voltage across a capacitor and the activator was the current through an inductor; therefore, the nonlinearity had to be implemented as an S-shaped I-V characteristic. (By contrast, in the circuit of figure 3.1, the tunnel diode I-V characteristic is N-shaped.) Also, a diffusive coupling mechanism had to be provided between the inductor currents. The purpose of their analog computer was for simulating gas discharge systems, which also have the S-shaped I-V characteristic [7].

The analog computer of Purwins et. al., was designed the way it was

because of the physical analogy with gas discharge systems, and because the implementation used discrete components rather than integrated circuit technology. For smart-systems applications, the only possible implementations of pattern-forming systems are in integrated circuit technology or in smart materials technology, since as was pointed out earlier, conventional approaches are only threatened when the number of actuators is in the millions. The analog computer of Purwins et. al. had only 31 by 31 sites. The circuit of figure 3.1 is implementable in integrated circuit technology, and CMOS amplifiers can be used instead of tunnel diodes, if desired.

3.2 Active transmission line

The basic cubic nonlinearity activator-inhibitor equation has a $+\eta$ coupling term in the $\partial_t\theta$ equation and a $-\theta$ coupling term in the $\partial_t\eta$ equation. A different but related equation in one spatial dimension takes the form

$$\begin{aligned} \tau_\theta \partial_t \theta &= l^2 \partial_{xx}\theta - \theta^3 + \theta - C - \partial_x \eta, \\ \tau_\eta \partial_t \eta &= L^2 \partial_{xx}\eta - \eta - \partial_x \theta, \end{aligned} \tag{3.5}$$

where for reasons that will become clear later we have moved the control (or bifurcation) parameter C from the $\partial_t\eta$ equation to the $\partial_t\theta$ equation.

The reason for calling this system an "active transmission line" is that when only the coupling terms are retained,

$$\begin{aligned} \tau_\theta \partial_t \theta &= -\partial_x \eta, \\ \tau_\eta \partial_t \eta &= -\partial_x \theta, \end{aligned} \tag{3.6}$$

the system reduces to the wave equation for a transmission line,

$$\begin{aligned} \partial_{tt}\theta &= \frac{1}{\tau_\theta \tau_\eta}\partial_{xx}\theta, \\ \partial_{tt}\eta &= \frac{1}{\tau_\theta \tau_\eta}\partial_{xx}\eta, \end{aligned} \tag{3.7}$$

where θ represents voltage, η represents current, τ_θ represents capacitance per unit length, τ_η represents inductance per unit length, and $1/\sqrt{\tau_\theta \tau_\eta}$ is the speed of traveling solutions. The additional terms in equation (3.5) add gain and dissipation.

There are two main circuit motivations for using active transmission lines. First, the active elements placed along the length of the transmission line could potentially serve as a simpler and more robust mechanism for overcoming transmission line losses than discrete repeaters. Second, for transmission lines on an integrated circuit chip, active transmission lines could be used to alleviate fanout problems [37]. This second application is important in the smart-system context, where it may be desirable to have large numbers of interconnections between processing elements. For example, the long-range coupling that could serve to stabilize patterns for the basic cubic nonlinearity model in two or more dimensions implies a relatively large fanout from each element to all its neighbors a certain distance away. Biological neural systems are also characterized by large fanout, and some neural interconnections use active transmission lines. The reason active transmission lines help with fanout problems is that the transmission line only needs to be excited at one end, and then the transmission line itself supplies the power necessary to propagate a pulse along its length. With passive transmission lines, the source needs to be able to drive enough current into each transmission line it is connected to in order to send sufficiently large pulses to the receivers.

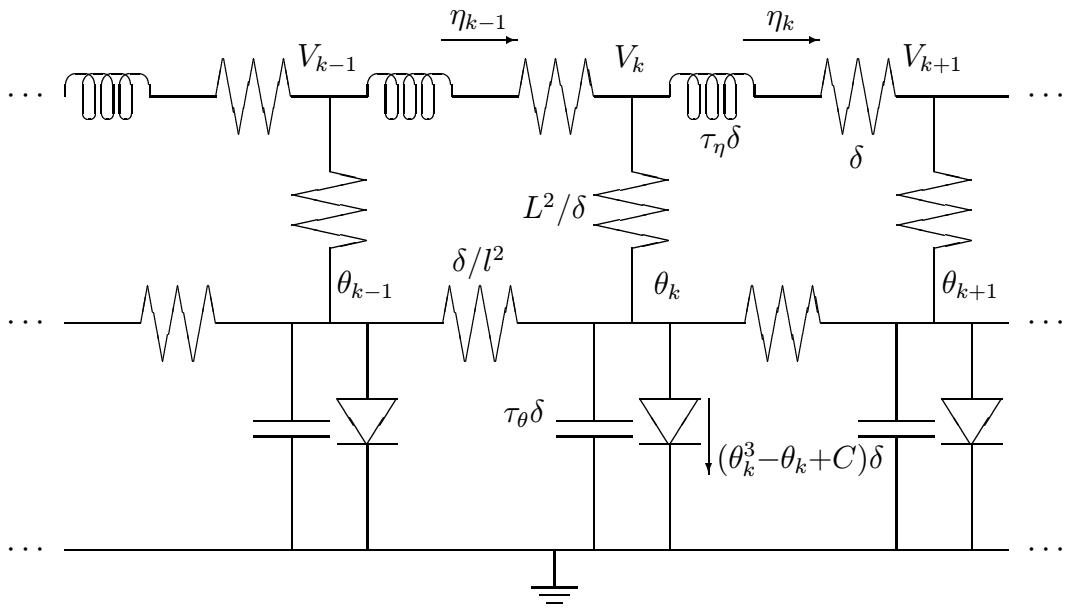

Figure 3.2: Active transmission-line circuit with inhibitor diffusion and dissipation

The circuit in figure 3.2 resembles a discrete approximation to a transmission line, with additional tunnel diodes added. The resistors in series with the inductors can be thought of as distributed resistance along the length of the inductors. Series resistance associated with the capacitors can be considered to be absorbed into the tunnel diode model. Series resistances (and the capacitances and inductances) scale with δ, and the parallel resistances scale as $1/\delta$. The equations for η_k, V_k, and θ_k are

$$\begin{aligned} V_k - \theta_k &= \frac{L^2}{\delta}(\eta_{k-1} - \eta_k), \\ (\tau_\theta\delta)\dot{\theta}_k + (\theta_k^3 - \theta_k + C)\delta + \frac{l^2}{\delta}(\theta_k - \theta_{k-1}) + \frac{l^2}{\delta}(\theta_k - \theta_{k+1}) &= \eta_{k-1} - \eta_k, \\ (\tau_\eta\delta)\dot{\eta}_k + (\delta)\eta_k &= V_k - V_{k+1}. \end{aligned} \tag{3.8}$$

These equations can be simplified to

$$\begin{aligned}
\tau_\theta \dot{\theta}_k &= \frac{l^2}{\delta^2}(\theta_{k-1} - 2\theta_k + \theta_{k+1}) - \theta_k^3 + \theta_k - C - \frac{1}{\delta}(\eta_k - \eta_{k-1}), \\
\tau_\theta \dot{\eta}_k &= -\eta_k + \frac{1}{\delta}\left[\theta_k + \frac{L^2}{\delta}(\eta_{k-1} - \eta_k) - \theta_{k+1} - \frac{L^2}{\delta}(\eta_k - \eta_{k+1})\right] \\
&= \frac{L^2}{\delta^2}(\eta_{k-1} - 2\eta_k + \eta_{k+1}) - \eta_k - \frac{1}{\delta}(\theta_{k+1} - \theta_k).
\end{aligned} \tag{3.9}$$

In the continuum limit (i.e., taking $\delta \to 0$), these equations become

$$\begin{aligned}
\tau_\theta \partial_t \theta &= l^2 \partial_{xx}\theta - \theta^3 + \theta - C - \partial_x \eta, \\
\tau_\eta \partial_t \eta &= L^2 \partial_{xx}\eta - \eta - \partial_x \theta.
\end{aligned} \tag{3.10}$$

Note that the control parameter is naturally associated with the tunnel diode characteristic. Although this is one motivation for moving the control parameter from the $\partial_t \eta$ equation to the $\partial_t \theta$ equation, it is not the only reason. The main reason is that the spatially uniform equilibria satisfy

$$\begin{aligned}
\theta^3 - \theta + C &= 0, \\
\eta &= 0,
\end{aligned} \tag{3.11}$$

so that there is no coupling between these equilibrium equations. In fact, adding a constant to the $\partial_t \eta$ equation has no effect on the dynamics, but adding a constant to the $\partial_t \theta$ equation does. Therefore, the control parameter for the active transmission line belongs with the $\partial_t \theta$ equation.

Figure 3.3 shows the active transmission line circuit without inhibitor diffusion or dissipation. The corresponding PDE system is

$$\begin{aligned}
\tau_\theta \partial_t \theta &= l^2 \partial_{xx}\theta - \theta^3 + \theta - C - \partial_x \eta, \\
\tau_\eta \partial_t \eta &= -\partial_x \theta.
\end{aligned} \tag{3.12}$$

The resistors in figure 3.3 could represent coupling between the biasing networks for the tunnel diodes, rather than resistors explicitly added to the cir-

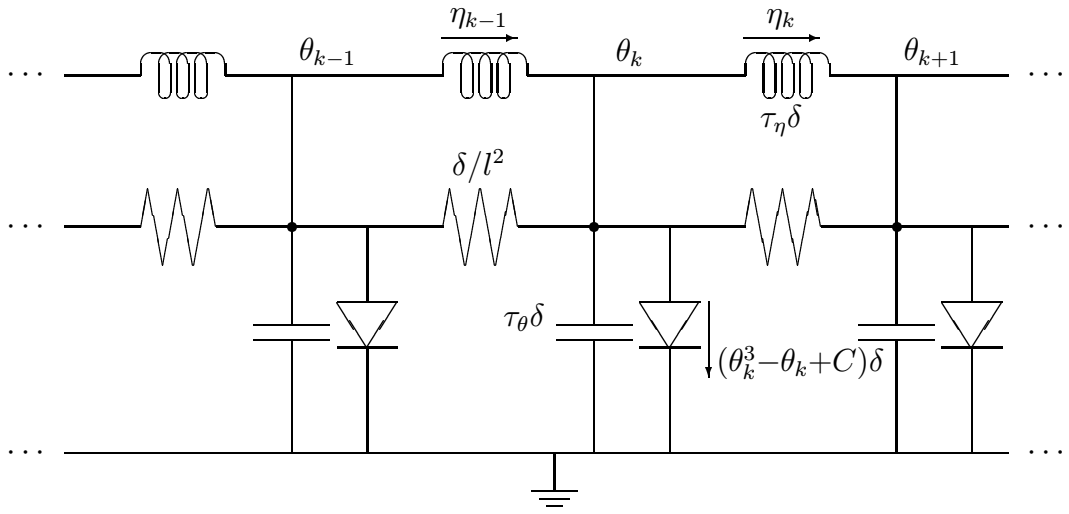

Figure 3.3: Active transmission-line circuit without inhibitor diffusion or dissipation

cuit. Since l determines the length scale of both the activator and inhibitor for this system, keeping these resistances large leads to a narrow traveling spike solution.

3.3 Complex activator-inhibitor equation

The complex activator-inhibitor equation

$$\begin{aligned} \tau_\theta \partial_t \theta &= l^2 \Delta\theta - |\theta|^2\theta + \theta + \eta, \\ \tau_\eta \partial_t \eta &= L^2 \Delta\eta - \eta - \theta + C, \end{aligned} \tag{3.13}$$

where θ, η, and C are complex, under suitable hypotheses, models the amplitude and phase evolution in the continuum limit of a network of coupled van der Pol oscillators (represented by θ), coupled to a network of resonant circuits (represented by η), with an external oscillating input (represented by C). The resonant frequencies of the van der Pol oscillators and the resonant circuits are assumed to be identical, and also equal to the frequency of the external input C.

The potential applications of the coupled van der Pol oscillator network modeled by the complex activator-inhibitor equation include quasi-optical power combining and phased-array antennas for microwave communications and radar [38, 39, 40]. As communications frequencies become higher and higher, for example, to provide high bandwidth for wireless LANs, oscillators built using solid state circuits are able to generate less and less microwave power. The only low-loss means of combining the power from many such oscillators is having the combining occur in free space, with the oscillators synchronized. Coupling between the oscillators, either through free space as well, or through electrical coupling, is used to cause the oscillators to synchronize, or frequency-lock with all oscillators in phase [41, 42, 43]. By having the oscillators not only frequency-lock, but also phase-lock with some prescribed phase relationship, it is possible to generate radiation patterns other than the simple broadside pattern which results from having all of the oscillators synchronized in phase as well as frequency.

To motivate the equations for the coupled van der Pol oscillator network model, we consider the microwave quasi-optical power-combining system. There are a number of nearly identical electrical oscillator circuits, which can be considered to be van der Pol oscillators, coupled together through some linear coupling network. Further assumptions on the oscillators and on the coupling will be introduced and explained as required.

We will first examine the coupled van der Pol oscillator part of the system, without the resonant circuit part. We will also consider a general linear coupling network instead of the specific network related to the Laplacian for the complex activator-inhibitor equation (3.13). One derivation of the coupled van der Pol oscillator network equations is based on an array of oscillators

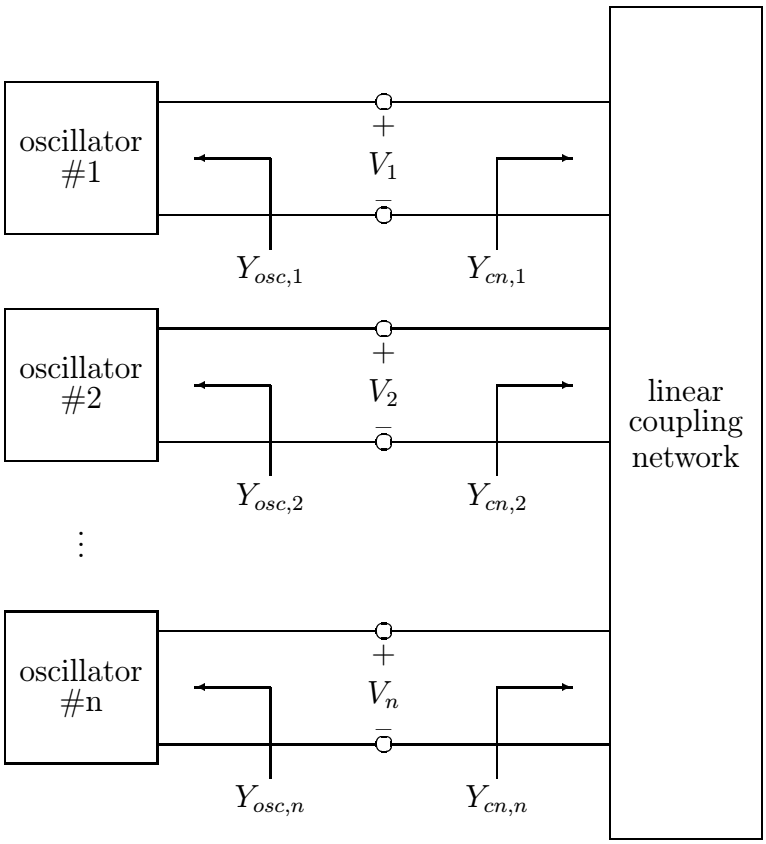

Figure 3.4: Oscillator array with linear coupling network

connected to an n-port coupling network described by Y-parameters [38]. Figure 3.4 illustrates the coupled oscillator network, and the various admittances used in the analysis.

The equation relating the terminal voltages and terminal admittances for the Y-parameter linear coupling network is

$$Y_{cn,j}(\omega_j, V_1, ..., V_n) = \frac{1}{V_j} \sum_k Y_{jk}(\omega_j) V_k. \tag{3.14}$$

Each oscillator in the array is taken to be the parallel RLC van der Pol oscillator circuit shown in figure 3.5.

The second-order differential equation describing a van der Pol oscillator

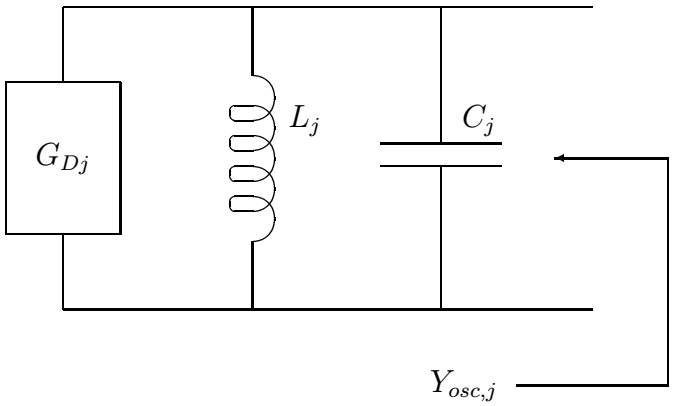

Figure 3.5: Van der Pol oscillator circuit model

can be put in the form

$$\frac{d^2V}{d\tau^2} - \epsilon(1 - V^2)\frac{dV}{d\tau} + V = 0, \tag{3.15}$$

where $\epsilon > 0$ and τ is an appropriately scaled time parameter (and the voltage V is appropriately scaled as well). If $\epsilon << 1$, then a perturbation analysis shows that the solution to the van der Pol equation can be approximated by a sine wave [44]. We also assume weak coupling, so that we can neglect deviation of the solution from a sine wave due to the effects of coupling. The parameter ϵ in the van der Pol equation is the reciprocal of the Q of the RLC circuit of figure 3.5, where $Q_j = \omega_{0j}C_j/|G_{0j}| = 1/(\omega_{0j}L_j|G_{0j}|)$ with $\omega_{0j} = 1/\sqrt{L_jC_j}$, and $G_{0j} < 0$ is the small-signal portion of G_{Dj} which produces the linear instability. Therefore, the first assumption required of the van der Pol oscillators is that the Q of each oscillator be large. (We will first derive the equations under the assumption that each oscillator has a different free-running frequency ω_{0j}, and later specialize to the case of identical free-running oscillator natural frequencies.)

With the assumption that each oscillator voltage signal is nearly sinusio-

dal, we can represent the voltages as

$$V_j(t) = A_j(t)e^{i(\omega_{0j}t+\phi_j(t))}, \tag{3.16}$$

where $A_j(t)$ is a slowly varying amplitude quantity and $\phi_j(t)$ is a slowly varying phase quantity. (The requirement that $A_j(t)$ and $\phi_j(t)$ be slowly varying will be made more precise later.) Under the large-Q assumption, we can therefore treat the negative-conductance circuit element as a simple conductance depending on the sine-wave amplitude A_j, and we further assume that form of the conductance as a function of A_j is given by

$$G_{Dj} = -|G_{0j}|(1 - \gamma_j A_j^2), \tag{3.17}$$

where γ_j is a scalar parameter. The admittance for each oscillator can then be written

$$Y_{osc,j}(\omega_j, V_j) = i\omega_j C_j + \frac{1}{i\omega_j L_j} - |G_{0j}|\left(1 - \gamma_j A_j^2\right), \tag{3.18}$$

where ω_j is the (slowly varying) frequency of the j^{th} oscillator.

The total admittance at each port of the coupling network is then the sum of the coupling network port admittance $Y_{cn,j}$ (given by equation (3.14)) and the oscillator admittance $Y_{osc,j}$:

$$\begin{aligned} Y_j(\omega_j, \mathbf{V}) &= Y_{osc,j}(\omega_j, V_j) + Y_{cn,j}(\omega_j, \mathbf{V}) \\ &= i\omega_j C_j + \frac{1}{i\omega_j L_j} - |G_{0j}|(1 - \gamma_j A_j^2) \\ &\quad + \sum_k Y_{jk}(\omega_j)\frac{A_k}{A_j}e^{i[(\omega_{0k}-\omega_{0j})t+(\phi_k-\phi_j)]}, \end{aligned} \tag{3.19}$$

where $\mathbf{V} = (V_1, ..., V_n)$. The classical harmonic balance condition for the existence of an oscillation at the (slowly varying) frequency ω_j is [45]

$$Y_j(\omega_j, \mathbf{V}) = 0, \tag{3.20}$$

which can be expanded in a Taylor series about ω_{0j} as

$$Y_j(\omega_{0j}, \mathbf{V}) + \left.\frac{\partial Y_j}{\partial \omega_j}\right|_{\omega_{0j}} (\omega_j - \omega_{0j}) + \cdots = 0. \tag{3.21}$$

But $\omega_j - \omega_{0j}$ can be expressed as follows:

$$\begin{aligned} \frac{dV_j}{dt} &= i\left[\omega_{0j} + \frac{d\phi_j}{dt} - i\frac{1}{A_j}\frac{dA_j}{dt}\right] V_j = i\omega_j V_j, \\ \omega_j - \omega_{0j} &= \frac{d\phi_j}{dt} - i\frac{1}{A_j}\frac{dA_j}{dt}. \end{aligned} \tag{3.22}$$

Thus, the explicit requirement that $A_j(t)$ and $\phi_j(t)$ be slowly varying is

$$\frac{d\phi_j}{dt} << \omega_{0j}, \quad \frac{1}{A_j}\frac{dA_j}{dt} << \omega_{0j}. \tag{3.23}$$

Then, under harmonic balance,

$$\frac{d\phi_j}{dt} - i\frac{1}{A_j}\frac{dA_j}{dt} = -\left.\frac{Y_j}{\partial Y_j/\partial \omega_j}\right|_{\omega_{0j}}, \tag{3.24}$$

which can be broken down into separate equations for A_j and ϕ_j as

$$\begin{aligned} \frac{d\phi_j}{dt} &= -\mathrm{Re}\left(\left.\frac{Y_j}{\partial Y_j/\partial \omega_j}\right|_{\omega_{0j}}\right), \\ \frac{dA_j}{dt} &= A_j \mathrm{Im}\left(\left.\frac{Y_j}{\partial Y_j/\partial \omega_j}\right|_{\omega_{0j}}\right). \end{aligned} \tag{3.25}$$

The quantity $\partial Y_j/\partial \omega_j$ evaluated at ω_{0j} is computed as follows:

$$\begin{aligned} \left.\frac{\partial Y_j}{\partial \omega_j}\right|_{\omega_{0j}} &= iC_j - \frac{1}{iL_j}\frac{1}{\omega_{0j}^2} + \sum_k \left.\frac{\partial Y_{jk}}{\partial \omega_j}\right|_{\omega_{0j}} \frac{A_k}{A_j} e^{i[(\omega_{0k}-\omega_{0j})t + (\phi_k - \phi_j)]} \\ &= 2iC_j + \sum_k \left.\frac{\partial Y_{jk}}{\partial \omega_j}\right|_{\omega_{0j}} \frac{A_k}{A_j} e^{i[(\omega_{0k}-\omega_{0j})t + (\phi_k - \phi_j)]}. \end{aligned} \tag{3.26}$$

Defining the normalized coupling parameters κ_{jk} by

$$\kappa_{jk} = Y_{jk}/|G_{0j}| \tag{3.27}$$

and substituting $Q_j = \omega_{0j}C_j/|G_{0j}|$, we obtain

$$\left.\frac{Y_j}{\partial Y_j/\partial \omega_j}\right|_{\omega_{0j}} = i\frac{\omega_{0j}}{2Q_j}\left[\frac{(1-\gamma_j A_j^2) - \sum_k \kappa_{jk}\frac{A_k}{A_j} e^{i[(\omega_{0k}-\omega_{0j})t + (\phi_k - \phi_j)]}}{1 - i\frac{\omega_{0j}}{2Q_j}\sum_k \left.\frac{\partial \kappa_{jk}}{\partial \omega_j}\right|_{\omega_{0j}} \frac{A_k}{A_j} e^{i[(\omega_{0k}-\omega_{0j})t + (\phi_k - \phi_j)]}}\right]. \tag{3.28}$$

Examining this expression, we see that considerable simplification can achieved if in the denominator,

$$\frac{\omega_{0j}}{2Q_j}\sum_k \frac{\partial \kappa_{jk}}{\partial \omega_j}\Big|_{\omega_{0j}} \frac{A_k}{A_j} << 1, \quad \forall j. \tag{3.29}$$

This is a condition on the coupling network; specifically, as pointed out by York et. al., it is a requirement that the coupling network characteristics vary with frequency much less than the oscillator characteristics, or in other words, that the coupling network be broadband compared to the oscillator networks [38].

With the broadband coupling network assumption, the magnitude and phase dynamics can be written as

$$\begin{aligned}
\frac{dA_j}{dt} &= \frac{\omega_{0j}}{2Q_j}(1-\gamma_j A_j^2)A_j \\
&\quad + \frac{\omega_{0j}}{2Q_j}\sum_k A_k K_{jk}\cos[(\omega_{0k}-\omega_{0j})t + (\phi_k - \phi_j) + \psi_{jk} + \pi], \\
\frac{d\phi_j}{dt} &= \frac{\omega_{0j}}{2Q_j}\frac{1}{A_j}\sum_k A_k K_{jk}\sin[(\omega_{0k}-\omega_{0j})t + (\phi_k - \phi_j) + \psi_{jk} + \pi],
\end{aligned} \tag{3.30}$$

where $\kappa_{jk} = K_{jk}e^{i\psi_{jk}}$. Defining

$$\frac{d\xi_j}{dt} = \omega_{0j} + \frac{d\phi_j}{dt}, \tag{3.31}$$

we can remove the explicit time dependence from the right-hand side of equation (3.30), obtaining

$$\begin{aligned}
\frac{dA_j}{dt} &= \frac{\omega_{0j}}{2Q_j}(1-\gamma_j A_j^2)A_j + \frac{\omega_{0j}}{2Q_j}\sum_k A_k K_{jk}\cos[\xi_k - \xi_j + \psi_{jk} + \pi], \\
\frac{d\xi_j}{dt} &= \omega_{0j} + \frac{\omega_{0j}}{2Q_j}\frac{1}{A_j}\sum_k A_k K_{jk}\sin[\xi_k - \xi_j + \psi_{jk} + \pi].
\end{aligned} \tag{3.32}$$

Now assume that the oscillators are identical. Then equation (3.30) in fact does not have an explicit time dependence on the right-hand side, and the dynamics simplify to

$$\begin{aligned}\frac{dA_j}{dt} &= c_1(1-\gamma A_j^2)A_j + c_2\sum_k A_k K_{jk}\cos(\phi_k-\phi_j-\varphi_{jk}),\\ \frac{d\phi_j}{dt} &= c_2\frac{1}{A_j}\sum_k A_k K_{jk}\sin(\phi_k-\phi_j-\varphi_{jk}),\end{aligned} \tag{3.33}$$

where c_1, c_2, and γ are constants and $\varphi_{jk} = -(\psi_{jk}+\pi)$. Under the assumption that κ_{jj} is purely real $\forall j$ and the same constant $\forall j$ (κ_{jj} is just the normalized admittance of the coupling network seen at port j when all of the other ports of the coupling network are short-circuited), the $A_j K_{jj}\cos(0)$ term can be pulled out of the sum in the dA_j/dt expression and combined with the nonlinear term, while in the $d\phi_j/dt$ expression, the $A_j K_{jj}\sin(0)$ term simply drops out, leaving

$$\begin{aligned}\frac{dA_j}{dt} &= c_1(c_3-\gamma A_j^2)A_j + c_2\sum_{k\neq j} A_k K_{jk}\cos(\phi_k-\phi_j-\varphi_{jk}),\\ \frac{d\phi_j}{dt} &= c_2\frac{1}{A_j}\sum_{k\neq j} A_k K_{jk}\sin(\phi_k-\phi_j-\varphi_{jk}).\end{aligned} \tag{3.34}$$

Rescaling to eliminate extraneous constants, we can finally write the dynamics in the form

$$\begin{aligned}\frac{dA_j}{dt} &= (1-\gamma A_j^2)A_j + \sum_k A_k K_{jk}\cos(\phi_k-\phi_j-\varphi_{jk}),\\ \frac{d\phi_j}{dt} &= \frac{1}{A_j}\sum_k A_k K_{jk}\sin(\phi_k-\phi_j-\varphi_{jk}),\end{aligned} \tag{3.35}$$

where $\gamma > 0$ is a scalar parameter determining the uncoupled equilibrium amplitude of the oscillators. The coordinate system is rotating at the natural frequency of the oscillators so that the $d\phi_j/dt$ equations represent the phase dynamics of the coupled oscillator network. These dynamics can also be written in the form

$$\frac{dx_j}{dt} = (1-\gamma|x_j|^2)x_j + \sum_k x_k\overline{w}_{jk}, \tag{3.36}$$

where the $x_j = A_j e^{i\phi_j}$ and $w_{jk} = K_{jk}e^{i\varphi_{jk}}$ are complex.

If the coupling between the oscillators is purely real nearest-neighbor passive coupling, the dynamics (3.36) can be thought of as a discretization of the complex Ginzburg-Landau equation in n dimensions with real coefficients:

$$\partial_t \theta = l^2 \Delta \theta + (1 - |\theta|^2)\theta, \quad \mathbf{x} \in \mathbb{R}^n, \quad t > 0, \quad \theta \in \mathbb{C}. \tag{3.37}$$

If the nonlinear conductance element G_{Lj} in figure 3.5 is replaced with a linear, positive conductance, the same analysis with the same assumptions leads to a network of coupled resonant circuits. With the same assumptions on the coupling network as for the coupled-oscillator case, the dynamics for the coupled resonant circuits can be written as

$$\partial_t \eta = L^2 \Delta \eta - \eta, \quad \mathbf{x} \in \mathbb{R}^n, \quad t > 0, \quad \eta \in \mathbb{C}. \tag{3.38}$$

The coupling between the oscillator array and resonator array needs to take a form analogous to the coupling between activator and inhibitor voltages for the real cubic nonlinearity model implementation shown in figure 3.1. Finally, injecting a sinusiodal signal of constant amplitude and phase at the common resonant frequency of the resonant circuits (which is also the same as the natural frequency of the oscillator circuits), we obtain the complex activator-inhibitor equation (3.13).

To summarize, the following assumptions were required on the network of coupled van der Pol oscillators and coupled resonant circuits to obtain the complex activator-inhibitor equation:

(1) The weak coupling assumption ensures that none of the oscillator waveforms is distorted by the coupling.

(2) The high-Q assumption on the oscillators ensures that each oscillator voltage is well-modeled as sinusoidal.

(3) The slowly-varying magnitude and phase condition is required to ensure the validity of the Taylor series expansion for finding the slowly varying frequency ω_j of each oscillator.

(4) The broadband-coupling-network assumption is required to keep the coupled oscillator equations managable.

(5) The free-running natural frequencies of the oscillators and resonant circuits are all assumed to be identical (and also equal to the frequency of the external input signal).

(6) The coupling networks give rise to Laplacian terms in the continuum limit. (Assumption (6) guarantees assumption (4) is satisfied, since a purely resistive coupling network has no frequency dependence.)

The boundary conditions that arise naturally in this coupled-oscillator context are Neumann boundary conditions involving the magnitudes of θ and η, and periodic boundary conditions. Dirichlet boundary conditions (i.e., $\theta = \eta = 0$ on $\partial\Omega$) could be physically implemented, but require "oscillator death" at the edges of the network. If we let $\theta_R = \mathrm{Re}\{\theta\}$ and $\theta_I = \mathrm{Im}\{\theta\}$, then the Neumann (or no-flux) boundary conditions are

$$\begin{aligned} \theta_R(\nabla\theta_R \cdot \mathbf{n}) + \theta_I(\nabla\theta_I \cdot \mathbf{n}) &= 0, \\ \eta_R(\nabla\eta_R \cdot \mathbf{n}) + \eta_I(\nabla\eta_I \cdot \mathbf{n}) &= 0, \end{aligned} \tag{3.39}$$

for $\mathbf{x} \in \partial\Omega$, where $\mathbf{n}$ is the unit outer normal for $\partial\Omega$.

Chapter 4

Basic Properties of Solutions

4.1 Introduction

To be on a secure mathematical footing for the dissipativity analysis at the end of this chapter and the Lyapunov functional analysis of the next chapter, we need to prove the existence and uniqueness of weak solutions for the PDE systems we are analyzing, and also show that the weak solutions have the required regularity. Another reason for showing the details of the existence, uniqueness, and regularity proofs is so that modified versions of the equations (e.g., with control inputs or feedback) can be easily checked for these properties. Also, to keep the classes of systems for which the results can be generalized as large as possible, we only seek to prove the minimum regularity necessary for the subsequent analysis.

The classes of models we analyze for existence and uniqueness of weak solutions divide along slightly different lines than the classifications based on their physical origins. The basic cubic nonlinearity model

$$\begin{aligned} \tau_\theta \partial_t \theta &= l^2 \Delta\theta - \theta^3 + \theta + \eta, \\ \tau_\eta \partial_t \eta &= L^2 \Delta\eta - \eta - \theta + C \end{aligned} \tag{4.1}$$

will be considered in the context of the more general class of models

$$\begin{aligned} \tau_\theta \partial_t \theta + L_\theta \theta + f_\theta(\theta) &= \eta, \\ \tau_\eta \partial_t \eta + L_\eta \eta + f_\eta(\eta) &= -\theta, \end{aligned} \tag{4.2}$$

which we will call the "general polynomial-nonlinearity model," where

L_θ = uniformly parabolic operator for the θ equation,

$$
\begin{aligned}
L_\eta &= \text{uniformly parabolic operator for the } \eta \text{ equation,} \\
f_\theta(\theta) &= \text{odd-order polynomial in } \theta \text{ with positive leading coefficient,} \\
f_\eta(\eta) &= \text{odd-order polynomial in } \eta \text{ with positive leading coefficient.}
\end{aligned}
$$

The active transmission-line model

$$
\begin{aligned}
\tau_\theta \partial_t \theta &= l^2 \partial_{xx} \theta - \theta^3 + \theta - C - \partial_x \eta, \\
\tau_\eta \partial_t \eta &= L^2 \partial_{xx} \eta - \eta - \partial_x \theta
\end{aligned}
\tag{4.3}
$$

lies in the general class

$$
\begin{aligned}
\tau_\theta \partial_t \theta + L_\theta \theta + f_\theta(\theta) &= -\partial_x \eta, \\
\tau_\eta \partial_t \eta + L_\eta \eta + f_\eta(\eta) &= -\partial_x \theta
\end{aligned}
\tag{4.4}
$$

in one space dimension, which we will call the "general parabolic active transmission-line model." The analysis of the general polynomial-nonlinearity model and the general parabolic active transmission-line model are so similar that the modifications required for the general parabolic active transmission-line model proofs will be stated as parenthetical remarks in the general polynomial-nonlinearity model proofs.

The cubic nonlinearity model with additional advective terms also falls within the general polynomial-nonlinearity model; for example,

$$
\begin{aligned}
\tau_\theta \partial_t \theta &= l^2 \Delta \theta - \theta^3 + \theta + \eta, \\
\tau_\eta \partial_t \eta &= L^2 \Delta \eta - \eta - \theta + C + \mathbf{v} \cdot \nabla \eta,
\end{aligned}
\tag{4.5}
$$

where $\mathbf{v}$ is a continuously differentiable function of $\mathbf{x}$.

The active transmission-line model without inhibitor diffusion,

$$
\begin{aligned}
\tau_\theta \partial_t \theta &= l^2 \partial_{xx} \theta - \theta^3 + \theta - C - \partial_x \eta, \\
\tau_\eta \partial_t \eta &= -\partial_x \theta,
\end{aligned}
\tag{4.6}
$$

requires a separate analysis, since it is both parabolic and hyperbolic in char-

acter. The existence and uniqueness proofs for this active transmission-line model actually require regularity results from the general parabolic active transmission-line model.

The bounded nonlinearity model,

$$\begin{aligned} \tau_\theta \partial_t \theta &= l^2 \Delta\theta - f(\theta) + \eta, \\ \tau_\eta \partial_t \eta &= L^2 \Delta\eta - \eta - \theta + C, \end{aligned} \tag{4.7}$$

where f is continuous and $\forall\theta$, $|f(\theta)| < M$ for some $M > 0$, actually has simpler proofs of existence and uniqueness of weak solutions than the general polynomial-nonlinearity model.

Existence and uniqueness of weak solutions for the complex activator-inhibitor equation,

$$\begin{aligned} \tau_\theta \partial_t \theta &= l^2 \Delta\theta - |\theta|^2\theta + \theta + \eta, \\ \tau_\eta \partial_t \eta &= L^2 \Delta\eta - \eta - \theta + C, \end{aligned} \tag{4.8}$$

follow analogously to the real case when the dynamics are written as a system of two coupled real activator-inhibitor systems. Another easy generalization of the general polynomial-nonlinearity model analysis is the addition of symmetric long-range coupling terms. (There are other generalizations as well, but only the complex activator-inhibitor equation and symmetric long-range coupling will be considered here.)

After existence, uniqueness, and regularity of weak solutions have been established, it is also possible to prove a dissipativity property for certain subclasses of the general models. We will establish dissipativity results for the cubic nonlinearity model (both real and complex), the active transmission-line model (with inhibitor diffusion and dissipation), the cubic nonlinearity model with an additional (suitably bounded) advective term, and the cubic

nonlinearity model with additional long-range coupling.

4.2 Existence and uniqueness of weak solutions for the general polynomial-nonlinearity model

4.2.1 Definition of weak solutions

We will now prove the existence and uniqueness of weak solutions for the system (4.2), the general polynomial-nonlinearity model. The existence and uniqueness results parallel those for parabolic PDEs, since the activator-inhibitor equations are a system of two parabolic PDEs [46, 47]. However, the linear form of the coupling terms between the activator and inhibitor equations is also key to the success of the analysis. Throughout this analysis, we are considering the domain $\Omega \subset \mathbb{R}^n$ in which $\mathbf{x}$ lies to be open and bounded.

First, we need to define the bilinear forms B_θ and B_η. A parabolic operator L_u can be written in either divergence form:

$$L_u u = -\sum_{i,j=1}^{n} \partial_{x_j}(a_{ij}(x,t)\partial_{x_i} u) + \sum_{i=1}^{n} b_i(x,t)\partial_{x_i} u + c(x,t)u, \tag{4.9}$$

or in nondivergence form

$$L_u u = -\sum_{i,j=1}^{n} a_{ij}(x,t)\partial_{x_j}(\partial_{x_i} u) + \sum_{i=1}^{n} b_i(x,t)\partial_{x_i} u + c(x,t)u, \tag{4.10}$$

where in either case, $a_{ij}, b_j, c \in \mathbb{R}$ and we further assume that $a_{ij} = a_{ji}$. If the a_{ij} are C^1 functions, then any operator written in divergence form can be written in nondivergence form and vice versa [46]. We will, in fact, assume that the a_{ij} are C^1 functions of both $\mathbf{x}$ and t, and that the b_i and c are bounded. We will consider only divergence form, because divergence form is more natural for energy-method approaches. The uniformly parabolic condition we require

is that there must exist a constant $A > 0$ such that

$$\sum_{i,j=1}^{n} a_{ij}(\mathbf{x},t)\xi_i\xi_j \geq A|\xi|^2, \ \ \forall \mathbf{x} \in \Omega, \ \forall t \in (0,T), \ \text{and} \ \forall \xi \in \mathbb{R}^n. \tag{4.11}$$

The bilinear form associated with L_u is defined as

$$B_u[u,v] = \int_\Omega \left[\sum_{i,j=1}^{n} a_{ij}(\mathbf{x},t)(\partial_{x_i} u)(\partial_{x_j} v) + \sum_{i=1}^{n} b_i(\mathbf{x},t)(\partial_{x_i} u)v + c(\mathbf{x},t)uv \right] d\mathbf{x}. \tag{4.12}$$

So B_θ is the bilinear form corresponding to L_θ, and B_η corresponds to L_η. For the special case of the cubic nonlinearity model,

$$\begin{aligned} B_\theta[\theta, v] &= \int_\Omega l^2(\nabla\theta)\cdot(\nabla v)d\mathbf{x}, \\ B_\eta[\eta, w] &= \int_\Omega L^2(\nabla\eta)\cdot(\nabla w)d\mathbf{x}, \end{aligned} \tag{4.13}$$

and there is no explicit t dependence.

To define weak solutions, we need to select an appropriate Sobolev space. Sobolev spaces are spaces of functions of $\mathbf{x}$ alone in which the solutions of the PDE under consideration are assumed to live at each time instant. The Sobolev space $W^{m,p}(\Omega)$ is defined as follows:

$$\begin{aligned} W^{m,p}(\Omega) = \Big\{ u \in L^p(\Omega) \Big| \ &\text{the distributional derivatives of u of order} \leq m \\ &\text{are in } L^p(\Omega) \Big\}. \end{aligned} \tag{4.14}$$

The Sobolev space $W^{m,p}(\Omega)$ is a Banach space with the norm

$$||u||_{W^{m,p}(\Omega)} = \left(\sum_{[\alpha]\leq m} ||D^\alpha u||^p_{L^p(\Omega)} \right)^{1/p}, \tag{4.15}$$

where $\alpha = \{\alpha_1, ..., \alpha_n\}$ is a multiindex, and $[\alpha] = \alpha_1 + \cdots + \alpha_n$.

When $p = 2$, $W^{m,2}(\Omega)$ is written as $H^m(\Omega)$. (This is because $H^m(\Omega)$ turns out to in fact be a Hilbert space.) In particular,

$$H^1(\Omega) = \left\{ u \in L^2(\Omega) | D_i u \in L^2(\Omega), 1 \leq i \leq n \right\}. \tag{4.16}$$

Since we need to define a space of functions in which the solutions of our PDE live at each time instant, we need to further restrict our Sobolev space to functions which adhere to the appropriate boundary conditions. There are three basic types of boundary conditions, which we will consider in parallel:

1. Dirichlet: $\theta = 0, \quad \eta = 0 \quad$ on $\partial\Omega$;
2. Neumann: $\nabla_{\mathbf{x}}\theta \cdot \mathbf{n} = 0, \quad \nabla_{\mathbf{x}}\eta \cdot \mathbf{n} = 0$ on $\partial\Omega$ where $\mathbf{n}$ is normal to $\partial\Omega$; or
3. periodic boundary conditions.

For Dirichlet boundary conditions, the space $H_0^1(\Omega)$ is considered, and it is defined as the closure of $C_0^\infty(\Omega)$ in $H^1(\Omega)$ (where $C_0^\infty(\Omega)$ is the space of C^∞ functions with compact support). Similarly, for periodic boundary conditions, we can work in the space $H^1_{\text{per}}(\Omega)$, defined in the obvious way. The norms for the Sobolev spaces $H_0^1(\Omega)$, $H^1_{\text{per}}(\Omega)$, etc., are the same as the norm for $H^1(\Omega)$, and therefore, we will refer to the $H^1(\Omega)$-norm, even though the function spaces we are actually working with are further restricted by the boundary conditions.

Even though we are used to writing solutions as $\theta(\mathbf{x}, t)$ and $\eta(\mathbf{x}, t)$, for purposes of the existence and uniqueness proofs, we will consider $\theta(t)$ and $\eta(t)$ to be evolving in time as elements of the appropriate Sobolev space.

To have a properly posed initial boundary value problem, we assume the initial conditions

$$\begin{aligned} \theta(0) &= g_\theta \in L^2(\Omega), \\ \eta(0) &= g_\eta \in L^2(\Omega). \end{aligned} \tag{4.17}$$

We also need norms that we can apply to $\theta(\cdot)$ and $\eta(\cdot)$ on any finite time interval

$[0, T]$. These norms are derived from Sobolev space norms; e.g.,

$$||\theta||_{L^2(0,T;H^1(\Omega))} = \left(\int_0^T ||\theta(t)||^2_{H^1(\Omega)} dt \right)^{1/2}. \tag{4.18}$$

(Technically, the boundary conditions and initial conditions should be thought of in the sense of trace [48].)

The last concept we need to properly define weak solutions is that of a negative Sobolev space, which is simply the dual space to the Sobolev space in which $\theta(t)$ and $\eta(t)$ lie. We denote the negative Sobolev space (to $H^1(\Omega)$ restricted by the boundary conditions) by $H^{-1}(\Omega)$, and we denote the pairing by

$$\langle u, v \rangle = \int_\Omega uv \, d\mathbf{x}, \tag{4.19}$$

for $u \in H^{-1}(\Omega)$ and $v \in H^1(\Omega)$. The time derivative of $\theta(t)$ and of $\eta(t)$ lie in $H^{-1}(\Omega)$, which we express as

$$\partial_t \theta \in H^{-1}(\Omega), \;\; \partial_t \eta \in H^{-1}(\Omega) \tag{4.20}$$

(even though $\theta(\cdot)$ and $\eta(\cdot)$ are thought of as functions of t only).

Finally, let $(\cdot, \cdot)$ denote the inner product

$$(u, v) = \int_\Omega uv \, d\mathbf{x}, \tag{4.21}$$

for $u, v \in L^2(\Omega)$. We say that the pair of functions θ and η are a weak solution of the system (4.2) provided

$$\theta, \eta \in L^2(0, T; H^1(\Omega)) \text{ with } \partial_t \theta, \partial_t \eta \in L^2(0, T; H^{-1}(\Omega)), \tag{4.22}$$

θ and η satisfy the appropriate boundary conditions and initial conditions, and

$$\begin{aligned} \tau_\theta < \partial_t \theta, v > + B_\theta[\theta, v; t] &= (-f_\theta(\theta) + \eta, v), \\ \tau_\eta < \partial_t \eta, w > + B_\eta[\eta, w; t] &= (-f_\eta(\eta) - \theta, w) \end{aligned} \tag{4.23}$$

for each $v, w \in H^1(\Omega)$ (and satisfying the boundary conditions), and for a.e. $t \in [0, T]$.

4.2.2 Galerkin approximations

The key tools for proving existence of weak solutions are Galerkin approximations and energy estimates. Let $\{w_k\}$ be a basis for $H^1(\Omega)$ and an orthonormal basis for $L^2(\Omega)$. (Since $H^1(\Omega) \subset L^2(\Omega)$, an orthonormal basis of $L^2(\Omega)$ that is contained in $H^1(\Omega)$ is a basis for $H^1(\Omega)$.) The Galerkin approximation consists of projecting the equations down to a space spanned by only a finite number of these basis functions $\{w_k\}$.

Define

$$\begin{aligned} \theta_m(t) &= \sum_{k=1}^{m} d_k^m(t) w_k, \\ \eta_m(t) &= \sum_{k=1}^{m} e_k^m(t) w_k, \end{aligned} \tag{4.24}$$

where we would like to be able to determine the coefficients d_k^m and e_k^m so they satisfy

$$\begin{aligned} d_k^m(0) &= (g_\theta, w_k) &= \int_\Omega g_\theta(\mathbf{x}) w_k(\mathbf{x}) d\mathbf{x}, \\ e_k^m(0) &= (g_\eta, w_k) &= \int_\Omega g_\eta(\mathbf{x}) w_k(\mathbf{x}) d\mathbf{x} \end{aligned} \tag{4.25}$$

and

$$\begin{aligned} \tau_\theta(\partial_t \theta_m, w_k) + B_\theta[\theta_m, w_k; t] &= (-f_\theta(\theta_m) + \eta_m, w_k), \\ \tau_\eta(\partial_t \eta_m, w_k) + B_\eta[\eta_m, w_k; t] &= (-f_\eta(\eta_m) - \theta_m, w_k), \end{aligned} \tag{4.26}$$

where $(\cdot, \cdot)$ denotes the usual inner product for $L^2(\Omega)$. In other words, we are trying to find functions θ_m, and η_m which satisfy the projection of the coupled PDEs onto a finite-dimensional subspace spanned by $\{w_k\}_{k=1}^m$. If we

substitute the expressions for θ_m in terms of d_k^m and for η_m in terms of e_k^m into the above equations, we obtain a system of ODEs in the d_k^m and e_k^m, along with appropriate initial conditions. To prove the existence of the d_k^m and e_k^m for all $t \in [0, T]$, it is sufficient to show that there are no finite escape times (since the necessary local Lipschitz condition is satisfied) [44]. In particular, if we can show that there is no finite escape time for either θ_m or η_m, then it follows from the fact that $\{w_k\}$ is a basis that there can be no finite escape time for any of the d_k^m or e_k^m.

4.2.3 Inequality for uniformly parabolic bilinear forms

The requirement that the parabolic operator be uniformly parabolic is needed for deriving an inequality that is used for determining energy estimates for θ_m and η_m. From the uniformly parabolic condition we have, for some $A > 0$,

$$A|\xi|^2 \leq \sum_{i,j=1}^{n} a_{ij}(\mathbf{x}, t)\xi_i\xi_j, \quad \forall \mathbf{x} \in \Omega, \ \forall t \in (0, T), \text{ and } \forall \xi \in \mathbb{R}^n, \tag{4.27}$$

from which it follows that

$$\begin{aligned}
A|\nabla u|^2 &\leq \sum_{i,j=1}^{n} a_{ij}(\mathbf{x}, t)(\partial_{x_i} u)(\partial_{x_j} u), \\
A\int_\Omega |\nabla u|^2 d\mathbf{x} &\leq \int_\Omega \sum_{i,j=1}^{n} a_{ij}(\mathbf{x}, t)(\partial_{x_i} u)(\partial_{x_j} u) d\mathbf{x} \\
&= B[u, u; t] - \int_\Omega \left[\sum_{i=1}^{n} b_i(\mathbf{x}, t)(\partial_{x_i} u)u + c(\mathbf{x}, t)u^2 \right] d\mathbf{x} \\
&\leq B[u, u; t] + \sum_{i=1}^{n} ||b_i||_{L^\infty(\Omega\times(0,T))} \int_\Omega |\nabla u||u| d\mathbf{x} \\
&\quad + ||c||_{L^\infty(\Omega\times(0,T))} \int_\Omega u^2 d\mathbf{x}.
\end{aligned} \tag{4.28}$$

Cauchy's inequality with ϵ implies

$$\int_\Omega |\nabla u||u| d\mathbf{x} \leq \epsilon \int_\Omega |\nabla u|^2 d\mathbf{x} + \frac{1}{4\epsilon} \int_\Omega u^2 d\mathbf{x}. \tag{4.29}$$

Therefore, we obtain

$$\begin{aligned} A\int_\Omega |\nabla u|^2 d\mathbf{x} &\leq B[u,u;t] + \epsilon \sum_{i=1}^{n} ||b_i||_{L^\infty(\Omega\times(0,T))} \int_\Omega |\nabla u|^2 d\mathbf{x} \\ &\quad + \left(\frac{1}{4\epsilon}\sum_{i=1}^{n} ||b_i||_{L^\infty(\Omega\times(0,T))} + ||c||_{L^\infty(\Omega\times(0,T))}\right)\int_\Omega u^2 d\mathbf{x}. \end{aligned} \tag{4.30}$$

Now choosing ϵ such that

$$\epsilon \sum_{i=1}^{n} ||b_i||_{L^\infty(\Omega\times(0,T))} < \frac{A}{2}, \tag{4.31}$$

we obtain

$$\beta \int_\Omega |\nabla u|^2 d\mathbf{x} \leq B[u,u;t] + \gamma \int_\Omega u^2 d\mathbf{x}, \tag{4.32}$$

where $\beta = A/2 > 0$ and γ is a constant. In terms of norms, this expression can be rewritten as

$$B[u,u;t] \geq \beta ||\nabla u||^2_{L^2(\Omega)} - \gamma ||u||^2_{L^2(\Omega)}. \tag{4.33}$$

4.2.4 $L^2(0,T;L^2(\Omega))$ and $L^\infty(0,T;L^2(\Omega))$ bounds for θ_m and η_m

Starting with (4.26), multiplying the first equation through by d_k^m and summing from $k=1$ to m while multiplying the second equation through by e_k^m and summing from $k=1$ to m, we obtain

$$\begin{aligned} \tau_\theta \int_\Omega (\partial_t \theta_m)\theta_m d\mathbf{x} + B_\theta[\theta_m,\theta_m;t] &= -\int_\Omega f_\theta(\theta_m)\theta_m d\mathbf{x} + \int_\Omega \eta_m \theta_m d\mathbf{x}, \\ \tau_\eta \int_\Omega (\partial_t \eta_m)\eta_m d\mathbf{x} + B_\eta[\eta_m,\eta_m;t] &= -\int_\Omega f_\eta(\eta_m)\eta_m d\mathbf{x} - \int_\Omega \theta_m \eta_m d\mathbf{x}. \end{aligned} \tag{4.34}$$

Summing these two equations gives

$$\begin{aligned} \tau_\theta \int_\Omega (\partial_t \theta_m)\theta_m d\mathbf{x} + \tau_\eta \int_\Omega (\partial_t \eta_m)\eta_m d\mathbf{x} + B_\theta[\theta_m,\theta_m;t] + B_\eta[\eta_m,\eta_m;t] \\ + \int_\Omega f_\theta(\theta_m)\theta_m d\mathbf{x} + \int_\Omega f_\eta(\eta_m)\eta_m d\mathbf{x} &= 0. \end{aligned} \tag{4.35}$$

(Exactly the same expression is obtained for the general parabolic active transmission-line model.) The first two terms can be rewritten as

$$\begin{aligned} \tau_\theta \int_\Omega (\partial_t \theta_m)\theta_m d\mathbf{x} &= \frac{1}{2}\tau_\theta \partial_t \int_\Omega \theta_m^2 d\mathbf{x} = \frac{1}{2}\tau_\theta \partial_t ||\theta_m||^2_{L^2(\Omega)} \\ \tau_\eta \int_\Omega (\partial_t \eta_m)\eta_m d\mathbf{x} &= \frac{1}{2}\tau_\eta \partial_t \int_\Omega \eta_m^2 d\mathbf{x} = \frac{1}{2}\tau_\eta \partial_t ||\eta_m||^2_{L^2(\Omega)}. \end{aligned} \tag{4.36}$$

For the third and fourth terms, we can use the inequality for uniformly parabolic bilinear forms,

$$\begin{aligned} B_\theta[\theta_m, \theta_m; t] &\geq \beta_\theta ||\nabla \theta_m||^2_{L^2(\Omega)} - \gamma_\theta ||\theta_m||^2_{L^2(\Omega)}, \\ B_\eta[\eta_m, \eta_m; t] &\geq \beta_\eta ||\nabla \eta_m||^2_{L^2(\Omega)} - \gamma_\eta ||\eta_m||^2_{L^2(\Omega)}, \end{aligned} \tag{4.37}$$

where β_θ, γ_θ, β_η, and γ_η are constants, with $\beta_\theta > 0$ and $\beta_\eta > 0$.

For the fifth and sixth terms, we can use the fact that $f_\theta(\theta_m)$ and $f_\eta(\eta_m)$ are odd-order polynomials with positive leading coefficients to obtain bounds. Suppose the leading term of $f_\theta(\theta_m)$ is $a_\theta \theta_m^{2p_\theta - 1}$ and the leading term of $f_\eta(\eta_m)$ is $a_\eta \eta_m^{2p_\eta - 1}$. Then there exist positive constants c_θ and c_η such that

$$\begin{aligned} f_\theta(\theta_m)\theta_m &\geq \frac{1}{2} a_\theta \theta_m^{2p_\theta} - c_\theta, \\ f_\eta(\eta_m)\eta_m &\geq \frac{1}{2} a_\eta \eta_m^{2p_\eta} - c_\eta \end{aligned} \tag{4.38}$$

so that

$$\begin{aligned} \int_\Omega f_\theta(\theta_m)\theta_m d\mathbf{x} &\geq \frac{1}{2} a_\theta \int_\Omega \theta_m^{2p_\theta} d\mathbf{x} - c_\theta |\Omega|, \\ \int_\Omega f_\eta(\eta_m)\eta_m d\mathbf{x} &\geq \frac{1}{2} a_\eta \int_\Omega \eta_m^{2p_\eta} d\mathbf{x} - c_\eta |\Omega|, \end{aligned} \tag{4.39}$$

where

$$|\Omega| = \int_\Omega d\mathbf{x}. \tag{4.40}$$

Next, we use Holder's inequality,

$$\int_\Omega |uv| d\mathbf{x} \leq ||u||_{L^p(\Omega)} ||v||_{L^q(\Omega)}, \tag{4.41}$$

and Young's inequality,

$$ab \leq \frac{a^p}{p} + \frac{b^q}{q}, \tag{4.42}$$

where $p, q > 1$ and $1/p + 1/q = 1$, to obtain

$$\begin{aligned}
\int_\Omega \theta_m^2 d\mathbf{x} &\leq \left(\int_\Omega \theta_m^{2p_\theta} d\mathbf{x}\right)^{1/p_\theta} |\Omega|^{1/q_\theta} \\
&\leq \frac{1}{p_\theta}\int_\Omega \theta_m^{2p_\theta} d\mathbf{x} + \frac{1}{q_\theta}|\Omega|, \\
\int_\Omega \theta_m^{2p_\theta} d\mathbf{x} &\geq p_\theta \int_\Omega \theta_m^2 d\mathbf{x} - \frac{p_\theta}{q_\theta}|\Omega|, \\
\int_\Omega f_\theta(\theta_m)\theta_m d\mathbf{x} &\geq \frac{1}{2}a_\theta p_\theta \int_\Omega \theta_m^2 d\mathbf{x} - \frac{1}{2}a_\theta \frac{p_\theta}{q_\theta}|\Omega| - c_\theta|\Omega| \\
&= \frac{1}{2}a_\theta p_\theta ||\theta_m||^2_{L^2(\Omega)} - c'_\theta|\Omega|, \\
\int_\Omega f_\eta(\eta_m)\eta_m d\mathbf{x} &\geq \frac{1}{2}a_\eta p_\eta ||\eta_m||^2_{L^2(\Omega)} - c'_\eta|\Omega|,
\end{aligned} \tag{4.43}$$

where $1/p_\theta + 1/q_\theta = 1$, $1/p_\eta + 1/q_\eta = 1$, $c'_\theta > 0$, and $c'_\eta > 0$.

Combining all of these inequalities, we obtain

$$\begin{aligned}
\frac{1}{2}\tau_\theta \partial_t ||\theta_m||^2_{L^2(\Omega)} + \frac{1}{2}\tau_\eta \partial_t ||\eta_m||^2_{L^2(\Omega)} + \beta_\theta ||\nabla\theta_m||^2_{L^2(\Omega)} - \gamma_\theta ||\theta_m||^2_{L^2(\Omega)} \\
+\beta_\eta ||\nabla\eta_m||^2_{L^2(\Omega)} - \gamma_\eta ||\eta_m||^2_{L^2(\Omega)} + \frac{1}{2}a_\theta p_\theta ||\theta_m||^2_{L^2(\Omega)} \\
-c'_\theta|\Omega| + \frac{1}{2}a_\eta p_\eta ||\eta_m||^2_{L^2(\Omega)} - c'_\eta|\Omega| \leq 0.
\end{aligned} \tag{4.44}$$

From this inequality, it follows that

$$\partial_t \left[\tau_\theta ||\theta_m||^2_{L^2(\Omega)} + \tau_\eta ||\eta_m||^2_{L^2(\Omega)}\right] \leq c_1 \left[\tau_\theta ||\theta_m||^2_{L^2(\Omega)} + \tau_\eta ||\eta_m||^2_{L^2(\Omega)}\right] + c_2, \tag{4.45}$$

for some constants c_1 and c_2.

Now we can apply the usual Gronwall lemma [47]: let g, h, y, and dy/dt be locally integrable on (t_0, ∞) satisfying

$$\frac{dy}{dt} \leq gy + h \text{ for } t \geq t_0. \tag{4.46}$$

Then

$$y(t) \leq y(t_0)\mathrm{e}^{\int_{t_0}^{t} g(\tau)d\tau} + \int_{t_0}^{t} h(s)\mathrm{e}^{-\int_{t}^{s} g(\tau)d\tau}ds. \tag{4.47}$$

Applied to the problem at hand, the usual Gronwall lemma, with

$$\begin{aligned} y &= \tau_\theta ||\theta_m||^2_{L^2(\Omega)} + \tau_\eta ||\eta_m||^2_{L^2(\Omega)}, \\ g &= c_1, \\ h &= c_2, \end{aligned} \tag{4.48}$$

implies

$$\begin{aligned} y(t) &\leq y(0)\mathrm{e}^{c_1 t} + \int_0^t c_2 \mathrm{e}^{c_1(t-s)}ds \\ &= y(0)\mathrm{e}^{c_1 t} - c_2\mathrm{e}^{c_1 t}\left(\frac{\mathrm{e}^{-c_1 s}}{c_1}\Big|_0^t\right) \\ &= y(0)\mathrm{e}^{c_1 t} + \frac{c_2}{c_1}(\mathrm{e}^{c_1 t} - 1). \end{aligned} \tag{4.49}$$

Therefore, for any $T > 0$,

$$\sup_{0\leq t\leq T}\left[\tau_\theta ||\theta_m||^2_{L^2(\Omega)} + \tau_\eta ||\eta_m||^2_{L^2(\Omega)}\right] \leq \rho_0^2, \tag{4.50}$$

for some $\rho_0 \in \mathbb{R}$. It then follows that for any $T > 0$, there exist constants ρ_θ^{max} and ρ_η^{max} such that

$$\begin{aligned} \sup_{0\leq t\leq T} ||\theta_m||_{L^2(\Omega)} &< \rho_\theta^{max}, \\ \sup_{0\leq t\leq T} ||\eta_m||_{L^2(\Omega)} &< \rho_\eta^{max}. \end{aligned} \tag{4.51}$$

Furthermore, ρ_θ^{max} and ρ_η^{max} depend only on the norm of the initial data and on T. We can also integrate the bound on $y(t)$ from 0 to T to obtain

$$\int_0^T y(t)dt \leq \int_0^T \left[y(0)\mathrm{e}^{c_1 t} + \frac{c_2}{c_1}(\mathrm{e}^{c_1 t} - 1)\right]dt = \rho_1^2, \tag{4.52}$$

for some $\rho_1 \in \mathbb{R}$. This lead to the bounds

$$\begin{aligned} ||\theta_m||_{L^2(0,T;L^2(\Omega))} &< \rho_\theta, \\ ||\eta_m||_{L^2(0,T;L^2(\Omega))} &< \rho_\eta, \end{aligned} \tag{4.53}$$

where ρ_θ and ρ_η are constants depending only on the initial data and on T. Thus,

$$\begin{aligned} \theta_m &\in L^2(0,T;L^2(\Omega)) \cap L^\infty(0,T;L^2(\Omega)), \\ \eta_m &\in L^2(0,T;L^2(\Omega)) \cap L^\infty(0,T;L^2(\Omega)), \end{aligned} \tag{4.54}$$

with bounds that depend only on the norm of the initial data and on T.

Because of the bounds we have just exhibited for θ_m and η_m, we can conclude that there are no finite escape times for the d_k^m or e_k^m. Hence, solutions d_k^m and e_k^m to the system of ODEs (4.26) exist and are unique. Therefore, θ_m and η_m also exist and are unique solutions for the finite-dimensional projected system. To complete the existence proof, we need to show that a subsequence of these approximate solutions θ_m and η_m converges to a weak solution of our original system of PDEs. However, this first requires another energy estimate on θ_m and η_m, as well as an energy estimate on $\partial_t\theta_m$ and $\partial_t\eta_m$.

4.2.5 $L^2(0,T;L^2(\Omega))$ bounds for $\nabla\theta_m$ and $\nabla\eta_m$

From inequality (4.44), it follows that

$$\begin{aligned} \frac{1}{2}\tau_\theta\partial_t||\theta_m||^2_{L^2(\Omega)} + \frac{1}{2}\tau_\eta\partial_t||\eta_m||^2_{L^2(\Omega)} + \beta_\theta||\nabla\theta_m||^2_{L^2(\Omega)} + \beta_\eta||\nabla\eta_m||^2_{L^2(\Omega)} \\ \leq c''_\theta||\theta_m||^2_{L^2(\Omega)} + c''_\eta||\eta_m||^2_{L^2(\Omega)} + c''|\Omega|, \end{aligned} \tag{4.55}$$

where c''_θ, c''_η, and c'' are constants, and we recall that $\beta_\theta > 0$ and $\beta_\eta > 0$. Integrating both sides from 0 to T, we obtain

$$\begin{aligned} &\frac{1}{2}\tau_\theta||\theta_m(T)||^2_{L^2(\Omega)} - \frac{1}{2}\tau_\theta||\theta_m(0)||^2_{L^2(\Omega)} + \frac{1}{2}\tau_\eta||\eta_m(T)||^2_{L^2(\Omega)} - \frac{1}{2}\tau_\eta||\eta_m(0)||^2_{L^2(\Omega)} \\ &\quad +\beta_\theta||\nabla\theta_m||^2_{L^2(0,T;L^2(\Omega))} + \beta_\eta||\nabla\eta_m||^2_{L^2(0,T;L^2(\Omega))} \\ &\qquad \leq c''_\theta||\theta_m||^2_{L^2(0,T;L^2(\Omega))} + c''_\eta||\eta_m||^2_{L^2(0,T;L^2(\Omega))} + c''|\Omega|T \\ &\qquad \leq c''_\theta\rho_\theta^2 + c''_\eta\rho_\eta^2 + c''|\Omega|T. \end{aligned} \tag{4.56}$$

It then follows that

$$\begin{aligned}\beta_\theta||\nabla\theta_m||^2_{L^2(0,T;L^2(\Omega))} + \beta_\eta||\nabla\eta_m||^2_{L^2(0,T;L^2(\Omega))} & \\ \leq\ c''_\theta\rho^2_\theta + c''_\eta\rho^2_\eta + c''|\Omega|T + \frac{1}{2}\tau_\theta||\theta_m(0)||^2_{L^2(\Omega)} + \frac{1}{2}\tau_\eta||\eta_m(0)||^2_{L^2(\Omega)} & \\ =\ \rho_2^2, & \end{aligned} \tag{4.57}$$

where ρ_2 is a constant depending only on T and on the norm of the initial data. Thus,

$$\begin{aligned}\nabla\theta_m &\in L^2(0,T;L^2(\Omega)), \\ \nabla\eta_m &\in L^2(0,T;L^2(\Omega)),\end{aligned} \tag{4.58}$$

with bounds that depend only on the norm of the initial data and on T.

4.2.6 $L^{2p_\theta}(0,T;L^{2p_\theta}(\Omega))$ and $L^{2p_\eta}(0,T;L^{2p_\eta}(\Omega))$ bounds for θ_m and η_m

Returning to (4.35), the first through fourth terms can be treated the same as before using (4.36) and (4.37). However, for the first and sixth terms, we use (4.39) instead of (4.43), to obtain

$$\begin{aligned}\frac{1}{2}\tau_\theta\partial_t||\theta_m||^2_{L^2(\Omega)} + \frac{1}{2}\tau_\eta\partial_t||\eta_m||^2_{L^2(\Omega)} + \beta_\theta||\nabla\theta_m||^2_{L^2(\Omega)} - \gamma_\theta||\theta_m||^2_{L^2(\Omega)} & \\ +\beta_\eta||\nabla\eta_m||^2_{L^2(\Omega)} - \gamma_\eta||\eta_m||^2_{L^2(\Omega)} + \frac{1}{2}a_\theta||\theta_m||^{2p_\theta}_{L^{2p_\theta}(\Omega)} - c_\theta|\Omega| & \\ +\frac{1}{2}a_\eta||\eta_m||^{2p_\eta}_{L^{2p_\eta}(\Omega)} - c_\eta|\Omega| \ \leq\ 0, & \end{aligned} \tag{4.59}$$

from which it follows that

$$\begin{aligned}\frac{1}{2}\tau_\theta\partial_t||\theta_m||^2_{L^2(\Omega)} + \frac{1}{2}\tau_\eta\partial_t||\eta_m||^2_{L^2(\Omega)} + \frac{1}{2}a_\theta||\theta_m||^{2p_\theta}_{L^{2p_\theta}(\Omega)} + \frac{1}{2}a_\eta||\eta_m||^{2p_\eta}_{L^{2p_\eta}(\Omega)} & \\ \leq \gamma_\theta||\theta_m||^2_{L^2(\Omega)} + \gamma_\eta||\eta_m||^2_{L^2(\Omega)} + (c_\theta + c_\eta)|\Omega|. & \end{aligned} \tag{4.60}$$

Integrating both sides from 0 to T then gives

$$\frac{1}{2}\tau_\theta||\theta_m(T)||^2_{L^2(\Omega)} - \frac{1}{2}\tau_\theta||\theta_m(0)||^2_{L^2(\Omega)} + \frac{1}{2}\tau_\eta||\eta_m(T)||^2_{L^2(\Omega)} - \frac{1}{2}\tau_\eta||\eta_m(0)||^2_{L^2(\Omega)}$$

$$+\frac{1}{2}a_\theta||\theta_m||^{2p_\theta}_{L^{2p_\theta}(0,T;L^{2p_\theta}(\Omega))} + \frac{1}{2}a_\eta||\eta_m||^{2p_\eta}_{L^{2p_\eta}(0,T;L^{2p_\eta}(\Omega))}$$
$$\leq \gamma_\theta||\theta_m||^2_{L^2(0,T;L^2(\Omega))} + \gamma_\eta||\eta_m||^2_{L^2(0,T;L^2(\Omega))} + (c_\theta + c_\eta)|\Omega|T, \tag{4.61}$$

from which it follows that

$$\begin{aligned}
&\frac{1}{2}a_\theta||\theta_m||^{2p_\theta}_{L^{2p_\theta}(0,T;L^{2p_\theta}(\Omega))} + \frac{1}{2}a_\eta||\eta_m||^{2p_\eta}_{L^{2p_\eta}(0,T;L^{2p_\eta}(\Omega))} \\
&\quad\leq \gamma_\theta||\theta_m||^2_{L^2(0,T;L^2(\Omega))} + \gamma_\eta||\eta_m||^2_{L^2(0,T;L^2(\Omega))} + (c_\theta + c_\eta)|\Omega|T \\
&\qquad+\frac{1}{2}\tau_\theta||\theta_m(0)||^2_{L^2(\Omega)} + \frac{1}{2}\tau_\eta||\eta_m(0)||^2_{L^2(\Omega)} \\
&\quad\leq \gamma_\theta\rho_\theta^2 + \gamma_\eta\rho_\eta^2 + (c_\theta + c_\eta)|\Omega|T + \frac{1}{2}\tau_\theta||\theta_m(0)||^2_{L^2(\Omega)} + \frac{1}{2}\tau_\eta||\eta_m(0)||^2_{L^2(\Omega)} \\
&\quad\leq \rho_3^2,
\end{aligned} \tag{4.62}$$

for some constant ρ_3 depending only on T and on the norm of the initial data. Thus,

$$\begin{aligned}
\theta_m &\in L^{2p_\theta}(0,T;L^{2p_\theta}(\Omega)), \\
\eta_m &\in L^{2p_\eta}(0,T;L^{2p_\eta}(\Omega))
\end{aligned} \tag{4.63}$$

with bounds that depend only on the norm of the initial data and on T.

To summarize, the energy estimates we have proved so far show that θ_m and η_m are bounded sequences in their respective Hilbert spaces, namely

$$\begin{aligned}
\theta_m &\in L^\infty(0,T;L^2(\Omega)) \cap L^2(0,T;H^1(\Omega)) \cap L^{2p_\theta}(0,T;L^{2p_\theta}(\Omega)), \\
\eta_m &\in L^\infty(0,T;L^2(\Omega)) \cap L^2(0,T;H^1(\Omega)) \cap L^{2p_\eta}(0,T;L^{2p_\eta}(\Omega)).
\end{aligned} \tag{4.64}$$

Later in the existence proof we will define weak convergence and use the fact that a bounded sequence in a Hilbert space contains a weakly convergent subsequence. But first we also need energy estimates for $\partial_t\theta_m$ and $\partial_t\eta_m$.

4.2.7 $L^2(0,T;H^{-1}(\Omega))$ bounds for $\partial_t\theta_m$ and $\partial_t\eta_m$

We will only do the calculation for the estimate for $\partial_t\theta_m$, because the

corresponding calculation for the estimate for $\partial_t \eta_m$ is identical. The bound we are trying to obtain (for $\partial_t \theta$) is

$$\int_0^T |(\partial_t \theta_m, v)| dt \leq \text{constant}, \ \forall v \in H^1(\Omega) \cap L^{2p_\theta}(\Omega). \tag{4.65}$$

Observe that the space $H^1(\Omega) \cap L^{2p_\theta}(\Omega)$ is the space of time-independent functions belonging to the same space as θ_m, namely

$$v \in L^\infty(0,T;L^2(\Omega)) \cap L^2(0,T;H^1(\Omega)) \cap L^{2p_\theta}(0,T;L^{2p_\theta}(\Omega)), \tag{4.66}$$

but v does not depend on t. (Whenever we write $v \in H^1(\Omega)$, it is understood that in addition v satisfies the boundary conditions.)

An alternative approach to proving existence would have been to ignore the $L^{2p_\theta}(0,T;L^{2p_\theta}(\Omega))$ bound and then prove a bound like (4.65) $\forall v \in H^1(\Omega)$. In fact, for the bounded nonlinearity model (4.7), that is exactly the approach we must take. For the generalized polynomial nonlinearity model, the results obtained using the $L^{2p_\theta}(0,T;L^{2p_\theta}(\Omega))$ bound are stronger than those that would be obtained without it. (Note that since Ω is bounded, $L^{2p_\theta}(\Omega) \subset L^2(\Omega)$.)

So fix $v \in H^1(\Omega)$ with $||v||_{H^1(\Omega)} \leq 1$ and $||v||_{L^{2p_\theta}(\Omega)} \leq 1$. We can decompose v as

$$v = v_1 + v_2, \tag{4.67}$$

where

$$\begin{aligned} &v_1 \in \text{span}\{w_k\}_{k=1}^m, \\ &(v_2, w_k) = 0 \text{ for } k = 1, ..., m. \end{aligned} \tag{4.68}$$

The $\{w_k\}$ are a basis for $H^1(\Omega)$ and $L^2(\Omega)$ so

$$\begin{aligned} ||v_1||_{H^1(\Omega)} &\leq ||v||_{H^1(\Omega)} \leq 1, \\ ||v_1||_{L^{2p_\theta}(\Omega)} &\leq ||v||_{L^{2p_\theta}(\Omega)} \leq 1. \end{aligned} \tag{4.69}$$

Therefore, from (4.26), it follows that

$$\tau_\theta(\partial_t\theta_m, v_1) + B_\theta[\theta_m, v_1; t] = (-f_\theta(\theta_m) + \eta_m, v_1), \tag{4.70}$$

so

$$\begin{aligned}\tau_\theta(\partial_t\theta_m, v) &= \tau_\theta(\partial_t\theta_m, v_1) \\ &= (-f_\theta(\theta_m) + \eta_m, v_1) - B_\theta[\theta_m, v_1; t] \\ &= (-f_\theta(\theta_m), v_1) + (\eta_m, v_1) - B_\theta[\theta_m, v_1; t]. \end{aligned} \tag{4.71}$$

Therefore,

$$\tau_\theta \int_0^T |(\partial_t\theta_m, v)|dt \leq \int_0^T |(f_\theta(\theta_m), v_1)|dt + \int_0^T |(\eta_m, v_1)|dt + \int_0^T |B_\theta[\theta_m, v_1; t]|dt \tag{4.72}$$

For the last term, we need to derive a bound involving the bilinear form (which does not, incidentally, require the uniformly parabolic condition):

$$\begin{aligned}|B[u, v; t]| &\leq \sum_{i,j=1}^n ||a_{ij}||_{L^\infty(\Omega\times(0,T))} \int_\Omega |\nabla u||\nabla v|d\mathbf{x} \\ &\quad + \sum_{i=1}^n ||b_i||_{L^\infty(\Omega\times(0,T))} \int_\Omega |\nabla u||v|d\mathbf{x} + ||c||_{L^\infty(\Omega\times(0,T))} \int_\Omega |u||v|d\mathbf{x} \\ &\leq \alpha||u||_{H^1(\Omega)}||v||_{H^1(\Omega)}, \end{aligned} \tag{4.73}$$

for some constant α. Therefore, for the last term of (4.72), we have the bound

$$\begin{aligned}|B_\theta[\theta_m, v_1; t]| &\leq \alpha_\theta||\theta_m||_{H^1(\Omega)}||v_1||_{H^1(\Omega)} \\ &\leq \alpha_\theta||\theta_m||_{H^1(\Omega)}, \end{aligned} \tag{4.74}$$

for some $\alpha_\theta > 0$, so that

$$\int_0^T |B_\theta[\theta_m, v_1; t]|dt \leq \alpha_\theta||\theta_m||_{L^2(0,T;H^1(\Omega))}. \tag{4.75}$$

For the middle term of (4.72), we have the bound

$$|(\eta_m, v_1)| \leq ||\eta_m||_{L^2(\Omega)}||v_1||_{L^2(\Omega)} \leq ||\eta_m||_{L^2(\Omega)}, \tag{4.76}$$

so that

$$\int_0^T |(\eta_m, v_1)|dt \leq ||\eta_m||_{L^2(0,T;L^2(\Omega))}. \tag{4.77}$$

(For the general parabolic active transmission line, the term $-(\partial_x \eta_m, v_1)$ appears in equation (4.71) in place of (η_m, v_1). Therefore, we obtain the bound

$$\int_0^T |(\partial_x \eta_m, v_1)|dt \leq ||\eta_m||_{L^2(0,T;H^1(\Omega))}, \tag{4.78}$$

instead of (4.77).)

For the first term of (4.72), we have to do a little more work. Since $f_\theta(\cdot)$ is an odd-order polynomial with positive leading coefficient, we have the upper bound

$$|f_\theta(\theta_m)| \leq \frac{3}{2} a_\theta |\theta_m|^{2p_\theta - 1} + b_\theta, \tag{4.79}$$

where $a_\theta > 0$ is the leading coefficient of $f_\theta(\cdot)$ and $b_\theta > 0$ is a constant. Then

$$\begin{aligned} \int_0^T |(f_\theta(\theta_m), v_1)|dt &= \int_0^T \left| \int_\Omega f_\theta(\theta_m) v_1 d\mathbf{x} \right| dt \\ &\leq \int_0^T \int_\Omega |f_\theta(\theta_m)||v_1| d\mathbf{x} dt \\ &\leq \int_0^T \int_\Omega \frac{3}{2} a_\theta |\theta_m|^{2p_\theta - 1} |v_1| d\mathbf{x} dt + \int_0^T \int_\Omega b_\theta |v_1| d\mathbf{x} dt. \end{aligned} \tag{4.80}$$

Holder's inequality applied to the second term on the right implies

$$\begin{aligned} \int_0^T b_\theta \int_\Omega |v_1| d\mathbf{x} dt &\leq \int_0^T b_\theta \left(\int_\Omega v_1^2 d\mathbf{x} \right)^{1/2} |\Omega|^{1/2} dt \\ &\leq \int_0^T b_\theta |\Omega|^{1/2} dt \\ &= b_\theta |\Omega|^{1/2} T \quad = \quad \text{constant}. \end{aligned} \tag{4.81}$$

Holder's inequality applied twice to the first term implies

$$\begin{aligned} &\frac{3}{2} a_\theta \int_0^T \int_\Omega |\theta_m^{2p_\theta - 1}||v_1| d\mathbf{x} dt \\ &\leq \frac{3}{2} a_\theta \int_0^T \left(\int_\Omega \left(|\theta_m|^{2p_\theta - 1} \right)^{\frac{2p_\theta}{2p_\theta - 1}} d\mathbf{x} \right)^{\frac{2p_\theta - 1}{2p_\theta}} \left(\int_\Omega |v_1|^{2p_\theta} d\mathbf{x} \right)^{\frac{1}{2p_\theta}} dt \end{aligned}$$

$$
\begin{aligned}
&= \frac{3}{2}a_\theta \int_0^T \left(\int_\Omega |\theta_m|^{2p_\theta} d\mathbf{x}\right)^{\frac{2p_\theta-1}{2p_\theta}} \left(\int_\Omega |v_1|^{2p_\theta} d\mathbf{x}\right)^{\frac{1}{2p_\theta}} dt \\
&\leq \frac{3}{2}a_\theta \left[\int_0^T \left(\int_\Omega |\theta_m|^{2p_\theta} d\mathbf{x}\right)^{\frac{2p_\theta-1}{2p_\theta}\frac{2p_\theta}{2p_\theta-1}} dt\right]^{\frac{2p_\theta-1}{2p_\theta}} \left[\int_0^T \left(\int_\Omega |v_1|^{2p_\theta} d\mathbf{x}\right)^{\frac{1}{2p_\theta}2p_\theta} dt\right]^{\frac{1}{2p_\theta}} \\
&= \frac{3}{2}a_\theta \left[\int_0^T \left(\int_\Omega |\theta_m|^{2p_\theta} d\mathbf{x}\right) dt\right]^{\frac{2p_\theta-1}{2p_\theta}} \left[\int_0^T \left(\int_\Omega |v_1|^{2p_\theta} d\mathbf{x}\right) dt\right]^{\frac{1}{2p_\theta}} \\
&\leq \frac{3}{2}a_\theta T^{\frac{1}{2p_\theta}} \left(||\theta_m||_{L^{2p_\theta}(0,T;L^{2p_\theta}(\Omega))}\right)^{2p_\theta-1}. \qquad (4.82)
\end{aligned}
$$

Thus,

$$\int_0^T |(f_\theta(\theta_m), v)| dt \leq \rho'_\theta, \quad \forall v \in H^1(\Omega) \cap L^{2p_\theta}(\Omega), \qquad (4.83)$$

where ρ'_θ is a constant depending only on T and the norm of the initial data. (By a similar calculation, we can also deduce that

$$\int_0^T |(f_\eta(\eta_m), v)| dt \leq \rho'_\eta, \quad \forall v \in H^1(\Omega) \cap L^{2p_\eta}(\Omega), \qquad (4.84)$$

where ρ'_η is a constant depending only on T and on the norm of the initial data.)

Now, θ_m lies in the Hilbert space

$$L^\infty(0,T;L^2(\Omega)) \cap L^2(0,T;H^1(\Omega)) \cap L^{2p_\theta}(0,T;L^{2p_\theta}(\Omega)),$$

with inner product

$$((u,v)) = \int_0^T \int_\Omega uv \, d\mathbf{x} \, dt, \quad \forall u, v \in L^2(0,T;H^1(\Omega)), \qquad (4.85)$$

and $\partial_t \theta_m$ lies in the dual space to this Hilbert space. Since by the Riesz representation theorem, there is a canonical isomorphism between any Hilbert space and its dual, the dual space of

$$L^\infty(0,T;L^2(\Omega)) \cap L^2(0,T;H^1(\Omega)) \cap L^{2p_\theta}(0,T;L^{2p_\theta}(\Omega))$$

must be smaller than $L^2(0,T;H^{-1}(\Omega))$. The dual space to $L^{2p_\theta}(0,T;L^{2p_\theta}(\Omega))$ can be deduced by appealing to Holder's inequality:

$$\begin{aligned}
\int_0^T < u, v > dt &= \int_0^T \int_\Omega uv \; d\mathbf{x} \; dt \\
&\leq \int_0^T \left(\int_\Omega |u|^p d\mathbf{x} \right)^{1/p} \left(\int_\Omega |v|^q d\mathbf{x} \right)^{1/q} dt \\
&\leq \left[\int_0^T \left(\int_\Omega |u|^p d\mathbf{x} \right)^{\frac{1}{p} \cdot p} dt \right]^{1/p} \left[\int_0^T \left(\int_\Omega |v|^q d\mathbf{x} \right)^{\frac{1}{q} \cdot q} dt \right]^{1/q} \\
&= \left(\int_0^T \int_\Omega |u|^p d\mathbf{x} dt \right)^{1/p} \left(\int_0^T \int_\Omega |v|^q d\mathbf{x} dt \right)^{1/q} \\
&= ||u||_{L^p(0,T;L^p(\Omega))} ||v||_{L^q(0,T;L^q(\Omega))}, \qquad (4.86)
\end{aligned}$$

so that if $v \in L^p(0,T;L^p(\Omega))$, then we need $u \in L^q(0,T;L^q(\Omega))$ to insure the existence of the inner product (where $1/p + 1/q = 1$). Hence,

$$\partial_t \theta_m \in L^2(0,T;H^{-1}(\Omega)) \cap L^{q_\theta}(0,T;L^{q_\theta}(\Omega)), \;\; \frac{1}{2p_\theta} + \frac{1}{q_\theta} = 1. \qquad (4.87)$$

Now we can turn to what is meant by weak convergence. The precise definition applies to Banach spaces, but since we are dealing with Hilbert spaces, we can restrict the definition to the Hilbert space setting. In this context, θ_m converges weakly to θ means

$$\begin{aligned}
\int_0^T \int_\Omega \theta_m v \; d\mathbf{x} \; dt \;\; &\rightarrow \;\; \int_0^T \int_\Omega \theta v \; d\mathbf{x} \; dt, \\
&\forall v \in L^\infty(0,T;L^2(\Omega)) \cap L^2(0,T;H^1(\Omega)) \cap L^{2p_\theta}(0,T;L^{2p_\theta}(\Omega)). \qquad (4.88)
\end{aligned}$$

Also, $\partial_t \theta_m$ converges weakly to ϕ means

$$\begin{aligned}
\int_0^T \int_\Omega \partial_t \theta_m v \; d\mathbf{x} \; dt \;\; &\rightarrow \;\; \int_0^T \int_\Omega \phi v \; d\mathbf{x} \; dt, \\
&\forall v \in L^\infty(0,T;L^2(\Omega)) \cap L^2(0,T;H^1(\Omega)) \cap L^{2p_\theta}(0,T;L^{2p_\theta}(\Omega)). \qquad (4.89)
\end{aligned}$$

Although these two statements appear identical, they have slightly different interpretations because θ_m and $\partial_t \theta_m$ lie in different spaces ($\partial_t \theta_m$ lies in the dual space to θ_m).

We can now formulate more precisely the definition of a weak solution to the general polynomial-nonlinearity model. Functions

$$\begin{aligned}\theta &\in L^\infty(0,T;L^2(\Omega)) \cap L^2(0,T;H^1(\Omega)) \cap L^{2p_\theta}(0,T;L^{2p_\theta}(\Omega)),\\ \eta &\in L^\infty(0,T;L^2(\Omega)) \cap L^2(0,T;H^1(\Omega)) \cap L^{2p_\eta}(0,T;L^{2p_\eta}(\Omega))\end{aligned}$$

with

$$\begin{aligned}\partial_t\theta &\in L^2(0,T;H^{-1}(\Omega)) \cap L^{q_\theta}(0,T;L^{q_\theta}(\Omega)), \quad \frac{1}{2p_\theta}+\frac{1}{q_\theta}=1,\\ \partial_t\eta &\in L^2(0,T;H^{-1}(\Omega)) \cap L^{q_\eta}(0,T;L^{q_\eta}(\Omega)), \quad \frac{1}{2p_\eta}+\frac{1}{q_\eta}=1\end{aligned}$$

are a weak solution of the PDE system (4.2) provided θ and η satisfy the boundary conditions and initial conditions, and

$$\begin{aligned}\tau_\theta < \partial_t\theta, v > + B_\theta[\theta, v; t] &= (-f_\theta(\theta)+\eta, v),\\ \tau_\eta < \partial_t\eta, w > + B_\eta[\eta, w; t] &= (-f_\eta(\eta)-\theta, w)\end{aligned} \tag{4.90}$$

for each

$$\begin{aligned}v &\in H^1(\Omega) \cap L^{2p_\theta}(\Omega),\\ w &\in H^1(\Omega) \cap L^{2p_\eta}(\Omega)\end{aligned}$$

(with v and w also satisfying the boundary conditions), and for a.e. $t \in [0,T]$.

4.2.8 Convergence lemma

Before we can show the existence of a weak solution in the sense of the definition given in the last subsection, we need to prove the following lemma.

Lemma 4.1 *Assume*

$$\begin{aligned}&\theta_m \text{ converges weakly to } \theta \text{ in } L^2(0,T;H^1(\Omega)) \cap L^{2p_\theta}(0,T;L^{2p_\theta}(\Omega)),\\ &\partial_t\theta_m \text{ converges weakly to } \phi \text{ in } L^2(0,T;H^{-1}(\Omega)) \cap L^{q_\theta}(0,T;L^{q_\theta}(\Omega)).\end{aligned} \tag{4.91}$$

Then

$$\phi = \partial_t\theta. \tag{4.92}$$

Proof: Let

$$\begin{aligned} \rho &\in C_c^1(0,T) \text{ (C^1 functions with compact support in } \Omega \text{ defined on } (0,T)), \\ w &\in H^1(\Omega) \cap L^{2p_\theta}(\Omega). \end{aligned} \tag{4.93}$$

Then

$$\begin{aligned} 0 &= -\int_0^T < \partial_t \theta_m, \rho w > dt + \int_0^T < \partial_t \theta_m, \rho w > dt \\ &= \int_0^T < \theta_m, (\partial_t \rho) w > dt + \int_0^T < \partial_t \theta_m, \rho w > dt, \end{aligned} \tag{4.94}$$

using integration by parts. But weak convergence of θ_m to θ and $\partial_t \theta_m$ to ϕ then implies

$$\begin{aligned} 0 &= \int_0^T < \theta, (\partial_t \rho) w > dt + \int_0^T < \phi, \rho w > dt \\ &= -\int_0^T < \partial_t \theta, \rho w > dt + \int_0^T < \phi, \rho w > dt \\ &= \int_0^T < \phi - \partial_t \theta, \rho w > dt, \end{aligned} \tag{4.95}$$

where again we have used integration by parts. But since ρ and w were arbitrary,

$$< \phi - \partial_t \theta, w >= 0, \quad \forall w \in H^1(\Omega) \cap L^{2p_\theta}(\Omega). \tag{4.96}$$

Hence, $\phi = \partial_t \theta$. □

4.2.9 Existence proof

Lemma 4.2 *There exists a weak solution (as defined in subsection 4.2.7) for the general polynomial-nonlinearity model (4.2).*

Proof: We have already shown that

$$
\begin{aligned}
\{\theta_m\} &\text{ is a bounded sequence in} \\
&\qquad L^\infty(0,T;L^2(\Omega)) \cap L^2(0,T;H^1(\Omega)) \cap L^{2p_\theta}(0,T;L^{2p_\theta}(\Omega)), \\
\{\partial_t\theta_m\} &\text{ is a bounded sequence in } L^2(0,T;H^{-1}(\Omega)) \cap L^{q_\theta}(0,T;L^{q_\theta}(\Omega)), \\
\{\eta_m\} &\text{ is a bounded sequence in} \\
&\qquad L^\infty(0,T;L^2(\Omega)) \cap L^2(0,T;H^1(\Omega)) \cap L^{2p_\eta}(0,T;L^{2p_\eta}(\Omega)), \\
\{\partial_t\eta_m\} &\text{ is a bounded sequence in } L^2(0,T;H^{-1}(\Omega)) \cap L^{q_\eta}(0,T;L^{q_\eta}(\Omega)).
\end{aligned}
\tag{4.97}
$$

Because these are all bounded sequences in Hilbert spaces, they contain weakly convergent subsequences [46]. The lemma proved in the previous subsection can therefore be invoked to conclude that

$$
\begin{aligned}
\{\theta_{m_k}\} &\text{ converges weakly to} \\
&\qquad \theta \in L^\infty(0,T;L^2(\Omega)) \cap L^2(0,T;H^1(\Omega)) \cap L^{2p_\theta}(0,T;L^{2p_\theta}(\Omega)), \\
\{\partial_t\theta_{m_k}\} &\text{ converges weakly to } \partial_t\theta \in L^2(0,T;H^{-1}(\Omega)) \cap L^{q_\theta}(0,T;L^{q_\theta}(\Omega)), \\
\{\eta_{m_k}\} &\text{ converges weakly to} \\
&\qquad \eta \in L^\infty(0,T;L^2(\Omega)) \cap L^2(0,T;H^1(\Omega)) \cap L^{2p_\eta}(0,T;L^{2p_\eta}(\Omega)), \\
\{\partial_t\eta_{m_k}\} &\text{ converges weakly to } \partial_t\eta \in L^2(0,T;H^{-1}(\Omega)) \cap L^{q_\eta}(0,T;L^{q_\eta}(\Omega)),
\end{aligned}
\tag{4.98}
$$

where by taking subsequences of subsequences we can assume without loss of generality that the subsequence indices are the same for all four subsequences. We thus have a candidate for the weak solution.

Now we need to verify that our candidate weak solution is in fact a weak solution. As usual, we will only consider the calculations for the θ equation, since the calculations for the η equation are identical. Fix an integer N and

let

$$v \in L^2(0,T;H^1(\Omega)) \cap L^{2p_\theta}(0,T;L^{2p_\theta}(\Omega)) \tag{4.99}$$

have the form

$$v(t) = \sum_{k=1}^{N} v_k(t) w_k, \tag{4.100}$$

where the $v_k(t)$ are given functions of t only. Let $m \geq N$, multiply

$$\tau_\theta(\partial_t \theta_m, w_k) + B_\theta[\theta_m, w_k; t] = (-f_\theta(\theta_m) + \eta_m, w_k), \tag{4.101}$$

equation (4.26), through by $v_k(t)$, sum from $k = 1$ to N, and integrate with respect to t to obtain

$$\int_0^T (\tau_\theta < \partial_t \theta_m, v > + B_\theta[\theta_m, v; t])dt = \int_0^T (-f_\theta(\theta_m) + \eta_m, v)dt. \tag{4.102}$$

Considering subsequences and passing to weak limits then gives

$$\int_0^T (\tau_\theta < \partial_t \theta, v > + B_\theta[\theta, v; t])dt = \int_0^T (-f_\theta(\theta) + \eta, v)dt. \tag{4.103}$$

This last equality then holds for all $v \in L^2(0,T;H^1(\Omega)) \cap L^{2p_\theta}(0,T;L^{2p_\theta}(\Omega))$ because functions of the form

$$v(t) = \sum_{k=1}^{N} v_k(t) w_k$$

are dense in this space. Hence,

$$\tau_\theta < \partial_t \theta, v > + B_\theta[\theta, v; t] = (-f_\theta(\theta) + \eta, v), \quad \forall v \in H^1(\Omega) \cap L^{2p_\theta}(\Omega), \tag{4.104}$$

and for a.e. $t \in [0,T]$. Similarly,

$$\tau_\eta < \partial_t \eta, w > + B_\eta[\eta, w; t] = (-f_\eta(\eta) - \theta, w), \quad \forall w \in H^1(\Omega) \cap L^{2p_\eta}(\Omega), \tag{4.105}$$

and for a.e. $t \in [0,T]$.

Finally, we need to verify that our candidate weak solution satisfies the initial conditions $\theta(0) = g_\theta$ and $\eta(0) = g_\eta$. Assume that v, as defined above,

is also C^1 and satisifies $v(T) = 0$. Then from (4.103), it follows that

$$-\tau_\theta(\theta(0), v(0)) + \int_0^T (-\tau_\theta < \partial_t v, \theta > + B_\theta[\theta, v; t])dt = \int_0^T (-f_\theta(\theta) + \eta, v)dt. \tag{4.106}$$

But also, from (4.102), it follows that

$$-\tau_\theta(\theta_m(0), v(0)) + \int_0^T (-\tau_\theta < \partial_t v, \theta_m > + B_\theta[\theta_m, v; t])dt = \int_0^T (-f_\theta(\theta_m) + \eta_m, v)dt, \tag{4.107}$$

which in passing to limits (with appropriate subsequences) gives

$$-\tau_\theta(g_\theta, v(0)) + \int_0^T (-\tau_\theta < \partial_t v, \theta > + B_\theta[\theta, v; t])dt = \int_0^T (-f_\theta(\theta) + \eta, v)dt, \tag{4.108}$$

since $\theta_{m_k}(0) \to g_\theta$ in $L^2(\Omega)$. Thus,

$$(\theta(0), v(0)) = (g_\theta, v(0)), \tag{4.109}$$

but because $v(0)$ is arbitrary, we conclude that $\theta(0) = g_\theta$. $\square$

4.2.10 Uniqueness proof

Lemma 4.3 *The weak solution for the general polynomial-nonlinearity model (4.2) is unique.*

Proof: Suppose there are two weak solutions, (θ_1, η_1) and (θ_2, η_2). Then

$$\begin{aligned}
\tau_\theta < \partial_t \theta_1, v > + B_\theta[\theta_1, v; t] &= (-f_\theta(\theta_1) + \eta_1, v), \quad \theta_1(0) = g_\theta, \\
\tau_\eta < \partial_t \eta_1, w > + B_\eta[\eta_1, w; t] &= (-f_\eta(\eta_1) - \theta_1, w), \quad \eta_1(0) = g_\eta, \\
\tau_\theta < \partial_t \theta_2, v > + B_\theta[\theta_2, v; t] &= (-f_\theta(\theta_2) + \eta_2, v), \quad \theta_2(0) = g_\theta, \\
\tau_\eta < \partial_t \eta_2, w > + B_\eta[\eta_2, w; t] &= (-f_\eta(\eta_2) - \theta_2, w), \quad \eta_2(0) = g_\eta, \\
\forall v \in H^1(\Omega) \cap L^{2p_\theta}(\Omega), \ \ \forall w \in H^1(\Omega) \cap L^{2p_\eta}(\Omega).
\end{aligned} \tag{4.110}$$

Letting $v = \theta_2 - \theta_1$ and $w = \eta_2 - \eta_1$, and using the bilinearity of B_θ and B_η, we obtain

$$\begin{aligned}
\tau_\theta < \partial_t(\theta_2 - \theta_1), (\theta_2 - \theta_1) > + B_\theta[\theta_2 - \theta_1, \theta_2 - \theta_1; t] & \\
= \quad (-(f_\theta(\theta_2) - f_\theta(\theta_1)) + (\eta_2 - \eta_1), \theta_2 - \theta_1), & \\
\tau_\eta < \partial_t(\eta_2 - \eta_1), (\eta_2 - \eta_1) > + B_\eta[\eta_2 - \eta_1, \eta_2 - \eta_1; t] & \\
= \quad (-(f_\eta(\eta_2) - f_\eta(\eta_1)) - (\theta_2 - \theta_1), \eta_2 - \eta_1), & \\
(\theta_2 - \theta_1)(0) = 0, & \\
(\eta_2 - \eta_1)(0) = 0. &
\end{aligned} \tag{4.111}$$

Letting $\delta\theta = \theta_2 - \theta_1$ and $\delta\eta = \eta_2 - \eta_1$, the above equations become

$$\begin{aligned}
\tau_\theta < \partial_t \delta\theta, \delta\theta > + B_\theta[\delta\theta, \delta\theta; t] &= (-(f_\theta(\theta_2) - f_\theta(\theta_1)) + \delta\eta, \delta\theta), \\
\tau_\eta < \partial_t \delta\eta, \delta\eta > + B_\eta[\delta\eta, \delta\eta; t] &= (-(f_\eta(\eta_2) - f_\eta(\eta_1)) - \delta\theta, \delta\eta), \\
\delta\theta(0) &= 0, \\
\delta\eta(0) &= 0.
\end{aligned} \tag{4.112}$$

Adding the $\delta\theta$ and $\delta\eta$ equations gives

$$\begin{aligned}
\frac{1}{2}\partial_t \left[\tau_\theta ||\delta\theta||^2_{L^2(\Omega)} + \tau_\eta ||\delta\eta||^2_{L^2(\Omega)}\right] + B_\theta[\delta\theta, \delta\theta; t] + B_\eta[\delta\eta, \delta\eta; t] & \\
= \quad (-(f_\theta(\theta_2) - f_\theta(\theta_1)), \delta\theta) + (-(f_\eta(\eta_2) - f_\eta(\eta_1)), \delta\eta). &
\end{aligned} \tag{4.113}$$

To handle the bilinear terms, we can use the inequalities (4.37),

$$\begin{aligned}
B_\theta[\delta\theta, \delta\theta; t] &\geq \beta_\theta ||\nabla\delta\theta||^2_{L^2(\Omega)} - \gamma_\theta ||\delta\theta||^2_{L^2(\Omega)}, \\
B_\eta[\delta\eta, \delta\eta; t] &\geq \beta_\eta ||\nabla\delta\eta||^2_{L^2(\Omega)} - \gamma_\eta ||\delta\eta||^2_{L^2(\Omega)},
\end{aligned} \tag{4.114}$$

where β_θ, γ_θ, β_η, and γ_η are constants, with $\beta_\theta > 0$ and $\beta_\eta > 0$. In fact, for our purposes here, we can simplify these inequalities to

$$\begin{aligned}
B_\theta[\delta\theta, \delta\theta; t] &\geq -\gamma_\theta ||\delta\theta||^2_{L^2(\Omega)}, \\
B_\eta[\delta\eta, \delta\eta; t] &\geq -\gamma_\eta ||\delta\eta||^2_{L^2(\Omega)},
\end{aligned} \tag{4.115}$$

leading to

$$\begin{aligned}\frac{1}{2}\partial_t \left[\tau_\theta ||\delta\theta||^2_{L^2(\Omega)} + \tau_\eta ||\delta\eta||^2_{L^2(\Omega)}\right] \\ \leq \ \gamma_\theta ||\delta\theta||^2_{L^2(\Omega)} + \gamma_\eta ||\delta\eta||^2_{L^2(\Omega)} + (-(f_\theta(\theta_2) - f_\theta(\theta_1)), \delta\theta) \\ +(-(f_\eta(\eta_2) - f_\eta(\eta_1)), \delta\eta). \end{aligned} \tag{4.116}$$

To handle the last two terms on the right, we need to use some simple facts about polynomials. Also, we will only consider the θ term, because the η term is handled identically. The first fact is that any term of the form $\theta_2^n - \theta_1^n$ can be factored as follows:

$$\theta_2^n - \theta_1^n = (\theta_2 - \theta_1)(\theta_2^{n-1} + \theta_2^{n-2}\theta_1 + \theta_2^{n-2}\theta_1^2 + \cdots + \theta_2\theta_1^{n-2} + \theta_1^{n-1}). \tag{4.117}$$

Furthermore, for n odd and $\theta_1 \neq \theta_2$,

$$(\theta_2^{n-1} + \theta_2^{n-2}\theta_1 + \theta_2^{n-2}\theta_1^2 + \cdots + \theta_2\theta_1^{n-2} + \theta_1^{n-1}) > 0. \tag{4.118}$$

Since $f_\theta(\cdot)$ is odd-order with a positive leading coefficient, we can write

$$\begin{aligned} f_\theta(\theta) &= a_\theta\theta^{2p_\theta-1} + a_{2p_\theta-2}\theta^{2p_\theta-2} + \cdots + a_1\theta + a_0, \\ f_\theta(\theta_2) - f_\theta(\theta_1) &= a_\theta(\theta_2^{2p_\theta-1} - \theta_1^{2p_\theta-1}) + a_{2p_\theta-2}(\theta_2^{2p_\theta-2} - \theta_1^{2p_\theta-2}) \\ &\quad + \cdots + a_1(\theta_2 - \theta_1) \\ &= a_\theta(\theta_2 - \theta_1)(\theta_2^{2p_\theta-2} + \theta_2^{2p_\theta-3}\theta_1 + \cdots + \theta_1^{2p_\theta-2}) \\ &\quad + a_{2p_\theta-2}(\theta_2 - \theta_1)(\theta_2^{2p_\theta-3} + \theta_2^{2p_\theta-4}\theta_1 + \cdots + \theta_1^{2p_\theta-3}) \\ &\quad + \cdots + a_1(\theta_2 - \theta_1). \end{aligned} \tag{4.119}$$

Defining

$$h_{\theta n}(\theta_1, \theta_2) = \theta_2^{n-1} + \theta_2^{n-2}\theta_1 + \theta_2^{n-3}\theta_1^2 + \cdots + \theta_2\theta_1^{n-2} + \theta_1^{n-1}, \tag{4.120}$$

then $h_{\theta(2p_\theta-1)}(\theta_1, \theta_2) \geq 0$, and we have the bounds

$$|h_{\theta n}(\theta_1, \theta_2)| \leq c_n + \frac{1}{2p_\theta} h_{\theta(2p_\theta-1)}(\theta_1, \theta_2), \quad n = 2, ..., 2p_\theta - 2, \quad \forall\theta_1, \theta_2, \tag{4.121}$$

where $c_n > 0$, $n = 2, ..., 2p_\theta - 2$. Therefore,

$$\begin{aligned}
&(-(f_\theta(\theta_2) - f_\theta(\theta_1)), \delta\theta) \\
&\quad = -a_\theta \int_\Omega \delta\theta^2 h_{\theta(2p_\theta-1)}(\theta_1, \theta_2) d\mathbf{x} - a_{2p_\theta-2} \int_\Omega \delta\theta^2 h_{\theta(2p_\theta-2)}(\theta_1, \theta_2) d\mathbf{x} \\
&\qquad + \cdots + a_1 \int_\Omega \delta\theta^2 d\mathbf{x} \\
&\quad \leq -a_\theta \frac{3}{2p_\theta} \int_\Omega \delta\theta^2 h_{\theta(2p_\theta-1)}(\theta_1, \theta_2) d\mathbf{x} + c_{(2p_\theta-2)} \int_\Omega \delta\theta^2 d\mathbf{x} \\
&\qquad + \cdots + c_2 \int_\Omega \delta\theta^2 d\mathbf{x} + a_1 \int_\Omega \delta\theta^2 d\mathbf{x} \\
&\quad \leq (c_{(2p_\theta-2)} + \cdots + c_2 + a_1) ||\delta\theta||^2_{L^2(\Omega)} \\
&\quad = c'_\theta ||\delta\theta||^2_{L^2(\Omega)}, \qquad (4.122)
\end{aligned}$$

where c'_θ is a constant. Similarly,

$$(-(f_\eta(\eta_2) - f_\eta(\eta_1)), \delta\eta) \leq c'_\eta ||\delta\eta||^2_{L^2(\Omega)}, \qquad (4.123)$$

where c'_η is a constant. Therefore we have

$$\begin{aligned}
\frac{1}{2}\partial_t \left[\tau_\theta ||\delta\theta||^2_{L^2(\Omega)} + \tau_\eta ||\delta\eta||^2_{L^2(\Omega)}\right] &\leq (\gamma_\theta + c'_\theta) ||\delta\theta||^2_{L^2(\Omega)} + (\gamma_\eta + c'_\eta) ||\delta\eta||^2_{L^2(\Omega)} \\
&\leq c'' \left[\tau_\theta ||\delta\theta||^2_{L^2(\Omega)} + \tau_\eta ||\delta\eta||^2_{L^2(\Omega)}\right], \qquad (4.124)
\end{aligned}$$

for some constant c''. The usual Gronwall lemma then implies

$$\begin{aligned}
||\delta\theta||^2_{L^2(\Omega)} &= 0, \\
||\delta\eta||^2_{L^2(\Omega)} &= 0, \quad \forall t \in [0, T]. \qquad (4.125)
\end{aligned}$$

Therefore, the weak solutions are unique. □

4.2.11 Continuous dependence on initial data

We can use the same calculation used to show uniqueness to show continuous dependence of the solutions on the initial data. Suppose now that (θ_1, η_1) and (θ_2, η_2) are two solutions with different initial data $(g_{\theta 1}, g_{\eta 1})$ and $(g_{\theta 2}, g_{\eta 2})$. Then we can define

$$\begin{aligned} \delta g_\theta &= g_{\theta 2} - g_{\theta 1}, \\ \delta g_\eta &= g_{\eta 2} - g_{\eta 1}. \end{aligned} \tag{4.126}$$

The usual Gronwall lemma then implies

$$\begin{aligned} ||\delta\theta||^2_{L^2(\Omega)} &\leq ||\delta g_\theta||^2_{L^2(\Omega)} \mathrm{e}^{c'' t}, \\ ||\delta\eta||^2_{L^2(\Omega)} &\leq ||\delta g_\eta||^2_{L^2(\Omega)} \mathrm{e}^{c'' t}. \end{aligned} \tag{4.127}$$

Thus, for each t, $||\delta\theta||_{L^2(\Omega)}$ and $||\delta\eta||_{L^2(\Omega)}$ can be made arbitrarily small by choosing $||\delta g_\theta||_{L^2(\Omega)}$ and $||\delta g_\eta||_{L^2(\Omega)}$ sufficiently small, which is what is meant by continuous dependence of the solutions on the initial data.

4.3 Generalizations of the basic existence and uniqueness results

4.3.1 Bounded nonlinearity model

For the bounded nonlinearity model, equation (4.7), the existence and uniqueness proofs are much simpler since we are given a (constant) bound on the nonlinearity $f(\theta)$. By the same general procedure as for the general polynomial nonlinearity model, we find

$$\begin{aligned} \theta &\in L^\infty(0,T;L^2(\Omega)) \cap L^2(0,T;H^1(\Omega)), \\ \eta &\in L^\infty(0,T;L^2(\Omega)) \cap L^2(0,T;H^1(\Omega)), \\ \partial_t\theta &\in L^2(0,T;H^{-1}(\Omega)), \\ \partial_t\eta &\in L^2(0,T;H^{-1}(\Omega)), \end{aligned} \tag{4.128}$$

with bounds that depend only on the norm of the initial data and on T.

4.3.2 Complex activator-inhibitor equation

Existence and uniqueness of weak solutions for the complex activator-

inhibitor equation (4.8) can be proved by considering the corresponding coupled pair of real activator-inhibitor equations,

$$\begin{aligned}
\tau_\theta \partial_t \theta_R &= l^2 \Delta \theta_R - (\theta_R^2 + \theta_I^2)\theta_R + \theta_R + \eta_R, \\
\tau_\theta \partial_t \theta_I &= l^2 \Delta \theta_I - (\theta_R^2 + \theta_I^2)\theta_I + \theta_I + \eta_I, \\
\tau_\eta \partial_t \eta_R &= L^2 \Delta \eta_R - \eta_R - \theta_R + C_R, \\
\tau_\eta \partial_t \eta_I &= L^2 \Delta \eta_I - \eta_I - \theta_I + C_I,
\end{aligned} \tag{4.129}$$

where $\theta_R = \mathrm{Re}\{\theta\}$, $\theta_I = \mathrm{Im}\{\theta\}$, etc. Because of the form of the coupling between the two activator equations, we obtain an inequality like (4.44), but with twice as many terms (i.e., for every term of (4.44) involving θ_m, there is a corresponding term with θ_{Rm} and another with θ_{Im}, and similarly for terms of (4.44) involving η_m). Also, the boundary conditions

$$\begin{aligned}
\theta_R(\nabla\theta_R \cdot \mathbf{n}) + \theta_I(\nabla\theta_I \cdot \mathbf{n}) &= 0, \\
\eta_R(\nabla\eta_R \cdot \mathbf{n}) + \eta_I(\nabla\eta_I \cdot \mathbf{n}) &= 0
\end{aligned} \tag{4.130}$$

on $\partial\Omega$ (where $\mathbf{n}$ is the unit outer normal to $\partial\Omega$) still cause the boundary terms from integrating

$$l^2 \left[\int_\Omega \theta_R \Delta\theta_R d\mathbf{x} + \int_\Omega \theta_I \Delta\theta_I d\mathbf{x} \right] + L^2 \left[\int_\Omega \eta_R \Delta\eta_R d\mathbf{x} + \int_\Omega \eta_I \Delta\eta_I d\mathbf{x} \right] \tag{4.131}$$

by parts to disappear. Therefore, the existence and uniqueness proofs go through just as for the general polynomial-nonlinearity model. In fact, the complex activator-inhibitor equation is just one example of how pairs of activator-inhibitor equations can be coupled so that the same types of energy bounds are still satisfied.

4.3.3 Additional symmetric long-range coupling

Symmetric long-range coupling can be added to the general polynomial-

nonlinearity model by adding a term

$$(z * \theta)(\mathbf{x}, t) = \int_\Omega z(\mathbf{x} - \mathbf{y})\theta(\mathbf{y}, t)d\mathbf{y} \tag{4.132}$$

to the $\partial_t\theta$ equation, where z is symmetric about the origin, and the operator norm of $z * \cdot$ is bounded:

$$\exists \rho_z > 0 \text{ such that } ||z * \theta||_{L^2(\Omega)} \leq \rho_z ||\theta||_{L^2(\Omega)}, \quad \forall \theta \in L^2(\Omega). \tag{4.133}$$

(For periodic boundary conditions, the convolution operation is interpreted as cyclic convolution.)

Since we have the bound

$$\begin{aligned} \left| \int_\Omega (z * \theta)(\mathbf{x})\theta(\mathbf{x})d\mathbf{x} \right| &\leq \int_\Omega |(z * \theta)(\mathbf{x})\theta(\mathbf{x})|d\mathbf{x} \\ &\leq \frac{1}{2}||z * \theta||_{L^2(\Omega)} + \frac{1}{2}||\theta||_{L^2(\Omega)} \\ &\leq \frac{1 + \rho_z}{2}||\theta||_{L^2(\Omega)}, \end{aligned} \tag{4.134}$$

inequality (4.44) is essentially unchanged. Furthermore, the additional term which would appear in equation (4.72) would be easily bounded, so the existence proof would go through as for the general polynomial-nonlinearity model. The uniqueness proof also requires only slight modification.

4.4 Existence and uniqueness of weak solutions for the active transmission-line model without inhibitor diffusion

The standard approach for proving existence and uniqueness of weak solutions for a hyperbolic system like (4.6) (without the $\partial_{xx}\theta$ term) is the vanishing viscosity method. Since the $\partial_{xx}\theta$ term is present, to use the vanishing viscosity method, we need only add a term $\epsilon\partial_{xx}\eta$ to the $\partial_t\eta$ equation:

$$\begin{aligned} \tau_\theta \partial_t \theta &= l^2 \partial_{xx}\theta - \theta^3 + \theta - C - \partial_x \eta, \\ \tau_\eta \partial_t \eta &= \epsilon \partial_{xx}\eta - \partial_x \theta. \end{aligned} \tag{4.135}$$

From the existence and uniqueness analysis for the general parabolic active transmission-line model, we have

$$\begin{aligned} \theta &\in L^{\infty}(0,T;L^2(\Omega)) \cap L^2(0,T;H^1(\Omega)) \cap L^4(0,T;L^4(\Omega)), \\ \eta &\in L^{\infty}(0,T;L^2(\Omega)) \cap L^2(0,T;H^1(\Omega)), \\ \partial_t\theta &\in L^2(0,T;H^{-1}(\Omega)) \cap L^{4/3}(0,T;L^{4/3}(\Omega)), \\ \partial_t\eta &\in L^2(0,T;H^{-1}(\Omega)), \end{aligned} \tag{4.136}$$

with bounds that depend on the norm of the initial data, on T, and on ϵ (the $-\eta$ term missing from the $\partial_t\eta$ equation is not required for obtaining the above energy estimates). The idea of the vanishing viscosity method is to obtain bounds like (4.136) which are uniform in ϵ, so that they still hold as we take $\epsilon \to 0$.

The bounds

$$\begin{aligned} \theta &\in L^{\infty}(0,T;L^2(\Omega)) \cap L^2(0,T;L^2(\Omega)) \cap L^4(0,T;L^4(\Omega)), \\ \eta &\in L^{\infty}(0,T;L^2(\Omega)) \cap L^2(0,T;L^2(\Omega)) \end{aligned} \tag{4.137}$$

are already uniform in ϵ (in fact, so is $\theta \in L^2(0,T;H^1(\Omega))$, since $l > 0$). We need the results

$$\begin{aligned} \theta &\in L^2(0,T;H^2(\Omega)), \\ \eta &\in L^2(0,T;H^2(\Omega)), \end{aligned} \tag{4.138}$$

where the bounds depends on ϵ, to proceed further. This second derivative bound is obtained in a similar fashion to the regularity proof for the general polynomial-nonlinearity model given in the next section. With this bound, we can define

$$\begin{aligned} \psi &= \partial_x\theta, \\ \zeta &= \partial_x\eta, \end{aligned} \tag{4.139}$$

and the system of equations

$$\begin{aligned} \tau_\theta \partial_t \psi &= l^2 \partial_{xx} \psi - 3\theta^2 \psi + \psi + \partial_x \zeta, \\ \tau_\eta \partial_t \zeta &= \epsilon \partial_{xx} \zeta - \partial_x \psi \end{aligned} \tag{4.140}$$

will be well-posed. (We will assume periodic or Neumann boundary conditions for the original system so that this system will have either periodic or Dirichlet boundary conditions.) By the same procedure as before, we can show that there exists a unique weak solution to the system (4.140), and

$$\begin{aligned} \psi &\in L^\infty(0,T;L^2(\Omega)) \cap L^2(0,T;H^1(\Omega)), \\ \zeta &\in L^\infty(0,T;L^2(\Omega)) \cap L^2(0,T;H^1(\Omega)), \\ \partial_t \psi &\in L^2(0,T;H^{-1}(\Omega)), \\ \partial_t \zeta &\in L^2(0,T;H^{-1}(\Omega)), \end{aligned} \tag{4.141}$$

with bounds depending only on T and on the norm of the initial data, for which we assume

$$\begin{aligned} \psi(0) &= \partial_x g_\theta \in L^2(\Omega), \\ \zeta(0) &= \partial_x g_\eta \in L^2(\Omega). \end{aligned} \tag{4.142}$$

By uniqueness of weak solutions for both the original system (4.135) and for the system (4.140), we can conclude that, indeed, $\partial_x \theta = \psi$ and $\partial_x \eta = \zeta$. Furthermore, the bounds

$$\begin{aligned} \psi &\in L^2(0,T;L^2(\Omega)), \\ \zeta &\in L^2(0,T;L^2(\Omega)) \end{aligned} \tag{4.143}$$

do not depend on ϵ, and so we have the necessary bounds independent of ϵ to conclude the existence and uniqueness of weak solutions for the active transmission line without inhibitor diffusion, equation (4.6). (The remaining details are exactly as in the analysis of hyperbolic systems using the vanishing viscosity method [46].)

4.5 Regularity of weak solutions for the general polynomial-nonlinearity model

4.5.1 Further energy bounds for θ and $\partial_t\theta$

Throughout the regularity analysis, we will only work with the θ equations, since the corresponding calculations for the η equations are identical. Although our basic goal here is to prove

$$\begin{aligned} \theta &\in L^2(0,T;H^2(\Omega)), \\ \eta &\in L^2(0,T;H^2(\Omega)), \end{aligned} \tag{4.144}$$

we need to first prove some simpler energy bounds. Specifically, we need to show

$$\begin{aligned} \theta &\in L^\infty(0,T;H^1(\Omega)) \cap L^\infty(0,T;L^{2p_\theta}(\Omega)), \\ \partial_t\theta &\in L^2(0,T;L^2(\Omega)). \end{aligned} \tag{4.145}$$

Even though we need to assume regularity of the boundary $\partial\Omega$ to prove the bounds (4.144), we can prove the bounds (4.145) without requiring boundary regularity. We do need to assume that the initial data satisfies

$$\begin{aligned} g_\theta &\in L^{2p_\theta}(\Omega), \\ g_\eta &\in L^{2p_\eta}(\Omega). \end{aligned} \tag{4.146}$$

Starting with equation (4.26),

$$\tau_\theta(\partial_t\theta_m, w_k) + B_\theta[\theta_m, w_k; t] = (-f(\theta_m) + \eta_m, w_k), \tag{4.147}$$

we now multiply by $\partial_t d_k^m$ and sum from $k = 1$ to m to obtain

$$\tau_\theta(\partial_t\theta_m, \partial_t\theta_m) + B_\theta[\theta_m, \partial_t\theta_m; t] = (-f(\theta_m) + \eta_m, \partial_t\theta_m). \tag{4.148}$$

Written out, the bilinear term looks like

$$B_\theta[\theta_m, \partial_t\theta_m; t] = \int_\Omega \sum_{i,j=1}^n a_{ij}(\partial_{x_i}\theta_m)[\partial_{x_j}(\partial_t\theta_m)]d\mathbf{x} + \int_\Omega \sum_{i=1}^n b_i(\partial_{x_i}\theta_m)(\partial_t\theta_m)d\mathbf{x} + \int_\Omega c\,\theta_m(\partial_t\theta_m)d\mathbf{x}. \quad (4.149)$$

Defining

$$A_\theta[u,v] = \int_\Omega \sum_{i,j=1}^n a_{ij}(\partial_{x_i}u)(\partial_{x_j}v)d\mathbf{x}, \;\; \forall u, v \in H^1(\Omega), \quad (4.150)$$

we then have

$$\frac{1}{2}\frac{d}{dt}A_\theta[u,v] = \frac{1}{2}\int_\Omega \sum_{i,j=1}^n a_{ij}[(\partial_{x_i}(\partial_t u))(\partial_{x_j}v) + (\partial_{x_i}u)(\partial_{x_j}(\partial_t v))]d\mathbf{x} + \frac{1}{2}\int_\Omega \sum_{i,j=1}^n (\partial_t a_{ij})(\partial_{x_i}u)(\partial_{x_j}v)d\mathbf{x}, \quad (4.151)$$

so

$$\begin{aligned}\int_\Omega \sum_{i,j=1}^n a_{ij}(\partial_{x_i}\theta_m)[\partial_{x_j}(\partial_t\theta_m)]d\mathbf{x} &= \frac{1}{2}\int_\Omega \sum_{i,j=1}^n a_{ij}[(\partial_{x_i}(\partial_t\theta_m))(\partial_{x_j}\theta_m) + (\partial_{x_i}\theta_m)(\partial_{x_j}(\partial_t\theta_m))]d\mathbf{x} \\ &= \frac{1}{2}\frac{d}{dt}A_\theta[\theta_m,\theta_m] - \frac{1}{2}\int_\Omega \sum_{i,j=1}^n (\partial_t a_{ij})(\partial_{x_i}\theta_m)(\partial_{x_j}\theta_m)d\mathbf{x}, \quad (4.152)\end{aligned}$$

since by assumption $a_{ij} = a_{ji}$. We assumed that $\partial_t a_{ij}$ was continuous $\forall i, j$, and if we further assume that $\partial_t a_{ij}$ is bounded $\forall i, j$, then

$$\left|\frac{1}{2}\int_\Omega \sum_{i,j=1}^n (\partial_t a_{ij})(\partial_{x_i}\theta_m)(\partial_{x_j}\theta_m)d\mathbf{x}\right| \leq C_0||\theta_m||^2_{H^1(\Omega)} \quad (4.153)$$

for some constant C_0. Also, using Holder's inequality and Cauchy's inequality with ϵ,

$$\int_\Omega \sum_{i=1}^n b_i(\partial_{x_i}\theta_m)(\partial_t\theta_m)d\mathbf{x} + \int_\Omega c\,\theta_m(\partial_t\theta_m)d\mathbf{x} \leq \frac{C_1}{\epsilon}||\theta_m||^2_{H^1(\Omega)} + \epsilon||\partial_t\theta_m||^2_{L^2(\Omega)}, \quad (4.154)$$

for all $\epsilon > 0$ and some constant $C_1 > 0$.

Next, we have

$$(-f(\theta_m)+\eta_m,\partial_t\theta_m)=-(f(\theta_m),\partial_t\theta_m)+(\eta_m,\partial_t\theta_m), \tag{4.155}$$

but again by Holder's inequality and Cauchy's inequality with ϵ we have

$$|(\eta_m,\partial_t\theta_m)|\leq\frac{C_2}{\epsilon}||\eta_m||^2_{L^2(\Omega)}+\epsilon||\partial_t\theta_m||^2_{L^2(\Omega)}. \tag{4.156}$$

We can also write

$$\begin{aligned}(f(\theta_m),\partial_t\theta_m) &= \int_\Omega\left(a_\theta\theta_m^{2p_\theta-1}+a_{2p_\theta-2}\theta_m^{2p_\theta-2}+\cdots+a_1\theta_m+a_0\right)\partial_t\theta_m d\mathbf{x}\\ &= \frac{a_\theta}{2p_\theta}\partial_t\int_\Omega\theta_m^{2p_\theta}d\mathbf{x}+\frac{a_{2p_\theta-2}}{2p_\theta-1}\partial_t\int_\Omega\theta_m^{2p_\theta-1}d\mathbf{x}+\cdots\\ &\quad+\frac{a_1}{2}\partial_t\int_\Omega\theta_m^2d\mathbf{x}+a_0\partial_t\int_\Omega\theta_m d\mathbf{x}.\end{aligned} \tag{4.157}$$

We thus obtain the following inequality:

$$\begin{aligned}&\tau_\theta||\partial_t\theta_m||^2_{L^2(\Omega)}+\frac{1}{2}\partial_tA_\theta[\theta_m,\theta_m]+\frac{a_\theta}{2p_\theta}\partial_t\int_\Omega\theta_m^{2p_\theta}d\mathbf{x}\\ &+\frac{a_{2p_\theta-2}}{2p_\theta-1}\partial_t\int_\Omega\theta_m^{2p_\theta-1}d\mathbf{x}+\cdots+\frac{a_1}{2}\partial_t\int_\Omega\theta_m^2d\mathbf{x}+a_0\partial_t\int_\Omega\theta_m d\mathbf{x}\\ &\qquad\leq\left(C_0+\frac{C_1}{\epsilon}\right)||\theta_m||^2_{H^1(\Omega)}+\frac{C_2}{\epsilon}||\eta_m||^2_{L^2(\Omega)}+2\epsilon||\partial_t\theta_m||^2_{L^2(\Omega)}.\end{aligned} \tag{4.158}$$

Integrating from 0 to $T'\leq T$, and taking $\epsilon=\tau_\theta/4$, we obtain

$$\begin{aligned}&\frac{\tau_\theta}{2}\int_0^{T'}||\partial_t\theta_m||^2_{L^2(\Omega)}dt+\frac{1}{2}\left(A_\theta[\theta_m(T'),\theta_m(T')]-A_\theta[\theta_m(0),\theta_m(0)]\right)\\ &+\frac{a_\theta}{2p_\theta}\left(||\theta_m(T')||^{2p_\theta}_{L^{2p_\theta}(\Omega)}-||\theta_m(0)||^{2p_\theta}_{L^{2p_\theta}(\Omega)}\right)\\ &+\frac{a_{2p_\theta-2}}{2p_\theta-1}\left(\int_\Omega\theta_m^{2p_\theta-1}(T')d\mathbf{x}-\int_\Omega\theta_m^{2p_\theta-1}(0)d\mathbf{x}\right)+\cdots\\ &+\frac{a_1}{2}\left(||\theta_m(T')||^2_{L^2(\Omega)}-||\theta_m(0)||^2_{L^2(\Omega)}\right)+a_0\left(\int_\Omega\theta_m(T')d\mathbf{x}-\int_\Omega\theta_m(0)d\mathbf{x}\right)\\ &\qquad\leq\left(C_0+\frac{4C_1}{\tau_\theta}\right)||\theta_m||^2_{L^2(0,T;H^1(\Omega))}+\frac{4C_2}{\tau_\theta}||\eta_m||^2_{L^2(0,T;L^2(\Omega))}.\end{aligned} \tag{4.159}$$

The terms involving $\theta_m(0)$ can all be taken to the right-hand side of the inequality and bounded, if necessary. For example,

$$\begin{aligned}\frac{a_{2p_\theta-2}}{2p_\theta-1}\int_\Omega(\theta_m(0))^{2p_\theta-1}d\mathbf{x} &\leq \left|\frac{a_{2p_\theta-2}}{2p_\theta-1}\right|\int_\Omega|\theta_m(0)|^{2p_\theta-1}d\mathbf{x}\\ &= \left|\frac{a_{2p_\theta-2}}{2p_\theta-1}\right|||\theta_m(0)||^{2p_\theta-1}_{L^{2p_\theta-1}(\Omega)}\\ &\leq C_{2p_\theta-1}||\theta_m(0)||^{2p_\theta-1}_{L^{2p_\theta}(\Omega)}, \end{aligned} \tag{4.160}$$

for some constant $C_{2p_\theta-1}>0$. The final step in the above equation follows from Holder's inequality:

$$\begin{aligned}||\theta_m(0)||^{2p_\theta-1}_{L^{2p_\theta-1}(\Omega)} &= \int_\Omega|\theta_m(0)|^{2p_\theta-1}d\mathbf{x}\\ &\leq C'_{2p_\theta-1}\left(\int_\Omega|\theta_m(0)|^{(2p_\theta-1)\left(\frac{2p_\theta}{2p_\theta-1}\right)}d\mathbf{x}\right)^{\frac{2p_\theta-1}{2p_\theta}}\\ &= C'_{2p_\theta-1}||\theta_m(0)||^{2p_\theta-1}_{L^{2p_\theta}(\Omega)}. \end{aligned} \tag{4.161}$$

The terms involving $\theta_m(T')$ (excluding the $A_\theta[\theta_m(T'),\theta_m(T')]$ term) can be bounded using Holder's inequality followed by Young's inequality with ϵ:

$$\begin{aligned}\int_\Omega(\theta_m(T'))^{2p_\theta-1}d\mathbf{x} &\leq \int_\Omega|\theta_m(T')|^{2p_\theta-1}d\mathbf{x}\\ &\leq C''_{2p_\theta-1}\left(\int_\Omega|\theta_m(T')|^{(2p_\theta-1)\left(\frac{2p_\theta}{2p_\theta-1}\right)}d\mathbf{x}\right)^{\frac{2p_\theta-1}{2p_\theta}}\\ &= C''_{2p_\theta-1}\left(\int_\Omega|\theta_m(T')|^{2p_\theta}d\mathbf{x}\right)^{\frac{2p_\theta-1}{2p_\theta}}\\ &\leq \epsilon\left(\int_\Omega|\theta_m(T')|^{2p_\theta}d\mathbf{x}\right)^{\frac{2p_\theta-1}{2p_\theta}\cdot\frac{2p_\theta}{2p_\theta-1}}+C'''_{2p_\theta-1}(\epsilon)\\ &= \epsilon||\theta_m(T')||^{2p_\theta}_{L^{2p_\theta}(\Omega)}+C'''_{2p_\theta-1}(\epsilon). \end{aligned} \tag{4.162}$$

By choosing the various epsilons sufficiently small, we can reduce inequality (4.159) to

$$\begin{aligned}&\frac{\tau_\theta}{2}\int_0^{T'}||\partial_t\theta_m||^2_{L^2(\Omega)}dt+\frac{1}{2}A_\theta[\theta_m(T'),\theta_m(T')]+c_{\theta1}||\theta_m(T')||^{2p_\theta}_{L^{2p_\theta}(\Omega)}\\ &\quad\leq \frac{1}{2}A_\theta[\theta_m(0),\theta_m(0)]+\left(C_0+\frac{4C_1}{\tau_\theta}\right)||\theta_m||^2_{L^2(0,T';H^1(\Omega))}\\ &\qquad+\frac{4C_2}{\tau_\theta}||\eta_m||^2_{L^2(0,T';L^2(\Omega))}+c_{\theta2}||\theta_m(0)||^{2p_\theta}_{L^{2p_\theta}(\Omega)}+c_{\theta3}, \end{aligned} \tag{4.163}$$

where $c_{\theta 1} > 0$ and all of $c_{\theta 1}$, $c_{\theta 2}$, and $c_{\theta 3}$ can be chosen independently of T' for $0 < T' < T$. We can change the T's on the right-hand side of the last inequality to Ts, and then observe that the right-hand side is bounded above by some constant independent of m due to the energy estimates we obtained in the existence/uniqueness proof. It then follows immediately that we have the bounds

$$\begin{aligned} \theta_m &\in L^\infty(0,T;L^{2p_\theta}(\Omega)), \\ \partial_t \theta_m &\in L^2(0,T;L^2(\Omega)). \end{aligned} \tag{4.164}$$

Furthermore, since by the uniformly parabolic condition satisfied by B_θ, A_θ satisfies

$$A_\theta[\theta_m(T'),\theta_m(T')] \geq A \int_\Omega |\nabla \theta_m(T')|^2 d\mathbf{x}, \tag{4.165}$$

it follows that we have $\nabla \theta_m$ bounded in $L^2(\Omega)$, $\forall t \in [0,T]$, which when combined with the bound

$$\theta_m \in L^\infty(0,T;L^2(\Omega)), \tag{4.166}$$

leads to

$$\theta_m \in L^\infty(0,T;H^1(\Omega)). \tag{4.167}$$

Since the bounds we have just derived for θ_m and $\partial_t \theta_m$ are independent of m, we can pass to limits, and conclude that (4.145) holds.

4.5.2 Outline of regularity proof

The details of the regularity proof (i.e., showing that the bounds (4.144) hold), are cumbersome and essentially similar to the standard approach for parabolic equations [46]. The idea behind the proof is as follows. We know from the existence and uniqueness theory that for a.e. $t \in [0,T]$,

$$\tau_\theta(\partial_t \theta, v) + B_\theta[\theta, v; t] = (-f_\theta(\theta) + \eta, v), \quad \forall v \in H^1(\Omega) \cap L^{2p_\theta}(\Omega). \tag{4.168}$$

We can rewrite this expression as

$$B_\theta[\theta, v; t] = (-\tau_\theta \partial_t \theta - f_\theta(\theta) + \eta, v), \tag{4.169}$$

and furthermore, expand $B_\theta[\theta, v; t]$ to obtain

$$\begin{aligned} \int_\Omega \sum_{i,j=1}^{n} a_{ij}(\partial_{x_i}\theta)(\partial_{x_j} v) d\mathbf{x} &= -\int_\Omega \left[\sum_{i=1}^{n} b_i(\partial_{x_i}\theta)v + c\,\theta v\right] d\mathbf{x} - \tau_\theta(\partial_t\theta, v) \\ &\quad -(f_\theta(\theta), v) + (\eta, v). \end{aligned} \tag{4.170}$$

Each term on the right-hand side of the above equation, when integrated from 0 to T, is bounded in absolute value due to the energy bounds we have already obtained (in the existence/uniqueness proof and in the previous subsection). What we would like to obtain is a bound involving the term on the left-hand side of the above equation and the second derivatives of θ.

The hypothesis of boundary regularity we need is $\partial\Omega \in C^2$. By definition, given $\Omega \subset \mathbb{R}^n$, open and bounded, $\partial\Omega$ is C^k if $\forall \mathbf{x}^0 \in \partial\Omega$, there exist $r > 0$, coordinates $\mathbf{x}_1, ..., \mathbf{x}_n$, and a C^k function $\gamma : \mathbb{R}^{n-1} \to \mathbb{R}$, such that

$$\Omega \cap B(\mathbf{x}^0, r) = \left\{\mathbf{x} \in B(\mathbf{x}^0, r) \mid \mathbf{x}_n > \gamma(\mathbf{x}_1, ..., \mathbf{x}_{n-1})\right\}, \tag{4.171}$$

where $B(\mathbf{x}^0, r)$ is the open ball of radius r centered at $\mathbf{x}^0$. If the boundary conditions are periodic boundary conditions, then we can think of Ω as an n-torus, a nice, compact manifold. The issue of boundary regularity therefore does not arise if the boundary conditions are periodic, and thus the bounds (4.144) hold.

For the general parabolic active transmission line, the same regularity result holds.

4.6 Dissipativity results

4.6.1 The notion of dissipativity

For finite-dimensional systems, the physical notion of dissipativity can be tied to the mathematical concept of the existence of an absorbing set. For infinite-dimensional systems, it is not so clear how dissipativity should be precisely defined, since there are systems which are considered "dissipative," but for which the existence of absorbing sets has not been established [47]. However, if for an infinite-dimensional system we can prove the existence of an absorbing set, we can certainly label the system dissipative. The cubic nonlinearity model does possess an absorbing set, and therefore we are justified in labeling it a dissipative system. The energy bounds required to show the existence of an absorbing set are stronger than those required to show existence, uniqueness, and regularity of solutions.

Let $\mathbf{u}(t) = (\theta(t), \eta(t))$ denote the solution for the cubic nonlinearity model, let $\mathbf{u}_0 = \mathbf{u}(0)$, and let $\mathbf{L} = L^2(\Omega) \times L^2(\Omega)$. Then the semigroup $\{S(t)\}_{t\geq 0}$ defined by

$$\begin{array}{rcl} S(t) : \mathbf{L} & \rightarrow & \mathbf{L} \\ \mathbf{u}_0 & \mapsto & \mathbf{u}(t) \end{array} \tag{4.172}$$

is well-defined for $\forall t \in [0, T]$ for T arbitrarily large. Note that $\mathbf{L} \supset \mathbf{H} = (H^1(\Omega) \cap L^{2p_\theta}(\Omega)) \times (H^1(\Omega) \cap L^{2p_\eta}(\Omega))$ where $\mathbf{H}$ is the Hilbert space in which $\mathbf{u}(t)$ lies for almost every t. However, writing $S(t) : \mathbf{L} \rightarrow \mathbf{L}$ reflects the fact that our initial conditions only need to be in $\mathbf{L}$ for the existence and uniqueness theory to hold.

The semigroup $\{S(t)\}_{t\geq 0}$ satisfies the basic semigroup properties,

$$\begin{aligned} S(t+s) &= S(t)\cdot S(s), \quad \forall s,t \geq 0, \\ S(0) &= I \text{ (the identity)}, \\ \mathbf{u}(t+s) &= S(t)\mathbf{u}(s) = S(s)\mathbf{u}(t), \end{aligned} \tag{4.173}$$

and in addition, because of the continuous dependence of solutions on initial data, we have that $S(t)$ is a continuous operator $\forall t \geq 0$.

For $\mathbf{u}_0 \in \mathbf{L}$, the trajectory starting at $\mathbf{u}_0$ is the set $\bigcup_{t\geq 0} S(t)\mathbf{u}_0$. For $\mathbf{u}_0 \in \mathbf{L}$ or $\mathcal{A} \in \mathbf{L}$, the ω-limit set is

$$\begin{aligned} \omega(\mathbf{u}_0) &= \bigcap_{s\geq 0} \overline{\bigcup_{t\geq s} S(t)\mathbf{u}_0}, \\ \omega(\mathcal{A}) &= \bigcap_{s\geq 0} \overline{\bigcup_{t\geq s} S(t)\mathcal{A}}, \end{aligned} \tag{4.174}$$

where the closures are taken in $\mathbf{L}$. The ω-limit set has the property that

$$\phi \in \omega(\mathcal{A}) \Longleftrightarrow \exists \phi_n \in \mathcal{A} \text{ and } t_n \to \infty \text{ such that } S(t_n)\phi_n \to \phi \text{ as } n \to \infty. \tag{4.175}$$

Note also that the ω-limit set of $\mathcal{A}$ is not the same as the union of the ω-limit sets of each $\mathbf{u}_0$ in $\mathcal{A}$.

The operators $S(t)$ are uniformly compact for large t if for all bounded sets $\mathcal{B}$ there exists t_0 depending on $\mathcal{B}$ such that $\bigcup_{t\geq t_0} S(t)\mathcal{B}$ is relatively compact in $\mathbf{L}$. By relatively compact, we mean the closure of a set is compact. We then have the following lemma (proved in [47]):

Lemma 4.4 *Assume that for some subset $\mathcal{A} \subset \mathbf{L}$, $\mathcal{A} \neq \emptyset$, and for some $t_0 > 0$, the set $\bigcup_{t\geq t_0} S(t)\mathcal{A}$ is relatively compact in $\mathbf{L}$. Then $\omega(\mathcal{A})$ is nonempty, compact, and invariant.*

An equilibrium point is a point $\mathbf{u}_0 \in \mathbf{L}$ such that $S(t)\mathbf{u}_0 = \mathbf{u}_0$, $\forall t \geq 0$. A set $X \subset \mathbf{L}$ is positively invariant for the semigroup $S(t)$ if $S(t)X \subset X$, $\forall t \geq 0$, negatively invariant if $S(t)X \supset X$, $\forall t \geq 0$, and invariant if $S(t)X = X$, $\forall t \geq 0$.

An attractor is a set $\mathcal{A} \subset \mathbf{L}$ such that

(i) $\mathcal{A}$ is invariant; i.e., $S(t)\mathcal{A} = \mathcal{A}$, $\forall t \geq 0$, and

(ii) $\exists\, \mathcal{U}$, open, such that $\forall \mathbf{u}_0 \in \mathcal{U}$, $S(t)\mathbf{u}_0 \to \mathcal{A}$ as $t \to \infty$; i.e.,

$\operatorname{dist}(S(t)\mathbf{u}_0, \mathcal{A}) \to 0$ as $t \to \infty$.

The largest such $\mathcal{U}$ is the basin of attraction of $\mathcal{A}$. If the basin of attraction of $\mathcal{A}$ is all of $\mathbf{L}$, then $\mathcal{A}$ is a global attractor for $\{S(t)\}_{t\geq 0}$.

Let $\mathcal{B} \subset \mathcal{U}$ where $\mathcal{U}$ is an open set in $\mathbf{L}$. Then $\mathcal{B}$ is an absorbing set in $\mathcal{U}$ if the orbit of any bounded set of $\mathcal{U}$ enters into $\mathcal{B}$ after a certain time (which may depend on the set); i.e., $\forall \mathcal{B}_0 \subset \mathcal{U}$, $\mathcal{B}_0$ bounded, $\exists t_1$ (depending on $\mathcal{B}_0$) such that $S(t)\mathcal{B}_0 \subset \mathcal{B}$, $\forall t \geq t_1$.

The existence of a global attractor implies the existence of an absorbing set. With an additional hypothesis, namely the uniform compactness of $S(t)$, the existence of an absorbing set implies the existence of an attractor. The following theorem is proved by Temam [47]:

Theorem 4.5 *Suppose* $\mathbf{L}$ *is a metric space and that the operators* $S(t)$ *satisfy the semigroup properties and are continuous operators from* $\mathbf{L}$ *into itself,* $\forall t > 0$. *Also, assume the* $S(t)$ *are uniformly compact. Suppose that there exists an open set* $\mathcal{U}$ *and a bounded set* $\mathcal{B}$ *of* $\mathcal{U}$ *such that* $\mathcal{B}$ *is absorbing in* $\mathcal{U}$. *Then the* ω*-limit set of* $\mathcal{B}$, $\mathcal{A} = \omega(\mathcal{B})$, *is a compact attractor which attracts the bounded*

sets of $\mathcal{U}$*. It is the maximal bounded attractor. Furthermore, if* $\mathbf{L}$ *is a Banach space and* $\mathcal{U}$ *is convex and connected, then* $\mathcal{A}$ *is connected, too.*

In applying the above theorem, we have $\mathbf{L}$ a Hilbert space, and $\mathcal{U} = \mathbf{L}$ so that the resulting attractor is a global attractor. Instead of using the above theorem of Temam as stated, we will instead specialize to a theorem whose hypotheses are easier to check for our examples of interest:

Theorem 4.6 *Suppose* $\mathbf{L}$ *is a Banach space and that the operators* $S(t)$ *satisfy the semigroup properties and are continuous operators from* $\mathbf{L}$ *into itself,* $\forall t > 0$*. Suppose that there exists an open set* $\mathcal{U}$ *and a bounded set* $\mathcal{B}$ *of* $\mathcal{U} \cap \mathbf{H}$ *such that* $\mathcal{B} \subset \mathbf{H} \subset\subset \mathbf{L}$ *and* $\mathcal{B}$ *is absorbing in* $\mathcal{U}$*. Then the* ω*-limit set of* $\mathcal{B}$*,* $\mathcal{A} = \omega(\mathcal{B})$*, is a compact attractor which attracts the bounded sets of* $\mathcal{U}$*. It is the maximal bounded attractor. Furthermore, if* $\mathcal{U}$ *is convex and connected, then* $\mathcal{A}$ *is connected, too.*

Remark: By $\mathbf{H} \subset\subset \mathbf{L}$, for $\mathbf{H}$ and $\mathbf{L}$ Banach spaces, we mean $\mathbf{H}$ is compactly embedded in $\mathbf{L}$. For our $\mathbf{H}$ and $\mathbf{L}$, $\mathbf{H} \subset\subset \mathbf{L}$ follows from standard compactness theory [46].

Proof: Since $\mathcal{B}$ is an absorbing set, $S(t)\mathcal{B} \subset \mathcal{B}, \ \ \forall t \geq t_1$. Thus, $\cup_{t \geq t_1} S(t)\mathcal{B} \subset \mathcal{B}$ is bounded in $\mathbf{H}$ and hence relatively compact in $\mathbf{L}$, so the earlier lemma applies: $\mathcal{A} = \omega(\mathcal{B})$ is nonempty, compact, and invariant. The rest of the proof is identical to the proof of the earlier theorem by Temam. □

4.6.2 Cubic nonlinearity model

Lemma 4.7 *The basic cubic nonlinearity model, equation (4.1), possess a compact, connected, global attractor.*

Proof: To demonstrate the dissipativity of the basic cubic nonlinearity model, equation (4.1), we need to exhibit an absorbing set in $\mathbf{H}$. In fact, this absorbing set will absorb all the bounded sets of $\mathbf{H}$. The existence of this absorbing set will then imply the existence of a global attractor by theorem 4.6.

The absorbing set in $\mathbf{H}$ is found by deriving strong enough energy bounds for the solutions θ and η, and also for $\nabla\theta$ and $\nabla\eta$. To obtain the energy bound for θ and η, we multiply the θ equation through by θ, the η equation through by η, integrate over Ω, and sum the results to obtain

$$\begin{aligned}\int_\Omega \tau_\theta\theta\partial_t\theta d\mathbf{x} + \int_\Omega \tau_\eta\eta\partial_t\eta d\mathbf{x} - l^2\int_\Omega \theta\Delta\theta d\mathbf{x} - L^2\int_\Omega \eta\Delta\eta d\mathbf{x} \\ + \int_\Omega(\theta^4-\theta^2)d\mathbf{x} + \int_\Omega(\eta^2 - C\eta)d\mathbf{x} &= 0, \qquad (4.176)\end{aligned}$$

for a.e. t. (That we can perform this calculation follows from the existence, uniqueness, and regularity theory.) We then compute

$$\begin{aligned}\frac{1}{2}\partial_t\left[\tau_\theta\int_\Omega\theta^2 d\mathbf{x} + \tau_\eta\int_\Omega\eta^2 d\mathbf{x}\right] + l^2\int_\Omega|\nabla\theta|^2 d\mathbf{x} + L^2\int_\Omega|\nabla\eta|^2 d\mathbf{x} \\ + \int_\Omega(\theta^4-\theta^2)d\mathbf{x} + \int_\Omega(\eta^2-C\eta)d\mathbf{x} &= 0. \qquad (4.177)\end{aligned}$$

Using Holder's inequality and Young's inequality, we have

$$\begin{aligned}\int_\Omega\theta^2 d\mathbf{x} &\le \left(\int_\Omega\theta^4 d\mathbf{x}\right)^{1/2}\left(\int_\Omega 1^2 d\mathbf{x}\right)^{1/2} \\ &= \sqrt{|\Omega|}\left(\int_\Omega\theta^4 d\mathbf{x}\right)^{1/2} \\ &\le \frac{1}{2}\int_\Omega\theta^4 d\mathbf{x} + \frac{1}{2}|\Omega|, \\ \int_\Omega\theta^4 d\mathbf{x} &\ge 2\int_\Omega\theta^2 d\mathbf{x} - |\Omega|, \qquad (4.178)\end{aligned}$$

where $|\Omega| = \int_\Omega d\mathbf{x}$. Similarly,

$$\begin{aligned}\int_\Omega|C\eta| d\mathbf{x} &\le \left(\int_\Omega C^2 d\mathbf{x}\right)^{1/2}\left(\int_\Omega\eta^2 d\mathbf{x}\right)^{1/2} \\ &= |C|\sqrt{|\Omega|}\left(\int_\Omega\eta^2 d\mathbf{x}\right)^{1/2} \\ &\le \frac{1}{2}\int_\Omega\eta^2 d\mathbf{x} + \frac{1}{2}C^2|\Omega|. \qquad (4.179)\end{aligned}$$

Substituting in these inequalities, we obtain

$$\begin{aligned}\frac{1}{2}\partial_t\left[\tau_\theta\int_\Omega\theta^2 d\mathbf{x}+\tau_\eta\int_\Omega\eta^2 d\mathbf{x}\right]+l^2\int_\Omega|\nabla\theta|^2 d\mathbf{x}&\\ +L^2\int_\Omega|\nabla\eta|^2 d\mathbf{x}+\int_\Omega\theta^2 d\mathbf{x}+\frac{1}{2}\int_\Omega\eta^2 \;&\leq\; \left(1+\frac{1}{2}C^2\right)|\Omega|. \quad (4.180)\end{aligned}$$

It then follows that

$$\partial_t\left[\tau_\theta\int_\Omega\theta^2 d\mathbf{x}+\tau_\eta\int_\Omega\eta^2 d\mathbf{x}\right]+c_1\left[\tau_\theta\int_\Omega\theta^2 d\mathbf{x}+\tau_\eta\int_\Omega\eta^2 d\mathbf{x}\right]\leq(2+C^2)|\Omega|, \quad (4.181)$$

where c_1 is a positive constant. If we identify

$$y_1(t)=\tau_\theta\int_\Omega\theta^2 d\mathbf{x}+\tau_\eta\int_\Omega\eta^2 d\mathbf{x}, \quad (4.182)$$

then the usual Gronwall lemma implies

$$\begin{aligned}y_1(t) &\leq y_1(0)\mathrm{e}^{-c_1 t}+\int_0^t(2+C^2)|\Omega|\mathrm{e}^{-\int_t^s(-c_1)d\tau}ds\\ &= y_1(0)\mathrm{e}^{-c_1 t}+(2+C^2)|\Omega|(1-e^{-t}). \quad (4.183)\end{aligned}$$

Thus, for sufficiently large t,

$$\tau_\theta\int_\Omega\theta^2 d\mathbf{x}+\tau_\eta\int_\Omega\eta^2 d\mathbf{x}\leq c_2, \quad (4.184)$$

for any $c_2>(2+C^2)|\Omega|$. Furthermore, the time t_0 after which this bound holds for a fixed c_2 can be given as a function of the $L^2(\Omega)$-norm of the initial data.

To obtain the energy bound for $\nabla\theta$ and $\nabla\eta$, we multiply the θ equation through by $\Delta\theta$, the η equation through by $\Delta\eta$, integrate over Ω, and sum the results to obtain

$$\begin{aligned}-\int_\Omega\tau_\theta\Delta\theta\partial_t\theta d\mathbf{x}-\int_\Omega\tau_\eta\Delta\eta\partial_t\eta d\mathbf{x}+\int_\Omega l^2(\Delta\theta)^2 d\mathbf{x}+\int_\Omega L^2(\Delta\eta)^2 d\mathbf{x}&\\ -\int_\Omega(\theta^3-\theta)\Delta\theta d\mathbf{x}-\int_\Omega(\eta-C)\Delta\eta d\mathbf{x}\;=\;0,&\end{aligned} \quad (4.185)$$

for almost every t. (That we can perform this calculation follows from the existence, uniqueness, and regularity theory.) The cross-term disappeared because

$$\int_\Omega \eta \Delta\theta d\mathbf{x} = -\int_\Omega \nabla\eta \cdot \nabla\theta d\mathbf{x} = \int_\Omega \theta\Delta\eta d\mathbf{x}. \tag{4.186}$$

We then compute

$$\begin{aligned}\tau_\theta \int_\Omega \nabla\theta \cdot (\partial_t(\nabla\theta))d\mathbf{x} + \tau_\eta \int_\Omega \nabla\eta \cdot (\partial_t(\nabla\eta))d\mathbf{x} + l^2 \int_\Omega (\Delta\theta)^2 d\mathbf{x} \\ + L^2 \int_\Omega (\Delta\eta)^2 d\mathbf{x} + \int_\Omega (3\theta^2 - 1)|\nabla\theta|^2 d\mathbf{x} + \int_\Omega |\nabla\eta|^2 d\mathbf{x} + \int_\Omega C\Delta\eta d\mathbf{x} \;=\; 0.\end{aligned} \tag{4.187}$$

The final term on the left-hand-side can be eliminated for Neumann or periodic boundary conditions. However, for Dirichlet boundary conditions, the final term is possibly nonzero. Using Holder's inequality and Young's inequality with epsilon, we have

$$\begin{aligned}\int_\Omega |C\Delta\eta| d\mathbf{x} &\leq \left(\int_\Omega C^2 d\mathbf{x}\right)^{1/2} \left(\int_\Omega (\Delta\eta)^2 d\mathbf{x}\right)^{1/2} \\ &= C\sqrt{|\Omega|}\left(\int_\Omega (\Delta\eta)^2 d\mathbf{x}\right)^{1/2} \\ &\leq \epsilon \int_\Omega (\Delta\eta)^2 d\mathbf{x} + c(\epsilon) C^2 |\Omega|.\end{aligned} \tag{4.188}$$

We can then choose $\epsilon = L^2/2$ to obtain

$$\begin{aligned}\frac{1}{2}\partial_t \left[\tau_\theta \int_\Omega |\nabla\theta|^2 d\mathbf{x} + \tau_\eta \int_\Omega |\nabla\eta|^2 d\mathbf{x}\right] + l^2 \int_\Omega (\Delta\theta)^2 d\mathbf{x} + \frac{L^2}{2}\int_\Omega (\Delta\eta)^2 d\mathbf{x} \\ + \int_\Omega 3\theta^2 |\Delta\theta|^2 d\mathbf{x} + \int_\Omega |\nabla\eta|^2 d\mathbf{x} \leq c_3 + \int_\Omega |\nabla\theta|^2 d\mathbf{x},\end{aligned} \tag{4.189}$$

where $c_3 > 0$ is a constant. It then follows that we can write

$$\partial_t \left[\tau_\theta \int_\Omega |\nabla\theta|^2 d\mathbf{x} + \tau_\eta \int_\Omega |\nabla\eta|^2 d\mathbf{x}\right] \leq \frac{2}{\tau_\theta}\left[\tau_\theta \int_\Omega |\nabla\theta|^2 d\mathbf{x} + \tau_\eta \int_\Omega |\nabla\eta|^2 d\mathbf{x}\right] + 2c_3, \tag{4.190}$$

where $2/\tau_\theta$ and $2c_3$ are both positive constants. Next, we need to apply the uniform Gronwall lemma [47]:

Lemma 4.8 *Let g, h, and y be positive locally integrable functions on $[t_0, \infty)$ such that dy/dt is locally integrable on $[t_0, \infty)$, and which satisfy*

$$\frac{dy}{dt} \leq gy + h, \quad \forall t \geq t_0. \tag{4.191}$$

Furthermore, suppose

$$\int_t^{t+r} g(s)ds \leq a_1, \quad \int_t^{t+r} h(s)ds \leq a_2, \quad \int_t^{t+r} y(s)ds \leq a_3, \quad \forall t \geq t_0, \tag{4.192}$$

where r, a_1, a_2, and a_3 are positive constants. Then

$$y(t+r) \leq \left(\frac{a_3}{r} + a_2\right) e^{a_1}, \quad \forall t \geq t_0. \tag{4.193}$$

Identifying

$$\begin{aligned} y_2(t) &= \tau_\theta \int_\Omega |\nabla\theta|^2 d\mathbf{x} + \tau_\eta \int_\Omega |\nabla\eta|^2 d\mathbf{x}, \\ g(t) &= 2/\tau_\theta, \\ h(t) &= 2c_3, \end{aligned} \tag{4.194}$$

we see that

$$\begin{aligned} a_1 &= \frac{2}{\tau_\theta} r, \\ a_2 &= 2c_3 r, \end{aligned} \tag{4.195}$$

and the remaining hypothesis we need to check is

$$\int_t^{t+r} y_2(s)ds \leq a_3, \quad \forall t \geq t_0, \tag{4.196}$$

for some t_0 and for some a_3 which can depend on r. We need to go back to inequality (4.180) and integrate from t to $t+r$ to obtain

$$\begin{aligned} &\frac{1}{2}\left[\tau_\theta ||\theta(t+r)||^2_{L^2(\Omega)} + \tau_\eta ||\eta(t+r)||^2_{L^2(\Omega)}\right] - \frac{1}{2}\left[\tau_\theta ||\theta(t)||^2_{L^2(\Omega)} + \tau_\eta ||\eta(t)||^2_{L^2(\Omega)}\right] \\ &+ \int_t^{t+r} \left[l^2 ||\nabla\theta||^2_{L^2(\Omega)} + L^2 ||\nabla\eta||^2_{L^2(\Omega)}\right] ds + \int_t^{t+r} ||\theta||^2_{L^2(\Omega)} ds \\ &+ \frac{1}{2}\int_t^{t+r} ||\eta||^2_{L^2(\Omega)} ds \leq \left(1 + \frac{1}{2}C^2\right) |\Omega| r. \end{aligned} \tag{4.197}$$

Throwing away some positive terms, we obtain the inequality

$$\int_t^{t+r} \left[l^2 ||\nabla\theta||^2_{L^2(\Omega)} + L^2 ||\nabla\eta||^2_{L^2(\Omega)} \right] ds \\ \leq \left(1 + \frac{1}{2}C^2\right) |\Omega| r + \frac{1}{2} \left[\tau_\theta ||\theta(t)||^2_{L^2(\Omega)} + \tau_\eta ||\eta(t)||^2_{L^2(\Omega)} \right], \quad (4.198)$$

and by appropriate choice of $c_4 > 0$, it follows that

$$c_4 \int_t^{t+r} \left[\tau_\theta ||\nabla\theta||^2_{L^2(\Omega)} + \tau_\eta ||\nabla\eta||^2_{L^2(\Omega)} \right] ds \\ \leq \left(1 + \frac{1}{2}C^2\right) |\Omega| r + \frac{1}{2} \left[\tau_\theta ||\theta(t)||^2_{L^2(\Omega)} + \tau_\eta ||\eta(t)||^2_{L^2(\Omega)} \right]. \quad (4.199)$$

Thus,

$$c_4 \int_t^{t+r} y_2(s) ds \leq \left(1 + \frac{1}{2}C^2\right) |\Omega| r + \frac{1}{2} y_1(t). \quad (4.200)$$

But the result of the energy bound calculation for θ and η is that there is some t_0 for which $y_1(t) \leq c_2$ when $t \geq t_0$, and so

$$\int_t^{t+r} y_2(s) ds \leq a_3 = \frac{\left(1 + \frac{1}{2}C^2\right) |\Omega| r}{c_4} + \frac{1}{2}\frac{c_2}{c_4}, \quad \forall t \geq t_0. \quad (4.201)$$

Thus, the hypotheses of the uniform Gronwall lemma are satisfied, and we can conclude that

$$\tau_\theta ||\nabla\theta||^2_{L^2(\Omega)} + \tau_\eta ||\nabla\eta||^2_{L^2(\Omega)} \leq c_5, \quad \forall t \geq t_1, \quad (4.202)$$

for some constant $c_5 > 0$ and some $t_1 > t_0 > 0$. Furthermore, we can take $t_1 = t_0 + r$ for some $r > 0$ which is fixed a priori. The constant c_5 can be chosen so as to depend on c_2 and r (and the other constants in the cubic nonlinearity PDEs) only.

Now, $\mathbf{H} = (H^1(\Omega) \cap L^4(\Omega)) \times (H^1(\Omega) \cap L^2(\Omega))$ is the Hilbert space in which we are looking for an absorbing set. $\mathbf{H}$ inherits a metric from $H^1(\Omega) \times H^1(\Omega)$, and if θ and η are bounded in $H^1(\Omega)$-norm, so too will $\mathbf{u} = (\theta, \eta)$ be bounded in $\mathbf{H}$-norm. We can fix $r > 0$ and $c_2 > (2 + C^2)|\Omega|$ a priori, and then we know

that after some time t_0 depending only on the $L^2(\Omega)$-norm of the initial data, we will have

$$\tau_\theta \int_\Omega \theta^2 d\mathbf{x} + \tau_\eta \int_\Omega \eta^2 d\mathbf{x} \leq c_2. \tag{4.203}$$

Also, the greater the magnitude of the initial data, the greater the t_0, and for sufficiently small initial data, $t_0 = 0$. Furthermore, having chosen c_2 and r, we can then find c_5 so that $\forall t \geq t_1 = t_0 + r$, we will have

$$\tau_\theta ||\nabla\theta||^2_{L^2(\Omega)} + \tau_\eta ||\nabla\eta||^2_{L^2(\Omega)} \leq c_5. \tag{4.204}$$

Thus, taking $\mathbf{u} = (\theta, \eta)$ we see that there is some ball $\mathcal{B}$ of radius $\rho > 0$ in $\mathbf{H}$ such that after some time t_1, which depends on the norm of $\mathbf{u}_0$, $\mathbf{u}(t) \in \mathcal{B}$, $\forall t \geq t_1$. In fact, for any bounded set $\mathcal{B}_0 \subset \mathbf{L}$, $\exists t_1$ (depending on $\mathcal{B}_0$) such that $S(t)\mathcal{B}_0 \subset \mathcal{B}$, $\forall t \geq t_1$, because only the $L^2(\Omega)$-norm of the initial data was used. Hence $\mathcal{B}$ satisfies the definition of an absorbing set in $\mathbf{L}$. Then since $\mathcal{B}$ is bounded and $\mathcal{B} \subset \mathbf{H} \subset\subset \mathbf{L}$, we can conclude from Theorem 4.6 that a compact, connected, global attractor $\mathcal{A} = \omega(\mathcal{B})$ exists for the cubic nonlinearity model. □

4.6.3 Active transmission-line models

The active transmission-line model with inhibitor dissipation and diffusion, equation (4.3), possesses the same dissipativity property as the basic cubic nonlinearity model, and the proof is nearly identical to the one given in the previous subsection.

The active transmission-line model without inhibitor diffusion, equation (4.6), cannot possess the same dissipativity property. In particular, adding a constant to η does not change the dynamics, so we cannot hope to find a bound eventually satisfied by $||\eta||_{L^2(\Omega)}$ that is independent of the initial data.

4.6.4 Cubic nonlinearity model with an additional advective term

With some slight modifications to the proof of dissipativity for the basic cubic nonlinearity model, it is also possible to prove the dissipativity property for the cubic nonlinearity model with an additional advective term, equation (4.5). The term $\mathbf{v} \cdot \nabla \eta$ is the advective term, meaning its effect is to cause steady-state solutions for η to the basic cubic nonlinearity model to translate spatially in time with a velocity $\mathbf{v}$. We will think of $\mathbf{v}$ for now as being a prescribed continuously differentiable function of $\mathbf{x}$ and t. The reason for adding the advective term to the basic cubic nonlinearity model is to allow equilibrium spike solutions of the basic cubic nonlinearity model to move around under some type of control (in this case, a control prescribed by choice of $\mathbf{v}(\mathbf{x}, t)$). We will assume that

$$\sup_{\Omega \times [0,T]} |\mathbf{v}(\mathbf{x}, t)| < L. \tag{4.205}$$

Even with the advective term, this system of PDEs lies within the class of systems for which we proved existence, uniqueness, and regularity.

Lemma 4.9 *The cubic nonlinearity model with additional advective term, equation (4.5), with the bound (4.205), possesses a compact, connected, global attractor.*

Proof: We will begin by deriving a bound for $B_\eta[\eta, \eta; t]$, where

$$B_\eta[u, w; t] = \int_\Omega \left[\sum_{i=1}^{n} L^2 (\partial_{x_i} u)(\partial_{x_i} w) + \sum_{i=1}^{n} v_i (\partial_{x_i} u) w \right] d\mathbf{x} \tag{4.206}$$

is the bilinear form associated with the η equation. Keep in mind that L is constant, whereas the v_i are functions of $\mathbf{x}$ and t. Then

$$L^2 \int_\Omega |\nabla \eta|^2 d\mathbf{x} \;\; = \;\; \int_\Omega \sum_{i=1}^{n} L^2 (\partial_{x_i} \eta)(\partial_{x_i} \eta)$$

$$
\begin{aligned}
&= B_\eta[\eta,\eta;t] - \int_\Omega \sum_{i=1}^{n} v_i(\partial_{x_i}\eta)\eta d\mathbf{x} \\
&\leq B_\eta[\eta,\eta;t] + (\sup_{\Omega\times[0,T]}|\mathbf{v}|)||\nabla\eta||_{L^2(\Omega)}||\eta||_{L^2(\Omega)} \\
&\leq B_\eta[\eta,\eta;t] + (\sup_{\Omega\times[0,T]}|\mathbf{v}|)\left(\epsilon||\nabla\eta||^2_{L^2(\Omega)} + \frac{1}{4\epsilon}||\eta||^2_{L^2(\Omega)}\right).
\end{aligned} \tag{4.207}
$$

If we take

$$
\epsilon(\sup_{\Omega\times[0,T]}|\mathbf{v}|) = \frac{L^2}{2}, \tag{4.208}
$$

then we obtain

$$
\frac{L^2}{2}||\nabla\eta||^2_{L^2(\Omega)} \leq B_\eta[\eta,\eta;t] + \frac{1}{2L^2}(\sup_{\Omega\times[0,T]}|\mathbf{v}|)^2||\eta||^2_{L^2(\Omega)}, \tag{4.209}
$$

or

$$
B_\eta[\eta,\eta;t] \geq \frac{L^2}{2}||\nabla\eta||^2_{L^2(\Omega)} - \frac{1}{2L^2}(\sup_{\Omega\times[0,T]}|\mathbf{v}|)^2||\eta||^2_{L^2(\Omega)}. \tag{4.210}
$$

Now when we multiply the η dynamical equation through by η and integrate over Ω, we obtain

$$
\begin{aligned}
&\int_\Omega \tau_\eta\eta(\partial_t\eta)d\mathbf{x} + \int_\Omega \left[-L^2\eta(\Delta\eta) + \eta(\mathbf{v}\cdot\nabla\eta)\right]d\mathbf{x} + \int_\Omega \theta\eta d\mathbf{x} + \int_\Omega \eta(\eta - C)d\mathbf{x} \\
&= \partial_t\left[\tau_\eta\int_\Omega \eta^2 d\mathbf{x}\right] + B_\eta[\eta,\eta;t] + \int_\Omega \theta\eta d\mathbf{x} + \int_\Omega \eta(\eta - C)d\mathbf{x}.
\end{aligned} \tag{4.211}
$$

Then proceeding as in the case of the basic cubic nonlinearity model, we obtain

$$
\begin{aligned}
&\frac{1}{2}\partial_t\left[\tau_\theta\int_\Omega \theta^2 d\mathbf{x} + \tau_\eta\int_\Omega \eta^2 d\mathbf{x}\right] + l^2\int_\Omega |\nabla\theta|^2 d\mathbf{x} + \frac{L^2}{2}\int_\Omega |\nabla\eta|^2 d\mathbf{x} \\
&\qquad + \int_\Omega \theta^2 d\mathbf{x} + \frac{1}{2}\left(1 - \frac{1}{L^2}(\sup_{\Omega\times[0,T]}|\mathbf{v}|)^2\right)\int_\Omega \eta^2 d\mathbf{x} \;\leq\; \left(1 + \frac{1}{2}C^2\right)|\Omega|.
\end{aligned} \tag{4.212}
$$

As a result of our assumption $\sup_{\Omega\times[0,T]}|\mathbf{v}| < L$, we obtain an energy bound for θ and η just as in the basic cubic nonlinearity model case.

For the energy bound on $\nabla\theta$ and $\nabla\eta$, when we multiply the θ and η equations through by $\Delta\theta$ and $\Delta\eta$ and then integrate over Ω, we obtain the

additional term

$$\int_\Omega (\mathbf{v}\cdot\nabla\eta)(\Delta\eta)d\mathbf{x}, \tag{4.213}$$

which was not present before. However, we can bound this term as follows:

$$\begin{aligned}\int_\Omega (\mathbf{v}\cdot\nabla\eta)\Delta\eta d\mathbf{x} &\leq (\sup_{\Omega\times[0,T]}|\mathbf{v}|)||\nabla\eta||_{L^2(\Omega)}||\Delta\eta||_{L^2(\Omega)} \\ &\leq (\sup_{\Omega\times[0,T]}|\mathbf{v}|)\left(\epsilon||\Delta\eta||^2_{L^2(\Omega)}+\frac{1}{4\epsilon}||\nabla\eta||^2_{L^2(\Omega)}\right). \end{aligned}\tag{4.214}$$

Choosing

$$\epsilon(\sup_{\Omega\times[0,T]}|\mathbf{v}|)=\frac{L^2}{2}, \tag{4.215}$$

we obtain

$$\begin{aligned}&\tau_\theta\int_\Omega\nabla\theta(\partial_t(\nabla\theta))d\mathbf{x}+\tau_\eta\int_\Omega\nabla\eta(\partial_t(\nabla\eta))d\mathbf{x}+l^2\int_\Omega(\Delta\theta)^2d\mathbf{x} \\ &+\frac{L^2}{2}\int_\Omega(\Delta\eta)^2d\mathbf{x}+\int_\Omega(3\theta^2-1)|\nabla\theta|^2d\mathbf{x}+\int_\Omega|\nabla\eta|^2d\mathbf{x}+\int_\Omega C\Delta\eta d\mathbf{x} \\ &\leq \frac{1}{2L^2}(\sup_{\Omega\times[0,T]}|\mathbf{v}|)^2\int_\Omega|\nabla\eta|^2d\mathbf{x}. \end{aligned}\tag{4.216}$$

As long as $\sup_{\Omega\times[0,T]}|\mathbf{v}|$ is bounded, we see that the necessary bound on $\nabla\theta$ and $\nabla\eta$ can be obtained in this case.

Thus, as was the case for the basic cubic nonlinearity model, we can claim that a compact, connected, global attractor exists for the cubic nonlinearity model with the additional advective term. □

4.6.5 Cubic nonlinearity model with additional symmetric long-range coupling

Lemma 4.10 *The basic cubic nonlinearity model with additional symmetric long-range coupling,*

$$\begin{aligned}\tau_\theta\partial_t\theta &= l^2\Delta\theta-\theta^3+\theta+\eta+z*\theta, \\ \tau_\eta\partial_t\eta &= L^2\Delta\eta-\eta-\theta+C, \end{aligned}\tag{4.217}$$

where the convolution term is bounded according to equation (4.133), possess a compact, connected, global attractor.

Proof: The proof is similar to that of lemma 4.7, but with a couple of modifications. Instead of inequality (4.178), Young's inequality with ϵ must be used to obtain

$$\int_\Omega \theta^4 d\mathbf{x} \geq \frac{1}{\epsilon}\int_\Omega \theta^2 d\mathbf{x} - \frac{4}{\epsilon^2}|\Omega|, \tag{4.218}$$

where we take ϵ sufficiently small that

$$\frac{1}{\epsilon} > \frac{1+\rho_z}{2} + 1. \tag{4.219}$$

Also, the extra term $\int_\Omega \Delta\theta(z*\theta)d\mathbf{x}$ can be integrated by parts, giving

$$\begin{aligned}\int_\Omega \Delta\theta(z*\theta)d\mathbf{x} &= \int_\Omega \Delta\theta \int_\Omega z(\mathbf{y})\theta(\mathbf{x}-\mathbf{y})d\mathbf{y}d\mathbf{x} \\ &= -\int_\Omega \nabla\theta \cdot \int_\Omega z(\mathbf{y})\nabla\theta(\mathbf{x}-\mathbf{y})d\mathbf{y}d\mathbf{x} \\ &= \int_\Omega \nabla\theta \cdot (z*\nabla\theta)d\mathbf{x}, \end{aligned} \tag{4.220}$$

where we have assumed that the boundary term from the integration by parts has vanished. Thus, the extra term appearing in equation (4.185) satisfies the bound

$$\Big|\int_\Omega \Delta\theta(z*\theta)d\mathbf{x}| \leq \frac{(1+\rho_z)n}{2}||\nabla\theta||_{L^2(\Omega)}, \tag{4.221}$$

and as for the basic cubic nonlinearity model, we can claim that a compact, connected, global attractor exists for the cubic nonlinearity model with additional symmetric long-range coupling. □

4.6.6 Complex activator-inhibitor equation

Lemma 4.11 *The complex activator-inhibitor equation (4.8) with periodic boundary conditions possess a compact, connected, global attractor.*

Proof: The proof is analogous to that of lemma 4.7, but with both real and imaginary parts of the θ and η appearing in the expressions. $\square$

Chapter 5

Lyapunov Functionals

5.1 Introduction

Since dissipation plays a crucial role in the behavior of activator-inhibitor equations, it is natural to try to apply energy methods. In fact, for the cubic nonlinearity model, it is easy to write down an energy functional V for which the system is a gradient system, but with respect to an indefinite metric. It turns out that for the cubic nonlinearity model, this energy functional, for certain parameter values, leads us to find a radially unbounded Lyapunov functional V^*, with $\dot{V}^* \leq 0$, and with $\dot{V}^* = 0$ only at equilibrium points of the dynamics. This result is an infinite-dimensional generalization of a corresponding result of Brayton and Moser for systems of ODEs [12, 49].

To illustrate the technique of Brayton and Moser, we spatially discretize the cubic nonlinearity model to obtain a system of ODEs. The discretized dynamics are shown to be gradient dynamics with respect to an energy function, in analogy with the PDE system. The procedure of Brayton and Moser is then applied to the system of ODEs, yielding a Lyapunov function, provided the ratio of time constants, $\alpha = \tau_\theta/\tau_\eta$, is greater than one. Since the Lyapunov function V^* is radially unbounded, and satisfies $\dot{V}^* \leq 0$ with $\dot{V}^* = 0$ only at equilibrium points of the dynamics, LaSalle's invariance principle enables us to conclude that all trajectories converge to the set of equilibrium points of the dynamics [44].

Having shown how the technique of Brayton and Moser applies to the

discretized system of ODEs, we then show how the technique extends to the infinite-dimensional setting for the basic cubic nonlinearity model. Having obtained the Lyapunov functional for the cubic nonlinearity model, we then show how related Lyapunov functionals can be obtained for the cubic nonlinearity model with additional long-range coupling, the complex activator-inhibitor equation, the bounded-nonlinearity model, and the active transmission line (with inhibitor diffusion and dissipation).

5.2 Gradient dynamics property of the cubic nonlinearity model

For the cubic nonlinearity model, there is an energy functional

$$V = \int_\Omega \left[\frac{l^2}{2} |\nabla \theta|^2 + \frac{1}{4}\theta^4 - \frac{1}{2}\theta^2 - \theta\eta - \frac{L^2}{2}|\nabla\eta|^2 - \frac{1}{2}\eta^2 + C\eta \right] d\mathbf{x}, \tag{5.1}$$

such that

$$\begin{aligned} \dot{V} &= \frac{\delta V}{\delta \theta} \cdot (\partial_t \theta) + \frac{\delta V}{\delta \eta} \cdot (\partial_t \eta) \\ &= -\int_\Omega \left[\tau_\theta (\partial_t \theta)^2 - \tau_\eta (\partial_t \eta)^2 \right] d\mathbf{x} \\ &= -\left(\begin{bmatrix} \partial_t \theta \\ \partial_t \eta \end{bmatrix}, \begin{bmatrix} \tau_\theta & 0 \\ 0 & -\tau_\eta \end{bmatrix} \begin{bmatrix} \partial_t \theta \\ \partial_t \eta \end{bmatrix} \right). \end{aligned} \tag{5.2}$$

An equivalent way of expressing this is

$$-J \begin{bmatrix} \partial_t \theta \\ \partial_t \eta \end{bmatrix} = \nabla V, \quad J = \begin{bmatrix} \tau_\theta & 0 \\ 0 & -\tau_\eta \end{bmatrix}, \tag{5.3}$$

so that

$$\dot{V} = \left(\nabla V, \begin{bmatrix} \partial_t \theta \\ \partial_t \eta \end{bmatrix} \right) = -\left(\begin{bmatrix} \partial_t \theta \\ \partial_t \eta \end{bmatrix}, J \begin{bmatrix} \partial_t \theta \\ \partial_t \eta \end{bmatrix} \right). \tag{5.4}$$

We thus have a gradient system with respect to an indefinite metric.

5.3 Lyapunov function derivation for the spatially discretized cubic nonlinearity model

To see how the technique of Brayton and Moser works for ODE systems, consider the simplest discretization of the cubic nonlinearity model in one spatial dimension with periodic boundary conditions,

$$\begin{aligned} \tau_\theta \dot{\theta}_k &= l^2 \left(\frac{\theta_{k-1} - 2\theta_k + \theta_{k+1}}{\delta^2} \right) - \theta_k^3 + \theta_k + \eta_k, \\ \tau_\eta \dot{\eta}_k &= L^2 \left(\frac{\eta_{k-1} - 2\eta_k + \eta_{k+1}}{\delta^2} \right) - \eta_k - \theta_k + C, \end{aligned} \tag{5.5}$$

where δ is the distance between the discretized points along the x-axis where we are evaluating θ_k and η_k, and the indices k are taken mod N, where $2N$ is the total number of ODEs. (The spatially discretized version of the cubic nonlinearity model satisfies dissipativity bounds analogous to those obtained in the PDE case. Since the necessary local Lipschitz condition is satisfied, and the dissipativity bounds preclude finite escape times, existence and uniqueness of solutions for the spatially discretized system of ODEs is easily established [44].)

As for the PDE system, we can write this discretized system as a gradient system with respect to an indefinite metric: let

$$\begin{aligned} V &= \frac{l^2}{\delta^2} \left(\sum_k \theta_k^2 - \sum_k \theta_k \theta_{k+1} \right) + \frac{1}{4} \sum_k \theta_k^4 - \frac{1}{2} \sum_k \theta_k^2 - \sum_k \theta_k \eta_k \\ &\quad - \frac{L^2}{\delta^2} \left(\sum_k \eta_k^2 - \sum_k \eta_k \eta_{k+1} \right) - \frac{1}{2} \sum_k \eta_k^2 + C \sum_k \eta_k, \end{aligned} \tag{5.6}$$

so that

$$\begin{aligned} \dot{V} &= \sum_k \frac{\partial V}{\partial \theta_k} \dot{\theta}_k + \sum_k \frac{\partial V}{\partial \eta_k} \dot{\eta}_k \\ &= -\sum_k \left[\tau_\theta (\dot{\theta}_k)^2 - \tau_\eta (\dot{\eta}_k)^2 \right] \end{aligned}$$

$$= -[\dot{\theta}^T \;\; \dot{\eta}^T] \begin{bmatrix} \tau_\theta I & 0 \\ 0 & -\tau_\eta I \end{bmatrix} \begin{bmatrix} \dot{\theta} \\ \dot{\eta} \end{bmatrix}, \tag{5.7}$$

where $\theta = (\theta_1, ..., \theta_N)$, $\eta = (\eta_1, ..., \eta_N)$, and I denotes the $N \times N$ identity matrix. As before, we can equivalently express this as

$$-J \begin{bmatrix} \dot{\theta} \\ \dot{\eta} \end{bmatrix} = \nabla V, \tag{5.8}$$

so that

$$\begin{aligned} \dot{V} &= [\dot{\theta}^T \;\; \dot{\eta}^T] \nabla V \\ &= -[\dot{\theta}^T \;\; \dot{\eta}^T] J \begin{bmatrix} \dot{\theta} \\ \dot{\eta} \end{bmatrix}, \end{aligned} \tag{5.9}$$

where

$$J = \begin{bmatrix} \tau_\theta I & 0 \\ 0 & -\tau_\eta I \end{bmatrix}. \tag{5.10}$$

The technique of Brayton and Moser involves first computing D^2V, which looks like

$$\begin{aligned} D^2V &= \begin{bmatrix} \partial_{\theta_1\theta_1} V & \cdots & \partial_{\theta_1\theta_N} V & \partial_{\theta_1\eta_1} V & \cdots & \partial_{\theta_1\eta_N} V \\ \vdots & & \vdots & \vdots & & \vdots \\ \partial_{\theta_1\theta_N} V & \cdots & \partial_{\theta_N\theta_N} V & \partial_{\theta_N\eta_1} V & \cdots & \partial_{\theta_N\eta_N} V \\ \partial_{\theta_1\eta_1} V & \cdots & \partial_{\theta_N\eta_1} V & \partial_{\eta_1\eta_1} V & \cdots & \partial_{\theta_1\eta_N} V \\ \vdots & & \vdots & \vdots & & \vdots \\ \partial_{\theta_1\eta_N} V & \cdots & \partial_{\theta_N\eta_N} V & \partial_{\eta_1\eta_N} V & \cdots & \partial_{\eta_N\eta_N} V \end{bmatrix} \\ &= \begin{bmatrix} P & -I \\ -I & Q \end{bmatrix}, \end{aligned} \tag{5.11}$$

where each block is $N \times N$. It turns out not to be necessary to compute P, but it is necessary to write down Q and show that Q is invertible. A simple calculation gives

$$Q = -\left(I + \frac{L^2}{\delta^2} R\right), \tag{5.12}$$

where

$$R = \begin{bmatrix} 2 & -1 & 0 & \cdots & 0 & -1 \\ -1 & 2 & -1 & 0 & \cdots & 0 \\ 0 & -1 & 2 & -1 & & \vdots \\ \vdots & 0 & & \ddots & & 0 \\ 0 & \vdots & & & 2 & -1 \\ -1 & 0 & \cdots & 0 & -1 & 2 \end{bmatrix}. \tag{5.13}$$

To show that Q is negative definite, and hence invertible, it suffices to show that R is positive semidefinite. But R can be directly shown to be positive semidefinite, because if $\mathbf{z}$ is any nonzero N-vector, then

$$\begin{aligned} \mathbf{z}^T R \mathbf{z} &= 2\sum_k z_k^2 - \sum_k z_k z_{k-1} - \sum_k z_k z_{k+1} \\ &= \sum_k (z_k^2 - 2 z_k z_{k+1} + z_{k+1}^2) \\ &= \sum_k (z_k - z_{k+1})^2 \\ &\geq 0. \end{aligned} \tag{5.14}$$

Then defining

$$M = \begin{bmatrix} 0 & 0 \\ 0 & -2Q^{-1} \end{bmatrix}, \tag{5.15}$$

we can define

$$\begin{aligned} J^* &= J + (D^2 V) M J \\ &= \begin{bmatrix} \tau_\theta I & 0 \\ 0 & -\tau_\eta I \end{bmatrix} + \begin{bmatrix} P & -I \\ -I & Q \end{bmatrix} \begin{bmatrix} 0 & 0 \\ 0 & -2Q^{-1} \end{bmatrix} \begin{bmatrix} \tau_\theta I & 0 \\ 0 & -\tau_\eta I \end{bmatrix} \\ &= \begin{bmatrix} \tau_\theta I & 0 \\ 0 & -\tau_\eta I \end{bmatrix} + \begin{bmatrix} 0 & -2\tau_\eta Q^{-1} \\ 0 & 2\tau_\eta I \end{bmatrix} \\ &= \begin{bmatrix} \tau_\theta I & -2\tau_\eta Q^{-1} \\ 0 & \tau_\eta I \end{bmatrix}. \end{aligned} \tag{5.16}$$

Corresponding to this J^*, there is a

$$V^* = V + \frac{1}{2}(\nabla V)^T M \nabla V, \tag{5.17}$$

such that

$$-J^* \begin{bmatrix} \dot{\theta} \\ \dot{\eta} \end{bmatrix} = \nabla V^*. \tag{5.18}$$

To see this, simply take the gradient of V^*:

$$\begin{aligned}\nabla V^* &= \nabla V + (D^2V)M\nabla V \\ &= -(J + (D^2V)MJ)\begin{bmatrix} \dot{\theta} \\ \dot{\eta} \end{bmatrix} \\ &= -J^*\begin{bmatrix} \dot{\theta} \\ \dot{\eta} \end{bmatrix}. \end{aligned} \tag{5.19}$$

If J^* were symmetric, there would be a well-defined metric, and the dynamics would be gradient dynamics. However, J^* is not symmetric. But if J^* is positive definite, V^* will still be decreasing along trajectories. If we can further show that V^* is radially unbounded and $\dot{V} = 0$ if and only if $\dot{\theta} = \dot{\eta} = 0$, we will be able to conclude that the trajectories of the system converge to the set of equilibrium points.

As for the positive definiteness of J^*, we have

$$\begin{aligned}&[\dot{\theta}^T \;\; \dot{\eta}^T]\begin{bmatrix} \tau_\theta I & -2\tau_\eta Q^{-1} \\ 0 & \tau_\eta I \end{bmatrix}\begin{bmatrix} \dot{\theta} \\ \dot{\eta} \end{bmatrix} \\ &\quad = \tau_\theta|\dot{\theta}|^2 + \tau_\eta|\dot{\eta}|^2 - 2\tau_\eta\dot{\theta}^TQ^{-1}\dot{\eta} \\ &\quad = \left|\sqrt{\tau_\theta}\dot{\theta} - \frac{1}{\sqrt{\alpha}}Q^{-1}(\sqrt{\tau_\eta}\dot{\eta})\right|^2 + \left|\sqrt{\tau_\eta}\dot{\eta}\right|^2 - \frac{1}{\alpha}\left|Q^{-1}(\sqrt{\tau_\eta}\dot{\eta})\right|^2, \end{aligned} \tag{5.20}$$

and if

$$\frac{1}{\sqrt{\alpha}}||Q^{-1}|| < 1, \tag{5.21}$$

then we see that J^* is positive definite. Furthermore, we can calculate $||Q^{-1}|| = 1$ by finding the smallest singular value of $-Q$, and then inverting it. Observing that for $||\mathbf{z}|| = 1$ we have

$$\mathbf{z}^T(-Q)\mathbf{z} = \mathbf{z}^T\left(I + \frac{L^2}{\delta^2}R\right)\mathbf{z} = 1 + \frac{L^2}{\delta^2}\mathbf{z}^TR\mathbf{z}, \tag{5.22}$$

and in light of the fact that R is positive semidefinite and $\mathbf{z}$ can be chosen such that $\mathbf{z}^TR\mathbf{z} = 0$, it is clear that the smallest singular value of $-Q$ is 1. Hence,

$||Q^{-1}|| = 1$, and we arrive at the condition that J^* is positive definite if

$$\alpha > 1. \tag{5.23}$$

Because

$$\dot{V}^* = -[\dot{\theta}^T \;\; \dot{\eta}^T] J^* \begin{bmatrix} \dot{\theta} \\ \dot{\eta} \end{bmatrix}, \tag{5.24}$$

we also see that if J^* is positive definite, then $\dot{V}^* \leq 0$, and $\dot{V}^* = 0$ if and only if $\dot{\theta} = \dot{\eta} = 0$.

Next, we need to compute V^* and determine that it is radially unbounded. We define

$$\nabla V^* = \begin{bmatrix} \nabla_\theta V^* \\ \nabla_\eta V^* \end{bmatrix}, \tag{5.25}$$

so that $\nabla_\theta V^*$ represents the gradient of V^* with respect to the θ_k only, and $\nabla_\eta V^*$ represents the gradient of V^* with respect to the η_k only. Then we can express V^* as

$$V^* = V - (\nabla_\eta V)^T Q^{-1} \nabla_\eta V. \tag{5.26}$$

Furthermore, we can directly calculate that

$$\frac{\partial V}{\partial \eta_k} = (-2\frac{L^2}{\delta^2} - 1)\eta_k + \frac{L^2}{\delta^2}\eta_{k-1} + \frac{L^2}{\delta^2}\eta_{k+1} - \theta_k + C, \tag{5.27}$$

and hence that

$$\nabla_\eta V = Q\eta - \theta + C \begin{bmatrix} 1 \\ 1 \\ \vdots \\ 1 \end{bmatrix}. \tag{5.28}$$

We thus compute

$$\begin{aligned} V^* \;\; = \;\; & \frac{l^2}{\delta^2}\left(\sum_k \theta_k^2 - \sum_k \theta_k \theta_{k+1}\right) + \frac{1}{4}\sum_k \theta_k^4 - \frac{1}{2}\sum_k \theta_k^2 \\ & + \frac{L^2}{\delta^2}\left(\sum_k \eta_k^2 - \sum_k \eta_k \eta_{k+1}\right) + \frac{1}{2}\sum_k \eta_k^2 - C\sum_k \eta_k \\ & + \sum_k \theta_k \eta_k - (\theta - C\gamma)^T Q^{-1}(\theta - C\gamma), \end{aligned} \tag{5.29}$$

where $\gamma = [1 \;\; 1 \;\; \cdots \;\; 1]^T$. We thus arrive at the conclusion that for the discretized one-dimensional system with periodic boundary conditions, regardless of the fineness of the discretization (N and δ), as long as $\alpha > 1$, we can find a radially unbounded Lyapunov function V^* such that $\dot{V}^* \leq 0$, and with $\dot{V}^* = 0$ if and only if $\dot{\theta} = \dot{\eta} = 0$. We can therefore conclude that all trajectories must converge to the set of equilibrium points, provided $\alpha > 1$.

If we have Dirichlet or Neumann boundary conditions, similar conclusions can be reached. For Neumann boundary conditions (still in one spatial dimension), the matrix R becomes

$$R = \begin{bmatrix} 1 & -1 & 0 & \cdots & 0 & 0 \\ -1 & 2 & -1 & 0 & \cdots & 0 \\ 0 & -1 & 2 & -1 & & \\ \vdots & & & \ddots & & \vdots \\ 0 & & & & 2 & -1 \\ 0 & 0 & \cdots & 0 & -1 & 1 \end{bmatrix} \tag{5.30}$$

This R is also positive semidefinite because

$$\begin{aligned} \mathbf{z}^T R \mathbf{z} &= z_1^2 + z_N^2 + 2\sum_{k=2}^{N-1} z_k^2 - \sum_{k=2}^{N} z_k z_{k-1} - \sum_{k=1}^{N-1} z_k z_{k+1} \\ &= \sum_{k=1}^{N-1} (z_k - z_{k+1})^2 \\ &\geq 0, \end{aligned} \tag{5.31}$$

for any nonzero vector $\mathbf{z}$. Thus, for Neumann boundary conditions, identical conclusions are reached as for the periodic boundary condition case.

For Dirichlet boundary conditions, there is a slight difference. The matrix R becomes

$$R = \begin{bmatrix} 2 & -1 & 0 & \cdots & 0 & 0 \\ -1 & 2 & -1 & 0 & \cdots & 0 \\ 0 & -1 & 2 & -1 & & \\ \vdots & & & \ddots & & \vdots \\ 0 & & & & 2 & -1 \\ 0 & 0 & \cdots & 0 & -1 & 2 \end{bmatrix}, \tag{5.32}$$

and this R is actually positive definite. This is because

$$\mathbf{z}^T R \mathbf{z} \;=\; z_1^2 + z_N^2 + \sum_{k=1}^{N-1} (z_k - z_{k+1})^2 \;>\; 0, \tag{5.33}$$

for any nonzero vector $\mathbf{z}$. However, the smallest eigenvalue of $(L^2/\delta^2)R$ remains bounded as $\delta \to 0$ and $N \to \infty$ with N proportional to $1/\delta$. Also, as long as the inhibitor diffusion length L is small compared to the overall system size, the smallest eigenvalue of $(L^2/\delta^2)R$ will be small. We therefore conclude that

$$||Q^{-1}|| < 1, \;\; \text{but } ||Q^{-1}|| \approx 1. \tag{5.34}$$

We then arrive at the same condition as before for positive definiteness of J^*, namely $\alpha > 1$.

For discretized systems in more than one spatial dimension, the results for the one-dimensional case carry over, as long as the domain Ω is rectangular. For example, in two spatial dimensions with periodic boundary conditions, the simplest discretization would be

$$\begin{aligned} \tau_\theta \dot{\theta}_{jk} &= l^2 \left(\frac{\theta_{j(k+1)} + \theta_{j(k-1)} + \theta_{(j+1)k} + \theta_{(j-1)k} - 4\theta_{jk}}{\delta^2} \right) - \theta_{jk}^3 + \theta_{jk} + \eta_{jk}, \\ \tau_\eta \dot{\eta}_{jk} &= L^2 \left(\frac{\eta_{j(k+1)} + \eta_{j(k-1)} + \eta_{(j+1)k} + \eta_{(j-1)k} - 4\eta_{jk}}{\delta^2} \right) - \eta_{jk} - \theta_{jk} + C. \end{aligned} \tag{5.35}$$

All the same calculations can be performed on this system as in the one-dimensional case, and the conclusions are the same.

5.4 Convergence result for the spatially discretized cubic nonlinearity model

With the Lyapunov function V^* given by equation (5.29) for the spatially discretized system, we can prove a rigorous convergence result using the following theorem, proved in [44]:

Theorem 5.12 (LaSalle's Invariance Principle) *Consider the system* $\dot{\nu} = f(\nu)$. *Let* Σ *be a compact set and suppose the solution* $\nu(t)$ *starting in* Σ *stays in* Σ *for all* $t > 0$. *Let* $V^* : \Sigma \to \mathbb{R}$ *be a continuous function such that* $V^*(\nu(t))$ *is a monotone nonincreasing function of* t. *Let* E *be the set of all points in* Ω *where* $\dot{V}^*(\nu)$ *exists and equals zero. Let* M *be the largest positively invariant set in* E. *Then* $\nu(t)$ *approaches* M *as* $t \to \infty$.

Our convergence result is the following:

Theorem 5.13 *Assume* $\alpha = \tau_\theta/\tau_\eta > 1$. *Then every trajectory of the spatially discretized system (5.5) (corresponding to periodic, Neumann, or Dirichlet boundary conditions for the original PDE system) converges to the set of equilibria of the dynamics.*

Proof: The existence of the compact invariant set Σ is guaranteed by the radial unboundedness of V^*. Also, $E = M$ is simply the set of equilibria of the dynamics, due to equation (5.24). Applying LaSalle's invariance principle completes the proof. $\Box$.

5.5 Lyapunov functional derivation for the cubic nonlinearity model

We can generalize the technique of Brayton and Moser to the infinite-dimensional setting and use it to find a Lyapunov functional for the basic cubic nonlinearity model.

The first step is to calculate the second derivative of the energy functional V. We have

$$V : X \to \mathbb{R}, \tag{5.36}$$

where X represents the space in which the (θ, η) lie. At each $\mathbf{p} \in X$, there is a derivative map,

$$\begin{aligned} DV_{\mathbf{p}} : X &\to \mathbb{R} \\ \mathbf{u} &\mapsto DV_{\mathbf{p}} \cdot \mathbf{u} = \frac{d}{d\epsilon} V(\mathbf{p} + \epsilon \mathbf{u})\Big|_{\epsilon=0}, \end{aligned} \tag{5.37}$$

which corresponds to the first variation of V evaluated at a particular (θ, η). By ∇V, we mean

$$\nabla V = \begin{bmatrix} -l^2 \Delta\theta + \theta^3 - \theta - \eta \\ L^2 \Delta\eta - \eta - \theta + C \end{bmatrix}, \tag{5.38}$$

for then

$$DV_{(\theta,\eta)} \cdot \begin{bmatrix} \delta\theta \\ \delta\eta \end{bmatrix} = \int_\Omega \nabla V \cdot \begin{bmatrix} \delta\theta \\ \delta\eta \end{bmatrix} d\mathbf{x}, \tag{5.39}$$

where $\int_\Omega \mathbf{u} \cdot \mathbf{v} \, d\mathbf{x}$ is our inner product. We can then define the second-derivative map at a point $\mathbf{p} \in X$ as

$$\begin{aligned} D^2 V_{\mathbf{p}} : X \times X &\to \mathbb{R} \\ (\mathbf{u}, \mathbf{v}) &\mapsto \frac{d^2}{d\epsilon d\xi} V(\mathbf{p} + \epsilon \mathbf{u} + \xi \mathbf{v})\Big|_{\epsilon=0,\xi=0}. \end{aligned} \tag{5.40}$$

We can define the second-derivative matrix D^2V by

$$D^2 V_{(\theta,\eta)} \cdot \left(\begin{bmatrix} \delta\theta_1 \\ \delta\eta_1 \end{bmatrix}, \begin{bmatrix} \delta\theta_2 \\ \delta\eta_2 \end{bmatrix} \right) = \int_\Omega \begin{bmatrix} \delta\theta_1 & \delta\eta_1 \end{bmatrix} D^2 V \begin{bmatrix} \delta\theta_2 \\ \delta\eta_2 \end{bmatrix} d\mathbf{x}. \tag{5.41}$$

The second-derivative matrix D^2V is computed to be

$$D^2 V = \begin{bmatrix} (3\theta^2 - 1 - l^2\Delta) & -1 \\ -1 & (-1 + L^2\Delta) \end{bmatrix}. \tag{5.42}$$

We thus see that the quantity that plays the role of the matrix Q in the discretized system is the operator $(-1 + L^2\Delta)$. Therefore, we need to address the issue of finding an inverse for $(-1 + L^2\Delta)$.

Suppose first that we have periodic boundary conditions. Since the functions $(\delta\theta, \delta\eta)$ we are working with are in $L^2(\Omega)$, their Fourier series are well-

defined (in the distributional sense):

$$\begin{aligned} u(\mathbf{x}) &= \sum_{\mathbf{k}} u_{\mathbf{k}} \mathrm{e}^{i\mathbf{k}\cdot\mathbf{x}}, \\ u_{\mathbf{k}} &= \frac{1}{|\Omega|} \int_{\Omega} u(\mathbf{x}) \mathrm{e}^{-i\mathbf{k}\cdot\mathbf{x}} d\mathbf{x}, \\ u(\mathbf{x}) &\in L^2(\Omega), \ \sum_{\mathbf{k}} |u_{\mathbf{k}}|^2 < \infty. \end{aligned} \tag{5.43}$$

(Here we are thinking of $\mathbf{k}$ as a vector containing indices which are not necessarily integer. For example, in the one-dimensional case, we would have $k = 2\pi m/\mathcal{L}$ where m is an integer and $\mathcal{L} = |\Omega|$ is the length of the interval Ω.) Then

$$(-1 + L^2\Delta)u(\mathbf{x}) = -\sum_{\mathbf{k}} (1 + L^2|\mathbf{k}|^2) u_{\mathbf{k}} \mathrm{e}^{i\mathbf{k}\cdot\mathbf{x}}, \tag{5.44}$$

so the inverse operator for $(-1 + L^2\Delta)$ has the form

$$(-1 + L^2\Delta)^{-1} v(\mathbf{x}) = w(\mathbf{x}) * v(\mathbf{x}) = \int_{\Omega} w(\mathbf{x} - \mathbf{y}) v(\mathbf{y}) d\mathbf{y}, \tag{5.45}$$

where $w(\mathbf{x})$ can be represented as

$$w(\mathbf{x}) = \sum_{\mathbf{k}} \frac{-1}{1 + L^2|\mathbf{k}|^2} \mathrm{e}^{i\mathbf{k}\cdot\mathbf{x}}. \tag{5.46}$$

Before we can conclude that we have an appropriate inverse, however, we need to verify, since $(-1+L^2\Delta)$ takes functions in $H^2(\Omega)$ to $L^2(\Omega)$, that $w(\mathbf{x})*\cdot$ takes functions in $L^2(\Omega)$ to $H^2(\Omega)$. But this is in fact the case, since an equivalent norm to the $H^2(\Omega)$ norm is [50]

$$||u||_2 = \left(\sum_{\mathbf{k}} |u_{\mathbf{k}}|^2 \left(1 + |\mathbf{k}|^2\right)^2 \right)^{1/2}. \tag{5.47}$$

Thus, from the form of $w(\mathbf{x}) * \cdot$, it is clear that $w(\mathbf{x}) * v(\mathbf{x}) \in H^2(\Omega)$ if $v(\mathbf{x}) \in L^2(\Omega)$. Thus, we have verified (at least for periodic boundary conditions) that $(-1 + L^2\Delta)^{-1} : L^2(\Omega) \to H^2(\Omega)$ is a well-defined operator.

Proceeding by analogy with the spatially discretized case, we can compute

$$V^* = V - (\nabla_\eta V, (-1 + L^2\Delta)^{-1} \nabla_\eta V), \tag{5.48}$$

where

$$\nabla_\eta V = L^2\Delta\eta - \theta - \eta + C = (-1 + L^2\Delta)\eta - \theta + C. \tag{5.49}$$

Calculating

$$\begin{aligned}
&(\nabla_\eta V, (-1 + L^2\Delta)^{-1}\nabla_\eta V) \\
&= \int_\Omega \Big[(-1 + L^2\Delta)\eta - \theta + C\Big] \Big[(-1 + L^2\Delta)^{-1} \Big[(-1 + L^2\Delta)\eta - \theta + C\Big]\Big] \, d\mathbf{x} \\
&= \int_\Omega \Big[(-1 + L^2\Delta)\eta - \theta + C\Big] \Big[\eta + (-1 + L^2\Delta)^{-1}(-\theta + C)\Big] \, d\mathbf{x} \\
&= \int_\Omega \Big[\eta(-1 + L^2\Delta)\eta - \theta\eta + C\eta + [(-1 + L^2\Delta)\eta][(-1 + L^2\Delta)^{-1}(-\theta + C)] \\
&\qquad +(-\theta + C)[(-1 + L^2\Delta)^{-1}(-\theta + C)]\Big] \, d\mathbf{x} \\
&= \int_\Omega \Big[-L^2|\nabla\eta|^2 - \eta^2 - \theta\eta + C\eta + \eta[(-1 + L^2\Delta)(-1 + L^2\Delta)^{-1}(-\theta + C)] \\
&\qquad +(-\theta + C)[(-1 + L^2\Delta)^{-1}(-\theta + C)]\Big] \, d\mathbf{x} \\
&= \int_\Omega \Big[-L^2|\nabla\eta|^2 - \eta^2 - 2\theta\eta + 2C\eta - (-\theta + C)[(-1 + L^2\Delta)^{-1}(-\theta + C)\Big] \, d\mathbf{x},
\end{aligned} \tag{5.50}$$

where integration by parts has been used (with the assumption of periodic boundary conditions), we finally obtain

$$\begin{aligned}
V^* \;=\; \int_\Omega \Big[&\frac{l^2}{2}|\nabla\theta|^2 + \frac{1}{4}\theta^4 - \frac{1}{2}\theta^2 + \frac{L^2}{2}|\nabla\eta|^2 + \frac{1}{2}\eta^2 - C\eta + \theta\eta \\
&-(\theta - C)[(-1 + L^2\Delta)^{-1}(\theta - C)]\Big] d\mathbf{x}.
\end{aligned} \tag{5.51}$$

From this expression for V^*, it is apparent that V^* is radially unbounded.

It now remains to determine ∇V^*, so that we can check whether (or under what conditions) $\dot{V}^* \leq 0$, with $\dot{V}^* = 0$ if and only if $\partial_t\theta = \partial_t\eta = 0$. The only term of V^* for which we have not yet computed the first variation is the $(-\theta + C)[(-1 + L^2\Delta)^{-1}(-\theta + C)]$ term. Using the representation $(-1 + L^2\Delta)^{-1}\cdot = w * \cdot$, we compute

$$\begin{aligned}
&\frac{\delta}{\delta\theta}\left[\int_\Omega (-\theta + C)[(-1 + L^2\Delta)^{-1}(-\theta + C)]d\mathbf{x}\right] \cdot u \\
&\qquad = \int_\Omega 2[(-1 + L^2\Delta)^{-1}(-\theta + C)]u d\mathbf{x}.
\end{aligned} \tag{5.52}$$

Therefore, we have

$$\begin{aligned}\nabla_\theta V^* &= -l^2\Delta\theta + \theta^3 - \theta + \eta + 2(-1+L^2\Delta)^{-1}(-\theta + C) \\ &= -\tau_\theta \partial_t \theta + 2[\eta + (-1+L^2\Delta)^{-1}(-\theta + C)], \qquad (5.53) \\ \nabla_\eta V^* &= -L^2\Delta\eta + \eta + \theta - C \;=\; -\tau_\eta \partial_t \eta.\end{aligned}$$

Observing that

$$\begin{aligned}2\tau_\eta(-1+L^2\Delta)^{-1}\partial_t\eta &= 2(-1+L^2\Delta)^{-1}(L^2\Delta\eta - \eta - \theta + C) \\ &= 2[\eta + (-1+L^2\Delta)^{-1}(-\theta + C)], \qquad (5.54)\end{aligned}$$

we conclude that ∇V^* can be expressed as

$$\nabla V^* = -\begin{bmatrix} \tau_\theta & -2\tau_\eta(-1+L^2\Delta)^{-1} \\ 0 & \tau_\eta \end{bmatrix} \begin{bmatrix} \partial_t\theta \\ \partial_t\eta \end{bmatrix}. \qquad (5.55)$$

Therefore

$$\begin{aligned}\dot{V}^* &= -\int_\Omega [\partial_t\theta \;\; \partial_t\eta] \begin{bmatrix} \tau_\theta & -2\tau_\eta(-1+L^2\Delta)^{-1} \\ 0 & \tau_\eta \end{bmatrix} \begin{bmatrix} \partial_t\theta \\ \partial_t\eta \end{bmatrix} d\mathbf{x} \\ &= -\int_\Omega \Big[\left(\sqrt{\tau_\theta}\partial_t\theta - \frac{1}{\sqrt{\alpha}}(-1+L^2\Delta)^{-1}(\sqrt{\tau_\eta}\partial_t\eta) \right)^2 + (\sqrt{\tau_\eta}\partial_t\eta)^2 \\ &\qquad -\frac{1}{\alpha}\left((-1+L^2\Delta)^{-1}(\sqrt{\tau_\eta}\partial_t\eta)\right)^2 \Big] d\mathbf{x}. \qquad (5.56)\end{aligned}$$

Thus, the sufficient condition for $\dot{V}^* \leq 0$ is

$$\frac{1}{\sqrt{\alpha}} ||(-1+L^2\Delta)^{-1}|| < 1, \qquad (5.57)$$

where we are using the operator norm for $||(-1+L^2\Delta)^{-1}||$ defined by

$$||(-1+L^2\Delta)^{-1}|| = \sup_{u\in U} ||(-1+L^2\Delta)^{-1}u||_{L^2(\Omega)}, \quad U = \left\{ u \;:\; ||u||_{L^2(\Omega)} = 1 \right\}. \qquad (5.58)$$

Since the eigenvalues of $(1 - L^2\Delta)$ are $(1 + L^2|\mathbf{k}|^2)$, and the eigenvalues of $(1 - L^2\Delta)^{-1}$are $1/(1 + L^2|\mathbf{k}|^2)$, with $\mathbf{k} = \mathbf{0}$ an admissible eigenvalue, it follows

as in the discretized case that $||(-1+L^2\Delta)^{-1}|| = 1$, and we arrive at the same sufficient condition for $\dot{V}^* \leq 0$, namely

$$\alpha > 1. \tag{5.59}$$

Thus, for periodic boundary conditions, we see that in analogy with the spatially discretized case, if $\alpha > 1$ then there is a radially unbounded Lyapunov functional V^* such that $\dot{V}^* \leq 0$, and with $\dot{V}^* = 0$ only at equilibria of the dynamics.

For Dirichlet or Neumann boundary conditions, we need to assume that the boundary of Ω is C^2 (so that we have the necessary second-derivative bounds required for calculating the variations of V and V^*), and we need to use Fourier transform techniques instead of Fourier series techniques. As in the Fourier series case, since we are working with functions in $L^2(\Omega)$, the Fourier transform is well-defined (in the distributional sense):

$$\begin{aligned} u(\mathbf{x}) &= \frac{1}{(2\pi)^{n/2}} \int_{\mathbf{R}^n} \hat{u}(\omega) \mathrm{e}^{i\omega\cdot\mathbf{x}} d\boldsymbol{\omega}, \\ \hat{u}(\boldsymbol{\omega}) &= \frac{1}{(2\pi)^{n/2}} \int_{\Omega} u(\mathbf{x}) \mathrm{e}^{-i\omega\cdot\mathbf{x}} d\mathbf{x}, \\ u(\mathbf{x}) &\in L^2(\Omega), \;\; \hat{u}(\boldsymbol{\omega}) \in L^2(\mathbb{R}^n). \end{aligned} \tag{5.60}$$

Then

$$(-1 + L^2\Delta)u(\mathbf{x}) = -\frac{1}{(2\pi)^{n/2}} \int_{\mathbf{R}^n} (1 + L^2|\boldsymbol{\omega}|^2)\hat{u}(\boldsymbol{\omega}) \mathrm{e}^{i\omega\cdot\mathbf{x}} d\boldsymbol{\omega}, \tag{5.61}$$

so the inverse operator for $(-1 + L^2\Delta)$ has the form

$$(-1 + L^2\Delta)^{-1} v(\mathbf{x}) = w(\mathbf{x}) * v(\mathbf{x}) = \int_{\Omega} w(\mathbf{x} - \mathbf{y}) v(\mathbf{y}) d\mathbf{y}, \tag{5.62}$$

where $w(\mathbf{x})$ can be represented as

$$w(\mathbf{x}) = \frac{1}{(2\pi)^{n/2}} \int_{\mathbf{R}^n} \frac{-1}{1 + L^2|\boldsymbol{\omega}|^2} \mathrm{e}^{i\omega\cdot\mathbf{x}} d\boldsymbol{\omega}. \tag{5.63}$$

Since an equivalent norm to the $H^2(\Omega)$ norm is

$$||u||_2 = \left(\frac{1}{(2\pi)^{n/2}} \int_{\mathbb{R}^n} (\hat{u}(\boldsymbol{\omega}))^2 \left(1 + L^2|\boldsymbol{\omega}|^2\right)^2 d\boldsymbol{\omega} \right)^{1/2}, \tag{5.64}$$

it is clear that just as in the Fourier series case, $w(\mathbf{x}) * v(\mathbf{x}) \in H^2(\Omega)$ if $v(\mathbf{x}) \in L^2(\Omega)$ [50].

The expression for V^* is then identical to what it was in the Fourier series case, and the rest of the calculations go through just as before. For Dirichlet boundary conditions, the operator norm $||(-1 + L^2\Delta)^{-1}||$ turns out to be less than one instead of equal to one, for the same reason as in the spatially discretized case with Dirichlet boundary conditions (i.e., $\boldsymbol{\omega} = \mathbf{0}$ is not an eigenvalue). But if L is small compared to the size of the system, we will have $||(-1 + L^2\Delta)^{-1}|| \approx 1$. For the Neumann case, in analogy with the spatially discretized system, we obtain $||(-1 + L^2\Delta)^{-1}|| = 1$. Thus, for Dirichlet or Neumann boundary conditions, if $\alpha > 1$, we have the same conclusion as before, that $\dot{V}^* \leq 0$, with $\dot{V}^* = 0$ only at equilibria.

So to summarize, whether we have periodic, Dirichlet, or Neumann boundary conditions, as long as $\alpha > 1$, we can find a Lyapunov functional V^* which is radially unbounded and has the property that $\dot{V}^* \leq 0$, with $\dot{V}^* = 0$ only at equilibrium points of the dynamics.

5.6 Generalizations of the basic Lyapunov functional

5.6.1 Cubic nonlinearity model with additional symmetric long-range coupling

The basic cubic nonlinearity model with additional symmetric long-range coupling is

$$\begin{aligned} \tau_\theta \partial_t \theta &= l^2 \Delta\theta - \theta^3 + \theta + \eta + z * \theta, \\ \tau_\eta \partial_t \eta &= L^2 \Delta\eta - \eta - \theta + C, \end{aligned} \tag{5.65}$$

where z is symmetric about the origin, and the operator norm of $z*\cdot$ is bounded:

$$\exists \rho_z > 0 \text{ such that } ||z * \theta||_{L^2(\Omega)} \leq \rho_z ||\theta||_{L^2(\Omega)}, \ \ \forall \theta \in L^2(\Omega). \tag{5.66}$$

(For periodic boundary conditions, the convolution operation is interpreted as cyclic convolution.)

This system has the Lyapunov functional

$$\begin{aligned} V^* = \int_\Omega \Big[&\frac{l^2}{2}|\nabla\theta|^2 + \frac{1}{4}\theta^4 - \frac{1}{2}\theta^2 - \frac{1}{2}\theta(z*\theta) + \frac{L^2}{2}|\nabla\eta|^2 + \frac{1}{2}\eta^2 - C\eta + \theta\eta \\ &-(\theta - C)[(-1 + L^2\Delta)^{-1}(\theta - C)] \Big] d\mathbf{x}, \end{aligned} \tag{5.67}$$

for $\alpha = \tau_\theta/\tau_\eta > 1$. The additional convolution term does not change the radial unboundedness property of V^*, because it is dominated by the θ^4 term.

5.6.2 Complex activator-inhibitor equation

The Lyapunov functional for the basic cubic nonlinearity model generalizes to the complex activator-inhibitor equation

$$\begin{aligned} \tau_\theta \partial_t \theta &= l^2 \Delta\theta - |\theta|^2\theta + \theta + \eta, \\ \tau_\eta \partial_t \eta &= L^2 \Delta\eta - \eta - \theta + C, \end{aligned} \tag{5.68}$$

where θ, η, and C are complex. The pair of complex activator-inhibitor equations can be written as two systems of real activator-inhibitor equations with nonlinear coupling between the two activator equations:

$$
\begin{aligned}
\tau_\theta \partial_t \theta_R &= l^2 \Delta \theta_R - (\theta_R^2 + \theta_I^2)\theta_R + \theta_R + \eta_R, \\
\tau_\theta \partial_t \theta_I &= l^2 \Delta \theta_I - (\theta_R^2 + \theta_I^2)\theta_I + \theta_I + \eta_I, \\
\tau_\eta \partial_t \eta_R &= L^2 \Delta \eta_R - \eta_R - \theta_R + C_R, \\
\tau_\eta \partial_t \eta_I &= L^2 \Delta \eta_I - \eta_I - \theta_I + C_I,
\end{aligned}
\tag{5.69}
$$

where $\theta_R = \mathrm{Re}\{\theta\}$, $\theta_I = \mathrm{Im}\{\theta\}$, $\eta_R = \mathrm{Re}\{\eta\}$, and $\eta_I = \mathrm{Im}\{\eta\}$.

The Lyapunov functional for the complex activator-inhibitor equation (expressed as in equation (5.69)) is

$$
\begin{aligned}
V^* = \int_\Omega \Big[& \frac{l^2}{2}\left(|\nabla\theta_R|^2 + |\nabla\theta_I|^2\right) + \frac{1}{4}\left(\theta_R^4 + 2\theta_R^2\theta_I^2 + \theta_I^4\right) - \frac{1}{2}\left(\theta_R^2 + \theta_I^2\right) \\
& + \frac{L^2}{2}\left(|\nabla\eta_R|^2 + |\nabla\eta_I|^2\right) + \frac{1}{2}\left(\eta_R^2 + \eta_I^2\right) - (C_R\eta_R + C_I\eta_I) \\
& + (\theta_R\eta_R + \theta_I\eta_I) - (\theta_R - C_R)\left[(-1 + L^2\Delta)^{-1}(\theta_R - C_R)\right] \\
& - (\theta_I - C_I)\left[(-1 + L^2\Delta)^{-1}(\theta_I - C_I)\right]\Big] d\mathbf{x}.
\end{aligned}
\tag{5.70}
$$

This Lyapunov functional can be written in terms of the complex variables θ, η, and C, as

$$
\begin{aligned}
V^* = \int_\Omega \Big[& \frac{l^2}{2}|\nabla\theta|^2 + \frac{1}{4}|\theta|^4 - \frac{1}{2}|\theta|^2 + \frac{L^2}{2}|\nabla\eta|^2 + \frac{1}{2}|\eta|^2 - \mathrm{Re}\{\overline{C}\eta\} + \mathrm{Re}\{\overline{\theta}\eta\} \\
& - (\overline{\theta} - \overline{C})\left[(-1 + L^2\Delta)^{-1}(\theta - C)\right]\Big] d\mathbf{x},
\end{aligned}
\tag{5.71}
$$

where the overbar denotes complex conjugation. Using V^* in the real variable form, we can compute $\dot{V}^*$ using

$$
\dot{V}^* = \frac{\delta V^*}{\delta \theta_R} \cdot (\partial_t \theta_R) + \frac{\delta V^*}{\delta \theta_I} \cdot (\partial_t \theta_I) + \frac{\delta V^*}{\delta \eta_R} \cdot (\partial_t \eta_R) + \frac{\delta V^*}{\delta \eta_I} \cdot (\partial_t \eta_I), \tag{5.72}
$$

which gives

$$\dot{V}^* = -\int_\Omega \begin{bmatrix} \partial_t\theta_R \\ \partial_t\theta_I \\ \partial_t\eta_R \\ \partial_t\eta_I \end{bmatrix}^T \begin{bmatrix} \tau_\theta & 0 & -2\tau_\eta(-1+L^2\Delta)^{-1} & 0 \\ 0 & \tau_\theta & 0 & -2\tau_\eta(-1+L^2\Delta)^{-1} \\ 0 & 0 & \tau_\eta & 0 \\ 0 & 0 & 0 & \tau_\eta \end{bmatrix} \begin{bmatrix} \partial_t\theta_R \\ \partial_t\theta_I \\ \partial_t\eta_R \\ \partial_t\eta_I \end{bmatrix} d\mathbf{x}. \tag{5.73}$$

When $\alpha = \tau_\theta/\tau_\eta > 1$, we can conclude that $\dot{V}^* \leq 0$, and $\dot{V}^* = 0$ only at equilibria. Since V^* is radially unbounded, it serves as a Lyapunov functional provided $\alpha > 1$.

5.6.3 Bounded nonlinearity model

The bounded nonlinearity model,

$$\begin{aligned} \tau_\theta \partial_t \theta &= l^2\Delta\theta - f(\theta) + \eta, \\ \tau_\eta \partial_t \eta &= L^2\Delta\eta - \eta - \theta + C, \end{aligned} \tag{5.74}$$

where f is continuous and $\forall\theta$, $|f(\theta)| < M$ for some $M > 0$, has a Lyapunov functional if we further restrict f. Assume that f can be decomposed as

$$f(\theta) = f_1(\theta) + f_2(\theta), \tag{5.75}$$

where

$$\begin{aligned} f_1(\theta) &= 0, \ \ \forall\theta \in (-\infty, -a) \cup (a, \infty) \text{ for some } a > 0, \\ \theta f_2(\theta) &> 0, \ \ \forall\theta \neq 0, \end{aligned} \tag{5.76}$$

and both f_1 and f_2 are continuous. Define

$$\begin{aligned} g_1(\theta) &= \int_{-a}^{\theta} f_1(\xi)d\xi, \\ g_2(\theta) &= \int_0^{\theta} f_2(\xi)d\xi. \end{aligned} \tag{5.77}$$

Then the Lyapunov functional is

$$\begin{aligned} V^* &= \int_\Omega \Big[\frac{l^2}{2}|\nabla\theta|^2 + g_1(\theta) + g_2(\theta) + \frac{L^2}{2}|\nabla\eta|^2 + \frac{1}{2}\eta^2 - C\eta + \theta\eta \\ &\qquad -(\theta - C)[(-1 + L^2\Delta)^{-1}(\theta - C)]\Big]d\mathbf{x}. \end{aligned} \tag{5.78}$$

What we need to check is that V^* is radially unbounded. If we can show that the energy functional

$$\begin{aligned} V^*_{f=0} &= \int_\Omega \Big[\frac{l^2}{2}|\nabla\theta|^2 + \frac{L^2}{2}|\nabla\eta|^2 + \frac{1}{2}\eta^2 - C\eta + \theta\eta \\ &\qquad -(\theta - C)[(-1 + L^2\Delta)^{-1}(\theta - C)]\Big]d\mathbf{x} \end{aligned} \tag{5.79}$$

is radially unbounded, then since g_1 is bounded and $\forall\theta$, $g_2(\theta) \geq 0$, it will follow that V^* is also radially unbounded. Let

$$\begin{aligned} \theta &= \sum_{\mathbf{k}} \theta_{\mathbf{k}} \mathrm{e}^{i\mathbf{k}\cdot\mathbf{x}}, \\ \eta &= \sum_{\mathbf{k}} \eta_{\mathbf{k}} \mathrm{e}^{i\mathbf{k}\cdot\mathbf{x}} \end{aligned} \tag{5.80}$$

be the Fourier series representations of θ and η. We have

$$\begin{aligned} \frac{1}{|\Omega|}\int_\Omega |\eta|^2 d\mathbf{x} &= \sum_{\mathbf{k}} |\eta_{\mathbf{k}}|^2, \\ \frac{1}{|\Omega|}\int_\Omega \theta\eta d\mathbf{x} &= \frac{1}{|\Omega|}\int_\Omega \left(\sum_{\mathbf{k}} \overline{\theta}_{\mathbf{k}} \mathrm{e}^{-i\mathbf{k}\cdot\mathbf{x}}\right)\left(\sum_{\mathbf{k}} \eta_{\mathbf{k}} \mathrm{e}^{i\mathbf{k}\cdot\mathbf{x}}\right) d\mathbf{x} = \sum_{\mathbf{k}} \overline{\theta}_{\mathbf{k}}\eta_{\mathbf{k}}, \\ \frac{1}{|\Omega|}\int_\Omega |\nabla\theta|^2 d\mathbf{x} &= \frac{1}{|\Omega|}\int_\Omega \left|\sum_{\mathbf{k}} i\mathbf{k}\theta_{\mathbf{k}} \mathrm{e}^{i\mathbf{k}\cdot\mathbf{x}}\right|^2 dx = \sum_{\mathbf{k}} |\mathbf{k}|^2|\theta_{\mathbf{k}}|^2, \\ \frac{1}{|\Omega|}\int_\Omega |\nabla\eta|^2 d\mathbf{x} &= \sum_{\mathbf{k}} |\mathbf{k}|^2|\eta_{\mathbf{k}}|^2. \end{aligned} \tag{5.81}$$

The $(-1 + L^2\Delta)^{-1}$ term can be analyzed also using Fourier methods:

$$\begin{aligned} -1 + L^2\Delta &\leftrightarrow -1 - L^2|\mathbf{k}|^2, \\ (-1 + L^2\Delta)^{-1} &\leftrightarrow \frac{-1}{1 + L^2|\mathbf{k}|^2}, \\ -\frac{1}{|\Omega|}\int_\Omega (\theta - C)[(-1 + L^2\Delta)^{-1}(\theta - C)]d\mathbf{x} &= \sum_{\mathbf{k}\neq\mathbf{0}} \frac{1}{1 + L^2|\mathbf{k}|^2}|\theta_{\mathbf{k}}|^2 + (\theta_{\mathbf{0}} - C)^2. \end{aligned} \tag{5.82}$$

We thus have

$$\begin{aligned}\frac{1}{|\Omega|}V^*_{f=0} &= \sum_{\mathbf{k}\neq\mathbf{0}}\Big[\frac{l^2}{2}|\mathbf{k}|^2|\theta_{\mathbf{k}}|^2+\frac{L^2}{2}|\mathbf{k}|^2|\eta_{\mathbf{k}}|^2+\frac{1}{2}|\eta_{\mathbf{k}}|^2-C\eta_{\mathbf{k}}\mathrm{e}^{i\mathbf{k}\cdot\mathbf{x}}+\overline{\theta}_{\mathbf{k}}\eta_{\mathbf{k}}\\ &\qquad+\frac{1}{1+L^2|\mathbf{k}|^2}|\theta_{\mathbf{k}}|^2\Big]+\frac{1}{2}\eta_{\mathbf{0}}^2-C\eta_{\mathbf{0}}+\theta_{\mathbf{0}}\eta_{\mathbf{0}}+(\theta_{\mathbf{0}}-C)^2\\ &= \sum_{\mathbf{k}\neq\mathbf{0}}\Big[\frac{l^2}{2}|\mathbf{k}|^2|\theta_{\mathbf{k}}|^2+\frac{1}{4}(1+L^2|\mathbf{k}|^2)|\eta_{\mathbf{k}}|^2-C\eta_{\mathbf{k}}\mathrm{e}^{i\mathbf{k}\cdot\mathbf{x}}\\ &\qquad+\Big|\frac{1}{\sqrt{1+L^2|\mathbf{k}|^2}}\theta_{\mathbf{k}}+\frac{\sqrt{1+L^2|\mathbf{k}|^2}}{2}\eta_{\mathbf{k}}\Big|^2\Big]\\ &\qquad+\frac{1}{6}\eta_{\mathbf{0}}^2-C\eta_{\mathbf{0}}+\frac{1}{4}\theta_{\mathbf{0}}^2-2C\theta_0+C^2+\left(\frac{\sqrt{3}}{2}\theta_{\mathbf{0}}+\frac{1}{\sqrt{3}}\eta_{\mathbf{0}}\right)^2. \quad (5.83)\end{aligned}$$

Thus $V^*_{f=0}$ is radially unbounded, and hence so is V^* given by equation (5.78).

5.6.4 Active transmission line (with inhibitor diffusion and dissipation)

The active transmission line dynamics (with inhibitor diffusion and dissipation) are

$$\begin{aligned}\tau_\theta\partial_t\theta &= l^2\partial_{xx}\theta-\theta^3+\theta-C-\partial_x\eta,\\ \tau_\eta\partial_t\eta &= L^2\partial_{xx}\eta-\eta-\partial_x\theta,\end{aligned} \quad (5.84)$$

The energy functional for which the active transmission line dynamics are gradient dynamics is

$$V=\int_\Omega\left[\frac{l^2}{2}(\partial_x\theta)^2+\frac{1}{4}\theta^4-\frac{1}{2}\theta^2+C\theta-\frac{L^2}{2}(\partial_x\eta)^2-\frac{1}{2}\eta^2+\theta\partial_x\eta\right]dx. \quad (5.85)$$

For periodic (or Dirichlet) boundary conditions,

$$\int_\Omega\theta\partial_x\eta\,dx=-\int_\Omega\eta\partial_x\theta\,dx, \quad (5.86)$$

so as was the case for the basic cubic nonlinearity model, the active transmission line dynamics are gradient with respect to an indefinite metric.

In analogy with the Lyapunov functional derivation for the basic cubic nonlinearity model, we compute

$$\begin{aligned}
&(\nabla_\eta V, (-1+L^2\partial_{xx})^{-1}\nabla_\eta V) \\
&= \int_\Omega [(-1+L^2\partial_{xx})\eta - \partial_x\theta][(-1+L^2\partial_{xx})^{-1}((-1+L^2\partial_{xx})\eta - \partial_x\theta)]dx \\
&= \int_\Omega [\eta(-1+L^2\partial_{xx})\eta - \eta\partial_x\theta + [(-1+L^2\partial_{xx})\eta][(-1+L^2\partial_{xx})^{-1}(-\partial_x\theta)] \\
&\qquad +(-\partial_x\theta)[(-1+L^2\partial_{xx})^{-1}(-\partial_x\theta)]]dx \\
&= \int_\Omega \left[\eta(-1+L^2\partial_{xx})\eta - 2\eta\partial_x\theta + (\partial_x\theta)[(-1+L^2\partial_{xx})^{-1}(\partial_x\theta)]\right] dx, \quad (5.87)
\end{aligned}$$

where integration by parts has been used (with the assumption of periodic boundary conditions), thus obtaining

$$\begin{aligned}
V^* &= \int_\Omega \left[\frac{l^2}{2}(\partial_x\theta)^2 + \frac{1}{4}\theta^4 - \frac{1}{2}\theta^2 + C\theta + \frac{L^2}{2}(\partial_x\eta)^2 + \frac{1}{2}\eta^2 + \eta\partial_x\theta \right. \\
&\qquad \left. -(\partial_x\theta)[(-1+L^2\partial_{xx})^{-1}(\partial_x\theta)]\right]dx. \quad (5.88)
\end{aligned}$$

This energy functional is radially unbounded. Furthermore,

$$\nabla V^* = -\begin{bmatrix} \tau_\theta & 2\tau_\eta\partial_x(-1+L^2\partial_{xx})^{-1} \\ 0 & \tau_\eta \end{bmatrix}\begin{bmatrix} \partial_t\theta \\ \partial_t\eta \end{bmatrix}, \quad (5.89)$$

and

$$\begin{aligned}
\dot{V}^* &= -\int_\Omega [\partial_t\theta \;\; \partial_t\eta]\begin{bmatrix} \tau_\theta & 2\tau_\eta\partial_x(-1+L^2\partial_{xx})^{-1} \\ 0 & \tau_\eta \end{bmatrix}\begin{bmatrix} \partial_t\theta \\ \partial_t\eta \end{bmatrix} dx \\
&= -\int_\Omega \left[\tau_\theta(\partial_t\theta)^2 + \tau_\eta(\partial_t\eta)^2 + (\partial_t\theta)2\tau_\eta\left[\partial_x(-1+L^2\partial_{xx})^{-1}\right](\partial_t\eta)\right] dx \\
&= -\int_\Omega \left[\left(\sqrt{\tau_\theta}\partial_t\theta + \frac{1}{\sqrt{\alpha}}\partial_x(-1+L^2\partial_{xx})^{-1}(\sqrt{\tau_\eta}\partial_t\eta)\right)^2 + (\sqrt{\tau_\eta}\partial_t\eta)^2 \right. \\
&\qquad \left. -\frac{1}{\alpha}\left[\partial_x(-1+L^2\partial_{xx})^{-1}(\sqrt{\tau_\eta}\partial_t\eta)\right]^2\right]dx. \quad (5.90)
\end{aligned}$$

To determine the parameter values for which V^* decreases along trajectories, we need to determine the operator norm of $\partial_x(-1+L^2\partial_{xx})^{-1}$. Using Fourier series, we have

$$u(x) = \sum_k u_k \mathrm{e}^{ikx},$$

$$\begin{aligned}\partial_x(-1+L^2\partial_{xx})^{-1}u(x) &= \partial_x(-1+L^2\partial_{xx})^{-1}\sum_k u_k \mathrm{e}^{ikx},\\ &= \partial_x \sum_k \frac{-1}{1+L^2k^2}u_k\mathrm{e}^{ikx},\\ &= \sum_k \frac{-ik}{1+L^2k^2}u_k\mathrm{e}^{ikx}. \end{aligned} \tag{5.91}$$

The operator norm is then

$$\max_k \left|\frac{-ik}{1+L^2k^2}\right| = \max_k \frac{k}{1+L^2k^2} = \frac{1}{2L}, \tag{5.92}$$

and the maximum occurs for $k = 1/L$. So for $\dot{V}^* \leq 0$, we need

$$\alpha > \frac{1}{2L}. \tag{5.93}$$

Thus, for $\alpha = \tau_\theta/\tau_\eta > \frac{1}{2L}$, we have a radially unbounded Lyapunov functional V^* satisfying $\dot{V}^* \leq 0$, and with $\dot{V}^* = 0$ only at equilibria. The existence of a Lyapunov functional for the transmission line system indicates that the dissipative character dominates the transmission-line character when $\alpha > \frac{1}{2L}$. If for fixed α we let L tend toward zero, then V^* loses its property of having $\dot{V}^* \geq 0$, and so ceases to be a Lyapunov functional.

5.6.5 Spatially-varying coefficients

In deriving the Lyapunov functional for the basic cubic nonlinearity model, we assumed constant coefficients τ_θ, τ_η, l, L and C. However, as long as l and L are constant, the other coefficients, τ_θ, τ_η, and C, can be functions of $\mathbf{x}$. In particular, thinking of C as a control input and taking it to be a function of $\mathbf{x}$ (and a slowly-varying function of time so that the system responds quasistatically) is one technique for exciting interesting (i.e., spatially nonuniform) equilibirium solutions. The same comments about spatially-varying coefficients also apply to the other generalizations of the Lyapunov functional.

Chapter 6

Analyzing Equilibria Using Lyapunov Functionals

6.1 Introduction

There are a couple of ways to try to use Lyapunov functionals for analyzing the stability of equilibria. One approach is to evaluate the Lyapunov functional for different equilibrium solutions. An equilibrium solution with a lower value for the Lyapunov functional is energetically favorable compared with a different equilibrium solution having a higher Lyapunov functional value. A second approach is to perturb the dynamical equations about a particular equilibrium solution, write down the Lyapunov functional for the perturbed dynamics, examine the lowest-order (i.e., quadratic) terms, and thereby assess whether or not the equilibrium solution is stable with respect to linear perturbations. Such an approach works in general for assessing the stability of spatially uniform equilibria, and also works for assessing the stability of the ideal helical pattern solution for the complex activator-inhibitor equation in one space dimension with $C = 0$.

We would like to be able to argue that energetically favorable equilibrium solutions are in fact stable. For the spatially discretized systems of ODEs possessing Lyapunov functions, if we could show that a spatially nonuniform equilibrium was energetically favorable compared with the spatially uniform equilibrium, we would be tempted to conclude that there must be some stable spatially nonuniform equilibrium (not necessarily the one shown to have lower energy than the spatially uniform equilibrium, although that one would

be a good candidate). Under these circumstances, if the spatially nonuniform equilibria were isolated, we would be able to conclude that some spatially nonuniform equilibrium was indeed stable. However, the spatially nonuniform equilibria are not isolated equilibria, since with periodic boundary conditions, any spatial translation of a given equilibrium solution is also an equilibrium solution. What LaSalle's invariance principle does imply for our spatially discretized systems is that trajectories that enter into a given sublevel set of the Lyapunov function must converge to the set of equilibria contained in that sublevel set. Although even in the finite-dimensional case we cannot make as strong statements about stability as we would like, the concept of energetically favorable equilibria is still important, and will be illustrated numerically. The other approach, perturbing the dynamical equations about a particular equilibrium solution, writing down the Lyapunov functional for the perturbed dynamics, and then assessing the stability of the equilibrium with respect to linear perturbations, will be illustrated analytically.

Another benefit of having a Lyapunov functional is that we can show for the complex activator-inhibitor equation in one space dimension that the modal dynamics for any finite number of modes possesses a Lyapunov function. Furthermore, we can show that a finite number of modal coefficients are sufficient to achieve any $L^2(\Omega)$ error tolerance in approximating an equilibrium solution. These results also carry over to the real cubic nonlinearity model.

6.2 Form of the Lyapunov functional at equilibria

6.2.1 Basic cubic nonlinearity model

Recall the dynamics and Lyapunov functional for the basic cubic nonlin-

earity model:

$$\begin{aligned}
\tau_\theta \partial_t \theta &= l^2 \Delta\theta - \theta^3 + \theta + \eta, \\
\tau_\eta \partial_t \eta &= L^2 \Delta\eta - \eta - \theta + C, \\
V^* &= \int_\Omega \Big[\frac{l^2}{2} |\nabla\theta|^2 + \frac{1}{4}\theta^4 - \frac{1}{2}\theta^2 + \frac{L^2}{2}|\nabla\eta|^2 + \frac{1}{2}\eta^2 - C\eta + \theta\eta \\
&\qquad -(\theta - C)[(-1 + L^2\Delta)^{-1}(\theta - C)] \Big] d\mathbf{x}.
\end{aligned} \tag{6.1}$$

For equilibria, we have

$$\begin{aligned}
0 &= L^2 \Delta\eta - \eta - \theta + C, \\
(-1 + L^2\Delta)\eta &= \theta - C, \\
\eta &= (-1 + L^2\Delta)^{-1}(\theta - C),
\end{aligned} \tag{6.2}$$

so that the Lyapunov functional reduces to

$$V_e^* = \int_\Omega \Big[\frac{l^2}{2} |\nabla\theta|^2 + \frac{1}{4}\theta^4 - \frac{1}{2}\theta^2 + \frac{L^2}{2}|\nabla\eta|^2 + \frac{1}{2}\eta^2 \Big] d\mathbf{x}. \tag{6.3}$$

This is the Lyapunov functional for the decoupled θ and η dynamics with $C = 0$. Furthermore, multiplying the $\partial_t\theta$ equation through by θ, the $\partial_t\eta$ equation through by η, summing the equations, and integrating over Ω yields the identity

$$\int_\Omega \Big[l^2 |\nabla\theta|^2 + \theta^4 - \theta^2 + L^2 |\nabla\eta|^2 + \eta^2 - C\eta \Big] d\mathbf{x} = 0. \tag{6.4}$$

Using this identity, we can eliminate the derivative operators from V_e^*:

$$V_e^* = \int_\Omega \Big[-\frac{1}{4}\theta^4 + \frac{1}{2} C\eta \Big] d\mathbf{x}. \tag{6.5}$$

We can use the equilibrium equation

$$0 = L^2 \Delta\eta - \theta - \eta + C, \tag{6.6}$$

and use the fact that, for periodic or Neumann boundary conditions, the divergence theorem implies

$$\int_\Omega \Delta\eta \, d\mathbf{x} = 0, \tag{6.7}$$

to conclude that

$$V_e^* = \int_\Omega \left[-\frac{1}{4}\theta^4 - \frac{1}{2}C\theta + \frac{1}{2}C^2 \right] d\mathbf{x}. \tag{6.8}$$

We see from this expression for V_e^* that it is energetically favorable for θ to have the greatest possible absolute value, and for θ to have the same sign as C. If $C = 0$, then it is energetically favorable to maximize $|\theta|$, and a spatially periodic pattern equilibrium is stable. If $|C|$ is large, then it is energetically favorable to maximize $|\theta|$ so that C and θ have the same sign, which leads to a stable spatially uniform equilibrium. For intermediate values of C, numerical analysis indicates that spike solutions can have lower energy than a competing stable spatially uniform equilibrium, provided $\beta = l/L$ is sufficiently small. This is because spike solutions can have lower energy density outside of the transition regions to make up for having a higher energy density within the transition regions. As the width of transition regions becomes small (i.e., for $\beta << 1$), the contribution of the transition regions to the energy density also becomes small. This will be illustrated numerically for the discretized cubic nonlinearity model later on.

For the cubic nonlinearity model with additional symmetric long-range coupling, V_e^* takes exactly the same form as for the basic cubic nonlinearity model. For the bounded nonlinearity model, a different expression for V_e^* is obtained, but it still can be written in a form that depends only on θ (and not on η, $\nabla\theta$, or $\nabla\eta$). The active transmission line (with inhibitor diffusion and dissipation) has

$$V_e^* = \int_\Omega \left[-\frac{1}{4}\theta^4 + \frac{1}{2}C\theta \right] d\mathbf{x}, \tag{6.9}$$

since C appears in the $\partial_t\theta$ equation instead of in the $\partial_t\eta$ equation.

6.2.2 Complex activator-inhibitor equation

Recall that the complex activator-inhibitor equation could be written as a pair of nonlinearly coupled real activator-inhibitor equations,

$$\begin{aligned}
\tau_\theta \partial_t \theta_R &= l^2 \Delta \theta_R - (\theta_R^2 + \theta_I^2)\theta_R + \theta_R + \eta_R, \\
\tau_\theta \partial_t \theta_I &= l^2 \Delta \theta_I - (\theta_R^2 + \theta_I^2)\theta_I + \theta_I + \eta_I, \\
\tau_\eta \partial_t \eta_R &= L^2 \Delta \eta_R - \eta_R - \theta_R + C_R, \\
\tau_\eta \partial_t \eta_I &= L^2 \Delta \eta_I - \eta_I - \theta_I + C_I.
\end{aligned} \tag{6.10}$$

In analogy to the basic cubic nonlinearity model, for equilibria, V^* in the $(\theta_R, \theta_I, \eta_R, \eta_I)$ variables reduces to

$$\begin{aligned}
V_e^* &= \int_\Omega \Big[\frac{l^2}{2}\left(|\nabla\theta_R|^2 + |\nabla\theta_I|^2\right) + \frac{1}{4}\left(\theta_R^4 + 2\theta_R^2\theta_I^2 + \theta_I^4\right) - \frac{1}{2}\left(\theta_R^2 + \theta_I^2\right) \\
&\quad + \frac{L^2}{2}\left(|\nabla\eta_R|^2 + |\nabla\eta_I|^2\right) + \frac{1}{2}\left(\eta_R^2 + \eta_I^2\right) \Big] d\mathbf{x}.
\end{aligned} \tag{6.11}$$

Furthermore, multiplying the $\partial_t\theta_R$ equation through by θ_R, etc., summing all four equations, and integrating, yields the identity

$$\begin{aligned}
\int_\Omega \Big[& l^2\left(|\nabla\theta_R|^2 + |\nabla\theta_I|^2\right) + \left(\theta_R^4 + 2\theta_R^2\theta_I^2 + \theta_I^4\right) - \left(\theta_R^2 + \theta_I^2\right) \\
& + L^2\left(|\nabla\eta_R|^2 + |\nabla\eta_I|^2\right) + \left(\eta_R^2 + \eta_I^2\right) - (C_R\eta_R + C_I\eta_I) \Big] d\mathbf{x} = 0,
\end{aligned} \tag{6.12}$$

at equilibria. Combining these expressions gives

$$V_e^* = \int_\Omega \Big[-\frac{1}{4}\left(\theta_R^4 + 2\theta_R^2\theta_I^2 + \theta_I^4\right) + \frac{1}{2}(C_R\eta_R + C_I\eta_I) \Big] d\mathbf{x}. \tag{6.13}$$

Using the equilibrium equations and divergence theorem (for periodic or Neumann boundary conditions) then gives

$$V_e^* = \int_\Omega \Big[-\frac{1}{4}\left(\theta_R^4 + 2\theta_R^2\theta_I^2 + \theta_I^4\right) - \frac{1}{2}(C_R\theta_R + C_I\theta_I) + \frac{1}{2}(C_R^2 + C_I^2) \Big] d\mathbf{x}. \tag{6.14}$$

In the complex variables, V_e^* takes the form

$$V_e^* = \int_\Omega \Big[-\frac{1}{4}|\theta|^4 - \frac{1}{2}\mathrm{Re}\{\overline{C}\theta\} + \frac{1}{2}|C|^2 \Big] d\mathbf{x}. \tag{6.15}$$

We see from this expression that it is energetically favorable for θ to have the greatest magnitude possible and for θ to be aligned with C. (The $(1/2)|C|^2$ term is simply an additive constant to the Lyapunov functional and can therefore be ignored.) If $C = 0$, then it is clearly energetically favorable to simply maximize the magnitude of the activator. If $|C|$ is very large, it is energetically favorable to align the activator with C. However, for intermediate values of $|C|$, there is a tradeoff between maximizing $|\theta|$ and aligning θ with C.

6.3 Stability analysis for spatially uniform equilibria

6.3.1 Basic cubic nonlinearity model

It is possible to analyze the stability of spatially uniform equilibria of activator-inhibitor equations by linearizing the dynamics [9, 29]. This linearization was carried out in chapter 2, and yielded formulas for the critical wave number,

$$k_0 = \left(\frac{(\partial_\theta q)(\partial_\eta Q) - (\partial_\theta Q)(\partial_\eta q)}{l^2 L^2} \right)^{1/4}, \tag{6.16}$$

and the point at which the bifurcation to a pattern equilibrium occurs,

$$\partial_\theta q = -\beta^2 \partial_\eta Q - 2\beta[(\partial_\theta q)(\partial_\eta Q) - (\partial_\theta Q)(\partial_\eta q)]^{1/2}, \tag{6.17}$$

under the assumption that the system is a K-system. For the cubic nonlinearity model, we have

$$\begin{aligned} q(\theta, \eta, C) &= \theta^3 - \theta - \eta, \\ Q(\theta, \eta, C) &= \eta + \theta - C. \end{aligned} \tag{6.18}$$

We thus compute

$$\begin{aligned} \partial_\theta q &= 3\theta^2 - 1, \quad \partial_\eta Q = 1, \\ \partial_\theta Q &= 1, \quad \partial_\eta q = -1. \end{aligned} \tag{6.19}$$

At equilibrium, we have $q(\theta, \eta, C) = Q(\theta, \eta, C) = 0$, from which it follows that

$$\begin{aligned} \theta &= C^{1/3}, \\ \eta &= C - C^{1/3}. \end{aligned} \tag{6.20}$$

Thus, at the bifurcation point,

$$\begin{aligned} 3\theta^2 - 1 &= -\beta^2 - 2\beta(3\theta^2 - 1 + 1)^{1/2}, \\ 3|\theta|^2 - 1 &= -\beta^2 - 2\sqrt{3}\beta|\theta|, \\ (\sqrt{3}|\theta| + \beta)^2 &= 1, \\ \sqrt{3}|\theta| + \beta &= 1, \\ \theta &= \frac{1}{\sqrt{3}}(1-\beta), \\ C &= \frac{1}{3\sqrt{3}}(1-\beta)^3, \end{aligned} \tag{6.21}$$

and

$$k_0 = \left(\frac{3(C^{1/3})^2}{l^2 L^2}\right)^{1/4} = \frac{((1-\beta)^2)^{1/4}}{\sqrt{lL}} = \frac{\sqrt{1-\beta}}{\sqrt{lL}}. \tag{6.22}$$

The direct linearization approach required the assumption that the system was a K-system, and also required the derivation of formulas (6.16) and (6.17). Since we have a Lyapunov functional, we know in advance that for $\alpha > 1$, the system is a K-system. For the spatially discretized system of ODEs, we could perform a second-derivative test using the Lyapunov function to assess stability of the spatially uniform equilibria. We use an analogous approach for the PDE system. Our approach is to write the (nonlinear) dynamics for perturbations about the spatially uniform equilibrium of interest, write down a Lyapunov functional for the perturbed dynamics, drop the higher-order terms from the Lyapunov functional, plug in Fourier series representations of the perturbed variables, and finally, determine whether the Lyapunov functional is positive definite in the Fourier coefficients. In other words, we are using the Lyapunov functional to assess the stability of the spatially uniform

equilibrium with respect to linear perturbations. (This is basically the same procedure used later to assess the stability of helical equilibria for the complex activator-inhibitor equation when $C = 0$. Applying the procedure to the basic cubic nonlinearity model illustrates the technique on a simpler system.)

Let $\delta\theta$ and $\delta\eta$ denote the perturbed variables, i.e.,

$$\begin{aligned} \theta &= C^{1/3} + \delta\theta, \\ \eta &= C - C^{1/3} + \delta\eta. \end{aligned} \tag{6.23}$$

The dynamics for $\delta\theta$ and $\delta\eta$ are then

$$\begin{aligned} \tau_\theta \partial_t \delta\theta &= l^2 \Delta\delta\theta - \delta\theta^3 - 3\delta\theta^2 C^{1/3} - 3\delta\theta C^{2/3} + \delta\theta + \delta\eta, \\ \tau_\eta \partial_t \delta\eta &= L^2 \Delta\delta\eta - \delta\eta - \delta\theta, \end{aligned} \tag{6.24}$$

and the corresponding Lyapunov functional is

$$\begin{aligned} V_p^* = \int_\Omega \Big[&\frac{l^2}{2}|\nabla\delta\theta|^2 + \frac{1}{4}\delta\theta^4 + C^{1/3}\delta\theta^3 + \frac{3}{2}C^{2/3}\delta\theta^2 - \frac{1}{2}\delta\theta^2 + \frac{L^2}{2}|\nabla\delta\eta|^2 \\ &+ \frac{1}{2}\delta\eta^2 + \delta\theta\delta\eta - (\delta\theta)[(-1 + L^2\Delta)^{-1}(\delta\theta)] \Big] d\mathbf{x}. \end{aligned} \tag{6.25}$$

Retaining only the quadratic terms of V_p^*, we obtain

$$\begin{aligned} V_q^* = \int_\Omega \Big[&\frac{l^2}{2}|\nabla\delta\theta|^2 + \frac{1}{2}(3C^{2/3} - 1)\delta\theta^2 + \frac{L^2}{2}|\nabla\delta\eta|^2 + \frac{1}{2}\delta\eta^2 + \delta\theta\delta\eta \\ &- (\delta\theta)[(-1 + L^2\Delta)^{-1}(\delta\theta)] \Big] d\mathbf{x}, \end{aligned} \tag{6.26}$$

where the subscript "q" is used because this Lyapunov functional is quadratic.

Next, we assume periodic boundary conditions and define the Fourier series

$$\begin{aligned} \delta\theta &= \sum_{\mathbf{k}} \delta\theta_k e^{i\mathbf{k}\cdot\mathbf{x}}, \\ \delta\eta &= \sum_{\mathbf{k}} \delta\eta_k e^{i\mathbf{k}\cdot\mathbf{x}}. \end{aligned} \tag{6.27}$$

Using the identities (calculated as in chapter 5),

$$\begin{aligned}
\frac{1}{|\Omega|}\int_\Omega |\delta\theta|^2 d\mathbf{x} &= \sum_{\mathbf{k}} |\delta\theta_{\mathbf{k}}|^2, \\
\frac{1}{|\Omega|}\int_\Omega |\delta\eta|^2 d\mathbf{x} &= \sum_{\mathbf{k}} |\delta\eta_{\mathbf{k}}|^2, \\
\frac{1}{|\Omega|}\int_\Omega \delta\theta\delta\eta d\mathbf{x} &= \sum_{\mathbf{k}} \overline{\delta\theta}_{\mathbf{k}}\delta\eta_{\mathbf{k}}, \\
\frac{1}{|\Omega|}\int_\Omega |\nabla\delta\theta|^2 d\mathbf{x} &= \sum_{\mathbf{k}} |\mathbf{k}|^2|\delta\theta_{\mathbf{k}}|^2, \\
\frac{1}{|\Omega|}\int_\Omega |\nabla\delta\eta|^2 d\mathbf{x} &= \sum_{\mathbf{k}} |\mathbf{k}|^2|\delta\eta_{\mathbf{k}}|^2, \\
-\frac{1}{|\Omega|}\int_\Omega (\delta\theta)[(-1+L^2\Delta)^{-1}(\delta\theta)] d\mathbf{x} &= \sum_{\mathbf{k}} \frac{1}{1+L^2|\mathbf{k}|^2}|\delta\theta_{\mathbf{k}}|^2, \qquad (6.28)
\end{aligned}$$

we have

$$\begin{aligned}
\frac{1}{|\Omega|}V_q^* &= \sum_{\mathbf{k}} \left[\frac{l^2}{2}|\mathbf{k}|^2 + \frac{1}{2}(3C^{2/3}-1) + \frac{1}{1+L^2|\mathbf{k}|^2}\right]|\delta\theta_{\mathbf{k}}|^2 \\
&\quad + \frac{1}{2}(1+L^2|\mathbf{k}|^2)|\eta_{\mathbf{k}}|^2 + \overline{\delta\theta}_{\mathbf{k}}\delta\eta_{\mathbf{k}} \\
&= \sum_{\mathbf{k}} \frac{1}{2}\left[l^2|\mathbf{k}|^2 + (3C^{2/3}-1) + \frac{1}{1+L^2|\mathbf{k}|^2}\right]|\delta\theta_{\mathbf{k}}|^2 \\
&\quad + \frac{1}{2}\left|\frac{1}{\sqrt{1+L^2|\mathbf{k}|^2}}\delta\theta_{\mathbf{k}} + \sqrt{1+L^2|\mathbf{k}|^2}\delta\eta_{\mathbf{k}}\right|^2. \qquad (6.29)
\end{aligned}$$

It is easily shown that

$$l^2|\mathbf{k}|^2 + \frac{1}{1+L^2|\mathbf{k}|^2} \geq -\beta^2 + 2\beta, \qquad (6.30)$$

and this leads to the stability criterion

$$|C| \geq \frac{1}{3\sqrt{3}}(1-\beta)^3, \qquad (6.31)$$

the same stability criterion for C that arises in the direct linearization of the dynamics. The critical wave number also agrees with that given by direct linearization, namely $k_0 = \sqrt{1-\beta}/\sqrt{lL}$.

6.3.2 Active transmission line (with inhibitor diffusion and dissipation)

The equation for the spatially uniform activator equilibrium is cubic,

$$\theta^3 - \theta + C = 0, \tag{6.32}$$

and so it can be solved for θ using the following formulas:

$$\begin{aligned} A &= \left(-\frac{C}{2} + \sqrt{\frac{C^2}{4} - \frac{1}{27}}\right)^{1/3}, \\ B &= \left(-\frac{C}{2} - \sqrt{\frac{C^2}{4} - \frac{1}{27}}\right)^{1/3}, \\ \theta &= A + B, \ -\frac{A+B}{2} + \frac{(A-B)}{2}\sqrt{-3}, \ -\frac{A+B}{2} - \frac{(A-B)}{2}\sqrt{-3}. \end{aligned} \tag{6.33}$$

If

$$\sqrt{\frac{C^2}{4} - \frac{1}{27}} \tag{6.34}$$

is positive, there is one real root; if it is zero, there is a simple real root and a double real root; and if it is negative, there are three unequal real roots.

Denote the spatially uniform equilibrium value of θ by $\hat{\theta}$ and perturb the dynamics about the spatially uniform equilibrium:

$$\begin{aligned} \theta &= \hat{\theta} + \delta\theta, \\ \eta &= \delta\eta. \end{aligned} \tag{6.35}$$

The perturbed dynamics are

$$\begin{aligned} \tau_\theta \partial_t \delta\theta &= l^2 \partial_{xx}\delta\theta - (\delta\theta)^3 - 3\hat{\theta}^2\delta\theta - 3\hat{\theta}(\delta\theta)^2 + \delta\theta - \partial_x\delta\eta, \\ \tau_\eta \partial_t \delta\eta &= L^2\partial_{xx}\delta\eta - \delta\eta - \partial_x\delta\theta. \end{aligned} \tag{6.36}$$

The Lyapunov functional for this perturbed system is

$$\begin{aligned} V_p^* = \int_\Omega \Big[&\frac{l^2}{2}|\partial_x\delta\theta|^2 + \frac{1}{4}\delta\theta^4 + \frac{3}{2}\hat{\theta}^2\delta\theta^2 + \hat{\theta}\delta\theta^3 - \frac{1}{2}\delta\theta^2 + \frac{L^2}{2}|\partial_x\delta\eta|^2 \\ &+ \frac{1}{2}\delta\eta^2 + \delta\eta\partial_x\delta\theta - (\partial_x\delta\theta)[(-1 + L^2\partial_{xx})^{-1}(\partial_x\delta\theta)]\Big] dx, \end{aligned} \tag{6.37}$$

and retaining only the quadratic part, we obtain

$$\begin{aligned} V_q^* &= \int_\Omega \Big[\frac{l^2}{2}|\partial_x\delta\theta|^2 + \frac{1}{2}(3\hat{\theta}^2-1)\delta\theta^2 + \frac{L^2}{2}|\partial_x\delta\eta|^2 + \frac{1}{2}\delta\eta^2 + \delta\eta\partial_x\delta\theta \\ &\quad -(\partial_x\delta\theta)[(-1+L^2\partial_{xx}^2)^{-1}(\partial_x\delta\theta)]\Big]dx, \end{aligned} \tag{6.38}$$

Using the Fourier series representations,

$$\begin{aligned} \delta\theta &= \sum_k \delta\theta_k \mathrm{e}^{ikx}, \\ \delta\eta &= \sum_k \delta\eta_k \mathrm{e}^{ikx}, \end{aligned} \tag{6.39}$$

we have the same identities as in the previous subsection, and also

$$\begin{aligned} \frac{1}{|\Omega|}\int_\Omega \delta\eta\partial_x\delta\theta dx &= \frac{1}{|\Omega|}\int_\Omega \left(\sum_k \delta\eta_k \mathrm{e}^{ikx}\right)\left(\sum_k ik\delta\theta_k \mathrm{e}^{ikx}\right)dx \\ &= \sum_k ik\overline{\delta\eta}_k\delta\theta_k, \\ -\frac{1}{|\Omega|}\int_\Omega (\partial_x\delta\theta)[(-1+L^2\partial_{xx})^{-1}(\partial_x\delta\theta)]dx & \\ &= \frac{1}{|\Omega|}\int_\Omega \left(\sum_k ik\delta\theta_k \mathrm{e}^{ikx}\right)\frac{1}{1+L^2k^2}\left(\sum_k ik\delta\theta_k \mathrm{e}^{ikx}\right)dx \\ &= \sum_k \frac{k^2}{1+L^2k^2}|\delta\theta_k|^2. \end{aligned} \tag{6.40}$$

We then obtain

$$\begin{aligned} \frac{1}{|\Omega|}V_q^* &= \sum_k \left[\frac{l^2k^2}{2} + \frac{1}{2}(3\hat{\theta}^2-1) + \frac{k^2}{1+L^2k^2}\right]|\delta\theta_k|^2 + \left[\frac{L^2k^2}{2}+\frac{1}{2}\right]|\delta\eta_k|^2 \\ &\quad + ik\overline{\delta\eta}_k\delta\theta_k \\ &= \sum_k \frac{1}{2}\left[l^2k^2 + 3\hat{\theta}^2 - 1 + \frac{k^2}{1+L^2k^2}\right]|\delta\theta_k|^2 \\ &\quad + \frac{1}{2}\left|\sqrt{1+L^2k^2}\delta\eta_k + \frac{ik}{\sqrt{1+L^2k^2}}\delta\theta_k\right|^2, \end{aligned} \tag{6.41}$$

from which we see that the spatially uniform equilibrium solution $\hat{\theta}$ is stable if $|\hat{\theta}| > 1/\sqrt{3}$. (Recall that the corresponding result for the basic cubic nonlinearity model was similar in the low-β limit, but that β did shift the stability boundary slightly.)

We can conclude from the above analysis that whenever C is such that $\theta^3 - \theta + C$ has three unequal real roots, the two that are greater than $1/\sqrt{3}$ in absolute value correspond to stable spatially uniform equilibria. (In fact, the root in between corresponds to an unstable spatially uniform equilibrium.) If C is such that $\theta^3 - \theta + C$ has only one real root, then it corresponds to a stable spatially uniform equilibrium. Thus, depending on the value of C, the system can be either monostable or bistable. Of course, these remarks only apply when $\alpha > \frac{1}{2L}$, so that V^* is a valid Lyapunov functional.

6.4 Analysis of equilibria for the complex activator-inhibitor equation

For purposes of analyzing equilibria, we will consider the complex activator-inhibitor equation in one space dimension,

$$\begin{aligned} \tau_\theta \partial_t \theta &= l^2 \partial_{xx} \theta - |\theta|^2 \theta + \theta + \eta, \\ \tau_\eta \partial_t \eta &= L^2 \partial_{xx} \eta - \eta - \theta + C, \end{aligned} \tag{6.42}$$

with periodic boundary conditions. For $C = 0$, there are stable spatially periodic pattern solutions, which in the one-dimensional case can be thought of as helical, since a three-dimensional (phasor) plot of the real and imaginary parts of either the activator or the inhibitor plotted along the single space dimension would trace out a helix. For $|C|$ sufficiently large, there is a stable spatially uniform equilibrium solution. The intermediate values of $|C|$ can produce patterns in which the direction of the activator (and inhibitor) vectors oscillate between two different directions as one moves along the space dimension (or, if $|C|$ is small enough, the helical solution is simply perturbed by higher spatial harmonics). If instead of thinking about the complex envelope, we instead return to the point of view of coupled oscillators, the helical solution corresponds to a traveling wave (or rotating wave), like the threads of a turning screw. In

this section, we will analyze the stability with respect to linear perturbations of helical equilibria for $C = 0$ and spatially uniform equilibria for $|C|$ large. We will also show how to express the dynamics and Lyapunov functional in polar coordinates. For the analysis in this section, we will assume throughout that $\alpha = \tau_\theta/\tau_\eta > 1$, and also that $\beta = l/L < 1$, although not necessarily $\beta << 1$.

6.4.1 Polar coordinate transformation

Since it is often natural to examine coupled oscillator equations in polar coordinates, we define

$$\begin{aligned} \theta_R + i\theta_I &= r_\theta \exp(i\psi_\theta), \\ \eta_R + i\eta_I &= r_\eta \exp(i\psi_\eta), \\ C_R + iC_I &= r_C \exp(i\psi_C). \end{aligned} \tag{6.43}$$

The dynamics in transformed coordinates are (see Appendix A),

$$\begin{aligned} \tau_\theta \partial_t r_\theta &= l^2 \left[\partial_{xx} r_\theta - r_\theta (\partial_x \psi_\theta)^2\right] - r_\theta^3 + r_\theta + r_\eta \cos(\psi_\eta - \psi_\theta), \\ \tau_\eta \partial_t r_\eta &= L^2 \left[\partial_{xx} r_\eta - r_\eta (\partial_x \psi_\eta)^2\right] - r_\eta - r_\theta \cos(\psi_\eta - \psi_\theta) + r_C \cos(\psi_\eta - \psi_C), \\ \tau_\theta \partial_t \psi_\theta &= l^2 \partial_{xx} \psi_\theta + \frac{2l^2}{r_\theta} (\partial_x r_\theta)(\partial_x \psi_\theta) + \frac{r_\eta}{r_\theta} \sin(\psi_\eta - \psi_\theta), \\ \tau_\eta \partial_t \psi_\eta &= L^2 \partial_{xx} \psi_\eta + \frac{2L^2}{r_\eta} (\partial_x r_\eta)(\partial_x \psi_\eta) + \frac{r_\theta}{r_\eta} \sin(\psi_\eta - \psi_\theta) - \frac{r_C}{r_\eta} \sin(\psi_\eta - \psi_C). \end{aligned} \tag{6.44}$$

We can also write the Lyapunov functional in transformed coordinates as

$$\begin{aligned} V^* = \int_\Omega \Big[& \frac{l^2}{2} |\partial_x r_\theta|^2 + \frac{l^2}{2} r_\theta^2 |\partial_x \psi_\theta|^2 + \frac{L^2}{2} |\partial_x r_\eta|^2 + \frac{L^2}{2} r_\eta^2 |\partial_x \psi_\eta|^2 + \frac{1}{4} r_\theta^4 - \frac{1}{2} r_\theta^2 \\ & + \frac{1}{2} r_\eta^2 - r_C r_\eta \cos(\psi_\eta - \psi_C) + r_\theta r_\eta \cos(\psi_\eta - \psi_\theta) \\ & - (r_\theta \cos\psi_\theta - r_C \cos\psi_C) \left[(-1 + L^2\Delta)^{-1} (r_\theta \cos\psi_\theta - r_C \cos\psi_C)\right] \\ & - (r_\theta \sin\psi_\theta - r_C \sin\psi_C) \left[(-1 + L^2\Delta)^{-1} (r_\theta \sin\psi_\theta - r_C \sin\psi_C)\right] \Big] d\mathbf{x}. \end{aligned} \tag{6.45}$$

We expect that the Lyapunov functional in transformed coordinates will depend only on relative phases and not on any absolute phases. All of the terms except those involving $(-1 + L^2\Delta)^{-1}$ clearly meet this requirement. For the terms involving $(-1 + L^2\Delta)^{-1}$, we can use the fact that the operator $(-1 + L^2\Delta)^{-1}$ can be represented as $(-1 + L^2\Delta)^{-1}v = w * v$, i.e., as a convolution with an even kernel w:

$$\begin{aligned}
&\int_\Omega [(r_\theta \cos\psi_\theta - r_C \cos\psi_C)[w * (r_\theta \cos\psi_\theta - r_C \cos\psi_C)] \\
&\qquad +(r_\theta \sin\psi_\theta - r_C \sin\psi_C)[w * (r_\theta \sin\psi_\theta - r_C \sin\psi_C)]]dx \\
&= \int_\Omega \int_\Omega [r_\theta(x,t)w(x-y)r_\theta(y,t)\,[\cos\psi_\theta(x,t)\cos\psi_\theta(y,t) \\
&\qquad\qquad + \sin\psi_\theta(x,t)\sin\psi_\theta(y,t)] \\
&\qquad -r_\theta(x,t)w(x-y)r_C\,[\cos\psi_\theta(x,t)\cos\psi_C + \sin\psi_\theta(x,t)\sin\psi_C] \\
&\qquad -r_C w(x-y)r_\theta(y,t)\,[\cos\psi_C\cos\psi_\theta(y,t) + \sin\psi_C\sin\psi_\theta(y,t)] \\
&\qquad +r_C w(x-y)r_C\,[\cos\psi_C\cos\psi_C + \sin\psi_C\sin\psi_C]\,]dydx \\
&= \int_\Omega \int_\Omega [r_\theta(x,t)w(x-y)r_\theta(y,t)\cos(\psi_\theta(x,t) - \psi_\theta(y,t)) \\
&\qquad -r_\theta(x,t)w(x-y)r_C\cos(\psi_\theta(x,t) - \psi_C) \\
&\qquad -r_C w(x-y)r_\theta(y,t)\cos(\psi_C - \psi_\theta(y,t)) + r_C w(x-y)r_C]dydx. \qquad (6.46)
\end{aligned}$$

Thus, the convolution terms also depend only on relative phases, not on any absolute phase.

Although $\dot{V}^*$ could in principle be calculated using

$$\dot{V}^* = \frac{\delta V^*}{\delta r_\theta}\cdot(\partial_t r_\theta) + \frac{\delta V^*}{\delta r_\eta}\cdot(\partial_t r_\eta) + \frac{\delta V^*}{\delta \psi_\theta}\cdot(\partial_t \psi_\theta) + \frac{\delta V^*}{\delta \psi_\eta}\cdot(\partial_t \psi_\eta), \qquad (6.47)$$

$\dot{V}^*$ will take a more complicated form in the $(r_\theta, r_\eta, \psi_\theta, \psi_\eta)$ variables than in the $(\theta_R, \theta_I, \eta_R, \eta_I)$ variables due to the $(-1 + L^2\Delta)^{-1}$ terms.

The ideal helical solution in the $C = 0$ case in one space dimension can be simply described in the transformed coordinates as

$$\begin{aligned} \partial_x \psi_\theta &= \partial_x \psi_\eta \equiv \phi = \text{constant}, \\ \psi_\theta &= \psi_\eta + \pi, \\ r_\theta &\equiv R_\theta = \text{constant}, \\ r_\eta &\equiv R_\eta = \text{constant}. \end{aligned} \tag{6.48}$$

(We are assuming that the boundary conditions are periodic, which will select specific possibilities for ϕ, of which it is possible that none or more than one will lead to ideal stable equilibria. If the domain Ω is large, we expect that there will be at least one ideal stable equilibrium. If the interval Ω has length $|\Omega|$, then the periodic boundary conditions imply that $\psi_\theta(x + |\Omega|) = \psi_\theta(x) + 2\pi m$ and $\psi_\eta(x + |\Omega|) = \psi_\eta(x) + 2\pi m$ for some integer m.)

In the $C = 0$ case, in addition to the ideal helical equilibrium solution taking a simple form, the Lyapunov functional at equilibria also takes a particularly simple form:

$$V_e^* = -\int_\Omega \frac{1}{4} r_\theta^4 \, dx. \tag{6.49}$$

Despite the simple form that the ideal equilibrium solutions and equilibrium energy take in polar coordinates, it turns out to be easier to analyze the stability of the ideal solutions using a different change of coordinates: one that retains the complex character of the dynamics, but rotates with the helical solution along the (single) space dimension.

6.4.2 Analysis of the ideal helical equilibria in the $C = 0$ case

The goal of our analysis of the ideal helical equilibrium solutions for the $C = 0$ case in one space dimension is to show that these equilibria are stable with respect to linear perturbations. The feature of the ideal helical solutions that makes this analysis tractable is that these solutions involve pure sinusoids

with a single spatial frequency (or wave number), ϕ, which (without loss of generality) we will assume to be positive.

The complex dynamics

$$\begin{aligned} \tau_\theta \partial_t \theta &= l^2 \partial_{xx}\theta - |\theta|^2\theta + \theta + \eta, \\ \tau_\eta \partial_t \eta &= L^2 \partial_{xx}\eta - \eta - \theta + C, \end{aligned} \tag{6.50}$$

are the starting point for this analysis. Let the ideal helical equilibrium solution of interest have the form

$$\begin{aligned} \theta &= R_\theta \mathrm{e}^{i\phi x}, \\ \eta &= R_\eta \mathrm{e}^{i\phi x}. \end{aligned} \tag{6.51}$$

We define the new coordinates θ_H and η_H such that θ_H is always aligned with the ideal helical equilibrium solution:

$$\begin{aligned} \theta_H &= \theta \mathrm{e}^{-i\phi x}, \\ \eta_H &= \eta \mathrm{e}^{-i\phi x}. \end{aligned} \tag{6.52}$$

We now calculate the dynamics for θ_H and η_H (for now, carrying along C in the equations, even though we will later set $C = 0$):

$$\begin{aligned} \tau_\theta \partial_t \theta_H &= l^2(\partial_{xx}\theta_H + i2\phi\partial_x\theta_H - \phi^2\theta_H) - |\theta_H|^2\theta_H + \theta_H + \eta_H, \\ \tau_\eta \partial_t \eta_H &= L^2(\partial_{xx}\eta_H + i2\phi\partial_x\eta_H - \phi^2\eta_H) - \theta_H - \eta_H + C_H, \end{aligned} \tag{6.53}$$

where $C_H = C\mathrm{e}^{-i\phi x}$, and the corresponding Lyapunov functional can be expressed in complex form as

$$\begin{aligned} V^* = \int_\Omega \Big[&\frac{l^2}{2}|\partial_x\theta_H + i\phi\theta_H|^2 + \frac{1}{4}|\theta_H|^4 - \frac{1}{2}|\theta_H|^2 + \frac{L^2}{2}|\partial_x\eta_H + i\phi\eta_H|^2 \\ &+\frac{1}{2}|\eta_H|^2 - \mathrm{Re}\{\overline{C}_H\eta_H\} + \mathrm{Re}\{\overline{\theta}_H\eta_H\} \\ &-(\overline{\theta}_H - \overline{C}_H)[(-1 + L^2(\partial_x + i\phi)^2)^{-1}(\theta_H - C_H)]\Big] dx. \end{aligned} \tag{6.54}$$

The ideal helical equilibrium solution of interest (with $C = 0$) is

$$\begin{aligned} \theta_H &= R_\theta = \text{constant}, \\ \eta_H &= R_\eta = \text{constant}. \end{aligned} \tag{6.55}$$

Solving for the constant values R_θ and R_η, we have

$$\begin{aligned} 0 &= -l^2\phi^2 R_\theta - R_\theta^3 + R_\theta + R_\eta, \\ 0 &= -L^2\phi^2 R_\eta - R_\eta - R_\theta, \end{aligned} \tag{6.56}$$

which leads to

$$\begin{aligned} R_\eta &= -\frac{1}{1+L^2\phi^2} R_\theta, \\ 0 &= -l^2\phi^2 R_\theta - R_\theta^3 + R_\theta - \frac{1}{1+L^2\phi^2} R_\theta, \\ R_\theta^2 &= 1 - l^2\phi^2 - \frac{1}{1+L^2\phi^2}. \end{aligned} \tag{6.57}$$

Note that

$$\max_\phi R_\theta = 1 - \beta, \tag{6.58}$$

and is attained for $\phi = \sqrt{1-\beta}/\sqrt{lL}$. Thus, the magnitude of the ideal helical solution is maximized for a value of ϕ near the reciprocal of the geometric mean of l and L, the activator and inhibitor length scales. (Keep in mind that we know from the form of the original Lyapunov functional on equilibria, V_e^*, that a larger R_θ corresponds to a lower energy V_e^*.) Figure 6.1 shows R_θ as a function of ϕ over the range of values $\phi > 0$ for which R_θ is well-defined.

Next, we perturb the dynamics using

$$\begin{aligned} \theta_H &= R_\theta + \delta\theta_H, \\ \eta_H &= R_\eta + \delta\eta_H. \end{aligned} \tag{6.59}$$

Noting that

$$\begin{aligned} &|R_\theta + \delta\theta_H|^2(R_\theta + \delta\theta_H) \\ &\quad = (R_\theta^2 + R_\theta\delta\theta_H + R_\theta\overline{\delta\theta}_H + |\delta\theta_H|^2)(R_\theta + \delta\theta_H) \end{aligned}$$

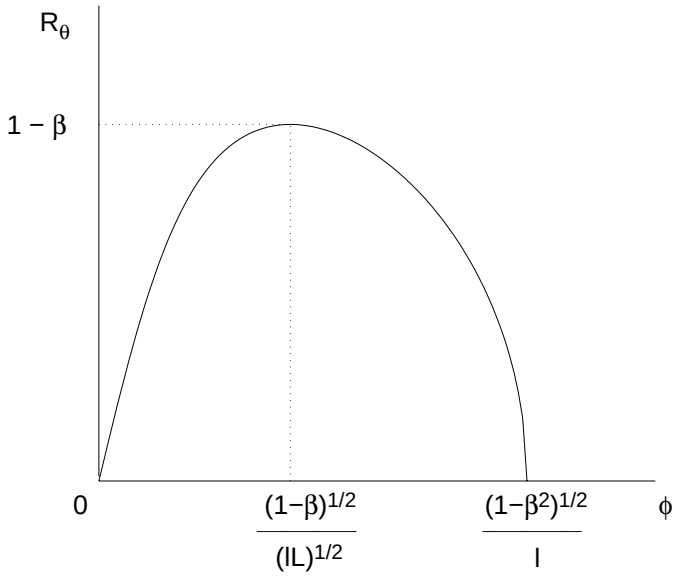

Figure 6.1: Plot of R_θ versus ϕ

$$
\begin{aligned}
&= R_\theta^3 + 2R_\theta^2\delta\theta_H + R_\theta^2\overline{\delta\theta}_H + 2R_\theta|\delta\theta_H|^2 + R_\theta(\delta\theta_H)^2 + |\delta\theta_H|^2\delta\theta_H \\
&= R_\theta^3 + 3R_\theta^2\mathrm{Re}\{\delta\theta_H\} + iR_\theta^2\mathrm{Im}\{\delta\theta_H\} + 3R_\theta(\mathrm{Re}\{\delta\theta_H\})^2 \\
&\quad +i2R_\theta\mathrm{Re}\{\theta_H\}\mathrm{Im}\{\theta_H\} + R_\theta(\mathrm{Im}\{\theta_H\})^2 + |\delta\theta_H|^2\delta\theta_H, \qquad (6.60)
\end{aligned}
$$

we find that the perturbed dynamics are

$$
\begin{aligned}
\tau_\theta\partial_t\delta\theta_H &= l^2(\partial_{xx}\delta\theta_H + i2\phi\partial_x\delta\theta_H - \phi^2\delta\theta_H) - |\delta\theta_H|^2\delta\theta_H - 3R_\theta^2\mathrm{Re}\{\delta\theta_H\} \\
&\quad -3R_\theta(\mathrm{Re}\{\delta\theta_H\})^2 - R_\theta(\mathrm{Im}\{\delta\theta_H\})^2 - iR_\theta^2\mathrm{Im}\{\delta\theta_H\} \\
&\quad -i2R_\theta\mathrm{Re}\{\delta\theta_H\}\mathrm{Im}\{\delta\theta_H\} + \delta\theta_H + \delta\eta_H, \\
\tau_\eta\partial_t\delta\eta_H &= L^2(\partial_{xx}\delta\eta_H + i2\phi\partial_x\delta\eta_H - \phi^2\delta\eta_H) - \delta\theta_H - \delta\eta_H. \qquad (6.61)
\end{aligned}
$$

The Lyapunov functional for this perturbed system is

$$
\begin{aligned}
V_p^* &= \int_\Omega \Big[\frac{l^2}{2}|\partial_x\delta\theta_H + i\phi\delta\theta_H|^2 + \frac{1}{4}|\delta\theta_H|^4 - \frac{1}{2}|\delta\theta_H|^2 + \frac{L^2}{2}|\partial_x\delta\eta_H + i\phi\delta\eta_H|^2 \\
&\quad +\frac{1}{2}|\delta\eta_H|^2 + \mathrm{Re}\{\overline{\delta\theta}_H\delta\eta_H\} + \frac{3}{2}R_\theta^2(\mathrm{Re}\{\delta\theta_H\})^2 + R_\theta(\mathrm{Re}\{\delta\theta_H\})^3 \\
&\quad +R_\theta(\mathrm{Re}\{\delta\theta_H\})(\mathrm{Im}\{\delta\theta_H\})^2 + \frac{1}{2}R_\theta^2(\mathrm{Im}\{\delta\theta_H\})^2 \\
&\quad -\overline{\delta\theta}_H[(-1 + L^2(\partial_x + i\phi)^2)^{-1}(\delta\theta_H)]\Big]dx. \qquad (6.62)
\end{aligned}
$$

The operator $(-1+L^2(\partial_x+i\phi)^2)^{-1}$ is well-behaved just like $(-1+L^2\partial_{xx})^{-1}$. The subscript "p" is to emphasize that this Lyapunov functional for the perturbed dynamics is different from the original Lyapunov functional for the θ_H and η_H dynamics, equation (6.54).

When the perturbation is zero (i.e., $\delta\theta_H = 0$ and $\delta\eta_H = 0$), clearly $V_p^* = 0$. If for sufficiently small but nonzero perturbations we can show that $V_p^* > 0$, then we could conclude that the ideal helical solution is stable. Since we are only concerned with small perturbations, we will neglect all of the higher-order terms in V_p^* and retain only the quadratic terms. Furthermore, we will divide up the $(3/2)R_\theta^2(\mathrm{Re}\{\delta\theta_H\})^2$ term into two terms, one of which can be merged with the corresponding term involving $(\mathrm{Im}\{\delta\theta_H\})^2$. The Lyapunov functional then becomes

$$\begin{aligned} V_q^* &= \int_\Omega \Big[\frac{l^2}{2}|\partial_x\delta\theta_H + i\phi\delta\theta_H|^2 - \frac{1}{2}(1-R_\theta^2)|\delta\theta_H|^2 + \frac{L^2}{2}|\partial_x\delta\eta_H + i\phi\delta\eta_H|^2 \\ &\quad + \frac{1}{2}|\delta\eta_H|^2 + \mathrm{Re}\{\overline{\delta\theta_H}\delta\eta_H\} - (\overline{\delta\theta_H})[(-1+L^2(\partial_x+i\phi)^2)^{-1}(\delta\theta_H)] \\ &\quad + R_\theta^2(\mathrm{Re}\{\delta\theta_H\})^2\Big]dx, \end{aligned} \tag{6.63}$$

where the subscript "q" is used because this Lyapunov functional is quadratic.

At this point, we consider Fourier series expansions of $\delta\theta_H$ and $\delta\eta_H$, and determine V_q^* in terms of the Fourier coefficients. The Fourier series representations for θ and η are

$$\begin{aligned} \delta\theta_H &= \sum_k \delta\theta_k \mathrm{e}^{ikx}, \\ \delta\eta_H &= \sum_k \delta\eta_k \mathrm{e}^{ikx}, \end{aligned} \tag{6.64}$$

The additional Fourier relationships we need are

$$
\begin{aligned}
\frac{1}{|\Omega|}\int_\Omega |\partial_x \delta\theta_H + i\phi\delta\theta_H|^2 dx &= \frac{1}{|\Omega|}\int_\Omega \left|\sum_k ik\delta\theta_k \mathrm{e}^{ikx} + \sum_k i\phi\delta\theta_k \mathrm{e}^{ikx}\right|^2 dx \\
&= \frac{1}{|\Omega|}\int_\Omega \left|\sum_k i(k+\phi)\delta\theta_k \mathrm{e}^{ikx}\right|^2 dx \\
&= \sum_k (k+\phi)^2 |\delta\theta_k|^2, \\
\frac{1}{|\Omega|}\int_\Omega |\partial_x \delta\eta_H + i\phi\delta\eta_H|^2 dx &= \sum_k (k+\phi)^2 |\delta\eta_k|^2, \qquad (6.65)
\end{aligned}
$$

and

$$
\begin{aligned}
-1 + L^2(\partial_x + i\phi)^2 &\leftrightarrow -1 - L^2(k+\phi)^2, \\
(-1 + L^2(\partial_x + i\phi)^2)^{-1} &\leftrightarrow \frac{-1}{1 + L^2(k+\phi)^2}, \\
-\frac{1}{|\Omega|}\int_\Omega (\overline{\delta\theta}_H)[(-1 + L^2(\partial_x + i\phi)^2)^{-1}(\delta\theta_H)]dx &= \sum_k \frac{1}{1 + L^2(k+\phi)^2}|\delta\theta_k|^2. \qquad (6.66)
\end{aligned}
$$

Finally, the $(\mathrm{Re}\{\theta\})^2$ term is analyzed as follows:

$$
\begin{aligned}
\delta\theta_H &= \sum_k \delta\theta_k \mathrm{e}^{ikx} = \delta\theta_0 + \sum_{k>0}\left[\delta\theta_k \mathrm{e}^{ikx} + \delta\theta_{-k}\mathrm{e}^{-ikx}\right] \\
&= \mathrm{Re}\{\delta\theta_0\} + i\mathrm{Im}\{\delta\theta_0\} + \sum_{k>0}\left[\left(\mathrm{Re}\{\delta\theta_k\} + i\mathrm{Im}\{\delta\theta_k\}\right)(\cos kx + i\sin kx)\right. \\
&\qquad \left. + \left(\mathrm{Re}\{\delta\theta_{-k}\} + i\mathrm{Im}\{\delta\theta_{-k}\}\right)(\cos kx - i\sin kx)\right] \\
&= \mathrm{Re}\{\delta\theta_0\} + \sum_{k>0}\left(\mathrm{Re}\{\delta\theta_k + \delta\theta_{-k}\}\cos kx - \mathrm{Im}\{\delta\theta_k - \delta\theta_{-k}\}\sin kx\right) \\
&\quad + i\left[\mathrm{Im}\{\delta\theta_0\} + \sum_{k>0}\left(\mathrm{Re}\{\delta\theta_k - \delta\theta_{-k}\}\sin kx + \mathrm{Im}\{\delta\theta_k + \delta\theta_{-k}\}\cos kx\right)\right], \\
&\frac{1}{|\Omega|}\int_\Omega (\mathrm{Re}\{\delta\theta_H\})^2 dx \\
&= (\mathrm{Re}\{\delta\theta_0\})^2 + \frac{1}{2}\sum_{k>0}\left[(\mathrm{Re}\{\delta\theta_k + \delta\theta_{-k}\})^2 + (\mathrm{Im}\{\delta\theta_k - \delta\theta_{-k}\})^2\right] \\
&= (\mathrm{Re}\{\delta\theta_0\})^2 + \frac{1}{2}\sum_{k>0}|\delta\theta_k + \overline{\delta\theta}_{-k}|^2. \qquad (6.67)
\end{aligned}
$$

We thus obtain

$$\begin{aligned}\frac{1}{|\Omega|}V_q^* &= \sum_k \Big[\frac{l^2}{2}(k+\phi)^2|\delta\theta_k|^2 - \frac{1}{2}(1-R_\theta^2)|\delta\theta_k|^2 + \frac{L^2}{2}(k+\phi)^2|\delta\eta_k|^2 + \frac{1}{2}|\delta\eta_k|^2 \\ &\qquad +\mathrm{Re}\{\overline{\delta\theta}_k\delta\eta_k\} + \frac{1}{1+L^2(k+\phi)^2}|\delta\theta_k|^2\Big] \\ &\quad +R_\theta^2(\mathrm{Re}\{\delta\theta_0\})^2 + \frac{1}{2}R_\theta^2\sum_{k>0}|\delta\theta_k + \overline{\delta\theta}_{-k}|^2. \end{aligned} \tag{6.68}$$

Plugging in the value of R_θ into the first term of V_q^* in which it appears then gives

$$\begin{aligned}\frac{1}{|\Omega|}V_q^* &= \sum_k \Big[\frac{l^2}{2}(k+\phi)^2|\delta\theta_k|^2 - \frac{1}{2}\left(l^2\phi^2 + \frac{1}{1+L^2\phi^2}\right)|\delta\theta_k|^2 + \frac{L^2}{2}(k+\phi)^2|\delta\eta_k|^2 \\ &\qquad +\frac{1}{2}|\delta\eta_k|^2 + \mathrm{Re}\{\overline{\delta\theta}_k\delta\eta_k\} + \frac{1}{1+L^2(k+\phi)^2}|\delta\theta_k|^2\Big] \\ &\quad +R_\theta^2(\mathrm{Re}\{\delta\theta_0\})^2 + \frac{1}{2}R_\theta^2\sum_{k>0}|\delta\theta_k + \overline{\delta\theta}_{-k}|^2 \\ &= \sum_k \Big[\left(\frac{l^2}{2}(k+\phi)^2 - \frac{l^2\phi^2}{2} - \frac{1}{2}\left(\frac{1}{1+L^2\phi^2}\right) + \frac{1}{1+L^2(k+\phi)^2}\right)|\delta\theta_k|^2 \\ &\qquad +\left(\frac{1+L^2(k+\phi)^2}{2}\right)|\delta\eta_k|^2 + \mathrm{Re}\{\overline{\delta\theta}_k\delta\eta_k\}\Big] \\ &\quad +R_\theta^2(\mathrm{Re}\{\delta\theta_0\})^2 + \frac{1}{2}R_\theta^2\sum_{k>0}|\delta\theta_k + \overline{\delta\theta}_{-k}|^2 \\ &= \sum_k \Big[\frac{1}{2}\left(l^2(k+\phi)^2 - l^2\phi^2 - \frac{1}{1+L^2\phi^2} + \frac{1}{1+L^2(k+\phi)^2}\right)|\delta\theta_k|^2 \\ &\qquad +\frac{1}{2}\left(\frac{1}{1+L^2(k+\phi)^2}\right)|\delta\theta_k|^2 + \frac{1}{2}\left(1+L^2(k+\phi)^2\right)|\delta\eta_k|^2 \\ &\qquad +\mathrm{Re}\{\overline{\delta\theta}_k\delta\eta_k\}\Big] \\ &\quad +R_\theta^2(\mathrm{Re}\{\delta\theta_0\})^2 + \frac{1}{2}R_\theta^2\sum_{k>0}|\delta\theta_k + \overline{\delta\theta}_{-k}|^2 \\ &= \sum_k \Big[\frac{1}{2}\left(l^2k^2 + 2l^2\phi k + \frac{1}{1+L^2(k+\phi)^2} - \frac{1}{1+L^2\phi^2}\right)|\delta\theta_k|^2 \\ &\quad +\frac{1}{2}\left|\frac{\delta\theta_k}{\sqrt{1+L^2(k+\phi)^2}} + \sqrt{1+L^2(k+\phi)^2}\delta\eta_k\right|^2\Big] \\ &\quad +R_\theta^2(\mathrm{Re}\{\delta\theta_0\})^2 + \frac{1}{2}R_\theta^2\sum_{k>0}|\delta\theta_k + \overline{\delta\theta}_{-k}|^2. \end{aligned} \tag{6.69}$$

Note that we always have

$$\begin{aligned} \left| \frac{\delta\theta_k}{\sqrt{1+L^2(k+\phi)^2}} + \sqrt{1+L^2(k+\phi)^2}\delta\eta_k \right|^2 &\geq 0, \\ R_\theta^2(\mathrm{Re}\{\delta\theta_0\})^2 &\geq 0, \\ \frac{1}{2}R_\theta^2 \sum_{k>0} |\delta\theta_k + \overline{\delta\theta}_{-k}|^2 &\geq 0. \end{aligned} \tag{6.70}$$

If we can show that $V_q^* > 0$ whenever θ and η are not both zero, then the ideal helical equilibrium solution with wave number ϕ will be stable with respect to linear perturbations. What we will in fact show is that for a certain range of values for ϕ, $V_q^* > 0$ whenever the small perturbation (6.64) is nonzero (except for a purely translational perturbation that is not of interest). We will then conclude that the helical solution, for a certain range of values of ϕ, is stable with respect to linear perturbations.

Lemma 6.14 *Consider the dynamics (6.50) with $\alpha = \tau_\theta/\tau_\eta > 1$ and the ideal helical equilibrium solution (6.51) with wave number ϕ. For $\phi \in [\phi_{min}, \phi_{max}]$, where $\phi_{min} = \sqrt{1-\beta}/\sqrt{lL}$ (with $\beta = l/L$) and where ϕ_{max} is a constant with $\phi_{max} - \phi_{min} > 0$ sufficiently small, the ideal helical equilibrium solution is stable with respect to linear perturbations; i.e., $V_q^* > 0$ for all small perturbations (6.64) of the ideal helical equilibrium solution (except for purely translational perturbations).*

Proof: First, consider the $k = 0$ term of V_q^*. If a perturbation satisfies

$$\delta\eta_0 = -\frac{1}{1+L^2\phi^2}\delta\theta_0, \tag{6.71}$$

with $\delta\theta_0$ and $\delta\eta_0$ both purely imaginary, then $V_q^* = 0$. This purely imaginary constant perturbation corresponds to a simple translation of the original ideal helical solution to the left or right, and so of course will not cause the energy

(either V^*, V_p^*, or V_q^*) to change (keep in mind that we are assuming periodic boundary conditions). This translational perturbation is not one we are interested in from the point of view of our stability analysis, so we will not consider it further.

Next, we will determine for what values of ϕ we have

$$l^2k^2 + 2l^2\phi k + \frac{1}{1+L^2(k+\phi)^2} - \frac{1}{1+L^2\phi^2} > 0, \quad \forall k > 0, \tag{6.72}$$

i.e, we are only considering positive values of k for now. (The $k < 0$ case is much more complicated, and we will return to it later.) We see that one dangerous limit is the $k \to 0$ limit. In this limit, we can neglect terms higher than linear in k and expand the third term above to yield

$$\begin{aligned}
2l^2\phi k + \frac{1}{1+L^2\phi^2}\left[\frac{1}{1+\frac{L^2(k^2+2k\phi)}{1+L^2\phi^2}}\right] - \frac{1}{1+L^2\phi^2} & \\
\approx \; 2l^2\phi k + \frac{1}{1+L^2\phi^2}\left[1 - \frac{L^2(k^2+2k\phi)}{1+L^2\phi^2}\right] - \frac{1}{1+L^2\phi^2} & \\
= \; 2l^2\phi k - \frac{L^2(k^2+2k\phi)}{(1+L^2\phi^2)^2} & \\
\approx \; \left[2l^2\phi - \frac{2L^2\phi}{(1+L^2\phi^2)^2}\right]k & \\
> \; 0. &
\end{aligned} \tag{6.73}$$

The limiting value of ϕ satisfying the above bound with equality is the value of ϕ that maximizes R_θ,

$$\phi > \frac{\sqrt{1-\beta}}{\sqrt{lL}}. \tag{6.74}$$

Furthermore, for $\phi > \sqrt{1-\beta}/\sqrt{lL}$,

$$f(k) = l^2k^2 + 2l^2\phi k + \frac{1}{1+L^2(k+\phi)^2} - \frac{1}{1+L^2\phi^2}. \tag{6.75}$$

is monotone increasing, since

$$\frac{df}{dk} \;=\; 2l^2k + 2l^2\phi - \frac{2L^2(k+\phi)}{(1+L^2(k+\phi)^2)^2}$$

$$
\begin{aligned}
&= \left(2l^2 - \frac{2L^2}{(1+L^2(k+\phi)^2)^2}\right)(k+\phi) \\
&> 0, \quad \forall k > 0.
\end{aligned} \tag{6.76}
$$

Now we consider the $k < 0$ terms of V_q^*. For $k < 0$, the term

$$
\frac{1}{2}\left(l^2k^2 + 2l^2\phi k + \frac{1}{1+L^2(k+\phi)^2} - \frac{1}{1+L^2\phi^2}\right)|\delta\theta_k|^2 \tag{6.77}
$$

of V_q^* will be negative for certain values of k, in particular, for $k \to 0$ with $k < 0$. Therefore, we need to regroup the terms in V_q^* to show that $V_q^* > 0$ for all nonzero perturbations of interest, for some range of values of $\phi \geq \phi_{min} = \sqrt{1-\beta}/\sqrt{lL}$.

Letting

$$
g(k) = \frac{l^2k^2 + 2l^2\phi k + \frac{1}{1+L^2(k+\phi)^2} - \frac{1}{1+L^2\phi^2}}{R_\theta^2}, \tag{6.78}
$$

we have

$$
\begin{aligned}
&\sum_k g(k)|\delta\theta_k|^2 + \sum_{k>0}|\delta\theta_k + \overline{\delta\theta}_{-k}|^2 \\
&= \sum_{k>0} g(k)|\delta\theta_k|^2 + g(-k)|\delta\theta_{-k}|^2 + |\delta\theta_k|^2 + |\delta\theta_{-k}|^2 + 2\mathrm{Re}\{\delta\theta_k\overline{\delta\theta}_{-k}\} \\
&= \sum_{k>0}(1+g(k))|\delta\theta_k|^2 + (1+g(-k))|\delta\theta_{-k}|^2 + 2\mathrm{Re}\{\delta\theta_k\overline{\delta\theta}_{-k}\} \\
&= \sum_{k>0}\left(1 + g(k) - \frac{1}{1+g(-k)}\right)|\delta\theta_k|^2 + \left|\frac{1}{\sqrt{1+g(-k)}}\delta\theta_k + \sqrt{1+g(-k)}\delta\theta_{-k}\right|^2.
\end{aligned} \tag{6.79}
$$

In the low k limit (where now, of course, k is positive since we have rewritten the sum over all k as a sum over positive k only), we know that $g(k) \to 0$. Therefore,

$$
\begin{aligned}
1 + g(k) - \frac{1}{1+g(-k)} &\to 1 + g(k) - (1 - g(-k) + (g(-k))^2) \\
&= g(k) + g(-k) - (g(-k))^2,
\end{aligned} \tag{6.80}
$$

and we only need to retain the lowest-order-in-k terms that appear, which are in fact the k^2 terms, since the first-order terms in k subtract out. We obtain

$$\begin{aligned}
&1+g(k)-\frac{1}{1+g(-k)} \\
&\quad\rightarrow\quad \frac{1}{R_\theta^2}\Bigg[l^2k^2+2l^2\phi k+\frac{1}{1+L^2(k+\phi)^2}-\frac{1}{1+L^2\phi^2} \\
&\qquad +l^2k^2-2l^2\phi k+\frac{1}{1+L^2(-k+\phi)^2}-\frac{1}{1+L^2\phi^2} \\
&\qquad -\frac{1}{R_\theta^2}\left(2l^2\phi-\frac{2L^2\phi}{(1+L^2\phi^2)^2}\right)^2k^2\Bigg] \\
&\quad=\quad \frac{1}{R_\theta^2}\left[2l^2k^2-\frac{2L^2k^2}{(1+L^2\phi^2)^2}+\frac{8L^4\phi^2k^2}{(1+L^2\phi^2)^3}-\frac{1}{R_\theta^2}\left(2l^2\phi-\frac{2L^2\phi}{(1+L^2\phi^2)^2}\right)^2k^2\right] \\
&\quad=\quad \frac{1}{R_\theta^2}\Bigg[\left(1-\frac{\phi^2}{R_\theta^2}\left(2l^2-\frac{2L^2}{(1+L^2\phi^2)^2}\right)\right)\left(2l^2-\frac{2L^2}{(1+L^2\phi^2)^2}\right)k^2 \\
&\qquad +\frac{8L^4\phi^2k^2}{(1+L^2\phi^2)^3}\Bigg]
\end{aligned} \tag{6.81}$$

For $\phi\geq\phi_{min}=\sqrt{1-\beta}/\sqrt{lL}$,

$$2l^2-\frac{2L^2}{(1+L^2\phi^2)^2}\geq 0, \tag{6.82}$$

and since we are also assuming ϕ is near ϕ_{min} so that $R_\theta^2>0$, it is clear that

$$1+g(k)-\frac{1}{1+g(-k)}>0 \tag{6.83}$$

in the low-k limit.

We still need to show that the stability condition, now reduced to

$$1+g(k)-\frac{1}{1+g(-k)}>0, \tag{6.84}$$

is satisfied $\forall k>0$, not just as $k\rightarrow 0$, for a range of values $\phi\geq\phi_{min}$. For convenience, define $h(k)=g(-k)$, and explicitly denote the parametric dependence of g and h on ϕ by using the subscript notation $g_\phi(k)$ and $h_\phi(k)$. For $\phi=\phi_{min}$, we have

$$\frac{dh_{\phi_{min}}}{dk}=-\frac{1}{R_\theta^2}\left(2l^2-\frac{2L^2}{1+L^2(-k+\phi_{min})^2}\right)(-k+\phi_{min}), \tag{6.85}$$

so that the critical points of $h_{\phi_{min}}(k)$ occur at $k = 0, \phi_{min}$, and $2\phi_{min}$. The values of $h_{\phi_{min}}(k)$ at these critical points are easily found to be

$$\begin{aligned} h_{\phi_{min}}(0) &= 0, \\ h_{\phi_{min}}(\phi_{min}) &= 1, \\ h_{\phi_{min}}(2\phi_{min}) &= 0, \end{aligned} \tag{6.86}$$

and $h_{\phi_{min}}(k) \to \infty$ as $k \to \infty$. Therefore, $\forall k$, $h_{\phi_{min}}(k) \geq 0$, and so we can conclude that

$$1 + g_{\phi_{min}}(k) - \frac{1}{1 + h_{\phi_{min}}(k)} \geq 0, \tag{6.87}$$

with equality only for $k = 0$. Defining $F(k, \phi) = 1 + g_{\phi}(k) - \frac{1}{1+h_{\phi}(k)}$, we note that $F(k, \phi)$ is a smooth function. Also, for $\phi > \phi_{min}$ but $\phi - \phi_{min} < \epsilon$ for ϵ sufficently small, we can find a $B > 0$ and a $\bar{k}$ such that

$$F(k, \phi) > B, \;\; \forall k \geq \bar{k}, \tag{6.88}$$

independent of ϕ. Therefore, since at $k = 0$,

$$\begin{aligned} \frac{\partial F}{\partial k}(0, \phi) &= 0, \\ \frac{\partial^2 F}{\partial k^2}(0, \phi) &> 0, \end{aligned} \tag{6.89}$$

for $\phi - \phi_{min} > 0$ sufficiently small, we can conclude that $F(k, \phi) > 0, \;\; \forall k > 0, \;\; \forall \phi \in [\phi_{min}, \phi_{max}]$, for some $\phi_{max} > \phi_{min} = \sqrt{1 - \beta}/\sqrt{lL}$. So finally we conclude that indeed there is a range of values $[\phi_{min}, \phi_{max}]$ for which the ideal helical equilibrium solutions are guaranteed to be stable with respect to linear perturbations. $\square$

Note that even though we have determined that an interval $[\phi_{min}, \phi_{max}]$ exists for which the ideal helical equilibrium solution with wave number ϕ is stable with respect to linear perturbations, this is not necessarily the largest such interval. One could, however, numerically calculate $[\phi_{min}, \phi_{max}]$ in the

above proposition, and plot the interval as a function of $\beta = l/L$ (while keeing $\sqrt{lL}$ fixed). This procedure would yield a (subset of the) "wedge of stability" for the ideal helical solution as a function of the parameter β.

6.4.3 Analysis of the spatially uniform equilibrium in the large-$|C|$ case

For the large-$|C|$ case, we expect to have a stable spatially uniform equilibrium solution. Returning to the (unperturbed) dynamics for $(\theta_R, \theta_I, \eta_R, \eta_I)$, equation (6.10), we set $C_I = 0$ and $C_R = \text{constant} > 0$. The spatially uniform equilibrium is then given by

$$\begin{aligned} \theta_R &= R_\theta = \text{constant}, \quad \theta_I = 0, \\ \eta_R &= R_\eta = \text{constant}, \quad \eta_I = 0. \end{aligned} \tag{6.90}$$

The value of R_θ is found from the equilibrium equations,

$$\begin{aligned} R_\eta &= -R_\theta + C_R, \\ R_\theta^3 &= R_\theta + R_\eta = C_R, \\ R_\theta &= C_R^{1/3}. \end{aligned} \tag{6.91}$$

Perturbing about the spatially uniform equilbrium using

$$\begin{aligned} \theta_R &= R_\theta + \delta\theta_R, \quad \theta_I = \delta\theta_I, \\ \eta_R &= R_\eta + \delta\eta_R, \quad \eta_I = \delta\eta_I, \end{aligned} \tag{6.92}$$

we obtain

$$
\begin{aligned}
\tau_\theta \partial_t \delta\theta_R &= l^2 \partial_{xx}\delta\theta_R - [(\delta\theta_R)^2 + (\delta\theta_I)^2]\delta\theta_R - 3R_\theta^2\delta\theta_R - 3R_\theta(\delta\theta_R)^2 \\
&\quad -R_\theta(\delta\theta_I)^2 + \delta\theta_R + \delta\eta_R, \\
\tau_\theta \partial_t \delta\theta_I &= l^2 \partial_{xx}\delta\theta_I - [(\delta\theta_R)^2 + (\delta\theta_I)^2]\delta\theta_I - R_\theta^2\delta\theta_I - 2R_\theta\delta\theta_R\delta\theta_I \\
&\quad +\delta\theta_I + \delta\eta_I, \\
\tau_\eta \partial_t \delta\eta_R &= L^2 \partial_{xx}\delta\eta_R - \delta\eta_R - \delta\theta_R, \\
\tau_\eta \partial_t \delta\eta_I &= L^2 \partial_{xx}\delta\eta_I - \delta\eta_I - \delta\theta_I.
\end{aligned}
\tag{6.93}
$$

Letting

$$
\begin{aligned}
\delta\theta &= \delta\theta_R + i\delta\theta_I, \\
\delta\eta &= \delta\eta_R + i\delta\eta_I,
\end{aligned}
\tag{6.94}
$$

we can rewrite the dynamics in complex form as

$$
\begin{aligned}
\tau_\theta \partial_t \delta\theta &= l^2 \partial_{xx}\delta\theta - |\delta\theta|^2\delta\theta - 3R_\theta^2 \mathrm{Re}\{\delta\theta\} - 3R_\theta(\mathrm{Re}\{\delta\theta\})^2 - R_\theta(\mathrm{Im}\{\delta\theta\})^2 \\
&\quad -iR_\theta^2\mathrm{Im}\{\delta\theta\} - i2R_\theta\mathrm{Re}\{\delta\theta\}\mathrm{Im}\{\delta\theta\} + \delta\theta + \delta\eta, \\
\tau_\eta \partial_t \delta\eta &= L^2 \partial_{xx}\delta\eta - \delta\eta - \delta\theta.
\end{aligned}
\tag{6.95}
$$

The Lyapunov functional for this perturbed system is

$$
\begin{aligned}
V_p^* &= \int_\Omega \Big[\frac{l^2}{2}|\partial_x\delta\theta|^2 + \frac{1}{4}|\delta\theta|^4 - \frac{1}{2}|\delta\theta|^2 + \frac{L^2}{2}|\partial_x\delta\eta|^2 + \frac{1}{2}|\delta\eta|^2 + \mathrm{Re}\{\overline{\delta\theta}\delta\eta\} \\
&\quad +\frac{3}{2}R_\theta^2(\mathrm{Re}\{\delta\theta\})^2 + R_\theta(\mathrm{Re}\{\delta\theta\})^3 + R_\theta(\mathrm{Re}\{\delta\theta\})(\mathrm{Im}\{\delta\theta\})^2 \\
&\quad +\frac{1}{2}R_\theta^2(\mathrm{Im}\{\delta\theta\})^2 - \overline{\delta\theta}[(-1 + L^2\partial_{xx})^{-1}(\delta\theta)] \Big] dx.
\end{aligned}
\tag{6.96}
$$

Retaining the quadratic terms of V_p^*, we obtain

$$
\begin{aligned}
V_q^* &= \int_\Omega \Big[\frac{l^2}{2}|\partial_x\delta\theta|^2 - \frac{1}{2}(1 - R_\theta^2)|\delta\theta|^2 + \frac{L^2}{2}|\partial_x\delta\eta|^2 + \frac{1}{2}|\delta\eta|^2 + \mathrm{Re}\{\overline{\delta\theta}\delta\eta\} \\
&\quad -\overline{\delta\theta}[(-1 + L^2\partial_{xx})^{-1}(\delta\theta)] + R_\theta^2(\mathrm{Re}\{\delta\theta\})^2 \Big] dx.
\end{aligned}
\tag{6.97}
$$

Unlike for the $C = 0$ case, here the analysis is simpler if we use separate Fourier

series for θ_R, θ_I, η_R, and η_I:

$$\begin{aligned}
\frac{1}{|\Omega|}V_q^* &= \sum_k \Bigg[\left(\frac{l^2k^2}{2} + \frac{3}{2}R_\theta^2 - \frac{1}{2} + \frac{1}{1+L^2k^2} \right) |\delta\theta_{Rk}|^2 + \left(\frac{1}{2} + \frac{L^2k^2}{2} \right) |\delta\eta_{Rk}|^2 \\
&\qquad + \overline{\delta\theta}_{Rk}\delta\eta_{Rk} + \left(\frac{l^2k^2}{2} + \frac{1}{2}R_\theta^2 - \frac{1}{2} + \frac{1}{1+L^2k^2} \right) |\delta\theta_{Ik}|^2 \\
&\qquad + \left(\frac{1}{2} + \frac{L^2k^2}{2} \right) |\delta\eta_{Ik}|^2 + \overline{\delta\theta}_{Ik}\delta\eta_{Ik} \Bigg] \\
&= \frac{1}{2}\sum_k \Bigg[\left(l^2k^2 + 3R_\theta^2 - 1 + \frac{1}{1+L^2k^2} \right) |\delta\theta_{Rk}|^2 \\
&\qquad + \left| \frac{1}{\sqrt{1+L^2k^2}}\delta\theta_{Rk} + \sqrt{1+L^2k^2}\delta\eta_{Rk} \right|^2 \\
&\qquad + \left(l^2k^2 + R_\theta^2 - 1 + \frac{1}{1+L^2k^2} \right) |\delta\theta_{Ik}|^2 \\
&\qquad + \left| \frac{1}{\sqrt{1+L^2k^2}}\delta\theta_{Ik} + \sqrt{1+L^2k^2}\delta\eta_{Ik} \right|^2 \Bigg].
\end{aligned} \tag{6.98}$$

The condition for V_q^* to be positive is

$$l^2k^2 + R_\theta^2 - 1 + \frac{1}{1+L^2k^2} > 0, \tag{6.99}$$

which holds if and only if $R_\theta > 1 - \beta$, or equivalently,

$$|C_R| > (1-\beta)^3. \tag{6.100}$$

6.4.4 Bifurcation from the spatially uniform equilibrium solution

For $|C_R| > (1-\beta)^3$, the spatially uniform equilibrium solution is stable, and furthermore, as that threshold is crossed, the unstable perturbations involve $\delta\theta_I$ and $\delta\eta_I$. In fact, if we set $|C_R| = (1-\beta)^3$ and $\delta\theta_R = \delta\eta_R = 0$, we are left with

$$\begin{aligned}
\tau_\theta \partial_t \delta\theta_I &= l^2\partial_{xx}\delta\theta_I - (\delta\theta_I)^3 + (2\beta - \beta^2)\delta\theta_I + \delta\eta_I, \\
\tau_\eta \partial_t \delta\eta_I &= L^2\partial_{xx}\delta\eta_I - \delta\eta_I - \delta\theta_I.
\end{aligned} \tag{6.101}$$

This real activator-inhibitor system is at the instability threshold for the spatially uniform equilibrium solution, and so for larger values of $(2\beta - \beta^2)$, a

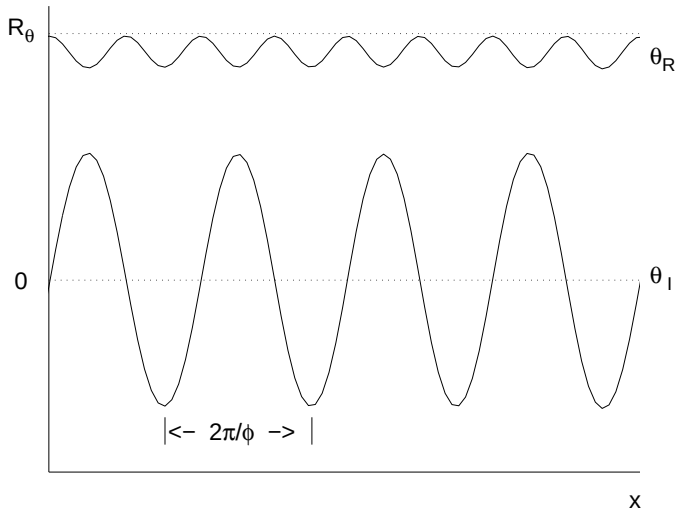

Figure 6.2: Complex activator-inhibitor equation near the bifurcation threshold

spatially periodic pattern solution is stable. For this reason, near threshold we expect there to be a stable pattern for which θ_I is spatially periodic and has mean value zero, while θ_R is spatially periodic with half the period of θ_I, and has its peak value near R_θ. Furthermore, a linear analysis (similar to the one for the basic cubic nonlinearity model earlier in this chapter) gives $\sqrt{1-\beta}/\sqrt{lL}$ as the instability wave number for equation (6.101) - precisely the wave number that minimized the Lyapunov functional for the ideal helical solution in the $C = 0$ case. Figure 6.2 shows θ_R and θ_I for the equilibrium solution with $0 < |C_R| < (1-\beta)^3$, but $|C_R|$ close to $(1-\beta)^3$.

6.5 Analysis of equilibria using modal equations

The fact that for $C = 0$ in the complex activator-inhibitor equation there is a stable helical solution is particularly suggestive that finite modal approximations of ideal spatially periodic pattern equilibria when $C \neq 0$ may be useful. Throughout the modal analysis we will make the following assumptions:

1. one spatial dimension,

2. periodic boundary conditions, and

3. $\Omega \subset \mathrm{R}$ is an interval with length equal to an integer number of periods of the ideal solution we are considering.

The first step is to rescale x by the wave number of the ideal solution. We assume the wave number is $\sqrt{1-\beta}/\sqrt{lL}$, since this is the wave number both for the linear instability in the (θ_I, η_I) dynamics as $|C|$ is decreased through $(1-\beta)^3$, and for the minimum-energy helical equilibrium solution when $C = 0$. Next, we obtain the dynamical equations for the modal coefficients. Then we find a Lyapunov function for any finite number of modes. The existence of the Lyapunov function ensures that our modal equations are well-posed and gives a numerical procedure for determining the modal coefficients. Next, we determine bounds on the higher-order modes so that we can justify retaining only the lower-order modes to obtain a good approximation of the equilibrium of interest. Finally, we generalize the results to the real cubic nonlinearity model.

6.5.1 Derivation of the modal dynamics

We assume that the ideal equilibrium solution of interest has wave number $\sqrt{1-\beta}/\sqrt{lL}$, and rescale the complex activator-inhibitor equation dynamics, obtaining

$$\begin{aligned} \tau_\theta \partial_t \theta &= \beta(1-\beta)\partial_{xx}\theta - |\theta|^2\theta + \theta + \eta, \\ \tau_\eta \partial_t \eta &= \frac{1-\beta}{\beta}\partial_{xx}\eta - \eta - \theta + C. \end{aligned} \tag{6.102}$$

Next, we write the Fourier series expansions for θ and η,

$$\begin{aligned} \theta &= \sum_k \theta_k \mathrm{e}^{ikx}, \\ \eta &= \sum_k \eta_k \mathrm{e}^{ikx}, \end{aligned} \tag{6.103}$$

where k takes integer values since by assumption 2π is the spatial period of the equilibrium solution for the rescaled dynamics. Plugging the Fourier series expansion into the dynamical equations gives

$$\begin{aligned} \sum_k \tau_\theta \dot{\theta}_k \mathrm{e}^{ikx} &= -\Big|\sum_k \theta_k \mathrm{e}^{ikx}\Big|^2 \left(\sum_k \theta_k \mathrm{e}^{ikx}\right) + \sum_k \left[1-\beta(1-\beta)k^2\right]\theta_k \mathrm{e}^{ikx} \\ &\quad + \sum_k \eta_k \mathrm{e}^{ikx}, \\ \sum_k \tau_\eta \dot{\eta}_k \mathrm{e}^{ikx} &= -\sum_k \left(1+\frac{1-\beta}{\beta}k^2\right)\eta_k \mathrm{e}^{ikx} - \sum_k \theta_k \mathrm{e}^{ikx} + C. \end{aligned} \tag{6.104}$$

In order to equate modes, we need to expand the cubic term. To see how to expand the cubic term, note that

$$\begin{aligned} &(\overline{x}_1+\overline{x}_2+\overline{x}_3+\cdots)(x_1+x_2+x_3+\cdots) \\ &\quad = \overline{x}_1x_1+\overline{x}_2x_2+\overline{x}_3x_3+\overline{x}_1x_2+\overline{x}_2x_1+\overline{x}_1x_3+\overline{x}_3x_1+\overline{x}_2x_3+\overline{x}_3x_2+\cdots, \\ &\left[(\overline{x}_1+\overline{x}_2+\overline{x}_3+\cdots)(x_1+x_2+x_3+\cdots)\right](x_1+x_2+x_3+\cdots) \\ &\quad = |x_1|^2x_1+|x_2|^2x_2+|x_3|^2x_3 \\ &\qquad +2|x_1|^2x_2+2|x_1|^2x_3+2|x_2|^2x_1+2|x_2|^2x_3+2|x_3|^2x_1+2|x_3|^2x_2 \\ &\qquad +\overline{x}_1x_2^2+\overline{x}_1x_3^2+\overline{x}_2x_1^2+\overline{x}_2x_3^2+\overline{x}_3x_1^2+\overline{x}_3x_2^2 \\ &\qquad +2\overline{x}_1x_2x_3+2x_1\overline{x}_2x_3+2x_1x_2\overline{x}_3+\cdots. \end{aligned} \tag{6.105}$$

We thus obtain

$$\begin{aligned}\Big|\sum_k \theta_k \mathrm{e}^{ikx}\Big|^2 \left(\sum_k \theta_k \mathrm{e}^{ikx}\right) &= \sum_k |\theta_k|^2\theta_k \mathrm{e}^{ikx} + 2\sum_j \sum_{k\neq j} |\theta_j|^2\theta_k \mathrm{e}^{ikx} + \sum_j \sum_{k\neq j} \overline{\theta}_j \theta_k^2 \mathrm{e}^{i(2k-j)x} \\ &\quad + \sum_j \sum_{k\neq j} \sum_{l\neq j,k} \overline{\theta}_j \theta_k \theta_l \mathrm{e}^{i(k+l-j)x}. \end{aligned} \tag{6.106}$$

The e^{imx} term of the above expression is

$$|\theta_m|^2\theta_m + 2\sum_{j\neq m} |\theta_j|^2\theta_m + \sum_{k\neq m} \overline{\theta}_{2k-m}\theta_k^2 + \sum_j \sum_{k\neq j,m,(m+j)/2} \overline{\theta}_j \theta_k \theta_{m+j-k}. \tag{6.107}$$

The modal dynamics are then

$$\begin{aligned}\tau_\theta \dot{\theta}_m &= \left(1 - m^2\beta(1-\beta)\right)\theta_m - \Bigg[|\theta_m|^2\theta_m + 2\sum_{j\neq m} |\theta_j|^2\theta_m + \sum_{k\neq m} \overline{\theta}_{2k-m}\theta_k^2 \\ &\quad + \sum_j \sum_{k\neq j,m,(m+j)/2} \overline{\theta}_j \theta_k \theta_{m+j-k}\Bigg] + \eta_m, \end{aligned} \tag{6.108}$$

$$\tau_\eta \dot{\eta}_m = -\left(1 + m^2 \frac{1-\beta}{\beta}\right)\eta_m - \theta_m + C\delta_{m0},$$

where

$$\delta_{jk} = \begin{cases} 1 & j = k \\ 0 & j \neq k. \end{cases} \tag{6.109}$$

6.5.2 Lyapunov function for the modal dynamics

Let

$$\begin{aligned} V &= -\frac{1}{2}\sum_m \left(1 - m^2\beta(1-\beta)\right)|\theta_m|^2 + \frac{1}{4}\sum_m |\theta_m|^4 + \frac{1}{2}\sum_m \sum_{j\neq m} |\theta_j|^2|\theta_m|^2 \\ &\quad + \mathrm{Re}\left\{\frac{1}{2}\sum_m \sum_{k\neq m} \overline{\theta}_{2k-m}\theta_k^2\overline{\theta}_m\right\} + \mathrm{Re}\left\{\frac{1}{4}\sum_m \sum_{j\neq m} \sum_{k\neq j,m,(m+j)/2} \overline{\theta}_j\theta_k\theta_{m+j-k}\overline{\theta}_m\right\} \\ &\quad + \frac{1}{2}\sum_m \left(1 + m^2\frac{1-\beta}{\beta}\right)|\eta_m|^2 - \mathrm{Re}\{C\overline{\eta}_0\} + \sum_m \mathrm{Re}\{\overline{\theta_m}\eta_m\} \\ &\quad + \sum_m \left(1 + m^2\frac{1-\beta}{\beta}\right)^{-1} |\theta_m - C\delta_{m0}|^2. \end{aligned} \tag{6.110}$$

Lemma 6.15 *The function V given by equation (6.110), appropriately truncated, is a Lyapunov function for the dynamics given by equation (6.108) for any finite number of modes.*

Proof: Differentiating the terms of V with respect to $\overline{\theta}_m$, we obtain

$$\begin{aligned}
\frac{\partial}{\partial\overline{\theta}_m}\left(\frac{1}{2}\sum_l\left(1-l^2\beta(1-\beta)\right)|\theta_l|^2\right) &= \left(1-m^2\beta(1-\beta)\right)\theta_m,\\
\frac{\partial}{\partial\overline{\theta}_m}\left(\frac{1}{4}\sum_l|\theta_l|^4\right) &= |\theta_m|^2\theta_m,\\
\frac{\partial}{\partial\overline{\theta}_m}\left(\frac{1}{2}\sum_l\sum_{j\neq l}|\theta_j|^2|\theta_l|^2\right) &= 2\sum_{j\neq m}|\theta_j|^2\theta_m,\\
\frac{\partial}{\partial\overline{\theta}_m}\left(\mathrm{Re}\left\{\frac{1}{2}\sum_l\sum_{k\neq l}\overline{\theta}_{2k-l}\theta_k^2\overline{\theta}_l\right\}\right) &= \sum_{k\neq m}\overline{\theta}_{2k-m}\theta_k^2+\sum_{l\neq m}\theta_{2m-l}\overline{\theta}_m\theta_l\\
&= \sum_{k\neq m}\overline{\theta}_{2k-m}\theta_k^2+\sum_{k\neq m}\overline{\theta}_m\theta_k\theta_{2m-k},\\
\frac{\partial}{\partial\overline{\theta}_m}\left(\mathrm{Re}\left\{\frac{1}{4}\sum_l\sum_{j\neq l}\sum_{k\neq j,l,(j+l)/2}\overline{\theta}_j\theta_k\theta_{l+j-k}\overline{\theta}_l\right\}\right) &= \sum_{j\neq m}\sum_{k\neq j,m,(j+m)/2}\overline{\theta_j}\theta_k\theta_{m+j-k},\\
\frac{\partial}{\partial\overline{\eta}_m}\left(\frac{1}{2}\sum_l\left(1+l^2\frac{1-\beta}{\beta}\right)|\eta_l|^2\right) &= \left(1+m^2\frac{1-\beta}{\beta}\right)\eta_m,\\
\frac{\partial}{\partial\overline{\eta}_0}\left(\mathrm{Re}\{C\overline{\eta}_0\}\right) &= C,\\
\frac{\partial}{\partial\overline{\theta}_m}\left(\sum_l\mathrm{Re}\{\overline{\theta_l}\eta_l\}\right) &= \eta_m,\\
\frac{\partial}{\partial\overline{\eta}_m}\left(\sum_l\mathrm{Re}\{\overline{\theta_l}\eta_l\}\right) &= \theta_m,\\
\frac{\partial}{\partial\overline{\theta}_m}\left(\sum_l\left(1+l^2\frac{1-\beta}{\beta}\right)^{-1}|\theta_l-C\delta_{l0}|^2\right) &= 2\left(1+m^2\frac{1-\beta}{\beta}\right)^{-1}(\theta_m-C\delta_{m0}).
\end{aligned} \tag{6.111}$$

Noting that

$$\sum_{k\neq m}\overline{\theta}_m\theta_k\theta_{2m-k}+\sum_{j\neq m}\sum_{k\neq j,m,(j+m)/2}\overline{\theta_j}\theta_k\theta_{m+j-k}=\sum_j\sum_{k\neq j,m,(j+m)/2}\overline{\theta_j}\theta_k\theta_{m+j-k}, \tag{6.112}$$

we see that

$$\begin{aligned}\tau_\eta \dot{\eta}_m &= -\frac{\partial V}{\partial \overline{\eta}_m}, \\ \tau_\theta \dot{\theta}_m &= -\frac{\partial V}{\partial \overline{\theta}_m} + 2\eta_m + 2\left(1 + m^2 \frac{1-\beta}{\beta}\right)^{-1} (\theta_m - C\delta_{m0}).\end{aligned} \tag{6.113}$$

But

$$\eta_m + \left(1 + m^2 \frac{1-\beta}{\beta}\right)^{-1} (\theta_m - C\delta_{m0}) = -\left(1 + m^2 \frac{1-\beta}{\beta}\right)^{-1} (\tau_\eta \dot{\eta}_m), \tag{6.114}$$

so

$$\begin{aligned}\dot{V} &= \sum_m \left[\frac{\partial V}{\partial \overline{\eta}_m} \cdot \dot{\eta}_m + \frac{\partial V}{\partial \overline{\theta}_m} \cdot \dot{\theta}_m\right] \\ &= -\sum_m \left[\tau_\theta |\dot{\theta}_m|^2 + \tau_\eta |\dot{\eta}_m|^2 + 2\tau_\eta \left(1 + m^2 \frac{1-\beta}{\beta}\right)^{-1} \left(\mathrm{Re}\{\dot{\overline{\theta}}_m \dot{\eta}_m\}\right)\right] \\ &= -\sum_m \left[\left|\sqrt{\tau_\theta}\dot{\theta}_m + \frac{1}{\sqrt{\alpha}}\left(1 + m^2 \frac{1-\beta}{\beta}\right)^{-1} (\sqrt{\tau_\eta}\dot{\eta}_m)\right|^2 + |\sqrt{\tau_\eta}\dot{\eta}_m|^2 \right. \\ &\qquad \left. -\frac{1}{\alpha}\left|\left(1 + m^2 \frac{1-\beta}{\beta}\right)^{-1} (\sqrt{\tau_\eta}\dot{\eta}_m)\right|^2\right]\end{aligned} \tag{6.115}$$

Thus, if $\alpha = \tau_\theta/\tau_\eta > 1$, then $\dot{V} \leq 0$, with $\dot{V} = 0$ only for equilibria (for any finite number of modes). V is also radially unbounded, and therefore is a valid Lyapunov function for any finite number of modes. □

6.5.3 Bounding the higher-order modes

At equilibrium for the modal dynamics, we have

$$\begin{aligned}&\eta_k = -\left(1 + k^2 \frac{1-\beta}{\beta}\right)^{-1} (\theta_k - C\delta_{k0}), \\ &\sum_k \left[1 - k^2\beta(1-\beta) - \frac{1}{1 + k^2 \frac{1-\beta}{\beta}}\right] \theta_k \mathrm{e}^{ikx} = \left|\sum_k \theta_k \mathrm{e}^{ikx}\right|^2 \left(\sum_k \theta_k \mathrm{e}^{ikx}\right) - C.\end{aligned} \tag{6.116}$$

Multiplying both sides by e^{-imx}, $m \neq 0$, and integrating over Ω gives

$$\begin{aligned}
\left[1 - m^2\beta(1-\beta) - \frac{1}{1+m^2\frac{1-\beta}{\beta}}\right]\theta_m|\Omega| &= \int_\Omega |\theta|^2 \left(\sum_k \theta_k \mathrm{e}^{ikx}\right)\mathrm{e}^{-imx}dx, \\
\left|1 - m^2\beta(1-\beta) - \frac{1}{1+m^2\frac{1-\beta}{\beta}}\right||\theta_m||\Omega| &\leq \int_\Omega |\theta|^2\Big|(\sum_k \theta_k \mathrm{e}^{ikx}\Big|dx \\
&= \int_\Omega |\theta|^3 dx \\
&\leq \frac{1}{2}\int_\Omega |\theta|^4 dx + \frac{1}{2}\int_\Omega |\theta|^2 dx \\
&= \frac{1}{2}\left(||\theta||^4_{L^4(\Omega)} + ||\theta||^2_{L^2(\Omega)}\right),
\end{aligned}$$

$$\begin{aligned}
|\theta_m| &\leq \frac{1}{2|\Omega|}\frac{1}{\left|m^2\beta(1-\beta) - \frac{m^2\frac{1-\beta}{\beta}}{1+m^2\frac{1-\beta}{\beta}}\right|}\left(||\theta||^4_{L^4(\Omega)} + ||\theta||^2_{L^2(\Omega)}\right) \\
&\leq \frac{1}{2|\Omega|}\frac{1}{m^2\beta(1-\beta)-1}\left(||\theta||^4_{L^4(\Omega)} + ||\theta||^2_{L^2(\Omega)}\right) \text{ for } m^2 > \frac{1}{\beta(1-\beta)} \\
&\leq \frac{1}{m^2}\left[\frac{1}{|\Omega|\beta(1-\beta)}\left(||\theta||^4_{L^4(\Omega)} + ||\theta||^2_{L^2(\Omega)}\right)\right] \text{ for } m^2 > \frac{2}{\beta(1-\beta)}.
\end{aligned} \tag{6.117}$$

We can derive bounds on $||\theta||^4_{L^4(\Omega)}$ and $||\theta||^2_{L^2(\Omega)}$ from the equilibrium equations

$$\begin{aligned}
0 &= \beta(1-\beta)\partial_{xx}\theta_R - (\theta_R^2+\theta_I^2)\theta_R + \theta_R + \eta_R, \\
0 &= \beta(1-\beta)\partial_{xx}\theta_I - (\theta_R^2+\theta_I^2)\theta_I + \theta_I + \eta_I, \\
0 &= \frac{1-\beta}{\beta}\partial_{xx}\eta_R - \eta_R - \theta_R + C_R, \\
0 &= \frac{1-\beta}{\beta}\partial_{xx}\eta_I - \eta_I - \theta_I + C_I.
\end{aligned} \tag{6.118}$$

We first obtain

$$\begin{aligned}
&\beta(1-\beta)\left(||\partial_x\theta_R||^2_{L^2(\Omega)} + ||\partial_x\theta_I||^2_{L^2(\Omega)}\right) + \int_\Omega (\theta_R^2+\theta_I^2)^2 dx \\
&-||\theta_R||^2_{L^2(\Omega)} - ||\theta_I||^2_{L^2(\Omega)} + \frac{1-\beta}{\beta}\left(||\partial_x\eta_R||^2_{L^2(\Omega)} + ||\partial_x\eta_I||^2_{L^2(\Omega)}\right) \\
&+||\eta_R||^2_{L^2(\Omega)} + ||\eta_I||^2_{L^2(\Omega)} - \int_\Omega (C_R\eta_R + C_I\eta_I)dx = 0.
\end{aligned} \tag{6.119}$$

Next, using

$$\begin{aligned}\left|\int_\Omega (C_R\eta_R + C_I\eta_I)dx\right| &\leq \int_\Omega |C_R\eta_R|dx + \int_\Omega |C_I\eta_I|dx \\ &\leq \frac{1}{2}\left(||\eta_R||^2_{L^2(\Omega)} + ||\eta_I||^2_{L^2(\Omega)}\right) + \frac{1}{2}|\Omega|(C_R^2 + C_I^2) \\ &= \frac{1}{2}\left(||\eta_R||^2_{L^2(\Omega)} + ||\eta_I||^2_{L^2(\Omega)}\right) + \frac{1}{2}|\Omega|C^2, \quad (6.120)\end{aligned}$$

we can conclude

$$\int_\Omega (\theta_R^2 + \theta_I^2)^2 dx - ||\theta_R||^2_{L^2(\Omega)} - ||\theta_I||^2_{L^2(\Omega)} \leq \frac{1}{2}|\Omega||C|^2. \quad (6.121)$$

Since

$$\int_\Omega (\theta_R^2 + \theta_I^2)dx \leq \frac{1}{2}\int_\Omega (\theta_R^2 + \theta_I^2)^2 dx + \frac{1}{2}|\Omega|, \quad (6.122)$$

we have

$$\int_\Omega (\theta_R^2 + \theta_I^2)^2 dx \geq 2\int_\Omega (\theta_R^2 + \theta_I^2)dx - |\Omega| = 2\left(||\theta_R||^2_{L^2(\Omega)} + ||\theta_I||^2_{L^2(\Omega)}\right) - |\Omega|, \quad (6.123)$$

so that

$$||\theta||^2_{L^2(\Omega)} = ||\theta_R||^2_{L^2(\Omega)} + ||\theta_I||^2_{L^2(\Omega)} \leq \left(1 + \frac{1}{2}|C|^2\right)|\Omega|. \quad (6.124)$$

Also,

$$\begin{aligned}\int_\Omega (\theta_R^2 + \theta_I^2)^2 dx - ||\theta_R||^2_{L^2(\Omega)} - ||\theta_I||^2_{L^2(\Omega)} &= \int_\Omega [(\theta_R^2 + \theta_I^2)^2 - (\theta_R^2 + \theta_I^2)]dx \\ &\geq \int_\Omega \left[\frac{1}{2}(\theta_R^2 + \theta_I^2)^2 - \frac{1}{2}\right]dx, \quad (6.125)\end{aligned}$$

so

$$\begin{aligned}\frac{1}{2}\int_\Omega (\theta_R^2 + \theta_I^2)^2 dx - \frac{1}{2}|\Omega| &\leq \frac{1}{2}|\Omega||C|^2, \\ ||\theta||^4_{L^4(\Omega)} &\leq (1 + |C|^2)|\Omega|. \quad (6.126)\end{aligned}$$

Therefore,

$$|\theta_m| \leq \frac{1}{m^2}\left[\frac{2(1 + |C|^2)}{\beta(1-\beta)}\right] \text{ for } m^2 \geq \frac{2}{\beta(1-\beta)}. \quad (6.127)$$

We can now bound the error in approximating the exact equilibrium solution θ with its finite modal approximation $\sum_{k=-N}^{N} \theta_k e^{ikx}$, for $N^2 \geq 2/(\beta(1-\beta))$:

$$\begin{aligned}
\left|\theta - \sum_{k=-N}^{N} \theta_k e^{ikx}\right| &\leq \sum_{k=N+1}^{\infty} |\theta_k| + \sum_{k=-(N+1)}^{-\infty} |\theta_k| \\
&= \left[\frac{2(1+|C|^2)}{\beta(1-\beta)}\right] \left(\sum_{k=N+1}^{\infty} \frac{1}{k^2} + \sum_{k=-(N+1)}^{-\infty} \frac{1}{k^2}\right) \\
&\leq \frac{1}{N}\left[\frac{4(1+|C|^2)}{\beta(1-\beta)}\right]. \qquad (6.128)
\end{aligned}$$

Thus, the error in approximating an exact periodic equilibrium solution θ of equation (6.108) using a finite number of modes approaches zero as the number of modes used becomes large. Furthermore, the smaller β is (for $\beta < 1/2$), the more terms are needed to achieve a given error tolerance, in accord with what one would expect, considering β represents the ratio of the two length scales present in the dynamics.

6.5.4 Modal results for the real cubic nonlinearity model

The real cubic nonlinearity model can be treated within the framework of the complex activator-inhibitor equation by choosing purely real initial conditions for the modal dynamics. From the form of the dynamics (6.108), it follows that if we take

$$\begin{aligned}
\theta_k &= \overline{\theta}_{-k}, \\
\eta_k &= \overline{\eta}_{-k} \qquad (6.129)
\end{aligned}$$

at $t = 0$, then equation (6.129) will also hold $\forall t > 0$.

For the complex activator-inhibitor equation, we considered $\beta < 1$ without requiring $\beta << 1$. For the real cubic nonlinearity model, however, we generally have considered $\beta << 1$. What the results of the modal analysis

tell us in the $\beta << 1$ case is that we many need to retain many modal coefficients to obtain a good approximation to the spike equilibrium, which is what we would expect, but that a finite number of modes is still sufficient to approximate the spike equilibrium solution.

6.6 Numerical results for the spatially discretized cubic nonlinearity model

We conclude this chapter with a look at some numerical results for equilibria of the spatially discretized cubic nonlinearity model in one space dimension. For $\beta << 1$, $\alpha > 1$, and C chosen so that the spatially uniform equilibrium solution is stable ($C = -\frac{2\sqrt{2}}{3\sqrt{3}}$ was used), the stable equilibria consist of a narrow spike equilibrium, a wide pulse equilibrium, and the spatially uniform equilibrium. As β is increased (by decreasing L while holding l fixed), the wide pulse solution narrows, and eventually coalesces with the narrow spike solution. If β becomes sufficiently large, the narrow spike solution becomes unstable, and only the spatially uniform equilibrium solution remains stable. If the Lyapunov function V^* is used as an energy measure for the equilibria, then when β is very small, the energy of the narrow spike solution is lowest, the energy of the wide pulse solution is higher, and the energy of the spatially uniform equilibrium is higher still. As β is increased, the energy of both the narrow spike solution and wide pulse solution increase (while the energy of the spatially uniform equilibrium remains unchanged). As the wide pulse and narrow spike solutions coalesce, their energy surpasses that of the spatially uniform equilibrium. This behavior is illustrated in figure 6.3. Figures 6.4 and 6.5 show waterfall diagrams of the wide pulse and narrow spike shapes for the values of β used to construct figure 6.3.

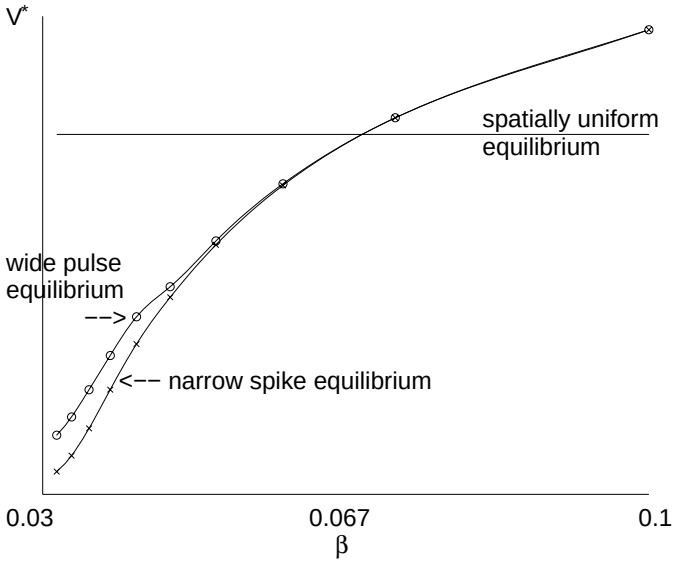

Figure 6.3: V^* energy for the cubic nonlinearity model equilibria as a function of β

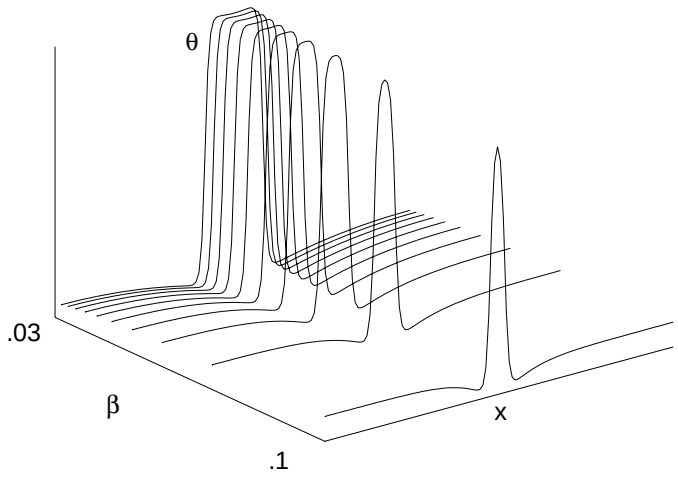

Figure 6.4: Wide pulse equilibrium shape as a function of β

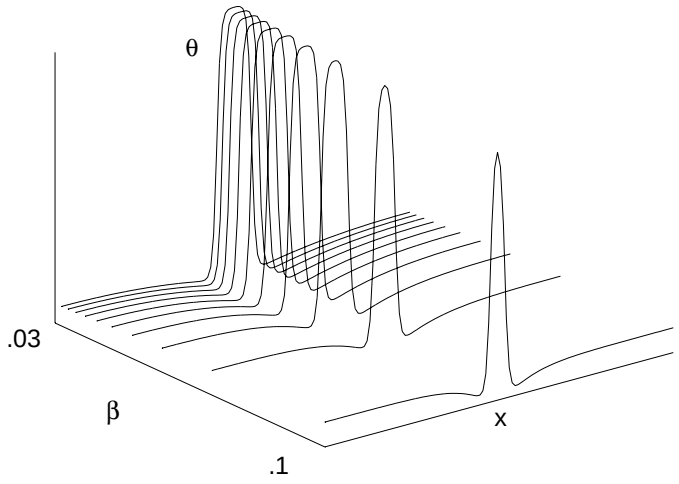

Figure 6.5: Narrow spike equilibrium shape as a function of β

Chapter 7

Smart Systems Applications

7.1 Introduction

There are a variety of ways in which the cubic nonlinearity model and its variants could potentially be used in smart-systems applications. We will consider potential MEMS actuator-array applications (sorting and micropositioning), a coupled-oscillator phased-array antenna application, and a real-time image-processing application. Other potential application areas not expanded on here are control of smart materials for ultrasonic motors and control of boundary-layer fluid flow. The purpose here is merely to illustrate some of the basic control issues, since a lot of engineering would be required to actually implement any of these systems. However, for each application, the technology either already exists or will exist in the forseeable future, so it is appropriate to consider how control systems might be implemented for them.

Before examining specific applications, we describe how spike solutions can be excited in one- and two-dimensional networks based on the cubic nonlinearity model. We assume that $\beta << 1$ and $\alpha > 1$ so that we have a Lyapunov functional and also the possibility of spike equilibria. One technique for exciting a spike is to choose appropriate initial conditions, but an alternative technique is to locally raise the control parameter above the bifurcation threshold. When the control parameter is in the pattern-forming regime over a localized region, the pattern solution forms in that region, but smoothly connects to the spatially uniform equilibrium outside that region. When the control parameter is then returned to the below-threshold value, the pattern

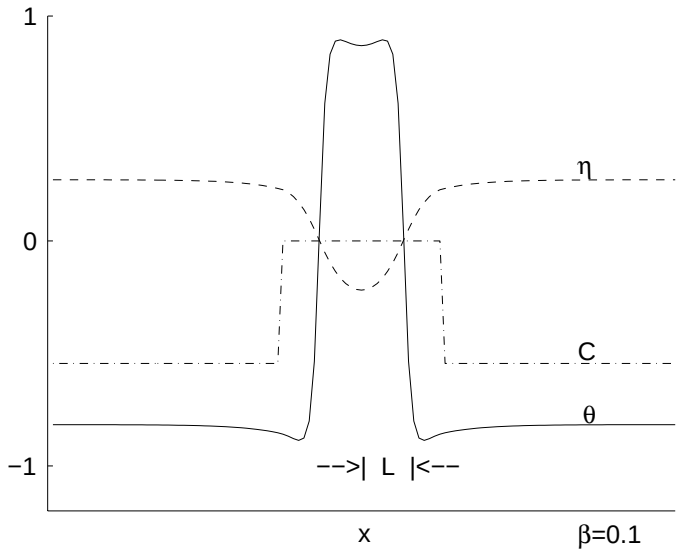

Figure 7.1: One cycle of the pattern solution excited by locally raising the control parameter for the one-dimensional discretization of the cubic nonlinearity model

solution relaxes to the corresponding spike solution. This method of exciting spikes is illustrated for one dimension in figures 7.1 and 7.2, and for two dimensions in figures 7.3 and 7.4. (The spatial discretization is such that there are ten sites within the length L.)

If the control parameter is raised over a larger region than required to excite a single spike, then in the two-dimensional system there are several possibilities, depending on the shape of the region in which the control parameter was raised, and also depending on the spatially uniform value of control parameter the system is returned to [8]. One possibility is a radially symmetric solution corresponding roughly to a one-dimensional off-center spike rotated through 360 degrees, as illustrated in figures 7.5 and 7.6. To excite the radially symmetric solution shown in figure 7.6, the control parameter (for figure 7.5) was raised in a circular region larger than that used in figure 7.3, in order to excite more of the pattern solution. A second possibility is that the pattern

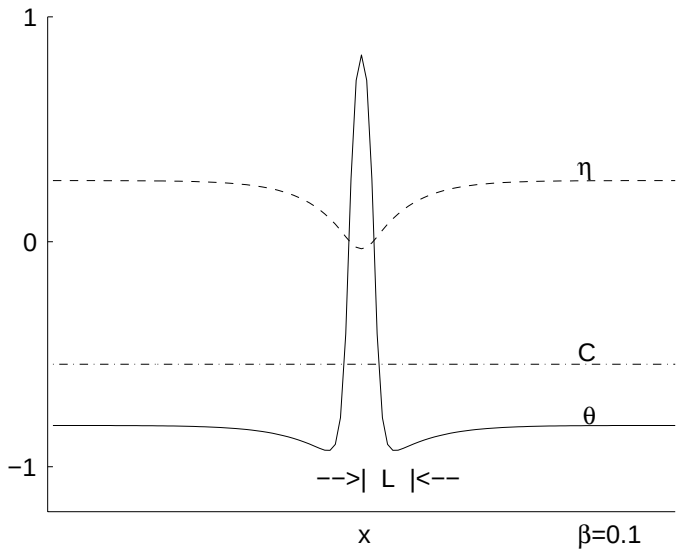

Figure 7.2: The resulting spike when the control parameter is restored to its original value after a cycle of the pattern solution has been excited as in figure 7.1

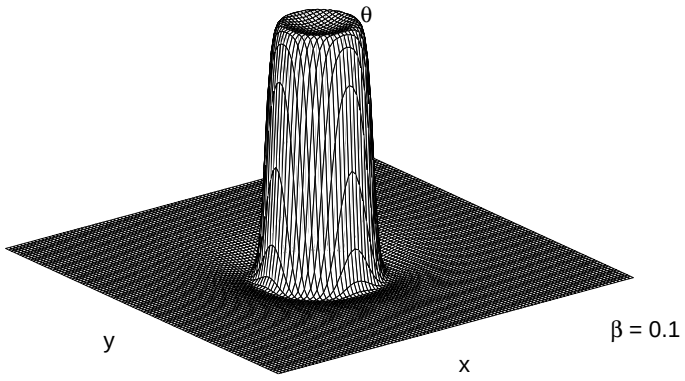

Figure 7.3: One cycle of the pattern solution excited by locally raising the control parameter for the two-dimensional discretization of the cubic nonlinearity model

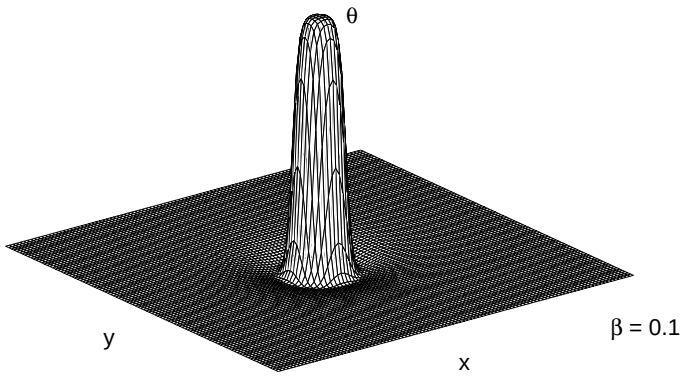

Figure 7.4: The resulting spike when the control parameter is restored to its original value after a cycle of the pattern solution has been excited as in figure 7.3

excited by raising the control parameter will separate into a number of spikes when the control parameter is returned to its spatially uniform value. This phenomenon is illustrated in figures 7.7 and 7.8, and in this case, the region in which the control parameter is raised is not circularly symmetric. For all of figures 7.1 through 7.8, the control parameter has the same value: $C = -\frac{2\sqrt{2}}{3\sqrt{3}}$.

Once spike solutions have been excited in various locations throughout a network, they can all be removed at once simply by taking the control parameter to a value where only a spatially uniform equilibrium is stable. Furthermore, since the control parameter only needs to be raised temporarily in a localized region to excite a spike, a sensor-driven mechanism for exciting a spike can be ac-coupled. A network can thereby act as an analog memory, forming spikes asynchronously and in parallel in response to local sensor driving. But then all the spikes can be eliminated at once by driving a single control input connected to all the sites in the network.

When spikes or circular walls are distributed throughout a network, any

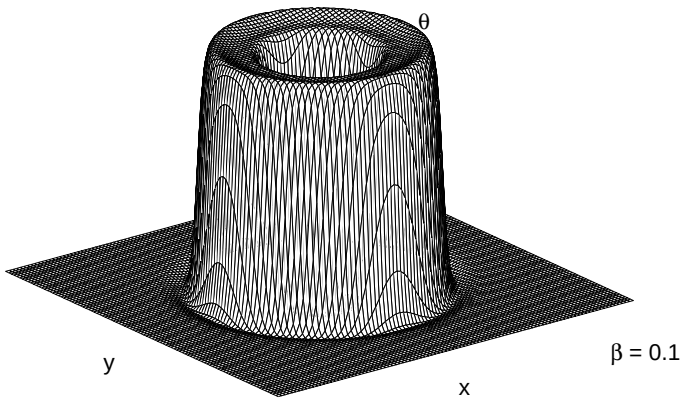

Figure 7.5: The pattern solution excited by locally raising the control parameter over a circular region larger than that of figure 7.3

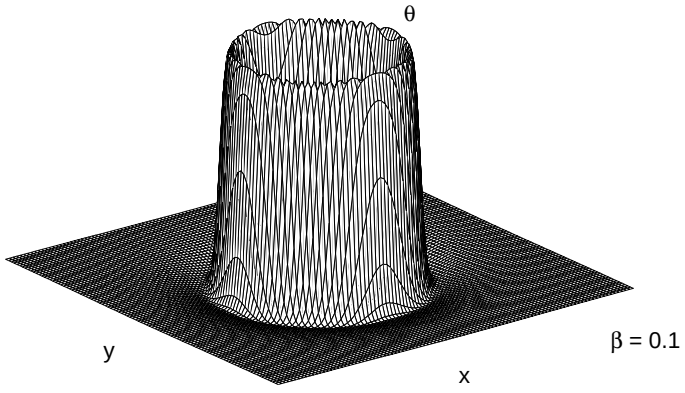

Figure 7.6: The resulting circularly symmetric solution when the control parameter is restored to its original value after the pattern solution of figure 7.5 has been excited

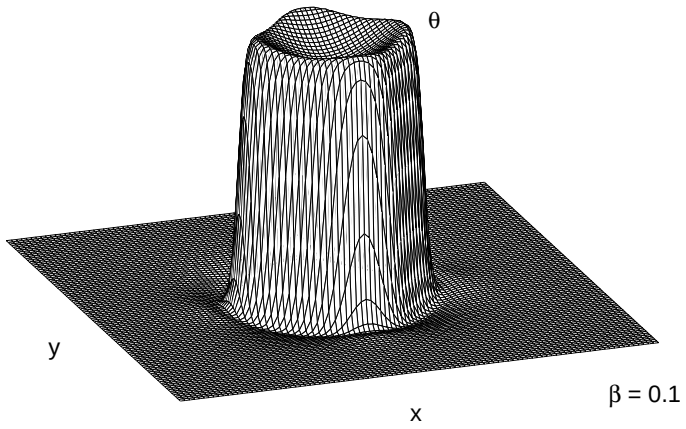

Figure 7.7: The pattern solution excited by locally raising the control parameter over a non-circular region larger than that of figure 7.3

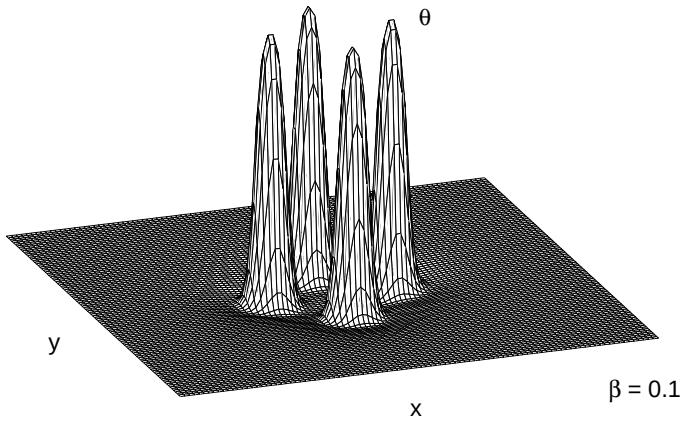

Figure 7.8: The resulting spikes when the control parameter is restored to its original value after the pattern solution of figure 7.7 has been excited

interaction between them decreases exponentially with distance [21]. Therefore, unless the activator-inhibitor system is highly homogeneous, one would not expect to observe interactions between spikes or walls that are not in close proximity. However, numerical study indicates that under some conditions in highly homogeneous systems, spikes can attract or repel each other, creating complicated "molecules," and similar results have been observed in gas discharge experiments [21]. Even in systems that are homogeneous enough for spikes to influence each other, presumably for spikes separated by a sufficiently large distance, the resulting motion of the spikes would be on a much longer time scale than τ_θ and τ_η (when $\tau_\theta > \tau_\eta$, but $\tau_\theta \approx \tau_\eta$).

So to summarize, interesting spatially nonuniform equilibria can be readily excited in spatial discretizations of the cubic nonlinearity model. In two dimensions, circularly symmetric solutions are possible in addition to spike solutions, depending on the value of the control parameter, and depending on how the spike is excited.

7.2 MEMS actuator-array applications

The MEMS actuator-array applications we will consider here involve moving microscopic items (for example, sorting small parts or bringing together small quantities of chemical reactants), or micropositioning small items [18]. It is also possible to use MEMS micromirror arrays for electro-optic applications, and it is potentially possible to use MEMS actuator arrays to control boundary-layer fluid flow [16, 17]. Although the specifics of pattern control differ for each of these applications, certain issues are inherent to the microactuators themselves, independent of the particular application: for example, the control voltages required, the forces and torques involved, and the way in which pattern-forming-system dynamics are translated into actuator motion.

We will assume for MEMS actuator arrays that there is a pattern-forming system implemented in a parallel, distributed fashion, collocated with the actuators, and that the control signal to each actuator is determined by a pattern-forming-system variable at its site. The pattern-forming system could be implemented in an analog or digital fashion, and the actuators could be driven in a linear regime of displacement proportional to control or a nonlinear regime of snapping between the two extremes of their range of motion, but in any case, the motion of the actuators is assumed not to influence the pattern-forming system directly. That way, we can consider control of the pattern independently of mechanical loads on the actuator array. When it is desirable to use information about the mechanical loads to help control the pattern, we will assume that separate pressure sensors provide the information, which can then be applied as input to the pattern-forming system.

Another way to state our approach to controlling MEMS actuator arrays is that we are assuming the actuators are "stiff" in the face of applied loads, and then deciding what patterns to excite in the pattern-forming system under the assumption that there is a direct correspondence between one of the pattern-forming system variables (generally the activator) and the actuators' positions. However, we then need to check whether, in fact, the actuators are stiff for the loading conditions and voltages applied. In the case where the actuators are assumed to snap between their two limits of motion, the pattern-forming-system dynamics might actually drive comparators, which would in turn drive the actuators. The actuator array surface might still vary smoothly, however, if the actuators are supporting a deformable membrane, as is the case for deformable mirrors, and as might be desirable for positioning microscopic items.

To clarify how an actuator array would be controlled by a pattern-forming system, a derivation of the dynamical equations for torsional microflaps is given. Then we determine the voltage levels required and discuss the condition for the actuators to be stiff. Finally, we discuss the positioning of microscopic items and micropositioning small (but not necessarily microscopic) items in more detail.

7.2.1 Derivation of torsional flap dynamical equations

The dynamical equations for an electrostatically driven torsional microflap were derived by P.S. Krishnaprasad [51]. An alternative derivation of these equations are presented here. (A different result is quoted in [52].) The torsional flap configuration is an important one because electrostatically actuated torsional joints are common in MEMS devices, and it is possible to obtain piston motion using torsional joints [15]. By deriving the dynamical equations for the torsional microflap, we can calculate the voltage levels required for a desired actuator displacement, and also derive the criterion for our actuators to be stiff.

We start by determining the torque as a function of applied voltage for a conducting flap connected to a pivot point located at a fixed distance above a conducting sheet (figure 7.9). Although the flap is symmetrical about the pivot point, there are really two separate conducting sheets below the flap, one to the left and one to the right of the pivot point. Therefore, for purposes of the analysis, we only consider the half of the flap to the right of the pivot point along with the single conducting sheet below it.

The analysis strategy is to solve Laplace's equation with the given boundary conditions to determine the potential field between the plates. From the

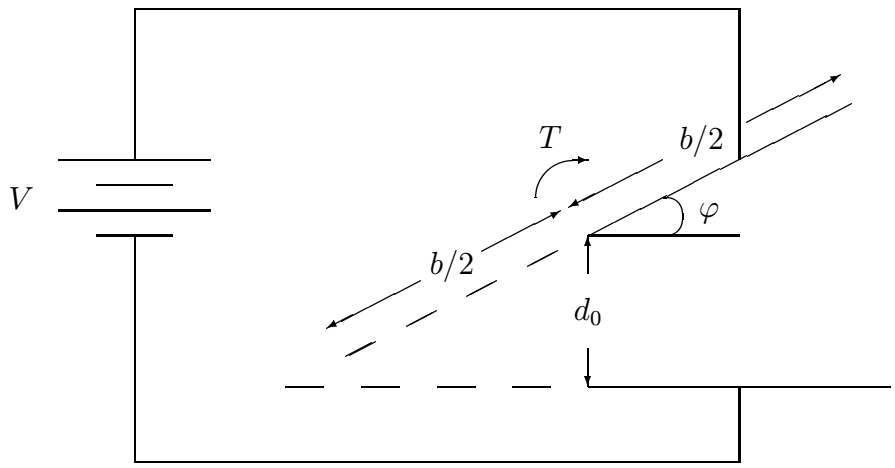

Figure 7.9: Torsional flap above a conducting sheet

solution to Laplace's equation, the electric field distribution can be determined. Next, the energy stored between the plates is determined by integrating the square of the electric field over the volume between the plates. This energy is then expressed solely in terms of the variable angle φ. Finally, the torque is computed by differentiating the energy with respect to φ. Fringing effects are neglected so that simple hand-calculations can be used.

Consider first the electrostatics problem of figure 7.10. There are two plates which, if extended, make an angle of ϕ with each other in the xy-plane. Using cylindrical coordinates, we let r_1 and r_2 denote the distance from the origin to the edges of the two plates in the xy-plane. The plates are assumed to be square with a z-dimension of length a. One plate is at a voltage V and the other is grounded.

The voltage distribution between the plates can be found by solving Laplace's equation with the given voltage boundary conditions on the plates. In the idealized case where the plates are infinite half-planes meeting at the z-axis in cylindrical coordinates, the equipotential surfaces are half-planes which when viewed in the xy-plane look like rays starting at the origin and heading

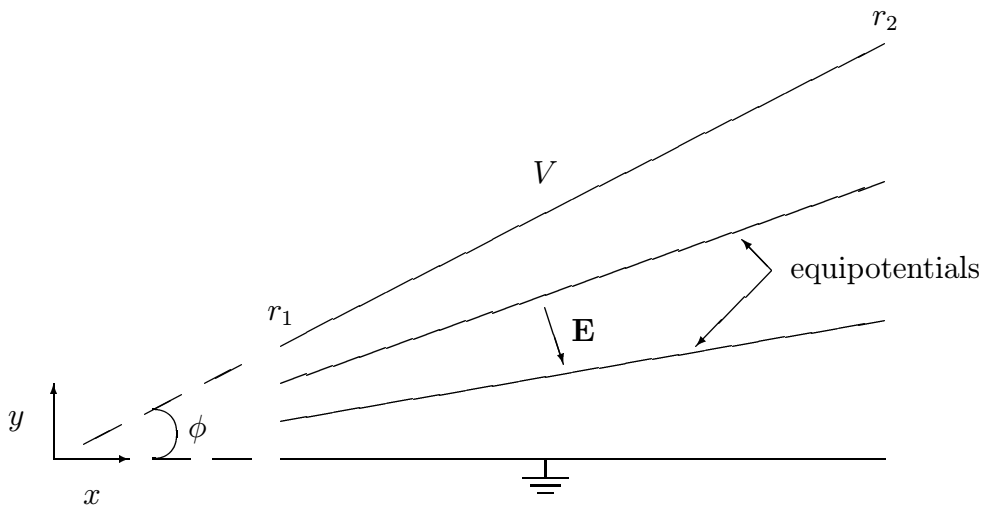

Figure 7.10: Electrostatics problem for the torsional flap above a conducting sheet

out radially between the two plates. Furthermore, by symmetry, equipotentials that differ by the same voltage are separated by equal angles.

The equation $\mathbf{E} = -\nabla V$ from electrostatics dictates that for this potential distribution, the electric field lines must lie on circular arcs between the two plates. From

$$V = -\int \mathbf{E} \cdot d\mathbf{l} \tag{7.1}$$

we conclude (since $|\mathbf{E}|$ is constant along each circular arc),

$$E_\phi(r) = -\frac{V}{r\phi}, \tag{7.2}$$

and the other components of $\mathbf{E}$ are zero.

We can now calculate the stored electrical energy between the plates:

$$\begin{aligned} W &= \frac{\epsilon}{2}\int_V |\mathbf{E}|^2 dv \\ &= \frac{\epsilon}{2}\frac{V^2}{\phi^2} a \int_{r_1}^{r_2}\int_0^{\phi} \frac{1}{r^2} r dr d\tilde{\phi} \end{aligned}$$

$$= \frac{\epsilon}{2}\frac{V^2}{\phi}a\ln\frac{r_2}{r_1}. \tag{7.3}$$

Now we return to the problem of figure 7.9. The goal is to express W in terms of the the angle φ, which enters into ϕ, r_1, and r_2:

$$\begin{aligned} \phi &= \varphi, \\ r_1 &= \frac{d_0}{\sin\varphi}, \\ r_2 &= \frac{d_0}{\sin\varphi} + \frac{b}{2}. \end{aligned} \tag{7.4}$$

Therefore, W in terms of φ is given by

$$\begin{aligned} W &= \frac{\epsilon V^2 a}{2\varphi}\ln\left[\frac{d_0/\sin\varphi + b/2}{d_0/\sin\varphi}\right] \\ &= \frac{\epsilon V^2 a}{2\varphi}\ln\left(1 + \frac{b}{2d_0}\sin\varphi\right) \\ &= \frac{\epsilon V^2 a}{2\varphi}\ln(1 + c_0\sin\varphi), \end{aligned} \tag{7.5}$$

where $c_0 = b/2d_0$. The torque is then

$$\begin{aligned} T &= -\frac{dW}{d\varphi} \\ &= \frac{\epsilon V^2 a}{2\varphi^2}\ln(1 + c_0\sin\varphi) - \frac{\epsilon V^2 a}{2\varphi}\left(\frac{1}{1 + c_0\sin\varphi}\right)c_0\cos\varphi \\ &= \frac{\epsilon V^2 a}{2\varphi^2}\left[\ln(1 + c_0\sin\varphi) - \frac{c_0\varphi\cos\varphi}{1 + c_0\sin\varphi}\right]. \end{aligned} \tag{7.6}$$

We can now use the following series expansions,

$$\begin{aligned} \sin\varphi &= \varphi - \frac{\varphi^3}{3!} + \cdots, \\ \cos\varphi &= 1 - \frac{\varphi^2}{2!} + \cdots, \\ \ln(1 + x) &= x - \frac{x^2}{2} + \frac{x^3}{3} - \cdots, \\ \frac{1}{1 + x} &= 1 - x + x^2 - x^3 + \cdots, \end{aligned} \tag{7.7}$$

to obtain, for $\varphi << 1$ and $x << 1$,

$$\begin{aligned}
\ln(1+c_0\sin\varphi) &\approx \ln\left[1+c_0\left(\varphi-\frac{\varphi^3}{6}\right)\right] \\
&\approx c_0\left(\varphi-\frac{\varphi^3}{6}\right)-\frac{1}{2}c_0^2\varphi^2+\frac{1}{3}c_0^3\varphi^3 \\
&= c_0\varphi-\frac{c_0^2}{2}\varphi^2+\left(\frac{c_0^3}{3}-\frac{c_0}{6}\right)\varphi^3, \qquad (7.8)\\
\frac{1}{1+c_0\sin\varphi} &\approx \frac{1}{1+c_0\left(\varphi-\frac{\varphi^3}{6}\right)} \\
&\approx 1-c_0\left(\varphi-\frac{\varphi^3}{6}\right)+c_0^2\varphi^2-c_0^3\varphi^3 \\
&= 1-c_0\varphi+c_0^2\varphi^2+\left(\frac{c_0}{6}-c_0^3\right)\varphi^3, \qquad (7.9)\\
c_0\varphi\cos\varphi &\approx c_0\varphi\left(1-\frac{\varphi^2}{2}\right) \\
&= c_0\varphi-\frac{c_0}{2}\varphi^3, \qquad (7.10)\\
\frac{c_0\varphi\cos\varphi}{1+c_0\sin\varphi} &\approx \left(c_0\varphi-\frac{c_0}{2}\varphi^3\right)\left[1-c_0\varphi+c_0^2\varphi^2+\left(\frac{c_0}{6}-c_0^3\right)\varphi^3\right] \\
&= c_0\varphi-\frac{c_0}{2}\varphi^3-c_0^2\varphi^2+c_0^3\varphi^3 \\
&= c_0\varphi-c_0^2\varphi^2+\left(c_0^3-\frac{c_0}{2}\right)\varphi^3. \qquad (7.11)
\end{aligned}$$

Therefore,

$$\begin{aligned}
T &= \frac{\epsilon V^2 a}{2\varphi^2}\left[\ln(1+c_0\sin\varphi)-\frac{c_0\varphi\cos\varphi}{1+c_0\sin\varphi}\right] \\
&\approx \frac{\epsilon V^2 a}{2\varphi^2}\left[c_0\varphi-\frac{c_0^2}{2}\varphi^2+\left(\frac{c_0^3}{3}-\frac{c_0}{6}\right)\varphi^3-c_0\varphi+c_0^2\varphi^2-\left(c_0^3-\frac{c_0}{2}\right)\varphi^3\right] \\
&= \frac{\epsilon V^2 a}{2\varphi^2}\left[\frac{c_0^2}{2}\varphi^2+\left(\frac{c_0}{3}-\frac{2c_0^3}{3}\right)\varphi^3\right] \\
&= \frac{\epsilon V^2 a}{2}\left[\frac{c_0^2}{2}+\left(\frac{c_0}{3}-\frac{2c_0^3}{3}\right)\varphi\right]. \qquad (7.12)
\end{aligned}$$

Defining

$$\gamma = c_0\varphi, \qquad (7.13)$$

so that γ is approximately the ratio of actual deflection to maximum possible

deflection for the flap, the torque expression can be rewritten as

$$T \approx \frac{\epsilon V^2 a b^2}{16 d_0^2} - \frac{\epsilon V^2 a b^2}{12 d_0^2}\left(1 - \frac{2 d_0^2}{b^2}\right)\gamma. \tag{7.14}$$

We will refer to γ as the "relative deflection." (In fact, the maximum possible deflection is typically less than 10 degrees for torsional microflaps, so we are justified in approximating the maximum angular deflection by $1/c_0$.) Letting $c_1 = \frac{\epsilon a b^2}{16 d_0^2}$, and assuming that $d_0 << b$, we can express the torque (approximately) as

$$T = c_1 V^2 \left(1 - \frac{4}{3}\gamma\right). \tag{7.15}$$

Modeling the mechanical part of the system as a linear torsional spring, we have

$$I\ddot{\varphi} + \frac{2K}{l}\varphi = -T, \tag{7.16}$$

where I is the moment of inertia of the flap, l is the length of the torsion bar on which the flap is suspended, and K is the torsional rigidity of the torsion bar on which the flap is suspended [51, 52]. We can write the linear torsional spring equation in terms of γ as

$$\ddot{\gamma} + \omega_0^2 \gamma = -\frac{c_0}{I} T, \tag{7.17}$$

where $\omega_0 = \sqrt{\frac{2K}{lI}}$.

Suppose now we actuate both sides of the flap with different voltages, as shown in figure 7.11. If we now apply a voltage V_1 to the right electrode, apply a voltage V_2 to the left electrode, and assume an external torque T_{ext}, we obtain

$$\begin{aligned} T_1 &= c_1 V_1^2 - c_1 V_1^2 \frac{4}{3}\gamma, \\ T_2 &= -c_1 V_2^2 - c_1 V_2^2 \frac{4}{3}\gamma, \\ T &= T_1 + T_2 - T_{\text{ext}} = c_1(V_1^2 - V_2^2) - c_1(V_1^2 + V_2^2)\frac{4}{3}\gamma - T_{\text{ext}}. \end{aligned} \tag{7.18}$$

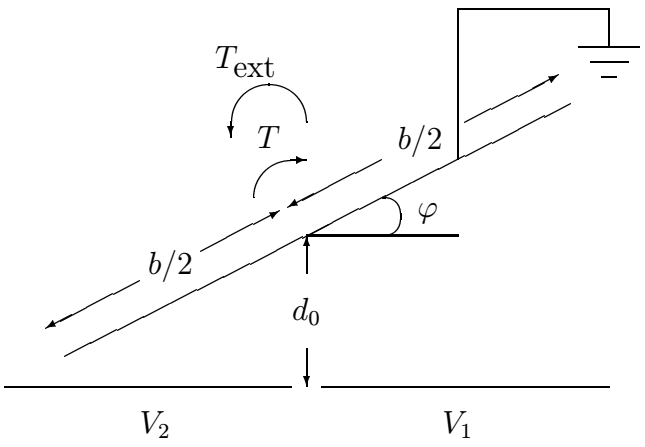

Figure 7.11: Torsional flap above two electrodes

The dynamical equation for the flap is then

$$\ddot{\gamma} + \left(\omega_0^2 - \frac{4}{3}\frac{c_0 c_1}{I}(V_1^2 + V_2^2)\right)\gamma = \frac{c_0 c_1}{I}(V_2^2 - V_1^2) + \frac{c_0}{I}T_{\text{ext}}. \tag{7.19}$$

The primary dissipative mechanism for small torsional flaps in air is aeordynamic drag, which contributes a term $c_3|\dot{\gamma}|\dot{\gamma}$ to the dynamics, yielding [51]

$$\ddot{\gamma} + c_3|\dot{\gamma}|\dot{\gamma} + \left(\omega_0^2 - \frac{4}{3}\frac{c_0 c_1}{I}(V_1^2 + V_2^2)\right)\gamma = \frac{c_0 c_1}{I}(V_2^2 - V_1^2) + \frac{c_0}{I}T_{\text{ext}}. \tag{7.20}$$

Suppose we consider the voltages V_1 and V_2 as having a common-mode component V and a differential component $\delta V << V$; i.e.,

$$V_1 = V - \frac{1}{2}\delta V, \;\; V_2 = V + \frac{1}{2}\delta V. \tag{7.21}$$

Then neglecting higher-order terms in δV, the dynamical equation becomes

$$\ddot{\gamma} + c_3|\dot{\gamma}|\dot{\gamma} + \left(\omega_0^2 - \frac{8V^2 c_0 c_1}{3I}\right)\gamma = \frac{V c_0 c_1}{I}\delta V + \frac{c_0}{I}T_{\text{ext}}, \tag{7.22}$$

where we think of V as constant and δV as a control input. We can view the dynamical equation (7.22) for the torsional microflap as being like a linear, second-order system with a control input. In fact, if a mechanical damping mechanism were added which dominated the aerodynamic drag dissipation (or

if the control δV were used to perform active damping), the system could be well-approximated by a linear second-order system.

We see from equation (7.22) that increasing the common-mode voltage V reduces the resonant frequency of the flap. We can compute the reduction in the resonant frequency as follows. The moment of inertia of the torsional flap is given by

$$I = \frac{1}{12}\rho a d b^3, \tag{7.23}$$

where $\rho = 2.3 \times 10^3 \text{kg/m}^3$ is the density of silicon and d is the thickness of the flap. Therefore,

$$\frac{8}{3}V^2\frac{c_0 c_1}{I} = \frac{8}{3}V^2\frac{b}{2d_0}\frac{\epsilon a b^2}{16 d_0^2}\frac{12}{\rho a d b^3} = \frac{V^2\epsilon}{\rho d_0^3 d}, \tag{7.24}$$

where $\epsilon = \epsilon_0 = 8.85 \times 10^{-12}$ F/m in air. Defining

$$f_V = \frac{1}{2\pi}\sqrt{\frac{V^2\epsilon}{\rho d_0^3 d}} = \frac{1}{2\pi}V\sqrt{\frac{\epsilon}{\rho d_0^3 d}}, \tag{7.25}$$

we find that for typical values of d_0 and d, and typical mechanical resonant frequencies for MEMS torsional microflaps, it is possible to have f_V comparable to $f_0 = \omega_0/2\pi$ for voltages of about 100V. For example, taking $d_0 = 5\mu$m, $d = .5\mu$m, and $V = 100$V, we find $f_V = 125\text{kHz} \approx f_0$ for a typical micromirror element [13].

Consider the case of V small enough that $f_V << f_0$. Then letting $\omega_e = \sqrt{\omega_0^2 - \omega_V^2}$, we have

$$\ddot{\gamma} + c_3|\dot{\gamma}|\dot{\gamma} + \omega_e^2\gamma = \frac{3}{8}\frac{V\epsilon}{\rho d_0^3 d}\delta V + \frac{c_0}{I}T_{\text{ext}} \tag{7.26}$$

Suppose d_0 and d are as before, but now $V = 10$V and $\omega_e = 100$kHz. We then obtain the equilibrium equation

$$\gamma = (.023)\delta V + \frac{c_0}{I\omega_e^2}T_{\text{ext}}, \tag{7.27}$$

which shows that $\delta V << V$ leads to tiny relative deflections. So there is a tradeoff between maintaining a high natural frequency and obtaining reasonable relative deflections. So we see that even without considering external torques, the common-mode voltages we require for reasonable deflections are on the order of 100V, and the differential voltages are on the order of volts when the common-mode voltage is 100V. In semiconductor processing, it is possible to achieve the 100V common-mode and few-volt differential signals, but care must be taken to ensure the 100V signal does not cause dielectric breakdown. (If the dimensions of the actuators and the external torques are small enough, low input voltages can provide sufficient displacement; for example, the Texas Instruments micromirror chip runs from a single 5V power supply [22, 23].)

When $f_V > f_0$, the coefficient ω_e^2 is negative. In this case, when $T_{\text{ext}} = 0$, the flap tends to snap to one extreme of its range of motion, or the other. Equation (7.22) does not provide a complete description of the dynamics in this regime, but since this would be a digital mode of operation, a complete description of the dynamics might not be necessary anyway, with parameters like transition time being more of interest.

The condition that the actuators be stiff can be expressed as

$$T_{\text{ext}} << V c_1(\max|\delta V|), \tag{7.28}$$

so that the external applied torque on the microflap only has a small effect on the equilibrium angle. We see that the larger the voltages used, the stiffer the actuators, as would be expected. Suppose there is a .23g mass on a 1cm^2 actuator array (corresponding to a 1mm-thick piece of silicon), which is being supported equally by 10 out of 100 actuators in the 1cm^2 array. The torque

on each actuator is

$$T_{\text{ext}} = \frac{1}{10} mg \frac{b}{2} = \frac{1}{10}(.00023\text{kg})(9.8\text{m/s}^2)(.0005\text{m}) = 1.1 \times 10^{-7}\text{Nm}, \quad (7.29)$$

and

$$c_1 = \frac{\epsilon a b^2}{16 d_0^2} = \frac{(8.85 \times 10^{-12}\text{F/m})(.001\text{m})(.001\text{m})^2}{(16)(5 \times 10^{-6}\text{m})^2} = 2.2 \times 10^{-11}\text{F}. \quad (7.30)$$

Even with $V = 100$V, we see that the actuators are far from stiff in this example.

To summarize, we have shown that it is indeed possible to achieve reasonable relative deflections with reasonable signal voltages (of a few volts) while keeping the natural frequency of the system positive, as long as there is a sufficiently high DC voltage available. The high voltage supply would not have to supply much power because there is essentially no DC current drawn by the high-voltage supply, only displacement current. However, the mechanical loading on the array has to be quite small for the actuators to be stiff (as it would be for micromirror arrays).

7.2.2 Manipulation of micro-scale items

For manipulating micro-scale items, consider a two-dimensional array of piston-type actuators underneath a flexible membrane [13]. Suppose that the actuators are controlled by a spatial discretization of the basic cubic nonlinearity model with $\beta << 1$ and $\alpha > 1$, with the control parameter in the regime where spike equilibria are stable. There are two types of solutions that could be used for manipulating items: ordinary spikes (figure 7.4 turned upside-down), and circular walls (as in figure 7.6). The advantage of using circular walls is that "containers" of different sizes could be generated in the same system. The challenges of using circular walls is that they require a more compex method

of excitation than is required for ordinary spikes, because if the walls bend too sharply, they become unstable and decay into spikes.

To give a more concrete picture of how a micro-manipulation or sorting system might work, suppose we have the ability to sense what objects are on the array, and where. We might obtain this information from pressure sensors in the array itself, or we might have an optical system above the array. For the sorting application, we are interested in separating out one type of object from others on the array. Where we sense the objects we want to separate, we excite spikes or walls (either electronically, or electro-optically by shining light down from above), and the network is designed to advect solutions in a particular direction (toward a bin at the edge of the array). As a wall surrounding an object moved along, it could push other objects in its path out of the way, something a spike probably could not do.

If it was desired to bring two items together, with more control effort, two walled regions with different items could be brought in proximity. A large wall surrounding both items could then be excited, and finally, the inner walls around each item could be made unstable. Of course, this type of scheme requires considerable additional control effort as compared with the simple sorting scheme.

Even for manipulation of small items, the walls or spikes that can be obtained using MEMS piston actuators are limited to a few microns or less in height. Therefore, even small objects we are trying to manipulate probably will be higher than the walls or the depth of the spikes. Therefore, surface and friction properties need to be considered carefully to determine if the objects we are attempting to manipulate can actually be manipulated this way. For example, in the case of manipulating fluids, we are really modulating surface

tension effects when we change the shape of a deformable membrane above the actuator array (presumably the fluid naturally beads on the membrane, and it is the beads that we are attempting to move with the walls or spikes). Allowing snapping to the limits of actuation is beneficial for the micromanipulation application because it increases the height of the walls or spikes by about a factor of 2.5 over the height we can otherwise achieve with the same geometry [13]. One disadvantage of snapping to the limits of actuation is stiction, particularly if the actuator spends too long snapped to one limit or the other. Allowing the actuators to snap to their limits of actuation is not a problem for the control scheme we are proposing: it simply means the actuator deflections will have a different shape than the corresponding three-dimensional plot of control voltages.

7.2.3 Micropositioning small (but not micro-scale) items

One approach to micropositioning small items using MEMS is to use an array of asymmetrical torsional resonators that each apply a small horizontal force in a fixed direction as they oscillate [18, 19]. Suppose we have (at least) three interlaced arrays of resonators with their directions of motion distributed evenly around the unit circle. We could then drive the actuators using electrical oscillator circuits, and couple the electrical oscillators so that each of the arrays would be separately governed by a complex activator-inhibitor equation. By controlling the patterns of rolls in the three networks, we could microposition an object atop the actuators.

Although an ideal pattern of rolls for the complex activator-inhibitor equation would work for conveying an object in the direction associated with that array, in fact the ideal pattern is not even required for this application. All we really want for motion in a single direction is that approximately equal

numbers of actutators be supporting the object at each instant of time, which is expected to be the case when $C = 0$ regardless of whether the roll pattern is ideal or not. Whether the helical solutions are left- or right-handed also makes no difference in this application, because the direction of rotation of each actuator is the same regardless of what the phase differences are between adjacent actuators.

So all we really need to control for the micropositioning application is where in each array (with each array corresponding to a different direction of motion) we excite the pattern solution. The alternative to exciting the pattern solution should be turning the oscillators off, i.e., fixing the corresponding actuator positions (either at the middle or bottom of their range of motion). Thus, the bifurcation parameter we want to use is not C, the injected external frequency, but is instead the coefficient of the linear instability term in the θ equation (as discussed below in the context of phased-array antennas).

So to implement our pattern-forming-system control scheme, we would lay out (at least) three co-located arrays of mechanical actuators, along with one electrical oscillator and one resonant electrical circuit for each actuator, couple the oscillators and resonators separately for each of the three arrays to implement three complex activator-inhibitor equations, and use the coefficient of the linear instability term in each complex activator-inhibitor equation as a spatially-variable control parameter that can be controlled by a high-level controller. Then to move an item in a certain direction, the high-level controller merely has to raise the control parameter for the array corresponding to the desired direction of motion in the vicinity of the object to be moved. If only one object is to be moved at a time, the control parameters can be common to each entire array.

7.3 Phased-array antenna applications

One method for implementing a phased-array antenna is to use an electro-optic system in which the optical part, using a micromirror array in which a certain pattern solution is used to create a pattern of optical phases, drives a photodetector array, which then controls the phase shifts in an array of electrical oscillator circuits [16]. The radiation pattern of the phased-array antenna is then controlled by controlling the pattern solution in the micromirror array.

However, we will consider a different type of phased-array antenna implementation here. As was shown in chapter 3, the complex activator-inhibitor equation can model a network of coupled oscillators (and coupled resonant circuits) if certain assumptions are met. It was also shown in chapter 6 that for $C = 0$, there is an ideal helical pattern equilibrium for the one-dimensional complex activator-inhibitor equation when $\alpha > 1$ and $\beta < 1$. This ideal helical pattern, in the coupled oscillator context, represents a constant phase shift between each pair of neighboring oscillators. The wave number of the helical pattern, which corresponds to the amount of phase shift between two adjacent oscillators, can be controlled by varying L, l, or both. Therefore, a potential application for the complex activator-inhibitor equation is phased-array antennas. A one-dimensional system would correspond to a linear array, and a two-dimensional system could be used as an endfire array [38, 39, 40].

7.3.1 Linear array

A linear array consists of a number of antennas equally spaced along a line, with one oscillator corresponding to each antenna. If the phased array is for transmitting, the oscillators drive the antennas, and if the array is for receiving, each (quadrature) oscillator output is mixed with the corresponding

antenna signal. The frequency of the oscillators determines the spacing of the antennas: if the antennas are a half-wavelength apart, then when adjacent oscillators are exactly out of phase, constructive interference occurs along the axis of the array, and when adjacent oscillators are in phase, destructive interference occurs along the axis of the array (and conversely for the normal direction to the axis of the array). The direction of constructive interference is also called the mainlobe direction.

For the coupled oscillator array we are considering based on the complex activator-inhibitor equation, however, we need the phase shift between oscillators to be considerably less than 180 degrees. Furthermore, we want to consider the case of a very large number of closely spaced oscillators, since then we can best approximate the purely resistive coupling needed between adjacent oscillators. Solid-state microwave oscillators, which have relatively low power output per oscillator but which can be fabricated in large numbers using semiconductor processing, are thus the main candidate for phased-array antennas based on the complex activator-inhibitor equation.

Suppose the parameter L, which corresponds to the strength of the coupling between the resonant circuits, can be varied between a very large value $L_{\max} >> l$ and a value $L_{\min} > l$. Suppose that the spacing between the oscillators is such that out-of-phase oscillators are a half-wavelength apart when $L = L_{\min}$ and $\phi_{\min} = \sqrt{1 - l/L_{\min}}/\sqrt{lL_{\min}}$. Then when $L = L_{\max}$, there is constructive interference (almost) perpendicular to the array and destructive interference along the axis of the array, and when $L = L_{\min}$, there is destructive interference perpendicular to the array and constructive interference along the axis of the array.

The parameter L corresponds to the coupling between the resonant cir-

cuits. When $L = L_{\max}$, the coupling between adjacent resonant circuits is large, and when $L = L_{\min}$, it is small (perhaps limited by stray coupling). So one parameter, common to all the resonant circuits, determines the phase shift between neighboring oscillators.

There is still the issue of how to excite the appropriate left-handed helical solution or right-handed helical solution. If we insist that the helical solution always be, say, left-handed, then we are restricting the useful angular range of the phased-array antenna to 90 degrees (as opposed to 180 degrees). But let us assume 90 degrees of angular range is acceptible. If we can force the system into the left-handed helical equlibrium, then as long as we vary L slowly enough, we expect that the system will remain in the left-handed helical state. So all we need to do is find a way to power up the oscillator array so that the left-handed helical solution is selected.

We can obtain the ideal helical solution by powering up the oscillators gradually from one side of the array to the other. This involves a slight modification to our usual complex activator-inhibitor equation: the addition of a control parameter multiplying the linear instability term in the activator equation,

$$\begin{aligned} \tau_\theta \partial_t \theta &= l^2 \Delta\theta - |\theta|^2 \theta + u\theta + \eta, \\ \tau_\eta \partial_t \eta &= L^2 \Delta\eta - \eta - \theta + C, \end{aligned} \tag{7.31}$$

where u is a real-valued control input varying between zero and one (or between a negative constant and one).

So we can bring the system up to an ideal helical solution. However, symmetry-breaking chooses between the left-handed and right-handed states. Two alternative ways to achieve an imperfect bifurcation (i.e., manually select

the left-handed helix) are to actually inject oscillating signals (e.g., using C) slightly out of phase into the first couple of oscillators powered up, or else have a slight asymmetry in the coupling between the first two oscillators. The conclusion is that with some engineering work, it should be possible to use the complex activator-inhibitor equation to help control a linear phased-array antenna. However, the need for a network of resonant circuits and coupling between the oscillators and resonant circuits would involve additional complexity as compared with other approaches [38, 39].

7.3.2 Endfire array

The endfire array operates on a slightly different principle than the linear array. The endfire array is a two-dimensional array, and we are interested in constructive and destructive interference in the plane containing the array. (Usually two-dimensional phased-array antennas are used for three-dimensional patterns outside the plane of the array, but the endfire configuration can also be used.) To have a useful endfire array, we can fix the parameters l and L, and vary the direction of constructive interference by controlling the pattern in the network.

The pattern we desire is an ideal pattern of parallel rolls, where along the direction perpendicular to the rolls we have ideal one-dimensional helical solutions. The spacing of the antennas is chosen such that oscillators 180 degrees out of phase are a half-wavelength apart, and therefore interfere constructively. For the endfire array configuration, there is no need to worry about whether the pattern is left-handed or right-handed. However, we still need to excite an ideal pattern of parallel rolls, and then be able to reorient it as required to change the mainlobe direction. The endfire antenna array example is particularly illustrative of the subtleties and difficulties one encounters in working

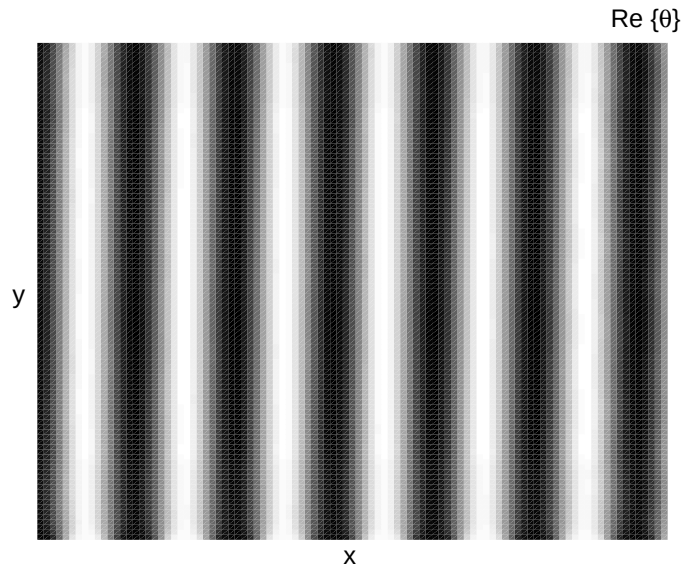

Figure 7.12: Ideal roll pattern for the endfire phased-array antenna with long-range coupling

with pattern-forming systems for control of large actuator arrays.

Suppose we first ask what the simplest technique would be for exciting the ideal roll pattern in a rectangular network. One approach would be to first power up a row of oscillators in the middle of the array, just as was done for the linear array, and then power up the rest of the oscillators from the middle row outward. This approach encounters the difficulty that the rolls tend to become disordered as they form outward from the center of the array. A simple solution to this problem is to add a small amount of long-range coupling to help stabilize the ideal pattern. In fact, it is likely if the antenna array is a transmit array, that there will, in fact, be some long-range coupling between oscillators through the antennas. The long-range coupling is indeed observed to stabilize the ideal roll pattern. The resulting roll pattern is shown in figure 7.12, and the corresponding (far-field) antenna pattern is shown in figure 7.13.

Once we have the initial ideal pattern of rolls, we would like to be able

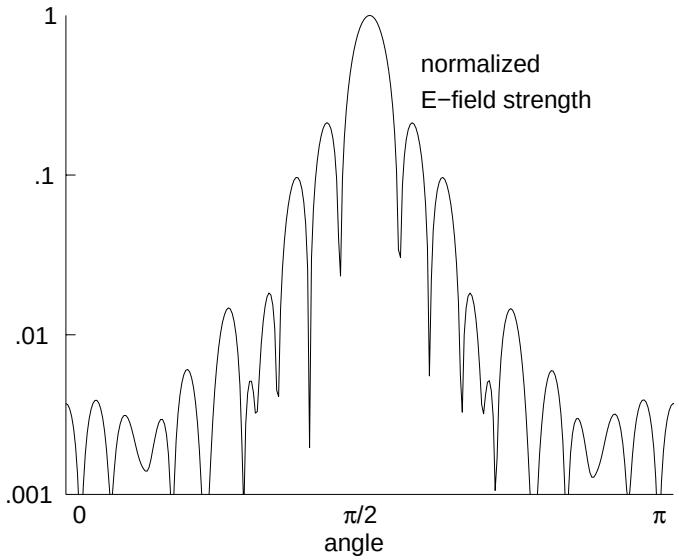

Figure 7.13: Antenna pattern for the ideal roll pattern of figure 7.12

to reorient the rolls in order to point the mainlobe in different directions. One way would be to use radially-dependent advective terms to rotate the entire pattern about its center at a constant angular velocity. However, physically, this would require complicated, asymmetric coupling between oscillators, and is therefore probably not realistic. So we might instead try to reorient the roll pattern using the boundary of the array. However, here we encounter an intrinsic limitation of the pattern approach: the pattern already present has a strong tendency to persist even if we perturb its edges. We cannot realistically expect to be able to move toward the bifurcation point and there try to reorient the pattern, because we cannot expect to have a sufficiently homogeneous system.

When we initially excited the ideal pattern of rolls, we were actually using the pattern-forming properties of the system very close to threshold, as we brought the system through threshold gradually across the network. If we could determine a simple way of powering up the oscillators in the right order

to achieve an arbitrary roll orientation, we could then achieve an arbitrary mainlobe direction by creating a new roll pattern instead of trying to reorient an existing one. Furthermore, since we want the system to be symmetric (so that no particular mainlobe direction is perferred, we will take the oscillator array to be circular instead of square.

One possible approach for trying to excite a roll pattern is to power up the array starting at a particular point on the circumference: if all went well, the resulting rolls would be approximately perpendicular to the diameter of the circular array intersecting that point. One way to achieve the desired pattern of turning on the oscillators is to use a second, bistable, two-dimensional, real activator-inhibitor network to control the power to each oscillator. A wave can then be excited in the real network that propagates radially outward from its source and turns on each oscillator as it passes.

With this type of system, long-range coupling can actually be detrimental to achieving the desired pattern. We want the rolls to be roughly parallel as they form, but the long-range coupling tries to force the rolls to be straight (which may break up the roll pattern into several subpatterns of rolls oriented in different directions). An example of a pattern excited using the approach of a second bistable network to turn on the oscillators is illustrated in figure 7.14. The partially-formed pattern as the wave is sweeping through the bistable system is shown in figure 7.15.

The bistable network and the coupled oscillator network (modeled by the complex activator-inhibitor equation), viewed independently, both possess Lyapunov functions. The bistable network drives the activator-inhibitor equation, but there is no feedback in the other direction. Furthermore, an asymptotically stable system driving another asymptotically stable system is

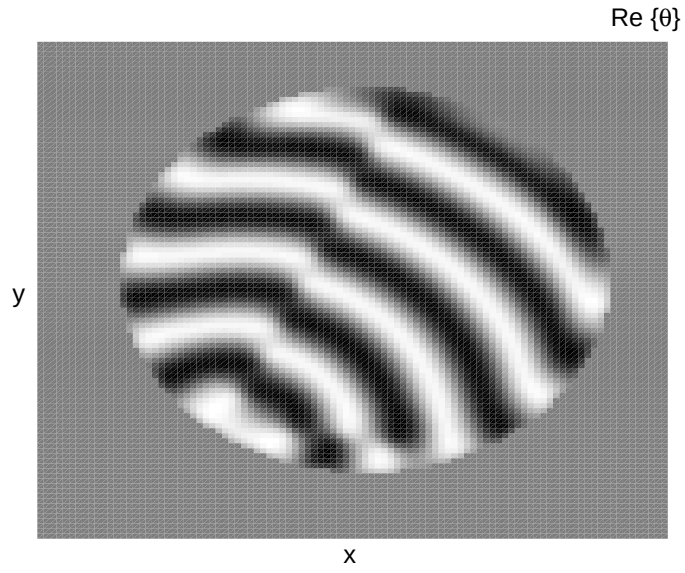

Figure 7.14: Roll pattern in a circular network with the oscillators turned on using a bistable activator-inhibitor network

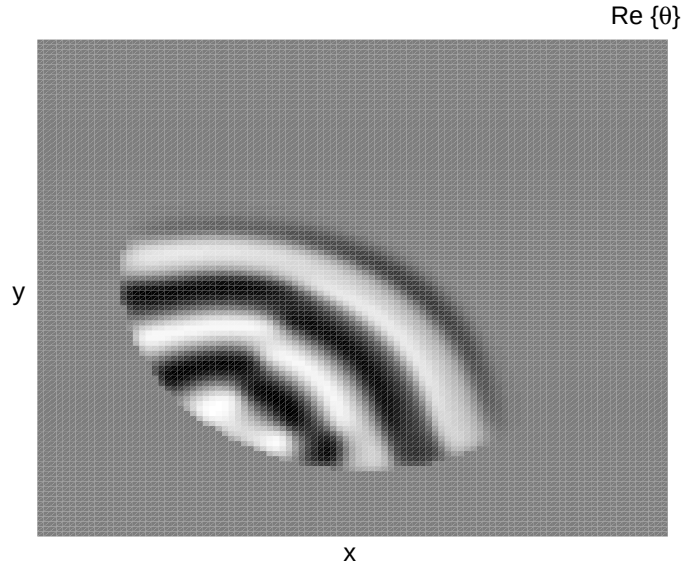

Figure 7.15: The roll pattern of figure 7.14 in the process of being formed as the wave in the bistable system sweeps across

asymptotically stable (provided the second system does not have a finite escape time due to the driving from the first system, which can be verified in this case) [53].

The roll pattern in the circular array is not as regular as that of the square array. Therefore the mainlobe of the antenna pattern is much wider for the circular array, but the point of this example was to illustrate some of the issues involved in actually using pattern-forming systems in applications. The key point is that it is important to excite the desired pattern as the pattern is being formed, because once formed, it will tend to resist change. Also, the approach of using an additional bistable network to bring the first system into the pattern-forming regime allows arbitrary orientations of a basic pattern to be excited in a rotationally symmetric two-dimensional system with access only to the edges (and to signals shared by the entire array).

7.4 Real-time image processing application

Consider the problem of detection of a particular type of item using image processing. Some of the most challenging instances of this problem occur in military applications, such as minesweeping and surveillance. The standard approach is to take lots of pictures, digitize the data, perform digital noise reduction and spatial filtering, and then try to correlate features in the data with matched filters developed for the target of interest. There is a receiver operating characteristic (ROC) for the detection problem, and detection threshold is set so that an acceptable detection probability and false alarm rate tradeoff is achieved [54].

Often, particularly in military applications, the targets are intentionally camouflauged to foil detection. However, camouflauge that works well in the

visible band (like green paint or foliage netting), is still succeptible to detection in the infrared band. Furthermore, it turns out that various features of objects can be best detected by fusing data from the near infrared, far infrared, and intermediate infrared [55]. (Sensory data fusion also plays an important role in biological systems. For example, in cats it has been found that the response to sound and light stimuli coming from the same peripheral point is much stronger than the response to sound stimulus or visual stimulus alone. This fusion of peripheral audio and visual information occurs reflexively; i.e., without conscious mental effort by the cat [56].) To facilitate data fusion for different IR bands, IR focal plane arrays have been developed with co-located sensors for near, intermediate, and far infrared [55]. By having a single detector (or three detectors stacked vertically) for all three IR bands, the problem of image registration (which arises when three different arrays are used to image the same scene) is overcome.

However, computation bandwidth is still a major issue in processing either simple images or fused images from three detectors. (For IR arrays, the processing is further complicated by the color-constancy issue: depending on the ambient lighting and temperature, infrared images of the same object can appear quite different. For purposes of this discussion, we will neglect the color-constancy issue.) The amount of computation required is far too great to hope to do in real-time.

However, biological systems use selective attention as a mechanism to overcome this computation bandwidth problem, and selective attention has been proposed for artificial visual recognition systems as well [57]. The idea behind selective attention is to have a large peripheral vision imager that can select potentially interesting features of the scene quickly and in parallel, and

then have a smaller, more complicated imager that can focus on the interesting features of the scene and assess in real-time whether the object one is trying to detect is in fact present. The peripheral imager only needs to determine where targets might be present, so it can use a much cruder matched filtering technique than would be used for analyzing a photograph. The more complicated matched filtering would be done by the much smaller imager that only focuses in on areas of the scene that are potentially of interest, and because this imager is small, the matched filtering can be done rapidly.

As we will outline, layered networks of pattern-forming systems could potentially be used to control such a selective-attention imaging scheme. Consider the following simplified version of the problem: we have a large square panorama in which we want to look for a particular type of target, amid a variety of clutter. Suppose we have a square imaging array with another small square array at the center capable of determining (within acceptable error criteria) whether it is looking at a target or not. We cannot scan the entire scene with the small array due to time constraints. However, the large array is capable of responding to features that look target-like, but with a very high probability of false detection. The approach is to scan the scene with the large array, and based on detections by the large array, point the small array toward features in the scene containing possible targets. The parts of the problem addressed by pattern-forming systems are related to recording where the large array has detected a feature, and positioning the small array to point in turn toward the detected features.

Suppose that under the large imaging array there is a cubic nonlinearity dynamical system implemented. When the feature detection algorithm (possibly a simple analog function of neighboring pixels) determines that a target-like

feature is present, the control parameter is locally raised above the bifurcation threshold for long enough to excite a spike solution in the cubic nonlinearity system. (As discussed earlier, the feature detection algorithm could drive the control parameter through ac-coupling, which is advantageous from a circuits point of view.) The feature detectors thoughout the array work in parallel, so that various spikes are excited in the cubic nonlinearity system.

Next, once the spikes have had a chance to form, the information about where the spikes are needs to be used to point the small array. For this purpose we use a second cubic nonlinearity network, this one with circular symmetry and an additional advective term. The activator state of the first network (i.e., the one now containing spikes) is periodically (with low duty cycle) applied as the control input to the second network, which otherwise has a spatially uniform control parameter value that permits spike equilibria. When the first-network activator is applied to the control input to the second network, spikes are excited in the second network where there are spikes in the first network. Spikes excited in the second network are then swept off by the advective term toward the periphery of the second network. Each spike in the first network thus produces a spike train at the same angle on the outer radius of the second network, and the phase of the spike train is related to the radial coordinate of the spike in the first network. This angle and radius information is then used to direct the small array. Once the small array has checked out each feature (i.e., each place a spike has been excited in the first network), the control parameter for the first network can be moved into the regime where only the spatially uniform equilibrium is stable, so that all spikes are removed. The large array is then positioned on the next part of the scene, the first array control parameter is moved back into the regime where spike solutions are possible, and the process is repeated.

The part of the selective attention problem that the layered network of cubic nonlinearity models addresses is how to convert features detected by the large array into information that can be used by the small array to decide where to point. The first network takes detected features and produces a managable collection of spikes. The second network takes a sparce, two-dimensional collection of spikes and multiplexes out a collection of polar coordinate data for directing the small imaging array. Both networks can consist of simple analog circuits, either integrated with the focal plane arrays or in a three-dimensional multilayered architecture.

The parts of the image processing task that the pattern-forming-system networks are being asked to perform are low-level, simple tasks, but tasks which it is helpful to perform in parallel. The networks simplify the interface between the sensors and the control system, and the interface between the control system and the actuators. The pattern-forming-system networks do not have to perform high-level tasks themselves to be useful, if they help simplify the job of the high-level controller. This appears to be a promising niche for pattern-forming-system networks from a controls point of view. As MEMS, microwave oscillator (and resonator), and imaging array technology improves to where we are thinking more about real-time systems than devices, we will have to develop some technique for performing the low-level functions which are then in turn regulated by high-level control.

Chapter 8

Conclusions and Directions for Future Research

On the theoretical side, for spatial discretizations of the models that have Lyapunov functions, it would be nice to be able to prove convergence to a particular equilibrium rather than having to settle for convergence to the set of equilibria. Such a result has been claimed for gradient systems where the energy function is analytic [58]. It does not appear, however, that the spatially discretized systems for which we have found Lyapunov functions can be written as gradient systems (with respect to a positive-definite metric).

On the engineering side, even though it may be technologically possible to incorporate electronics to implement a pattern-forming system with a MEMS actuator array, the prototyping cost is much higher than the cost of implementing the MEMS actuator array alone. It still remains to provide a compelling argument that a particular actuator array controlled using a particular pattern-forming system would so outperform standard approaches that it would be worth prototyping.

If there is one conclusion to be drawn from this investigation of applying pattern-forming systems to the control of actuator arrays, it is that the problem is multidisciplinary. The control aspects of the problem, which have been the primary focus here, are not enough to supply a useful system. Beyond the obvious mechanical engineering and solid state engineering required to actually construct the systems, there also has to be detailed knowledge of the application. If the application is to control boundary layer fluid flow, then

the fluid system needs to be understood well enough to know what type of actuation is required, which is currently an open question [17]. If the application is to manipulate small quantities of fluid, then the physics of surface tension, and the chemistry to be achieved, need to be understood and used in deciding what type of actuation is needed [20]. If microwave coupled oscillators are the application, then the electromagnetics and circuit design needs to be understood, since both impact the pattern-forming system design. In optics, there has been some investigation of what types of patterns might be useful for micromirror arrays, but this work is still in its early stages, and requires an understanding of adaptive optics [14].

Knowing what types of potentially useful solutions are readily achieved with pattern-forming systems is a necessary first step toward developing a viable concrete application, and that is essentially the contribution of this work. The potentially useful solutions are not only the equilibria, but the relaxational character of the dynamics as the equilibria are approached: for example, in a bistable system, the only stable equilibria may be uninteresting spatially uniform equilibria, but the way the system transitions from one spatially uniform equilibrium to the other is actually the behavior of interest. Above all, we desire qualitative information about solutions that can be rigorously supported mathematically, without the need to rely on simulation for more than simply illustration. This is particularly important when we need to incorporate sensor data and integrate arrays of actuators into larger control systems.

Appendix A

Derivations

A.1 Derivation of the phase equation for *K*-systems

The starting point is the reaction-diffusion equation

$$\partial_t \mathbf{u} = \mathbf{D}\Delta\mathbf{u} + \mathbf{f}(\mathbf{u}), \tag{A.1}$$

where $\mathbf{D}$ is symmetric. We have introduced the change of coordinates

$$\mathbf{X} = \epsilon\mathbf{x}, \quad T = \epsilon^2 t, \tag{A.2}$$

and the variables

$$\begin{aligned} \nabla\phi(\mathbf{x},t) &= \mathbf{k}(\mathbf{x},t), \\ \Phi(\mathbf{X},T,\epsilon) &= \epsilon\phi(\mathbf{x},t) \end{aligned} \tag{A.3}$$

so that

$$\hat{\mathbf{k}}(\mathbf{X},T) = \mathbf{k}(\mathbf{x},t) = \nabla_{\mathbf{x}}\phi(\mathbf{x},t) = \nabla_{\mathbf{X}}\Phi(\mathbf{X},T). \tag{A.4}$$

We will now drop the caret and consider $\mathbf{k}$ to be a function of $\mathbf{X}$ and T. The first step is to expand the solution as

$$\mathbf{u}(\phi,\mathbf{X},T) = \mathbf{u}^{(0)}(\phi,\mathbf{X},T) + \epsilon\mathbf{u}^{(1)}(\phi,\mathbf{X},T) + \cdots, \tag{A.5}$$

where $\mathbf{u}^{(0)}$ is the ideal pattern, and each of the $\mathbf{u}^{(i)}$ are periodic in ϕ with period 2π.

To recast equation (A.1) in $(\mathbf{X},T)$ coordinates, we need to apply the chain rule to obtain some derivative formulas:

$$
\begin{aligned}
\nabla_{\mathbf{x}} f(\phi, \mathbf{X}, T) &= (\partial_\phi f)(\nabla_{\mathbf{x}} \phi) + \epsilon \nabla_{\mathbf{X}} f \\
&= \mathbf{k} \partial_\phi f + \epsilon \nabla_{\mathbf{X}} f, \qquad \text{(A.6)} \\
\partial_t f(\phi, \mathbf{X}, T) &= (\partial_\phi f)(\partial_t \phi) + \epsilon^2 \partial_T f \\
&= \epsilon^2 (\partial_\phi f)(\partial_T \phi) + \epsilon^2 \partial_T f \\
&= \epsilon (\partial_\phi f)(\partial_T \Phi) + \epsilon^2 \partial_T f, \qquad \text{(A.7)} \\
|\nabla_{\mathbf{x}} f|^2 &= |\mathbf{k} \partial_\phi f + \epsilon \nabla_{\mathbf{X}} f|^2 \\
&= k^2 (\partial_\phi f)^2 + 2\epsilon (\partial_\phi f)(\mathbf{k} \cdot \nabla_{\mathbf{X}}) f + O(\epsilon^2), \qquad \text{(A.8)} \\
\nabla_{\mathbf{x}} \cdot \mathbf{F}(\phi, \mathbf{X}, T) &= (\partial_\phi \mathbf{F}) \cdot (\nabla_{\mathbf{x}} \phi) + (\nabla_{\mathbf{X}} \cdot \mathbf{F})(\epsilon) \\
&= \mathbf{k} \cdot (\partial_\phi \mathbf{F}) + \epsilon \nabla_{\mathbf{X}} \cdot \mathbf{F}, \qquad \text{(A.9)} \\
\Delta_{\mathbf{x}} f &= \nabla_{\mathbf{x}} \cdot \nabla_{\mathbf{x}} f \\
&= \nabla_{\mathbf{x}} \cdot (\mathbf{k} \partial_\phi f + \epsilon \nabla_{\mathbf{X}} f) \\
&= (\nabla_{\mathbf{x}} \cdot \mathbf{k})(\partial_\phi f) + \mathbf{k} \cdot \nabla_{\mathbf{x}} (\partial_\phi f) + \epsilon \nabla_{\mathbf{x}} \cdot \nabla_{\mathbf{X}} f \\
&= \epsilon (\nabla_{\mathbf{X}} \cdot \mathbf{k})(\partial_\phi f) + \mathbf{k} \cdot [\mathbf{k} (\partial_\phi^2 f) + \epsilon \nabla_{\mathbf{X}} (\partial_\phi f)] \\
&\quad + \epsilon [\mathbf{k} \cdot \partial_\phi (\nabla_{\mathbf{X}} f) + \epsilon \nabla_{\mathbf{X}} \cdot \nabla_{\mathbf{X}} f] \\
&= k^2 (\partial_\phi^2 f) + \epsilon (\nabla_{\mathbf{X}} \cdot \mathbf{k})(\partial_\phi f) + \epsilon (\mathbf{k} \cdot \nabla_{\mathbf{X}})(\partial_\phi f) \\
&\quad + \epsilon [\mathbf{k} \cdot \nabla_{\mathbf{x}} (\partial_\phi f) + \epsilon \Delta_{\mathbf{X}} f] \\
&= k^2 (\partial_\phi^2 f) + \epsilon (\nabla_{\mathbf{X}} \cdot \mathbf{k})(\partial_\phi f) + \epsilon 2 (\mathbf{k} \cdot \nabla_{\mathbf{X}})(\partial_\phi f) + \epsilon^2 \Delta_{\mathbf{X}} f. \\
& \qquad \text{(A.10)}
\end{aligned}
$$

Using the intermediate calculations just derived, we obtain

$$
\begin{aligned}
\partial_t \mathbf{u}(\phi, \mathbf{X}, T) &= \epsilon (\partial_\phi \mathbf{u})(\partial_T \Phi) + \epsilon^2 (\partial_T \mathbf{u}), \\
\Delta_{\mathbf{x}} u_i &= k^2 (\partial_\phi^2 u_i) + \epsilon (\nabla_{\mathbf{X}} \cdot \mathbf{k})(\partial_\phi u_i) + \epsilon 2 (\mathbf{k} \cdot \nabla_{\mathbf{X}})(\partial_\phi u_i) + \epsilon^2 \Delta_{\mathbf{X}} u_i, \\
\Delta_{\mathbf{x}} \mathbf{u} &= k^2 (\partial_\phi^2 \mathbf{u}) + \epsilon (\nabla_{\mathbf{X}} \cdot \mathbf{k})(\partial_\phi \mathbf{u}) + \epsilon 2 (\nabla_{\mathbf{X}} (\partial_\phi \mathbf{u}))^T \mathbf{k} + \epsilon^2 \Delta_{\mathbf{X}} \mathbf{u}. \\
& \qquad \text{(A.11)}
\end{aligned}
$$

(Recall that the gradient of a vector is defined as the transpose of the derivative matrix.) Plugging into the reaction-diffusion equation, expanding the nonlinear term in a Taylor series, and retaining only the terms of up to order ϵ, we then obtain

$$\begin{aligned}\epsilon\partial_\phi \mathbf{u}^{(0)}\partial_T\Phi &= \mathbf{D}\Big[k^2(\partial_\phi^2\mathbf{u}^{(0)}) + \epsilon(\nabla_{\mathbf{X}}\cdot\mathbf{k})(\partial_\phi\mathbf{u}^{(0)}) + \epsilon 2(\nabla_{\mathbf{X}}(\partial_\phi\mathbf{u}^{(0)}))^T\mathbf{k} \\ &\quad +\epsilon k^2(\partial_\phi^2\mathbf{u}^{(1)})\Big] + \mathbf{f}(\mathbf{u}^{(0)}) + \epsilon\frac{\partial\mathbf{f}}{\partial\mathbf{u}}\Big|_{\mathbf{u}=\mathbf{u}^{(0)}}\mathbf{u}^{(1)}. \qquad \text{(A.12)}\end{aligned}$$

The part of this equation which is of order zero in ϵ is simply the equation satisfied by the ideal pattern

$$0 = \mathbf{D}k^2(\partial_\phi^2\mathbf{u}^{(0)}) + \mathbf{f}(\mathbf{u}^{(0)}). \qquad \text{(A.13)}$$

Letting $\mathbf{g} = \partial\mathbf{f}/\partial\mathbf{u}$, the part which is of order ϵ gives rise to the equation

$$\begin{aligned}\partial_\phi\mathbf{u}^{(0)}\partial_T\Phi &= \mathbf{D}\left[(\nabla_{\mathbf{X}}\cdot\mathbf{k})(\partial_\phi\mathbf{u}^{(0)}) + 2(\nabla_{\mathbf{X}}(\partial_\phi\mathbf{u}^{(0)}))^T\mathbf{k} + k^2(\partial_\phi^2\mathbf{u}^{(1)})\right] + \\ &\quad \mathbf{g}(\mathbf{u}^{(0)})\mathbf{u}^{(1)}, \\ \left[\mathbf{D}k^2\partial_\phi^2 + \mathbf{g}(\mathbf{u}^{(0)})\right]\mathbf{u}^{(1)} &= -\mathbf{D}\left[(\nabla_{\mathbf{X}}\cdot\mathbf{k})(\partial_\phi\mathbf{u}^{(0)}) + 2(\nabla_{\mathbf{X}}(\partial_\phi\mathbf{u}^{(0)}))^T\mathbf{k}\right] + \partial_\phi\mathbf{u}^{(0)}\partial_T\Phi, \qquad \text{(A.14)}\end{aligned}$$

and this equation has the form

$$\mathcal{L}_1\mathbf{u}^{(1)} = \mathcal{N}, \qquad \text{(A.15)}$$

where $\mathcal{L}_1$ and $\mathcal{N}$ are operators.

Due to the translation-invariance of the original reaction-diffusion equation, $\partial_\phi\mathbf{u}^{(0)}$ is a zero-eigenvalue eigenvector of $\mathcal{L}_1$:

$$\begin{aligned}\mathcal{L}_1(\partial_\phi\mathbf{u}^{(0)}) &= \left[\mathbf{D}k^2\partial_\phi^2 + \mathbf{g}(\mathbf{u}^{(0)})\right]\partial_\phi\mathbf{u}^{(0)} \\ &= \partial_\phi\left[\mathbf{D}k^2\partial_\phi^2\mathbf{u}^{(0)} + \mathbf{f}(\mathbf{u}^{(0)})\right] \\ &= 0. \qquad \text{(A.16)}\end{aligned}$$

Next, we observe that the operator $\mathcal{L}_1$ is self-adjoint:

$$\begin{aligned} < \mathcal{L}_1 \mathbf{w}, \mathbf{v} > &= \frac{1}{2\pi} \int_0^{2\pi} \mathbf{v}^T \mathcal{L}_1 \mathbf{w} d\phi \\ &= \frac{1}{2\pi} \int_0^{2\pi} \mathbf{v}^T \left[k^2 \partial_\phi^2 + \mathbf{g}(\mathbf{u}^{(0)}) \right] \mathbf{w} d\phi \\ &= \frac{1}{2\pi} \int_0^{2\pi} \mathbf{w}^T \left[k^2 \partial_\phi^2 + \mathbf{g}(\mathbf{u}^{(0)}) \right] \mathbf{v} d\phi \\ &= < \mathbf{w}, \mathcal{L}_1 \mathbf{v} >, \end{aligned} \tag{A.17}$$

where we have used integration by parts. Then because $\mathcal{L}_1$ is self-adjoint and has $\partial_\phi \mathbf{u}^{(0)}$ as a zero-eigenvalue eigenvector, it follows from $\mathcal{L}_1 \mathbf{u}^{(1)} = \mathcal{N}$ that

$$\begin{aligned} < \mathcal{N}, \partial_\phi \mathbf{u}^{(0)} > &= < \mathcal{L}_1 \mathbf{u}^{(1)}, \partial_\phi \mathbf{u}^{(0)} > \\ &= < \mathbf{u}^{(1)}, \mathcal{L}_1 (\partial_\phi \mathbf{u}^{(0)}) > \\ &= 0. \end{aligned} \tag{A.18}$$

Calculating the various terms of $< \mathcal{N}, \partial_\phi \mathbf{u}^{(0)} >$, and using the notation

$$[\mathbf{f}^T \mathbf{g}] =< \mathbf{f}, \mathbf{g} >, \tag{A.19}$$

gives

$$\begin{aligned} < (\partial_\phi \mathbf{u}^{(0)}) \partial_T \Phi, \partial_\phi \mathbf{u}^{(0)} > &= \partial_T \Phi \left[|\partial_\phi \mathbf{u}^{(0)}|^2 \right], \\ < \mathbf{D}(\nabla_{\mathbf{X}} \cdot \mathbf{k}) \partial_\phi \mathbf{u}^{(0)}, \partial_\phi \mathbf{u}^{(0)} > &= (\nabla_{\mathbf{X}} \cdot \mathbf{k}) < \mathbf{D} \partial_\phi \mathbf{u}^{(0)}, \partial_\phi \mathbf{u}^{(0)} > \\ &= (\nabla_{\mathbf{X}} \cdot \mathbf{k}) \left[(\partial_\phi \mathbf{u}^{(0)})^T \mathbf{D} (\partial_\phi \mathbf{u}^{(0)}) \right], \\ < 2\mathbf{D}(\nabla_{\mathbf{X}} (\partial_\phi \mathbf{u}^{(0)}))^T \mathbf{k}, \partial_\phi \mathbf{u}^{(0)} > &= 2 < \mathbf{k}, (\nabla_{\mathbf{X}} (\partial_\phi \mathbf{u}^{(0)})) \mathbf{D}^T (\partial_\phi \mathbf{u}^{(0)}) > . \end{aligned} \tag{A.20}$$

To simplify the last expression, we need the symmetry assumption on $\mathbf{D}$. This is because, in general, if we have $\mathbf{u}(\mathbf{x})$, a constant matrix $\mathbf{A}$, and let D denote the derivative operator,

$$D_{\mathbf{x}} \left(\frac{1}{2} \mathbf{u}^T \mathbf{A} \mathbf{u} \right) = D_{\mathbf{u}} \left(\frac{1}{2} \mathbf{u}^T \mathbf{A} \mathbf{u} \right) D_{\mathbf{x}} \mathbf{u}$$

$$
\begin{aligned}
&= \left(\mathbf{A}_{\rm sym}\mathbf{u}\right)^T D_{\mathbf{x}}\mathbf{u}, \\
\nabla_{\mathbf{x}}\left(\frac{1}{2}\mathbf{u}^T\mathbf{A}\mathbf{u}\right) &= \left(D_{\mathbf{x}}\left(\frac{1}{2}\mathbf{u}^T\mathbf{A}\mathbf{u}\right)\right)^T \\
&= \left(D_{\mathbf{x}}\mathbf{u}\right)^T \mathbf{A}_{\rm sym}\mathbf{u} \\
&= \left(\nabla_{\mathbf{x}}\mathbf{u}\right)\mathbf{A}_{\rm sym}\mathbf{u}, \qquad \text{(A.21)}
\end{aligned}
$$

where $\mathbf{A}_{\rm sym} = (\mathbf{A} + \mathbf{A}^T)/2$ is the symmetric part of $\mathbf{A}$. Then we obtain

$$
\begin{aligned}
< 2\mathbf{D}(\nabla_{\mathbf{X}}(\partial_\phi \mathbf{u}^{(0)}))^T\mathbf{k}, \partial_\phi\mathbf{u}^{(0)} > &= 2 < \mathbf{k}, \nabla_{\mathbf{X}}\left(\frac{1}{2}(\partial_\phi\mathbf{u}^{(0)})^T\mathbf{D}(\partial_\phi\mathbf{u}^{(0)})\right) > \\
&= \mathbf{k}\cdot\nabla_{\mathbf{X}}\left[(\partial_\phi\mathbf{u}^{(0)})^T\mathbf{D}(\partial_\phi\mathbf{u}^{(0)})\right]. \qquad \text{(A.22)}
\end{aligned}
$$

The orthogonality condition $< \mathcal{N}, \partial_\phi\mathbf{u}^{(0)} >= 0$ thus gives rise to the following equation for Φ:

$$
\left[|\partial_\phi\mathbf{u}^{(0)}|^2\right]\partial_T\Phi = \left[(\partial_\phi\mathbf{u}^{(0)})^T\mathbf{D}(\partial_\phi\mathbf{u}^{(0)})\right](\nabla_{\mathbf{X}}\cdot\mathbf{k}) + \mathbf{k}\cdot\nabla_{\mathbf{X}}\left[(\partial_\phi\mathbf{u}^{(0)})^T\mathbf{D}(\partial_\phi\mathbf{u}^{(0)})\right], \qquad \text{(A.23)}
$$

which can be put in the form

$$
\partial_T\Phi = f_1(k)(\nabla_{\mathbf{X}}\cdot\mathbf{k}) + f_2(k)(\mathbf{k}\cdot\nabla_{\mathbf{X}})k, \qquad \text{(A.24)}
$$

since the ideal solution $\mathbf{u}^{(0)}$ only depends on $(\mathbf{X}, T)$ through the magnitude of $\mathbf{k}(\mathbf{X}, T)$.

Finally, we need to convert back to the original coordinates $(\mathbf{x}, t)$:

$$
\partial_t\phi = f_1(k)(\nabla_{\mathbf{x}}\cdot\mathbf{k}) + f_2(k)(\mathbf{k}\cdot\nabla_{\mathbf{x}})k, \qquad \text{(A.25)}
$$

where $\mathbf{k}$ is now thought of as a function of $(\mathbf{x}, t)$.

As we will now show, in two dimensions, this equation for $\Phi(\mathbf{X}, T)$ is closely related to the diffusion equation,

$$
\partial_T\Phi = D_1\partial_X^2\Phi + D_2\partial_Y^2\Phi, \qquad \text{(A.26)}
$$

where $\mathbf{X} = (X, Y)$, and D_1 and D_2 are diffusion coefficients.

To see how the diffusion equation plays a role, fix a point $\mathbf{X}$ in space, and suppose that $\mathbf{k}$ takes on the value $\mathbf{k}(\mathbf{X}, T)$ at that point $\mathbf{X}$ at some time T. Define the unit vector $\hat{\mathbf{v}}_{\|}$ to be in the direction of $\mathbf{k}(\mathbf{X}, T)$, and let the $\hat{\mathbf{v}}_{\perp}$ unit vector be orthogonal to $\hat{\mathbf{v}}_{\|}$. Then at any point in a small enough neighborhood of $(\mathbf{X}, T)$, we can do a coordinate transformation and write

$$\mathbf{k} = \nabla_{\mathbf{X}}\Phi = (\partial_{\|}\Phi)\hat{\mathbf{v}}_{\|} + (\partial_{\perp}\Phi)\hat{\mathbf{v}}_{\perp}, \tag{A.27}$$

where $\partial_{\|}$ is interpreted as the spatial partial derivative with respect to the transformed coordinate corresponding to the $\hat{\mathbf{v}}_{\|}$ direction, and $\partial_{\perp}$ is interpreted as the spatial partial derivative with respect to the transformed coordinate corresponding to the $\hat{\mathbf{v}}_{\perp}$ direction, and furthermore,

$$\partial_{\|}\Phi >> \partial_{\perp}\Phi. \tag{A.28}$$

Therefore, we can use the binomial formula to write

$$\begin{aligned} k &= [(\partial_{\|}\Phi)^2 + (\partial_{\perp}\Phi)^2]^{1/2} \\ &= [(\partial_{\|}\Phi)^2]^{1/2} + \frac{1}{2}[(\partial_{\|}\Phi)^2]^{-1/2}[(\partial_{\perp}\Phi)^2] + \cdots \\ &= \partial_{\|}\Phi + \frac{1}{2}\frac{(\partial_{\perp}\Phi)^2}{\partial_{\|}\Phi} + \cdots. \end{aligned} \tag{A.29}$$

Moreover, the expression $(\mathbf{k} \cdot \nabla_{\mathbf{X}})$ in the term $(\mathbf{k} \cdot \nabla_{\mathbf{X}})k$ can be approximately represented near $(\mathbf{X}, T)$ as

$$(\mathbf{k} \cdot \nabla_{\mathbf{X}}) \approx k(\hat{\mathbf{v}}_{\|} \cdot \nabla_{\mathbf{X}}) = k\partial_{\|}, \tag{A.30}$$

so that the linearization of the term $(\mathbf{k} \cdot \nabla_{\mathbf{X}})k$ is $k\partial_{\|}^2\Phi$.

Returning to equation (A.24), we can now plug in $\mathbf{k} = \nabla_{\mathbf{X}}\Phi$ and $(\mathbf{k} \cdot \nabla_{\mathbf{X}})k \approx k\partial_{\|}^2\Phi$, and using the fact that

$$\nabla_{\mathbf{X}} \cdot \nabla_{\mathbf{X}}\Phi = \Delta_{\mathbf{X}}\Phi = \partial_{\|}^2\Phi + \partial_{\perp}^2\Phi, \tag{A.31}$$

obtain the following approximate equation for Φ:

$$\begin{aligned} \partial_T \Phi &= (f_1(k) + k f_2(k))\partial_\parallel^2 \Phi + f_1(k)\partial_\perp^2 \Phi \\ &= D_\parallel \partial_\parallel^2 \Phi + D_\perp \partial_\perp^2 \Phi. \end{aligned} \tag{A.32}$$

The sense in which this is an approximate equation for Φ is that it is a linearization of the full equation for Φ about a point $(\mathbf{X}, T)$. The constants $D_\parallel$ and $D_\perp$ are the diffusion coefficients, and they describe the rate at which the phase relaxes in the direction of $\mathbf{k}$ and in the direction perpendicular to $\mathbf{k}$, respectively.

The diffusion coefficients are functions of ϵ and k, the reduced control parameter and the wave number. As long as both diffusion coefficients are positive, the diffusion equation for Φ is stable. Where one diffusion coefficient or the other becomes negative represents a stability boundary in the $k - \epsilon$ plane.

A.2 Derivation of the complex activator-inhibitor dynamics in polar coordinates

Starting with the dynamical system

$$\begin{aligned} \tau_\theta \partial_t \theta_R &= l^2 \partial_{xx} \theta_R - (\theta_R^2 + \theta_I^2)\theta_R + \theta_R + \eta_R, \\ \tau_\theta \partial_t \theta_I &= l^2 \partial_{xx} \theta_I - (\theta_R^2 + \theta_I^2)\theta_I + \theta_I + \eta_I, \\ \tau_\eta \partial_t \eta_R &= L^2 \partial_{xx} \eta_R - \eta_R - \theta_R + C_R, \\ \tau_\eta \partial_t \eta_I &= L^2 \partial_{xx} \eta_I - \eta_I - \theta_I + C_I, \end{aligned} \tag{A.33}$$

and using the coordinate transformation

$$\begin{aligned} \theta_R + i\theta_I &= r_\theta \exp(i\psi_\theta), \\ \eta_R + i\eta_I &= r_\eta \exp(i\psi_\eta), \\ C_R + iC_I &= r_C \exp(i\psi_C), \end{aligned} \tag{A.34}$$

the $\partial_t r_\theta$ equation is derived as follows. From $r_\theta^2 = \theta_R^2 + \theta_I^2$, we obtain

$$\begin{aligned} r_\theta \partial_t r_\theta &= \theta_R \partial_t \theta_R + \theta_I \partial_t \theta_I, \\ (\partial_x r_\theta)^2 + r_\theta(\partial_{xx} r_\theta) &= (\partial_x \theta_R)^2 + \theta_R(\partial_{xx}\theta_R) + (\partial_x \theta_I)^2 + \theta_I(\partial_{xx}\theta_I). \end{aligned} \tag{A.35}$$

From $\theta_R = r_\theta \cos\psi_\theta$ and $\theta_I = r_\theta \sin\psi_\theta$, we obtain

$$\begin{aligned} \partial_x \theta_R &= (\partial_x r_\theta)\cos\psi_\theta - r_\theta \sin\psi_\theta(\partial_x \psi_\theta), \\ \partial_x \theta_I &= (\partial_x r_\theta)\sin\psi_\theta + r_\theta \cos\psi_\theta(\partial_x \psi_\theta), \\ (\partial_x \theta_R)^2 + (\partial_x \theta_I)^2 &= (\partial_x r_\theta)^2 + r_\theta^2(\partial_x \psi_\theta)^2. \end{aligned} \tag{A.36}$$

From $\eta_R = r_\eta \cos\psi_\eta$ and $\eta_I = r_\eta \sin\psi_\eta$, we obtain

$$\begin{aligned} \theta_R \eta_R &= r_\theta r_\eta \cos\psi_\theta \cos\psi_\eta, \\ \theta_I \eta_I &= r_\theta r_\eta \sin\psi_\theta \sin\psi_\eta, \\ \theta_R \eta_R + \theta_I \eta_I &= r_\theta r_\eta \cos(\psi_\theta - \psi_\eta). \end{aligned} \tag{A.37}$$

Next, multiplying the equation for $\partial_t \theta_R$ through by θ_R, multiplying the equation for $\partial_t \theta_I$ through by θ_I, and summing the results, we obtain

$$\begin{aligned} &\tau_\theta \left[\theta_R(\partial_t \theta_R) + \theta_I(\partial_t \theta_I)\right] \\ &\quad = l^2 \left[\theta_R(\partial_{xx}\theta_R) + \theta_I(\partial_{xx}\theta_I)\right] - \left[r_\theta^2 \theta_R^2 + r_\theta^2 \theta_I^2\right] + \left[\theta_R^2 + \theta_I^2\right] \\ &\qquad + \left[\theta_R \eta_R + \theta_I \eta_I\right], \\ \tau_\theta r_\theta(\partial_t r_\theta) &= l^2 \left[(\partial_x r_\theta)^2 + r_\theta(\partial_{xx} r_\theta) - (\partial_x \theta_R)^2 - (\partial_x \theta_I)^2\right] - r_\theta^4 + r_\theta^2 + \theta_R \eta_R \\ &\qquad + \theta_I \eta_I \\ &\quad = l^2 \left[r_\theta(\partial_{xx} r_\theta) - r_\theta^2(\partial_x \psi_\theta)^2\right] - r_\theta^4 + r_\theta^2 + r_\theta r_\eta \cos(\psi_\theta - \psi_\eta), \\ \tau_\theta \partial_t r_\theta &= l^2 \left[\partial_{xx} r_\theta - r_\theta(\partial_x \psi_\theta)^2\right] - r_\theta^3 + r_\theta + r_\eta \cos(\psi_\theta - \psi_\eta). \end{aligned} \tag{A.38}$$

Similarly, we obtain

$$\tau_\eta \partial_t r_\eta = L^2 \left[\partial_{xx} r_\eta - r_\eta(\partial_x \psi_\eta)^2\right] - r_\eta - r_\theta \cos(\psi_\eta - \psi_\theta) + r_C \cos(\psi_\eta - \psi_C). \tag{A.39}$$

To determine the equation for $\partial_t \psi_\theta$, we first note that from $\theta_R = r_\theta \cos\psi_\theta$ and $\theta_I = r_\theta \sin\psi_\theta$ we have

$$\begin{aligned}
\partial_t \theta_R &= (\partial_t r_\theta)\cos\psi_\theta - r_\theta \sin\psi_\theta (\partial_t \psi_\theta), \\
\partial_t \theta_I &= (\partial_t r_\theta)\sin\psi_\theta + r_\theta \cos\psi_\theta (\partial_t \psi_\theta), \\
\sin\psi_\theta(\partial_t \theta_R) &= (\partial_t r_\theta)\sin\psi_\theta\cos\psi_\theta - r_\theta \sin^2\psi_\theta (\partial_t \psi_\theta), \\
\cos\psi_\theta(\partial_t \theta_I) &= (\partial_t r_\theta)\sin\psi_\theta\cos\psi_\theta + r_\theta \cos^2\psi_\theta (\partial_t \psi_\theta), \\
r_\theta \partial_t \psi_\theta &= -\sin\psi_\theta(\partial_t\theta_R) + \cos\psi_\theta(\partial_t\theta_I). \qquad \text{(A.40)}
\end{aligned}$$

Plugging in the expressions for $\partial_t\theta_R$ and $\partial_t\theta_I$ then yields

$$\begin{aligned}
\tau_\theta r_\theta \partial_t\psi_\theta &= -\sin\psi_\theta\left[l^2\partial_{xx}\theta_R - r_\theta^2\theta_R + \theta_R + \eta_R\right] \\
&\quad + \cos\psi_\theta\left[l^2\partial_{xx}\theta_I - r_\theta^2\theta_I + \theta_I + \eta_I\right] \\
&= -\sin\psi_\theta\Big\{l^2\Big[(\partial_{xx}r_\theta)\cos\psi_\theta - 2(\partial_x r_\theta)\sin\psi_\theta(\partial_x\psi_\theta) - r_\theta\cos\psi_\theta(\partial_x\psi_\theta)^2 \\
&\quad - r_\theta\sin\psi_\theta(\partial_{xx}\psi_\theta)\Big] - r_\theta^3\cos\psi_\theta + r_\theta\cos\psi_\theta + r_\eta\cos\psi_\eta\Big\} \\
&\quad + \cos\psi_\theta\Big\{l^2\Big[(\partial_{xx}r_\theta)\sin\psi_\theta + 2(\partial_x r_\theta)\cos\psi_\theta(\partial_x\psi_\theta) - r_\theta\sin\psi_\theta(\partial_x\psi_\theta)^2 \\
&\quad + r_\theta\cos\psi_\theta(\partial_{xx}\psi_\theta)\Big] - r_\theta^3\sin\psi_\theta + r_\theta\sin\psi_\theta + r_\eta\sin\psi_\eta\Big\} \\
&= l^2\left[2(\partial_x r_\theta)(\partial_x\psi_\theta) + r_\theta(\partial_{xx}\psi_\theta)\right] + r_\eta\sin(\psi_\eta - \psi_\theta), \\
\tau_\theta\partial_t\psi_\theta &= l^2\partial_{xx}\psi_\theta + \frac{2l^2}{r_\theta}(\partial_x r_\theta)(\partial_x\psi_\theta) + \frac{r_\eta}{r_\theta}\sin(\psi_\eta - \psi_\theta). \qquad \text{(A.41)}
\end{aligned}$$

Similarly, we obtain

$$\tau_\eta\partial_t\psi_\eta = L^2\partial_{xx}\psi_\eta + \frac{2L^2}{r_\eta}(\partial_x r_\eta)(\partial_x\psi_\eta) - \frac{r_\theta}{r_\eta}\sin(\psi_\theta - \psi_\eta) + \frac{r_C}{r_\eta}\sin(\psi_C - \psi_\eta). \qquad \text{(A.42)}$$

The dynamics in transformed coordinates are thus

$$
\begin{aligned}
\tau_\theta \partial_t r_\theta &= l^2 \left[\partial_{xx} r_\theta - r_\theta (\partial_x \psi_\theta)^2 \right] - r_\theta^3 + r_\theta + r_\eta \cos(\psi_\eta - \psi_\theta), \\
\tau_\eta \partial_t r_\eta &= L^2 \left[\partial_{xx} r_\eta - r_\eta (\partial_x \psi_\eta)^2 \right] - r_\eta - r_\theta \cos(\psi_\eta - \psi_\theta) + r_C \cos(\psi_\eta - \psi_C), \\
\tau_\theta \partial_t \psi_\theta &= l^2 \partial_{xx} \psi_\theta + \frac{2l^2}{r_\theta} (\partial_x r_\theta)(\partial_x \psi_\theta) + \frac{r_\eta}{r_\theta} \sin(\psi_\eta - \psi_\theta), \\
\tau_\eta \partial_t \psi_\eta &= L^2 \partial_{xx} \psi_\eta + \frac{2L^2}{r_\eta} (\partial_x r_\eta)(\partial_x \psi_\eta) + \frac{r_\theta}{r_\eta} \sin(\psi_\eta - \psi_\theta) - \frac{r_C}{r_\eta} \sin(\psi_\eta - \psi_C).
\end{aligned}
\tag{A.43}
$$

Appendix B

Simulations

The simulations were performed for illustration purposes more than for discerning the behavior of the systems being studied. Certainly one could use a supercomputer and perform a thorough study, but the purpose of the theoretical results is to obviate the need to do so. The purpose of this appendix is to indicate what level of effort is required to simulate these systems in the context of the applications outlined in chapter 7.

The spatially discretized versions of the cubic nonlinearity model and its generalizations are quite amenable to numerical simulation when there is a Lyapunov function (i.e., when $\alpha > 1$ for the cubic nonlinearity model). The approach is to formulate a system of $2N$ ODEs for an N-point spatial discretization, and then use a numerical integration technique starting from some initial state to obtain an approximation to a system trajectory, which then appears to approach an equilibrium solution for the $2N$-dimensional system of ODEs. The simulation results can be interpreted in two ways: either as approximating the time-evolution of the system, or simply as a numerical method for finding an approximation to the equilibria.

The numerical integration technique used was the forward Euler method. The forward Euler method is only stable if the step size is chosen sufficiently small. Some simulations were performed using both the forward Euler method and a fourth-order Runge-Kutta method, but no advantage was observed in using the fourth-order Runge-Kutta method over the forward Euler method, despite the Runge-Kutta method being a higher-order method. Although ana-

log approaches for implementing the spatially discretized cubic nonlinearity model and its variants were considered in chapters 3 and 7, an alternative digital implementation approach would be to implement the forward Euler numerical integration method in a parallel fashion. (In principle, the fourth-order Runge-Kutta algorithm could also be implemented digitally in a parallel fashion, but the complexity would be far greater.)

The time required to run a simulation (for the forward Euler method) is determined by the step size, which is in turn limited by the ratios of time constants and length scales (i.e., by α and β). (The fineness of the spatial discretization also plays a role, but we take the spatial discretization spacing δ equal to the activator diffusion length l. If $\delta < l$, then the step size needs to be reduced, and if $\delta > l$, we risk having too coarse a discretization to accurately approximate the continuous variable $\theta(\mathbf{x}, t)$ of the PDE system.) Since we need $\alpha > 1$, we can take $\alpha \approx 1$, so that α does not limit our step size. So, in fact, β is the parameter that determines the step size. If $\beta << 1$, we must use a correspondingly small step size, but if β is only less than one, we can use a larger step size. The cases for which $\beta < 1$ is of interest are

(1) the pattern regime for the basic cubic nonlinearity model,

(2) the complex activator-inhibitor equation, and

(3) the basic cubic nonlinearity model in the bistable regime when the behavior of interest is a wave that switches the system from one spatially uniform equilibrium to another.

However, we must use $\beta << 1$ when we are interested in analyzing spike solutions, because stable spike equilibria only exist for $\beta << 1$.

Simulations on two-dimensional domains take correspondingly longer to run than simulations in one dimension, but the actual code is similar. The main modification required is one extra vector-matrix multiplication per update to take into account diffusion in both spatial directions. For the two-dimensional simulations, the matrices used were 100 by 100, and the simulation times were on the order of several hours (using 1998 workstation technology). Of course, if the computations were done in a parallel distributed fashion in an array of actuators, there would be no limit on the size of the system, since the speed of the numerical method would be independent of the system size.

When necessary, random initial conditions were used. Where symmetry-breaking phenomena are possible, not using random initial conditions can lead to misleading results. But when, for example, spikes are being excited by locally raising the control parameter, a spatially uniform initial condition near the spatially uniform equilibrium solution is acceptable.

References

[1] M.C. Cross and P.C. Hohenberg, "Pattern formation outside of equilibrium," *Reviews of Modern Physics,* Vol. 65, No. 3, pp. 851-1112, 1993.

[2] G.B. Ermentrout and J.D. Cowan, "A mathematical theory of visual hallucination patterns," *Biological Cybernetics,* Vol. 34, No. 3, pp. 137-150, 1979.

[3] Ge Li, Qi Ouyang, Valery Petrov, and Harry L. Swinney, "Transistion from Simple Rotating Chemical Spirals to Meandering and Traveling Spirals," *Physical Review Letters,* Vol. 77, No. 10, pp. 2105-2108, 1996.

[4] M. Sheintuch and S. Shvartsman, "Spatiotemporal patterns in Catalytic Reactor: Journal Review," *American Institute of Chemical Engineers Journal,* Vol. 42, No. 4, pp. 1041-1068, 1996.

[5] M. Bar, I.G. Kevrekidis, H.H. Rotermund, and G. Ertl, "Pattern formation in composite excitable media," *Physical Review E,* Vol. 52, No. 6, pp. R5739-R5742, 1995.

[6] P.B. Umbanhowar, F. Melo, and H.L. Swinney, "Localized excitations in a vertically vibrated granular layer," *Nature,* Vol. 382, pp. 793-796, 1996.

[7] M. Bode and H.-G. Purwins, "Pattern formation in reaction-diffusion systems - dissipative solitons in physical systems," *Physica D*, Vol. 86, pp. 53-63, 1995.

[8] B.S. Kerner and V.V. Osipov, "Autosolitons," *Soviet Physics Uspekhi,* Vol. 32, No. 2, pp. 101-138, 1989.

[9] B.S. Kerner and V.V. Osipov. *Autosolitons.* Boston: Kluwer Academic Publishers, 1994.

[10] M. Barahona, E. Trias, T.P. Orlando, A.E. Duwel, H.S.J. van der Zant, S. Watanabe, and S.H. Strogatz, "Resonances of dynamical checkerboard states in Josephson arrays with self-inductance," *Physical Review B,* Vol. 55, No. 18, pp. 11989-11992, 1997.

[11] Kwok Yeung Tsang, Renato E. Mirollo, Steven H. Strogatz, and Kurt Wiesenfeld, "Dynamics of a Globally Coupled Oscillator Array," *Physica D,* Vol. 48, pp. 102-112, 1991.

[12] E.W. Justh and P.S. Krishnaprasad, "A Lyapunov functional for the cubic nonlinearity activator-inhibitor model equation." To appear in the *Proceedings of the 37th IEEE Conference on Decision and Control,* 1998.

[13] Thomas G. Bifano, Julie Perreault, Raji Krishnamoorthy Mali, and Mark N. Horenstein, "Microelectromechanical Deformable Mirrors," preprint, 1998.

[14] B.A. Samson and M.A. Vorontsov, "Localized states in a nonlinear optical system with a binary-phase slice and a feedback mirror," *Physical Review A,* Vol. 56, No. 2, pp. 1621-1626, 1997.

[15] Larry J. Hornbeck, "Deformable-Mirror Spatial Light Modulators," Spatial Light Modulators and Applications III, *SPIE Critical Reviews,* Vol. 1150, pp. 86-102, 1989.

[16] Edward N. Toughlian, Henry Zmuda, and Philipp Kornreich, "A Deformable Mirror-Based Optical Beamforming System for Phased Array Antennas," *IEEE Photonics Technology Letters,* Vol. 2, No. 6, pp. 444-446, 1990.

[17] Promode R. Bandyopadhyay, "Microfabricated Silicon Surfaces for Turbulence Diagnostics and Control," *Proceedings of the Active 95 Conference,* pp. 1327-1338, 1995.

[18] Karl-Friedrich Bohringer, Bruce Randall Donald, and Noel C. MacDonald, "Single-Crystal Silicon Actuator Arrays for Micro Manipulation Tasks," *Proceedings, IEEE Workshop on Micro Electro Mechanical Structures (MEMS),* 1996.

[19] Dan Reznik, Stan Brown, and John Canny, "Dynamic Simulation as a Design Tool for a Microactuator Array," Preprint, 1997.

[20] C.M. Ho and Y.C. Tai, "Micro-electro-mechanical-systems (MEMS) and fluid flows," *Annual Review of Fluid Mechanics,* Vol. 30, pp. 579-612, 1998.

[21] C.P. Schenk, P. Schutz, M. Bode, and H.-G. Purwins, "Interaction of self-organized quasiparticles in a two-dimensional reaction-diffusion system: the formation of molecules," *Physical Review E,* Vol. 57, No. 6, pp. 6480-6486, 1998.

[22] Edison H. Chiu, Can Tran, Takeshi Honzawa, and Shigeki Numaga. "Design and Implementation of a 525mm^2 CMOS Digital Micromirror Device (DMD) Display Chip," *Proceedings, IEEE VLSI Conference,* pp. 137-139, 1995.

[23] Gary A. Feather and David W. Monk, "The Digital Micromirror Device for Projection Display," *Proceedings, IEEE International Conference on Wafer Scale Integration,* pp. 43-51, 1995.

[24] F. H. Busse, "Non-linear properties of thermal convection," *Reports on Progess in Physics,* Vol. 41, pp. 1929-1967, 1978.

[25] Gerard Iooss and Moritz Adelmeyer. *Topics in Bifurcation Theory and Applications.* World Scientific Publishing Co., 1992.

[26] Klaus Kirchgassner, "Bifurcation in nonlinear hydrodynamic stability," *SIAM Review,* Vol. 17, No. 4, pp. 652-683, 1975.

[27] Alan C. Newell, "Envelope Equations." *Lectures in Applied Mathematics,* Vol. 15, pp. 157-163, Providence, RI: American Mathematical Society, 1974.

[28] D. H. Sattinger. *Group Theoretic Methods in Bifurcation Theory.* Lecture Notes in Mathematics, No. 762, Springer-Verlag, 1979.

[29] B.S. Kerner and V.V. Osipov, "Self-organization in active distributed media: scenarios for the spontaneous formation and evolution of dissipative structures," *Soviet Physics Uspekhi,* Vol. 33, No. 9, pp. 679-719, 1990.

[30] Gemunu H. Gunaratne, "Pattern formation in the presence of symmetries," *Physical Review E,* Vol. 50, No. 4, pp. 2802-2820, 1994.

[31] G.H. Gunaratne, R.E. Jones, Q. Ouyang, and H.L. Swinney, "An Invariant Measure of Disorder in Patterns," *Physical Review Letters,* Vol. 75, No. 18, pp. 3281-3284, 1995.

[32] A.S. Landsberg and E. Knobloch, "Oscillatory bifurcation with broken translation symmetry," *Physical Review E,* Vol 53, No. 4, pp. 3579-3600, 1996.

[33] M.A. Vorontsov and A. Yu. Karpov, "Pattern formation due to interballoon spatial mode coupling," *Journal of the Optical Society of America,* Vol. 14, No. 1, pp. 34-50, 1997.

[34] Harold T. Davis. *Introduction to Nonlinear Differential and Integral Equations.* Washington: U.S. Government Printing Office, 1960.

[35] Woodward Yang, "A Wide-Dynamic-Range, Low-Power Photosensor Array," *Proceedings of the IEEE International Solid-State Circuits Conference,* pp. 230-231, 1994.

[36] H.-G. Purwins and Ch. Radehaus, "Pattern Formation on Analogue Parallel Networks," *Neural and Synergetic Computers,* Hermann Haken, Ed., pp.137-154, 1988.

[37] Larry Cauler and Andy Penz, "Neurointeractivism: Emergence by Real-time Environmental Dynamics," Neuromorphic VLSI PI Meeting, Naval Research Laboratory, Washington, DC, June 23-24, 1998.

[38] R.A. York, P. Liao, and J.L. Lynch, "Oscillator Array Dynamics with Broadband N-Port Coupling Networks." *IEEE Transactions on Microwave Theory and Techniques*, Vol. 42, No. 11, pp. 2040-2045, 1994.

[39] R.A. York, "Nonlinear Analysis of Phase Relationships in Quasi-Optical Oscillator Arrays," *IEEE Transactions on Microwave Theory and Techniques*, Vol. 41, No. 10, pp. 1799-1809, 1993.

[40] Merrill Skolnik. *Introduction to Radar Systems.* McGraw-Hill, Inc., 1980. (Chapter 7)

[41] Robert Adler, "A Study of Locking Phenomena in Oscillators," *Proceedings of the IEEE*, Vol. 61, No. 10, pp. 1380-1385, 1973. (Reprinted from *Proceedings of the IRE*, Vol. 34, pp. 351-357, 1946.)

[42] Kaneyuki Kurokawa, "Injection Locking of Microwave Solid-State Oscillators," *Proceedings of the IEEE*, Vol. 61, No. 10, pp. 1386-1410, 1973.

[43] N. Kopell and G.B. Ermentrout, "Symmetry and phaselocking in chains of weakly coupled oscillators," *Communications on Pure and Applied Mathematics*, Vol. 39, No. 5, pp. 623-660, 1986.

[44] H. Khalil. *Nonlinear Systems.* New York: Macmillan Publishing Co., 1992.

[45] Y.S. Tang, A.I. Mees, and L.O. Chua, "Hopf Bifurcation Via Volterra Series." *IEEE Transactions on Automatic Control*, Vol. AC-28, No. 1, pp. 42-53, 1983.

[46] Lawrence Evans. *Partial Differential Equations.* Berkeley Mathematics Lecture Notes, 1994.

[47] Roger Temam. *Infinite-Dimensional Dynamical Systems in Mechanics and Physics, 2nd ed.* Springer-Verlag, 1997.

[48] Stuart Antman. *Nonlinear Problems of Elasticity.* Springer-Verlag, 1995.

[49] R.K. Brayton and J.K. Moser, "A Theory of Nonlinear Networks - I," *Quarterly of Applied Mathematics*, Vol. XXII, No. 1, pp. 1-33, 1964.

[50] Peter B. Gilkey. *The Index Theorem and the Heat Equation.* Mathematics Lecture Series 4, Boston: Publish or Perish, Inc., 1974.

[51] P.S. Krishnaprasad, "Spatial Light Modulator," preprint, 1998.

[52] Kari Gustafsson and Bertil Hok, "A silicon light modulator," *Journal of Physics E: Scientific Instruments*, Vol. 21, No. 7, pp. 680-685, 1988.

[53] E.D. Sontag, "Feedback stabilization of nonlinear systems." *Robust Control of Linear Systems and Nonlinear Control. Proceedings of the International Symposium MTNS-89 Vol. II*, pp. 61-81, 1990.

[54] Harry L. Van Trees. *Detection, estimation, and modulation theory, part 1.* New York: Wiley, 1968.

[55] Dean Scribner, "Infrared Color Vision from Fusion of Multi-band Imagery," Neuromorphic VLSI PI Meeting, Naval Research Laboratory, Washington, DC, June 23-24, 1998.

[56] Barry E. Stein and M. Alex Meredith. *The Merging of the Senses.* Cambridge: MIT Press, 1993.

[57] Christof Koch, "Attention, Eye Movements, and Visual Search: A Neuromorphic, Analog VLSI Model," Neuromorphic VLSI PI Meeting, Naval Research Laboratory, Washington, DC, June 23-24, 1998.

[58] Robert Mahony, "Convergence of Gradient Flows and Gradient Descent Algorithms for Analytic Cost Functions," *Proceedings of the International Symposium MTNS-98*, to appear, 1998.